LAYER-ADAPTED MESH METHODS FOR SINGULARLY PERTURBED PARABOLIC PARTIAL DIFFERENTIAL EQUATIONS WITH ROBIN BOUNDARY CONDITIONS

by

FASIKA WONDIMU GELU

JIMMA UNIVERSITY

October, 2023

JIMMA UNIVERSITY
SCHOOL OF GRADUATE STUDIES

LAYER-ADAPTED MESH METHODS FOR SINGULARLY PERTURBED PARABOLIC PARTIAL DIFFERENTIAL EQUATIONS WITH ROBIN BOUNDARY CONDITIONS

A Ph.D. DISSERTATION SUBMITTED TO THE SCHOOL OF GRADUATE STUDIES OF JIMMA UNIVERSITY FOR THE AWARD OF THE DEGREE OF DOCTOR OF PHILOSOPHY (Ph.D.) IN MATHEMATICS

by

FASIKA WONDIMU GELU

Under the Supervision of

GEMECHIS FILE DURESSA

October, 2023
JIMMA UNIVERSITY

Examination Board Dissertation Approval Sheet

We, the undersigned members of the board of examiners of the final open defense by Fasika Wondimu Gelu, have read and evaluated his dissertation entitled "LAYER-ADAPTED MESH METHODS FOR SINGULARLY PERTURBED PARABOLIC PARTIAL DIFFERENTIAL EQUATIONS WITH ROBIN BOUNDARY CONDITIONS" and examined the oral presentation of the candidate. This is, therefore, to certify that the dissertation has been accepted in partial fulfillment of the requirements for the degree of Doctor of Philosophy in Mathematics.

Board Members of Examiner

Name of Chairman	Signature	Date
Name of External Examiner	Signature	Date
Name of External Examiner	Signature	Date
Name of Internal Examiner	Signature	Date
Name of the Supervisor	Signature	Date

Dedication

This work is dedicated to my lovely wife, Mrs. Tadelech Adisu Adare, beloved daughter, Ruhama Fasika Wondimu, and entire families.

Declaration

I declare that the dissertation entitled “LAYER-ADAPTED MESH METHODS FOR SINGULARLY PERTURBED PARABOLIC PARTIAL DIFFERENTIAL EQUATIONS WITH ROBIN BOUNDARY CONDITIONS” is carried out by me under the supervision of Prof. Gemechis File Duressa for the award of Doctor of Philosophy in Mathematics. I declare that this dissertation has not been presented for the award of any degree elsewhere, either wholly or partly, and that all sources of data and scholarly information used in this dissertation are duly acknowledged.

Fasika Wondimu Gelu October, 2023

Signature ____________________

Abbreviations and Nomenclatures

PDE	Partial differential equation
RBC	Robin boundary condition
SPP	Singular perturbation problem
RPP	Regular perturbation problem
TPP	Turning point problem
FOFDM	Fitted operator finite difference method
FMFDM	Fitted mesh finite difference method
MATLAB	MATrix LABoratory
S-mesh	Shishkin mesh
BS-mesh	Bakhvalov-Shishkin mesh
VS-mesh	Vulanović-Shishkin mesh
$u(x,t)$	Solution of continuous problem
$u_0(x,t)$	Solution of reduced problem
N, M	Number of mesh intervals in space and time directions, respectively
$U^{N,M}$	Numerical solution on N, M number of mesh intervals
ε	Singular perturbation parameter
σ	Boundary layer transition parameter
τ	Delay parameter
$O(.)$	Landau order symbol
x, x_i	Continuous and discrete space variables
t, t_j	Continuous and discrete time variables
Ω_x, $\bar{\Omega}_x$	Space domain, closed space domain
$\\| . \\|$ or $\\| . \\|_\Omega$	Supremum norm over the domain Ω
$C^{(k)}(\Omega), C^{(k)}(\bar{\Omega})$	k times continuously differentiable functions in the respective domain
C	Generic positive constant independent of ε and mesh points
Ω_x^N, Ω_t^M	Discrete domain of space and time directions, respectively
$\Omega_x^N \times \Omega_t^M$	Discrete space-time domain
T	Maximum/Final time
$h, H, h_i; \Delta t$	Space mesh size and time mesh size, respectively
$\mathcal{L}_\varepsilon$	Differential operator
$\mathcal{L}_\varepsilon^{N,M}$	Difference operator
$E_\varepsilon^{N,\Delta t}, E^{N,\Delta t}$	Maximum absolute error and $\varepsilon-$uniform error, respectively
$R_\varepsilon^{N,\Delta t}, R^{N,\Delta t}$	Rate of convergence and uniform rate of convergence, respectively

Contents

List of Tables

List of Figures

List of Publications

Part of this dissertation has been published/submitted in the form of the following papers.

1. A parameter-uniform numerical method for singularly perturbed Robin type parabolic convection-diffusion turning point problems. *Applied Numerical Mathematics*, **190**:50-64, 2023.

2. Parameter-uniform numerical scheme for singularly perturbed parabolic convection-diffusion Robin type problems with a boundary turning point. *Results in Applied Mathematics*, **15**(2):100324, 2022.

3. A novel numerical approach for singularly perturbed parabolic convection-diffusion problems on layer-adapted meshes. *Research in Mathematics*, **9**(1):1-15, 2022.

4. Computational method for singularly perturbed parabolic reaction-diffusion equations with Robin boundary conditions. *Journal of Applied Mathematics & Informatics,* **40**(1-2), 25-45, 2022.

5. A uniformly convergent collocation method for singularly perturbed delay parabolic reaction-diffusion problem. *Abstract and Applied Analysis*, **2021**:8835595, 2021.

6. Hybrid scheme on S-type meshes for singularly perturbed parabolic reaction-diffusion problems with Robin boundary conditions (Under Review).

7. Hybrid numerical scheme for singularly perturbed parabolic convection-diffusion problems on Shishkin Mesh (Under Review).

Abstract

The main purpose of this dissertation is to present layer-adapted mesh methods for singularly perturbed parabolic partial differential equations of convection-diffusion and reaction-diffusion types with Robin boundary conditions. A singularly perturbed parabolic differential equation with Robin boundary conditions is a partial differential equation in which the highest space derivative in the differential equation and the first derivatives in the boundary conditions are multiplied by a small parameter $\varepsilon(0 < \varepsilon \ll 1)$. The parameter ε is known as the perturbation parameter. Because of the presence of ε, the solution of such differential equations exhibits a thin layer in which the solution varies rapidly near the layer while changing slowly and smoothly away from it. The presence of the layer phenomenon makes it difficult to solve such differential equations analytically. Thus, it is desirable to develop parameter-uniform numerical methods that help to solve singularly perturbed parabolic differential equations with Robin boundary conditions. As a result, this dissertation presents some parameter-uniform numerical methods for singularly perturbed parabolic partial differential equations with Robin boundary conditions on well-known layer-adapted meshes of Shishkin, Bakhvalov-Shishkin and Vulanović-Shishkin types. Furthermore, the stability and convergence analysis of the present numerical methods are well established. To support the theoretical findings, extensive numerical computations are carried out in all the chapters. The numerical results using the present methods improved the existing methods in the literature. At the end of the dissertation, a brief summary, conclusions and possible future scope are provided.

Acknowledgment

First and foremost, I would like to thank the Almighty God for giving me the strength to be able to withstand all the ups and downs to successfully complete my Ph.D. dissertation.

I very appreciate the help and guidance received from my supervisor Prof. Gemechis File Duressa and I am grateful for numerous corrections, constructive criticisms and advices he gave me throughout my dissertation work. Dear Prof. Gemechis, I thank you for your follow up and help to complete my study.

I am most grateful to my lovely wife, Mrs. Tadelech Adisu Adare, and my daughter, Ruhama Fasika, who gave me love and support for the completion of this Ph.D. dissertation. I appreciate their understanding, prayers, and cooperation. Indeed, they are my "good things" and I love them so much.

I acknowledge my gratitude to Jimma University, College of Natural Sciences, for the academic and financial support. Furthermore, I thank Dilla University for the financial and academic support. Moreover, I would like to thank "Simons Foundation Research and Graduate Studies in Mathematics and its Applications for Sub-Saharan Africa Nationals" at the Department of Mathematics and Statistical Sciences, Botswana International University of Science and Technology for partial financial support.

I am grateful to my classmates Dr. Masho and Dr. Wakjira, as well as my colleague Dr. Imiru, for their direct or indirect contributions to the completion of my dissertation.

October, 2023

Fasika Wondimu Gelu

Chapter 1

General Introduction

This chapter comprises of the general overview of singularly perturbed problems, the objectives of the study, the significance of the study, theoretical framework, research design and general mathematical procedures of the study. Finally, the organization of the dissertation is presented at the end of this chapter.

1.1 Background of the Study

Mathematical models are developed to ensure a thorough understanding of physical phenomena. A mathematical model is a description of a system that employs mathematical concepts and language. The model that would maintain the small parameters is called the perturbed model, whereas the simplified model (the one that does not include the small parameters) is called the unperturbed model (or reduced model) [6]. Mathematical models commonly produce equations involving derivatives of one or more dependent variables in relation to one or more independent variables, which is known as a differential equation. Many scientific and engineering problems are modelled using differential equations with or without delay and a small positive parameter(s). The behavior of the solution to these equations is based on the magnitude of the parameter(s). The solutions to these equations are affected by a small change in these parameter(s). This small change is called a perturbation or disturbance, and the corresponding parameter is called the perturbation parameter. The model that would be obtained by maintaining the small parameters is called the perturbed model, whereas the simplified model (the one that does not include the small parameters) is called unperturbed model (reduced model). A differential equation with a small parameter $\varepsilon(0 < \varepsilon \ll 1)$ multiplying the highest order derivative term subject to the specified boundary conditions belongs to a class of problems known as SPPs, and the parameter ε is known as perturbation parameter.

The birth of the singular perturbation was given by Prandtl at the Third International Congress of Mathematicians at Heidelberg in 1904, and it was reported in the proceedings of the conference [99]. Though Prandtl introduced the term "boundary layer" in this conference, it got much greater generality in the substantial work of Wasow [122]. The term "singular perturbation" was first introduced in the 1940s by Friedrichs and Wasow in their paper [37].

A boundary layer is defined to be a region of the independent variable over which the dependent variable changes rapidly [86]. The solution to SPPs exhibit a multi-scale character as $\varepsilon \to 0$, which means that there are thin transition layer(s) where the solution varies rapidly or jumps suddenly in some parts, which is known as the boundary layer region (inner region), and away from the layer(s), the solution behaves regularly and varies slowly, which is known as the outer region. When a layer is located near the boundary of the domain, SPP is referred to as a boundary layer problem, whereas if the layer is located inside the domain, SPP is known as an interior layer problem.

SPPs are significant in diversified fields of physical sciences, for example, fluid mechanics, fluid dynamics, elasticity, aerodynamics, plasma dynamics, rarefied gas dynamics, oceanography, in the modelling of steady and unsteady viscous flow problems with large Reynolds numbers, convective heat transport problems with large Pećlet numbers, magneto-hydrodynamics duct problems at high Hartman numbers, and other allied areas of fluid motion.

It is a well-known fact that singularly perturbed problem possesses boundary or interior layers. As a result, they are commonly known as boundary layers in fluid mechanics, edge layers in solid mechanics, skin layers in electrical applications, shock layers in fluid and solid mechanics, transition points in quantum mechanics, and Stokes lines and surfaces in mathematics [111].

Asymptotic methods, which are qualitative, and numerical methods, which are quantitative, are the two main types of methods for solving SPPs. There are several asymptotic methods available in the literature to approximate the solution of SPPs [12], [96] and [120]. However, the most widely used methods are multiple scales and matched asymptotic expansions. When applied to the SPP, the asymptotic method yields a single solution valid in the entire domain of interest, whereas the numerical method yields two solutions, known as inner and outer solutions. Though the asymptotic methods do provide approximate solutions, no quantitative information can be obtained with these approaches. As a result, numerical methods are needed.

Solving SPPs using the standard numerical methods such as finite difference, finite element, or finite volume methods on uniform meshes fail to resolve the layers when $\varepsilon \to 0$. It is well-known that small ε bring the so-called boundary layer phenomena, which makes the classical numerical methods lose their accuracy and stability [57]. Standard numerical methods on uniform mesh give oscillatory solutions in these problems due to the small parameter ε and are typically unstable when $\varepsilon \to 0$. Consequently, a large number of mesh points are needed, which is computationally expensive, in order to achieve the required numerical solution [106]. In this circumstances, the numerical experiments show that the standard numerical methods fail to decrease the maximum absolute errors as the mesh is refined, until the mesh size and the perturbation parameter have the same order of magnitude [36]. These difficulties can be overcome by the use of fitted numerical methods whose accuracies do not depend on the perturbation parameter, i.e., methods which are $\varepsilon-$uniformly convergent. By $\varepsilon-$uniform convergence, we mean that the numerical approximations converge independently of the small parameter ε.

Many scholars were inspired to develop $\varepsilon-$uniformly convergent numerical methods. The construction of $\varepsilon-$uniform numerical methods can be classified into two approaches. The first approach is the fitted operator finite difference methods (FOFDMs), and it is carried out on a uniform mesh. These methods are generally categorized into two groups. Exponentially fitted method and non-standard finite difference method. In the first group, an exponentially fitting factor along with the diffusion coefficient is introduced to control the rapid growth or decay of the solution in the boundary layer region. This method was first introduced by Allen and Southwell in [30]. The latter group is constructed by replacing the denominator functions of the classical finite differences with positive functions derived in such a way that they capture some significant properties of the governing differential equation and provide trustworthy numerical results. This method was first introduced by Mickens in [83]. The major drawback of FOFDMs is that they are sometimes difficult to extend to higher dimensional problems.

The second approach to the construction of $\varepsilon-$uniform numerical method involves the use of classical finite difference operators on a layer-adapted mesh, and thus it is carried out on non-uniform meshes. Such methods are referred to as fitted mesh finite difference methods (FMFDMs). Fitted (also called layer-adapted) meshes lie under two classes: graded and piecewise uniform meshes. The well-known layer-adapted fitted meshes are the Bakhvalov mesh and Shishkin mesh. Bakhvalov mesh is the first layer-adapted mesh introduced by Bakhvalov [5] and it is a *graded mesh* which is designed in such a way that in the layer region the mesh is fine at one end and gradually becomes coarse, and outside the layer region the mesh is uniform. Shishkin mesh is first introduced by Shishkin [112] and it is a *piecewise uniform mesh* which is finer at boundary layer region and coarser outer region. Methods using fitted meshes are recommended, whenever possible, because they are usually simpler to implement than methods using fitted operators. Moreover, we use FMFDMs to solve higher dimensional and nonlinear problems. However, they necessitate prior knowledge of the size and location of the layers. FMFDMs use nonuniform grids, which is fine in the boundary layer regions and coarse outside the layer regions.

The majority of science and engineering problems involving rates of change in time and space are mathematically expressed as parabolic partial differential equations (PDEs). A parabolic PDE subject to initial and boundary conditions is called initial-boundary value problem [23]. A singularly perturbed parabolic differential equation with Robin boundary conditions (RBCs) is a partial differential equation in which the highest space derivative in the differential equation and the first derivatives in the boundary conditions are multiplied by a small parameter $\varepsilon(0 < \varepsilon \ll 1)$. A singularly perturbed RBCs are a linear combination of both the Dirichlet and a singularly perturbed Neumann boundary conditions [53]. Because Neumann boundary conditions are a particular type of RBCs, the term RBCs in this study can refer to either Robin or Neumann boundary conditions.

Robin boundary conditions for a partial differential equation enjoys a long history in science and engineering applications [74]. It arises in a variety of physical situations and is often used as a way to homogenize complex boundary dynamics. In biology and chemistry, the Robin condition for the diffusion equation is often invoked to represent reactive or semipermeable boundaries. Problems with Robin boundary conditions are encountered in many practical situations such as problems concerned with fluid flow, electrolysis, semiconductor device modelling and chemical reactions [31]. The presence of ε multiplying the derivative terms in Robin boundary conditions amplifies the significance of the boundary layer whereas in the absence of ε, the layer is sufficiently weak for Robin type problems [2].

A singularly perturbed problem is said to be of the convection-diffusion type if the order of the differential equation is reduced by one when the perturbation parameter ε is set equal to zero. Thus, the solution to this type of differential equation exhibits one or two layers. The convection-diffusion-reaction equation consists of three processes [89]. The convection is due to the movement of materials from one region to another. The diffusion is due to the movement of materials from a region of high concentration to a region of low concentration. The reaction is due to the decay, absorption, and reaction of substances with other components. If the order of the differential equation is reduced by two when the perturbation parameter ε is set equal to zero, then the differential equation is known as a singularly perturbed reaction-diffusion type. Therefore, the solution to this type of differential equation exhibits two layers. Numerical solution of singularly perturbed parabolic convection-diffusion having turning or non-turning points and reaction-diffusion with or without time delay with Dirichlet boundary conditions have attracted many researchers. A few scholars developed various numerical methods to solve singularly perturbed parabolic Robin type differential equations of convection-diffusion-reaction type with non-turning point in [3], [53], [71], and [80], convection-diffusion-reaction type having a boundary turning point in [56], reaction-diffusion with time delay in [108], reaction-diffusion without delay in [44], [51], [68] [70] and [115], and convection-diffusion-reaction with two-parameter in [61]. However, the numerical solution of the aforementioned type of singularly perturbed parabolic partial differential equations with RBCs still need a lot of attention. Thus, the main aim of this dissertation is to formulate parameter-uniform numerical methods for singularly perturbed parabolic convection-diffusion type and reaction-diffusion type differential equations with RBCs.

1.2 Objectives

The efficiency of a numerical method is determined by its accuracy of the obtained discrete solution. Since the numerical methods developed for solving singularly perturbed problems depend upon the value of the perturbation parameter, errors in the numerical solution depend upon the mesh points and become small only when the mesh size in the layer region is much less than the value of the perturbation parameter ε. These motivate scholars to develop parameter-uniform numerical methods.

1.2.1 General Objective

The main objective of this study is to formulate parameter-uniform numerical methods for singularly perturbed parabolic partial differential equations with RBCs.

1.2.2 Specific Objectives

The specific objectives of this study are to

- develop layer-adapted mesh methods for families of singularly perturbed parabolic partial differential equations with RBCs.
- establish the stability analysis of the methods.
- prove parameter-uniform convergence analysis of the developed methods.

1.3 Significance of the Study

The outcome of this study helps the scholar not only acquire research skills and scientific knowledge but also comes up with the completion of his Ph.D. study. The work in this dissertation may provide some background information for scholars who are working on numerical methods to solve singularly perturbed differential equations with RBCs.

1.4 Theoretical Framework

A brief review of research achievements in singularly perturbed parabolic differential equations of both convection-diffusion-reaction and reaction-diffusion types with Robin boundary conditions are highlighted below. The works are presented in the chronological order and categorized into two types of differential equations as follows.

1.4.1 Singularly Perturbed Convection-diffusion Type Problems

The convection-diffusion-reaction partial differential equation is applied in a wide range of applications such as the water quality problem in river networks [10], simulation of oil extraction from under-ground reservoirs [35], convective heat transport problems with large Pećlet numbers [34], electromagnetic field problems in moving media [47], financial modeling of option pricing [13], turbulence model [73], drift diffusion equations of semiconductor device modeling [98], atmospheric pollution [101], fluid flow with high Reynolds numbers [55], ground water transport [11] and chemical reactor theory [85]. The next works are the review of singularly perturbed parabolic convection-diffusion-reaction type problem with non-turning points.

Bobisud [14] considered linear second-order singularly perturbed parabolic problem in the domain $(x,t) \in \Omega = (0,1) \times (0,T]$

$$\mathcal{L}_\varepsilon u(x,t) \equiv \varepsilon a(x,t)\frac{\partial^2 u(x,t)}{\partial x^2} - \frac{\partial u(x,t)}{\partial x} - b(x,t)u(x,t) - \frac{\partial u(x,t)}{\partial t} = f(x,t), \tag{1.1}$$

with initial and boundary conditions

$$\begin{cases} u(x,0) = \varphi(x), & 0 \le x \le 1, \\ u(0,t) = \psi_0(t), \quad u(1,t) = \psi_1(t), & 0 < t \le T, \end{cases} \tag{1.2}$$

where $0 < \varepsilon \ll 1$ is perturbation parameter. The coefficients $a(x,t), b(x,t), f(x,t)$, $(x,t) \in \Omega$ and $\varphi(x), \psi_0(t), \psi_1(t)$ are smooth and bounded functions satisfying $a(x,t) \ge a_0 > 0, b(x,t) \ge b_0 > 0, (x,t) \in \bar{\Omega}$. The next five reviews consider Eqs. (1.1) and (1.2).

Ng-Stynes et al. [95] discussed various difference schemes generated by means of a semi-discrete Petrov-Galerkin finite element method. They analyzed and compared both lumped and non-lumped time discretizations. Their schemes are first-order $\varepsilon-$uniformly convergent. Numerical results are also presented.

Hemker et al. [52] constructed a standard finite difference method on a piecewise uniform mesh for space and an implicit Euler method on a uniform mesh for time. The order of convergence for the proposed scheme is exactly one and close to one up to a small logarithmic factor with respect to the time and space variables, respectively.

Hemker et al. [54] constructed $\varepsilon-$uniformly convergent schemes with the second-order accuracy (up to a logarithmic factor) with respect to x and with the second, third, and higher orders of accuracy with respect to t using a defect-correction method. The computation of a numerical example demonstrated that the theoretical findings are in consistent with the second-order convergence with regard to the space and time variables.

Stynes and O'Riordan [117] examined a family of difference schemes with an exponentially fitted $x-$variable and using classical differencing in the $t-$variable, on rectangular grids which are arbitrarily spaced in both the x and t directions. The errors at the grid points first-order both in space and time directions. The corresponding result for a two-point boundary value problem is also derived.

Cai and Liu [21] developed a numerical method using Shishkin scheme, Bakhvalov-Shishkin scheme, and the multi-transition points scheme. They computed the maximum absolute errors using an example and noticed that the multi-transition scheme is more accurate than Shishkin scheme.

Hemker et al. [53] considered singularly perturbed parabolic convection-diffusion-reaction problem in the domain $(x,t) \in \Omega = (0,1) \times (0,T]$

$$\mathcal{L}_\varepsilon u(x,t) \equiv \varepsilon \frac{\partial^2 u(x,t)}{\partial x^2} + a(x)\frac{\partial u(x,t)}{\partial x} - b(x)u(x,t) - \frac{\partial u(x,t)}{\partial t} = f(x,t), \tag{1.3}$$

with initial and Robin boundary conditions

$$\begin{cases} u(x,0) = s(x), & 0 \le x \le 1, \\ B_{L,\varepsilon} u(0,t) \equiv u(0,t) - \varepsilon \frac{\partial u(0,t)}{\partial x} = q_0(t), & 0 < t \le T, \\ B_{R,\varepsilon} u(1,t) \equiv u(1,t) + \varepsilon \frac{\partial u(1,t)}{\partial x} = q_1(t), & 0 < t \le T, \end{cases} \tag{1.4}$$

where $0 < \varepsilon \ll 1$ is perturbation parameter and the coefficients $a(x),\ b(x),\ f(x,t)$, $\forall (x,t) \in \Omega$ and $s(x),\ q_0(t),\ q_1(t)$ are smooth and bounded functions satisfying $a(x) \ge \alpha > 0,\ b(x) \ge 0,\ x \in \bar{\Omega}$. The problem has left layer of width $O(\varepsilon)$. The authors studied the problem for the first time via an upwind finite difference scheme on a piecewise uniform Shishkin mesh and the backward Euler for the space and time discretisations. They obtained first-order in time and first-order with logarithmic factor in space direction.

Mbroh et al. [80] developed the scheme, which is a combination of a non-standard finite difference scheme and the backward Euler finite difference scheme on a uniform mesh for Eqs. (1.3) and (1.4). They established first-order accuracy for both the time and space variables and later improved to second-order by applying Richardson extrapolation. An example was considered to validate the theoretical findings.

SPPs with turning points arise as mathematical models for various physical phenomena. Among these, the problem with interior turning points represents the one-dimensional version of stationary convection-diffusion problems with a dominant convective term and a speed field that changes its sign in the catch basin. On the other hand, boundary turning point problems arise in geophysics [49] and in the modelling of thermal boundary layers in laminar flow [107]. The author in [49] presented a model for heat flow and mass transport near an oceanic rise. It is a single boundary turning point problem because of the assumption that the velocity distribution is linear. If one allows for a higher order of velocity distribution, then it becomes multiple boundary turning point problems [107].

The problem in which the convection coefficient vanishes inside the domain by changing signs is turning point problem with interior layer, whereas the problem in which the convection coefficient vanishes at the boundary of the domain is turning point problem with a boundary layer. Thus, singularly perturbed turning point problem can be classified into two classes, viz problem with boundary turning point and problem with interior turning point. This gives rise to the presence of boundary and/or interior layers depending on the number of zeros and the sign of convection coefficient.

Singularly perturbed parabolic convection-diffusion problem with a turning point is the differential equation where the coefficient of a convective term is zero along with certain parts of the boundary of the domain. Zeros that coincide with the boundary are referred to as boundary turning points, whereas zeros inside the domain of differential equations are interior turning points. The point in the domain where the convection coefficient vanishes is known as turning point.

Singularly perturbed turning point problems received systematic attention from the late 1960s [111]. Many researchers have proposed different numerical methods for singularly perturbed parabolic convection-diffusion problem having a boundary turning point with Dirichlet boundary conditions. Next, we present the reviews of singularly perturbed parabolic convection-diffusion-reaction problems having a boundary turning point.

Dunne and O'Riordan [33] considered singularly perturbed parabolic convection-diffusion problem having a boundary turning point on the domain $(x,t) \in \Omega \equiv (0,1) \times (0,T]$

$$\mathcal{L}_\varepsilon u(x,t) \equiv \varepsilon \frac{\partial^2 u(x,t)}{\partial x^2} + a(x,t)\frac{\partial u(x,t)}{\partial x} - b(x,t)u(x,t) - \frac{\partial u(x,t)}{\partial t} = f(x,t), \qquad (1.5)$$

with initial and boundary conditions

$$\begin{cases} u(x,0) = u_0(x), & 0 \le x \le 1, \\ u(0,t) = q_0(t), \quad u(1,t) = q_1(t), & 0 < t \le T, \end{cases} \qquad (1.6)$$

where $0 < \varepsilon \ll 1$ is perturbation parameter and $a(x,t) = a_0(x,t)x^p,\ p \ge 1, \forall (x,t) \in \bar{\Omega},\ a_0(x,t) \ge \alpha > 0,\ b(x,t) \ge \beta > 0$. Their method consists of a standard upwind finite difference method on a fitted piecewise uniform mesh for space discretization and an implicit Euler method on a uniform mesh for time discretization. They analyzed for uniform convergence and tested the proposed method using an example. The next eight reviews are based on Eqs. (1.5) and (1.6).

Gupta and Kadalbajoo [45] employed the implicit Euler method to discretize the time variable on a uniform mesh and the cubic B-spline collocation method defined on a piecewise uniform Shishkin mesh to discretize the space variable. Their method is analyzed and has been shown to be almost second-order accurate in space and first-order accurate in time. The scheme presented is shown to produce better compared to the results with the upwind finite difference method.

Majumdar and Natesan [78] discretized the domain into piecewise-uniform Shishkin mesh in the space direction using an upwind finite difference scheme and uniform mesh in the time direction using the implicit-Euler scheme. Applying the Richardson extrapolation technique, they improved the accuracy of the numerical solution from $O(N^{-1}\ln^2 N+\Delta t)$ to $O(N^{-2}\ln^2 N+\Delta t^2)$. They derived error estimates and carried out some numerical experiments to validate the theoretical results.

Majumdar and Natesan [79] used the backward Euler finite difference scheme to discretize the time derivative on a uniform mesh and the hybrid finite difference scheme, which is a combination of the central difference scheme and the midpoint upwind scheme on a piecewise uniform Shishkin mesh, to discretize the space derivative of the resulting time semi-discrete problem. They derived the error estimates, and the proposed scheme is $\varepsilon-$uniformly convergent of almost second-order (up to a logarithmic factor) in space and first-order in time. Numerical results are carried out.

Yadav et al. [126] proposed a numerical scheme that combines an implicit finite difference method for time discretization on a uniform mesh with a hybrid scheme for space discretization on a generalized Shishkin mesh. They applied the Richardson extrapolation technique to increase the order of convergence in the time direction. The resulting scheme has second-order convergence (up to a logarithmic factor) in space and second-order convergence in time. They conducted some numerical experiments to demonstrate the theoretical results and compare them with the existing methods in the literature.

Kumar et al. [69] constructed a numerical method using the implicit Euler scheme on a uniform mesh in the time direction and the upwind finite difference scheme on a layer adaptive non-uniform mesh in the space direction. The layer adaptive non-uniform mesh in the space direction is generated through the equidistribution of a suitably chosen monitor function. They performed error analysis through the truncation error and barrier function approaches and proved that the method is uniformly convergent with first-order in both time and space. Numerical results are given in support of the theoretical findings.

Mbroh et al. [81] developed a numerical scheme via Rothe's method. By means of the Crank-Nicolson finite difference scheme, the time derivative is discretised to obtain a set of semi-discrete boundary value problems. Using a fitted operator finite difference scheme based on the midpoint downwind scheme, the system of boundary value problems is discretized and analyzed for convergence. Second-order accuracy is established for each discretization. Numerical simulations are carried out to validate the theoretical estimate.

Ku Sahoo and Gupta [59] proposed a scheme consisting of an implicit Euler method on uniform mesh in time and a simple upwind scheme on piece-wise uniform mesh in space. Then, they applied the Richardson extrapolation scheme in both space and time directions. Theoretically, they proved that the proposed scheme is almost second-order parameter uniform convergent and verified it by doing some numerical experiments.

Singh et al. [116] semi-discretized the problem using the Crank-Nicolson scheme for the time and then the quadratic spline basis functions were used to discretize the semi-discrete problem. A rigorous error analysis shows that the proposed method is boundary layer resolving and second-order parameter uniformly convergent. They devised some numerical experiments to support the theoretical findings.

Rai and Yadav [102] considered the following singularly perturbed parabolic convection-diffusion time delay problem with a boundary turning point

$$\begin{aligned}\mathcal{L}_\varepsilon u(x,t) \equiv \varepsilon\frac{\partial^2 u(x,t)}{\partial x^2} + a(x,t)\frac{\partial u(x,t)}{\partial x} - b(x,t)u(x,t) - \frac{\partial u(x,t)}{\partial t} \\ = -c(x,t)u(x,t-\tau) + f(x,t), \quad (x,t) \in (0,1)\times(0,T],\end{aligned}$$

with initial and boundary conditions

$$\begin{cases} u(x,t) = s(x,t), & (x,t) \in [0,1]\times[-\tau,0], \\ u(0,t) = q_0(t), \quad u(1,t) = q_1(t), & 0 < t \le T, \end{cases}$$

where $0 < \varepsilon \ll 1$ is perturbation parameter, $\tau >$ is the delay parameter and coefficients $a(x,t) = a_0(x,t)x^p,\ p \ge 1, \forall (x,t) \in \bar{\Omega},\ a_0(x,t) \ge \alpha > 0,\ b(x,t) \ge \beta > 0,\ c(x,t) > 0$. To approximate the solution, they proposed a numerical method that consists of the backward

Euler scheme for time discretization on a uniform mesh and a combination of midpoint upwind and central difference schemes for the space discretization on a modified Shishkin mesh. They improved the order of convergence in time direction via the Richardson extrapolation technique. Numerical results are presented and a comparison is made.

Yadav and Rai [125] considered the following singularly perturbed parabolic convection-diffusion time delay turning point problem with interior layer

$$\begin{aligned}\mathcal{L}_\varepsilon u(x,t) &\equiv \varepsilon\frac{\partial^2 u(x,t)}{\partial x^2} + a(x,t)\frac{\partial u(x,t)}{\partial x} - b(x,t)u(x,t) - d(x,t)\frac{\partial u(x,t)}{\partial t}\\ &= c(x,t)u(x,t-\tau) + f(x,t), \quad (x,t) \in (-1,1)\times(0,T],\end{aligned}$$

with initial and boundary conditions

$$\begin{cases} u(x,t) = s(x,t), & (x,t) \in [-1,1]\times[-\tau,0],\\ u(-1,t) = q_0(t), \qquad u(1,t) = q_1(t), & 0 < t \le T,\end{cases}$$

where $0 < \varepsilon \ll 1$ is perturbation parameter and $\tau > 0$ is the delay parameter, $a(x,t) = a_0(x,t)x^p,\ p \geq 1, \forall (x,t) \in \bar{\Omega},\ a_0(x,t) \geq \alpha > 0,\ b(x,t) \geq \beta > 0,\ c(x,t) > 0$. They solved the problem by using the fitted mesh method and analyzing the upwind scheme on a non-uniform mesh. The proposed scheme has an order of convergence of almost one both in space and time variables. The numerical findings support the theoretical results.

Munyakazi et al. [92] considered the following singularly perturbed parabolic convection-diffusion turning point problem with interior layer for $(x,t) \in \Omega \equiv (-1,1)\times(0,T]$

$$\mathcal{L}_\varepsilon u(x,t) \equiv \varepsilon\frac{\partial^2 u(x,t)}{\partial x^2} + a(x,t)\frac{\partial u(x,t)}{\partial x} - b(x,t)u(x,t) - d(x,t)\frac{\partial u(x,t)}{\partial t} = f(x,t),$$

with initial and boundary conditions

$$\begin{cases} u(x,0) = u_0(x), & x \in [0,1],\\ u(-1,t) = \alpha, \qquad u(1,t) = \gamma, & 0 < t \le T,\end{cases}$$

where $0 < \varepsilon \ll 1$ is perturbation parameter. They discretized the time variable using the classical Euler method and the space variable using a fitted operator finite difference method. Through a rigorous error analysis, they showed that the scheme is uniformly convergent of order one with respect to both time and space variables. They used Richardson extrapolation to improve the proposed scheme's accuracy and order of convergence. Numerical investigations are carried out to demonstrate the efficacy.

Janani Jayalakshmi and Tamilselvan [56] solved the following singularly perturbed convection-diffusion turning point problem posed on $(x,t) \in \Omega = (0,1) \times (0,T]$

$$\mathcal{L}_\varepsilon u(x,t) \equiv \varepsilon \frac{\partial^2 u(x,t)}{\partial x^2} + a(x,t)\frac{\partial u(x,t)}{\partial x} - \frac{\partial u(x,t)}{\partial t} - b(x,t)u(x,t) = f(x,t),$$

with initial and Robin boundary conditions

$$\begin{cases} u(x,0) = \phi_B(x), & 0 \le x \le 1, \\ B_{L,\varepsilon}u(0,t) \equiv u(0,t) - \sqrt{\varepsilon}\frac{\partial u(0,t)}{\partial x} = \phi_L(t), & 0 < t \le T, \\ B_{R,\varepsilon}u(1,t) \equiv u(1,t) + \sqrt{\varepsilon}\frac{\partial u(1,t)}{\partial x} = \phi_R(t), & 0 < t \le T, \end{cases}$$

where $0 < \varepsilon \ll 1$ is perturbation parameter and $a(x,t) = a_0(x,t)x^p,\ p \ge 1,\ \forall (x,t) \in \bar{\Omega},\ a_0(x,t) \ge \alpha > 0,\ b(x,t) \ge \beta > 0$. The problem has left layer of width $O(\sqrt{\varepsilon})$. They proposed the upwind finite difference method for space on a Shishkin mesh and the backward Euler method for time on a uniform mesh to discretize the problem. They employed forward and backward finite difference approximations to discretize Robin boundary condition. Their overall discretization gives first-order uniform convergence, which is confirmed by computing two numerical examples.

1.4.2 Singularly Perturbed Reaction-diffusion Type Problems

Many of the real-life processes, both natural and man-made, in biology, medicine, chemistry, physics, engineering, economics, etc., involve time delays, and time delays are also known as transport lags, dead times, or time lags [60]. In addition, time delays have appeared in the study of chemostat models, circadian rhythms, epidemiology, the respiratory system, population ecology, tumor growth, and neural networks; see [60] and [124]. In epidemiology, a delay can represent the duration of incubation time or the time a host stays infected. A time delay may be defined as the time interval between the start of an event at one point in a system and its resulting action at another point in the system. Any system involving feedback control almost always involves a time delay. A singularly perturbed time delay parabolic problem is one in which a small parameter $\varepsilon(0 < \varepsilon \ll 1)$ multiplies the highest space derivative and contains a delay term in the time direction.

The reviews on singularly perturbed parabolic reaction-diffusion problem with time delay are given below.

Ansari et al. [1] considered the following singularly perturbed time delay parabolic reaction-diffusion problem on the domain $(x, t) \in \Omega = (0, 1) \times (0, T]$

$$\mathcal{L}_\varepsilon u(x,t) \equiv \frac{\partial u(x,t)}{\partial t} - \varepsilon \frac{\partial^2 u(x,t)}{\partial x^2} + a(x,t)u(x,t) = -b(x,t)u(x,t-\tau) + f(x,t), \quad (1.7)$$

with initial and boundary conditions

$$\begin{cases} u(x,t) = \phi_B(x,t), & (x,t) \in [0,1] \times [-\tau, 0], \\ u(0,t) = \phi_L(t), \qquad u(1,t) = \phi_R(t), & 0 < t \leq T, \end{cases} \quad (1.8)$$

where $0 < \varepsilon \ll 1$ is perturbation parameter and $\tau > 0$ is a delay parameter. They proposed a centered finite difference operator in space direction on a piecewise uniform mesh and an implicit Euler in time direction. In the maximum norm, their errors are bounded by $O(N^{-2} \ln^2 N + \Delta t)$.

Bashier and Patidar [8] proposed a Crank-Nicolson finite difference method on a mesh of Shishkin type for Eqs. (1.7) and (1.8). They investigated the method's stability and convergence and proved that the method is unconditionally stable and converges with order $O(\Delta t^2 + N^{-2} \ln^2 N)$. Their method was illustrated through numerical experiments.

Bashier and Patidar [9] designed a robust fitted operator finite difference method for Eqs. (1.7) and (1.8). Their method is unconditionally stable and convergent with first-order in time and second-order in space directions, respectively. Their method is demonstrated through numerical experiments and also compared with those obtained by the finite difference method in the literature.

Bashier and Patidar [7] considered the following singularly perturbed time delay parabolic problem of the following form on the domain $(x,t) \in \Omega = (0,1) \times (0,T]$

$$\mathcal{L}_\varepsilon u(x,t) \equiv \frac{\partial u(x,t)}{\partial t} - \varepsilon \frac{\partial^2 u(x,t)}{\partial x^2} = -b(x,t)u(x,t-\tau) + f(x,t),$$

with initial and boundary conditions

$$\begin{cases} u(x,t) = \theta(x,t), & (x,t) \in [0,1] \times [-\tau,0], \\ u(0,t) = \Gamma_L(t), \quad u(1,t) = \Gamma_R(t), & 0 < t \leq T, \end{cases}$$

where $0 < \varepsilon \ll 1$ is perturbation parameter and $\tau > 0$ is a delay parameter. They constructed a second-order fitted operator difference method via the Crank-Nicolson discretization. Their proposed method is found to be unconditionally stable and convergent with second-order time and space directions, respectively. The performance of their method is illustrated through a numerical example.

Kumar and Kumar [66] proposed a hybrid scheme on a generalized Shishkin mesh in space direction and the implicit Euler scheme on a uniform mesh in time direction for Eqs. (1.7) and (1.8). They then designed a Richardson extrapolation scheme to increase the order of convergence in time direction. Their resulting scheme is shown to be second-order accurate in time and fourth-order (with a logarithmic factor) accurate in space. Numerical experiments are performed to support the theoretical results.

Gowrisankar and Natesan [42] discretized the domain by a uniform mesh in the time direction and a nonuniform mesh in the space direction, obtained via the equidistribution of a monitor function for Eqs. (1.7) and (1.8). Their numerical scheme consists of the implicit Euler scheme for the time derivative and the classical central difference scheme for the space derivative. They showed that the method converges uniformly with an optimal error bound. Error estimates are derived, and numerical examples are presented.

Peiraviminaei and Ghoreishi [97] considered the following singularly perturbed time delay parabolic problem on the domain $(x,t) \in \Omega = (-1,1) \times (0,T]$

$$\mathcal{L}_\varepsilon u(x,t) \equiv \frac{\partial u(x,t)}{\partial t} - 4\varepsilon \frac{\partial^2 u(x,t)}{\partial x^2} + a(x,t)u(x,t) = -b(x,t)u(x,t-\tau) + f(x,t),$$

with initial and Dirichlet boundary conditions

$$\begin{cases} u(x,t) = \phi_B(x,t), & (x,t) \in [-1,1] \times [-\tau, 0], \\ u(0,t) = \phi_L(t), \quad u(1,t) = \phi_R(t), & 0 < t \le T, \end{cases}$$

where $0 < \varepsilon \ll 1$ is perturbation parameter and $\tau > 0$ is a delay parameter. They proposed Chebyshev spectral collocation for space discretization.

Singh et al. [114] designed and analyzed a domain decomposition method to solve Eqs. (1.7) and (1.8). They discretized the problem using the backward Euler scheme in the time direction and the central difference scheme in the space direction. Their proposed method is almost second order in space and first order in time. Numerical results were performed for the support of theoretical findings.

Govindarao et al. [40] used the implicit Euler scheme on the uniform mesh for time and the central difference scheme for the space discretization on the Shishkin mesh for Eqs. (1.7) and (1.8). To enhance the order of convergence, they applied the Richardson extrapolation technique. Then, they prove that the proposed method converges uniformly with respect to the perturbation parameter and also attains an almost fourth-order convergence rate. They presented some numerical experiments.

Govindarao and Mohapatra [39] used the Crank-Nicolson scheme on the uniform mesh for time and the central difference scheme on the Shishkin mesh for space discretization, which provides a second order convergence rate for Eqs. (1.7) and (1.8). To enhance the order of convergence, they applied the Richardson extrapolation technique. They attained an almost fourth-order convergence rate. They presented numerical experiments.

Kumar and Ravi Kanth [65] semi-discretized Eqs. (1.7) and (1.8) in the time derivative by the Crank-Nicolson scheme and then in the space derivative by the tension spline scheme on non-uniform Shishkin mesh. Their error estimation for the discretized problem is derived. They tested the numerical outcomes for linear and nonlinear problems.

Selvi and Ramanujam [108] considered the singularly perturbed time delay parabolic reaction-diffusion problem on $(x,t) \in \Omega = (0,1) \times (0,T]$

$$\mathcal{L}_\varepsilon u(x,t) \equiv \frac{\partial u(x,t)}{\partial t} - \varepsilon \frac{\partial^2 u(x,t)}{\partial x^2} + a(x,t)u(x,t) = -b(x,t)u(x,t-\tau) + f(x,t),$$

with initial and Robin boundary conditions

$$\begin{cases} u(x,t) = \phi_B(x,t), & (x,t) \in [0,1] \times [-\tau,0], \\ B_{L,\varepsilon} u(0,t) \equiv u(0,t) - \sqrt{\varepsilon}\frac{\partial u(0,t)}{\partial x} = \phi_L(t), & 0 < t \leq T, \\ B_{R,\varepsilon} u(1,t) \equiv u(1,t) + \sqrt{\varepsilon}\frac{\partial u(1,t)}{\partial x} = \phi_R(t), & 0 < t \leq T, \end{cases}$$

where $0 < \varepsilon \ll 1$ is perturbation parameter and $\tau > 0$ is a delay parameter. The problem has boundary layers of width $O(\sqrt{\varepsilon})$ near $x = 0$ and $x = 1$. They suggested a numerical method comprising a central finite difference scheme on a piecewise uniform mesh condensing in the boundary layers. They proved the error is of the form $O(N^{-2}\ln^2 N + \Delta t)$. They considered an example to validate the theoretical result.

Reaction-diffusion problems usually arise in the modelling of various chemical, biological, and physical systems. Some applications of reaction-diffusion problems involve chemical kinetics, mathematical models of liquid crystal materials, and heat transport problems with high Pećlet numbers [85]. Various numerical methods have been developed for singularly perturbed parabolic reaction-diffusion problems without delay.

Miller et al. [84] considered the following singularly perturbed parabolic reaction-diffusion problem in the domain $(x,t) \in \Omega = (0,1) \times (0,T]$

$$\mathcal{L}_\varepsilon u(x,t) \equiv \frac{\partial u(x,t)}{\partial t} - \varepsilon \frac{\partial^2 u(x,t)}{\partial x^2} + a(x,t)u(x,t) = f(x,t), \tag{1.9}$$

with initial and boundary conditions

$$\begin{cases} u(x,0) = u_0(x), & 0 \le x \le 1, \\ u(0,t) = q_0(t), \qquad u(1,t) = q_1(t), & 0 < t \le T, \end{cases} \tag{1.10}$$

where $0 < \varepsilon \ll 1$ is perturbation parameter. The coefficient $a(x,t)$ and source function $f(x,t)$ are smooth and bounded satisfying the condition $a(x,t) \ge \alpha > 0$. They suggested a numerical method comprising a standard finite difference operator (centered in space, implicit in time) on a rectangular piecewise uniform mesh condensing in the boundary layers and proved to be parameter-uniform in the sense that its numerical solutions converge in the maximum norm to the exact solution uniformly well for all values of the parameter. It was demonstrated that the errors are bounded by $O(N^{-2}\ln^2 N + \Delta t)$. The next thirteen reviews are based on Eqs. (1.9) and (1.10).

In [93], Natesan and Deb developed a numerical scheme which combines the cubic spline scheme in layer region and the central finite difference scheme in outer region for the space derivative on the Shishkin mesh and a backward difference scheme for the time derivative. They obtained stability analysis and error estimates and solved a test problem.

Kumar and Chandra Sekhara Rao [64] constructed a numerical method by combining the Crank-Nicolson method on a uniform mesh in the time direction with a hybrid scheme, which is a suitable combination of a fourth-order compact difference scheme and the standard central difference scheme on a generalized Shishkin mesh in the space direction. They proved that the numerical method is uniformly convergent to second-order in time and almost fourth-order in space variables. Numerical experiments are presented.

Clavero and Gracia [24] proposed a numerical scheme combining the backward Euler method for time and central differencing defined on some special meshes such as Shishkin, Bahkvalov and Vulanovic meshes for space. The analysis of uniform convergence is established. Some numerical results are shown, corroborating the theoretical results.

Clavero and Gracia [25] developed a numerical method which combines the implicit Euler method on a uniform mesh to discretize time and a HODIE compact fourth order finite difference scheme to discretize space defined on a Vulanović mesh. The method is uniformly convergent, having first order in time and almost fourth order in space. A uniform convergence analysis is performed. Some numerical results are given.

Natesan and Gowrisankar [94] discretized the problem with the implicit Euler scheme on a uniform mesh in the time direction and the classical central difference scheme on a nonuniform mesh, obtained via equidistribution of a monitor function for the space variable. Truncation error and stability analysis are carried out. Error estimates are derived, and numerical examples are presented.

In [91], Munyakazi and Patidar semi-discretized the problem in time by means of the classical backward Euler method and a fitted operator finite difference method in space to solve the resulting set of linear problems. They proved that their method is shown to be first-order uniformly convergent in time and second-order convergent in space. They tested the method on several numerical examples to confirm its theoretical findings.

Gowrisankar and Natesan [41] used a modified backward Euler scheme for time and a central finite difference method on a layer adapted nonuniform mesh obtained by equidistribution of a positive monitor function, which involves the second-order space derivative. The truncation error and the stability analysis are obtained. To support the theoretical results, numerical experiments are carried out.

Clavero and Gracia [26] constructed a high-order uniformly convergent finite difference scheme, which combines an implicit Euler method to discretize in time and a HODIE scheme to discretize in space. They applied the Richardson extrapolation technique and performed numerical experiments for different test problems.

Kumar and Rao [67] developed an overlapping Schwarz domain decomposition method for space on a Shishkin mesh and an implicit Euler method for time on a uniform mesh. They established that the method is first-order in time and almost second-order in space. They proved that when ε is small, just one iteration is required to achieve the desired accuracy. Numerical experiments support the theoretical results.

Gracia and O'Riordan [43] proposed a classical finite difference method on a piecewise uniform Shishkin mesh. First order convergence of these numerical approximations is established in an appropriately weighted C^1-norm. Numerical results are given to illustrate the theoretical error bounds.

In [104], Rao et al. constructed a discrete Schwarz waveform relaxation method of higher order for their numerical solution. The method is shown to be parameter-uniformly convergent, having almost fourth order in space and first order in time. Numerical results demonstrate the efficiency of the proposed method.

Mishra et al. [87] used orthogonal spline collocation with C^1 splines of degree $r \geq 3$ on a Shishkin mesh for space discretization, and the Crank-Nicolson method. The results of numerical experiments validate the theoretical analysis.

Bullo et al. [19] introduced an average finite difference approximation for time and a fitted operator finite difference method for space on uniform mesh. To accelerate the rate of convergence of the method, the Richardson extrapolation technique is applied. The consistency and stability of the proposed method have been established very well. Numerical experimentation is carried out on some numerical examples. Their results are compared with the findings of some methods existing in the literature.

Kumar et al. [68] considered the following singularly perturbed parabolic reaction-diffusion problem posed on $(x,t) \in \Omega = (0,1) \times (0,T]$

$$\mathcal{L}_\varepsilon u(x,t) \equiv \frac{\partial u(x,t)}{\partial t} - \varepsilon \frac{\partial^2 u(x,t)}{\partial x^2} + a(x,t)u(x,t) = f(x,t), \tag{1.11}$$

with initial and Robin boundary conditions

$$\begin{cases} u(x,0) = \phi_B(x), & 0 \le x \le 1, \\ B_{L,\varepsilon} u(0,t) \equiv u(0,t) - \sqrt{\varepsilon}\frac{\partial u(0,t)}{\partial x} = \phi_L(t), & 0 < t \le T, \\ B_{R,\varepsilon} u(1,t) \equiv u(1,t) + \sqrt{\varepsilon}\frac{\partial u(1,t)}{\partial x} = \phi_R(t), & 0 < t \le T, \end{cases} \tag{1.12}$$

where $0 < \varepsilon \ll 1$ is perturbation parameter such that boundary layers of width $O(\sqrt{\varepsilon})$ appear in the neighbourhood of both $x = 0$ and $x = 1$. They discretization the problem by means of a modified Euler scheme in time using uniform mesh and a central difference scheme in space using equidistribution mesh, and a special finite difference scheme for Robin boundary conditions. They discussed error analysis and proved that their method is parameter-uniformly convergent of second-order in space and first-order in time. They performed some numerical experiments.

Gupta et al. [44] claimed an efficient hybrid difference scheme which is the combination of a modified backward difference scheme in time and a hybrid spline difference scheme in space using adaptive mesh. They applied the cubic spline difference scheme for the discretization of Robin boundary conditions for Eqs. (1.11) and (1.12). Their error analysis of the proposed discretization reveals parameter-uniform second-order convergence in space and first-order convergence in time. The numerical results presented corroborate the theoretical findings.

Kumar et al. [70] constructed and analyzed a domain decomposition method known as the Schwarz waveform relaxation method for Eqs. (1.11) and (1.12). Their method considers three subdomains, of which two are finely meshed and the other is coarsely meshed. The Robin boundary conditions are approximated using a special finite difference scheme to maintain accuracy. They proved that their numerical results are parameter-uniform and that the convergence of the iterates is optimal for small values of the perturbation parameters. The numerical results support the theoretical results.

A non-polynomial basis consisting of trigonometric B-spline functions discretization for space variable using two different piecewise uniform meshes and the Crank-Nicolson discretization for time variable were developed in Singh et al. [115] for Eqs. (1.11) and (1.12). Their present scheme is shown to be convergent, independent of the perturbation and mesh parameters, through meticulous analysis. They checked the performance of their method through several graphs and tables. Their results obtained using improved Shishkin mesh were more accurate than standard Shishkin mesh.

Despite the fact that numerical treatments of singularly perturbed parabolic differential equations with Dirichlet boundary conditions have received a great deal of attention in the literature, there is little experience in developing parameter-uniform numerical methods for solving singularly perturbed parabolic differential equations with Robin boundary conditions. Motivated by this, the theoretical framework of this dissertation focuses on developing and analyzing parameter-uniform numerical methods for solving singularly perturbed parabolic differential equations of the reaction-diffusion and convection-diffusion types with Robin boundary conditions.

1.5 Research Design and Mathematical Procedures

1.5.1 Study Design

An extensive documentary review of advanced, up-to-date, relevant sources and supplementary papers related to the problem under investigation is used in this dissertation. Detailed derivations of the numerical methods have been done, and further valid numerical experiments are also being carried out using MATLAB software.

1.5.2 General Mathematical Procedures

The mathematical procedures are used to design the framework of this dissertation. To achieve the stated objectives, this dissertation followed the following mathematical procedures.

- Defining the differential equations.
- Analyzing the properties of the continuous solution.
- Developing the numerical schemes.
- Establishing the stability and convergence analysis of the developed schemes.
- Writing the MATLAB codes for the schemes.
- Validating the schemes using numerical examples or numerical experimentation.
- Presenting the numerical results using tables and graphs.
- Discussing the results against the existing methods and providing conclusions.

1.5.3 Preliminaries and Definitions

This subsection introduces some essential definitions and notations used in this dissertation. To begin with, we denote the space and time domain as $\Omega = (0, 1) \times (0, T]$. The notations Ω and $\bar{\Omega}$ are domain and closed domain, respectively. We used $C^{(i,j)}(\Omega)$ to represents the space of all continuous derivatives up to the orders i in space direction and j in time direction, where i, j are positive integers.

For analysis, we use standard supermum norm, which is denoted by $\|.\|_\infty$ and is defined by $\|g\|= \max|g(x, t)|$, and in discrete case $\|g\|= \max\limits_{(x_i,t_j)\in\Omega}|g(x_i, t_j)|$. Through out this dissertation C denotes a generic positive constant independent of ε, the meshes (x_i, t_j) and the step sizes $h_i, \Delta t$. Note that C may take different values in different places.

Let Ω_x^N the discrete version of Ω_x be an arbitrary mesh in space direction and Ω_t^M the discrete version of Ω_t be an arbitrary mesh in time direction. Consider the arbitrary meshes in the space direction as $\Omega_x^N = \{0 = x_0 < x_1 < \cdots , x_N = 1\}$ and in the time direction $\Omega_t^M = \{0 = t_0 < t_1 < \cdots , t_M = T\}$. We define the standard finite difference operators which are useful for describing the difference schemes in the subsequent chapters.

For a given discrete mesh function $z(x_i, t_j) = z_i^j$, define the forward, backward and central difference operators D_x^+, D_x^- and D_x^0 in space direction by

$$D_x^+ z_i^j = \frac{z_{i+1}^j - z_i^j}{h_{i+1}}, \quad D_x^- z_i^j = \frac{z_i^j - z_{i-1}^j}{h_i}, \quad D_x^0 z_i^j = \frac{z_{i+1}^j - z_{i-1}^j}{h_{i+1} + h_i},$$

respectively, and we define the second-order central difference operator δ_x^2 by

$$\delta_x^2 z_i^j = \frac{2(D_x^+ z_i^j - D_x^- z_i^j)}{h_i + h_{i+1}},$$

and define the backward difference operator δ_t^- in time direction by

$$D_t^- z_i^j = \frac{z_i^j - z_i^{j-1}}{\Delta t}.$$

The following is the definition of an M-matrix which is used the dissertation.

Definition 1.1. *[106] A matrix A is said to be an M-matrix if its entries $a_{i,j}$ such that $a_{i,j} \leq 0$ for $i \neq j$ and its inverse A^{-1} exists with $A^{-1} \geq 0$.*

Definition 1.2. *[15] A numerical method is said to be* **stable** *if the errors at any stage of the computation do not grow in the course of the computational processes.*

Definition 1.3. *[15] A numerical scheme is* **consistent** *if the method of approximating differential equations becomes exact as the step sizes tend to zero. For a method to be consistent, the truncation error should vanish as the step size approaches zero.*

Definition 1.4. *[15] A numerical method is said to be* **convergent** *if the solution of the numerical method approaches the exact solution of the original differential equation in the course of the computation. A stable and consistent process of discretization leads to convergence of the solution.*

We shall frequently use the maximum norm for our error analysis. The $\varepsilon-$uniform convergence of the proposed numerical methods is defined as follows:

Definition 1.5. *[106]* **($\varepsilon-$uniform convergence)**
Consider P a family of singularly perturbed parabolic PDEs parametrized by a singular perturbation parameter $\varepsilon(0<\varepsilon\ll 1)$. Assume that each problem in P has exact solution denoted by u and that each u is approximated by sequence of numerical solutions $\{(U^N,\bar{\Omega}^{N,\Delta t})\}$ obtained by using a numerical method $P^{N,\Delta t}$ where U^N is defined on the mesh $\bar{\Omega}^{N,\Delta t}$ and; N and Δt are discretization parameters. Then, U^N is said to converge $\varepsilon-$uniformly to the exact solution u, if there exists positive integers N_0, M_0 and positive numbers C, p and q, such that for all $N\geq N_0$ and $M\geq M_0$, where $M=T/\Delta t$, for N_0, M_0, C, p and q are all independent of ε, we have

$$\sup_{0<\varepsilon\leq 1}\|U^N-u\|_\infty\leq C\big(N^{-q}+(\Delta t)^p\big),$$

where q and p are the $\varepsilon-$uniform order of convergence of the space and time directions respectively, and C is the $\varepsilon-$uniform error constant.

1.5.4 Governing Differential Equations

The following four governing differential equations are considered. These governing equations are categorized into convection-diffusion and reaction-diffusion type equations.
Governing Equation-I: Consider the following singularly perturbed parabolic convection-diffusion equation with non-turning point [53] on the domain $(x,t)\in\Omega=(0,1)\times(0,T]$

$$\mathcal{L}_\varepsilon u(x,t)\equiv\varepsilon\frac{\partial^2 u(x,t)}{\partial x^2}+a(x)\frac{\partial u(x,t)}{\partial x}-b(x)u(x,t)-\frac{\partial u(x,t)}{\partial t}=f(x,t),$$

with initial condition and Robin boundary conditions

$$\begin{aligned} u(x,0)&=s(x), && 0\leq x\leq 1,\\ B_{L,\varepsilon}u(0,t)&\equiv u(0,t)-\varepsilon\frac{\partial u(0,t)}{\partial x}=q_0(t), && 0<t\leq T,\\ B_{R,\varepsilon}u(1,t)&\equiv u(1,t)+\varepsilon\frac{\partial u(1,t)}{\partial x}=q_1(t), && 0<t\leq T,\end{aligned}$$

where $0 < \varepsilon \ll 1$ is perturbation parameter and $a(x) \geq \alpha > 0,\ b(x) \geq 0,\ x \in [0,1]$.

Governing Equation-II: The following singularly perturbed parabolic convection-diffusion equation having a boundary turning point from [56] is considered on the domain $(x,t) \in \Omega = (0,1) \times (0,T]$

$$\mathcal{L}_\varepsilon u(x,t) \equiv \varepsilon \frac{\partial^2 u(x,t)}{\partial x^2} + a(x,t)\frac{\partial u(x,t)}{\partial x} - \frac{\partial u(x,t)}{\partial t} - b(x,t)u(x,t) = f(x,t),$$

with initial condition and Robin boundary conditions

$$\begin{aligned}
u(x,0) &= \phi_B(x), && 0 \leq x \leq 1,\\
B_{L,\varepsilon}u(0,t) \equiv u(0,t) - \sqrt{\varepsilon}\frac{\partial u(0,t)}{\partial x} &= \phi_L(t), && 0 < t \leq T,\\
B_{R,\varepsilon}u(1,t) \equiv u(1,t) + \sqrt{\varepsilon}\frac{\partial u(1,t)}{\partial x} &= \phi_R(t), && 0 < t \leq T,
\end{aligned}$$

where $0 < \varepsilon \ll 1$ is perturbation parameter and $a(x,t) = a_0(x,t)x^p,\ p \geq 1,\ \forall (x,t) \in \bar{\Omega},\ a_0(x,t) \geq \alpha > 0,\ b(x,t) \geq \beta > 0,\ (x,t) \in \bar{\Omega}$.

Governing Equation-III: From [108], the following singularly perturbed parabolic reaction-diffusion time delay equation is considered on the domain $(x,t) \in \Omega = (0,1) \times (0,T]$

$$\mathcal{L}_\varepsilon u(x,t) \equiv \frac{\partial u(x,t)}{\partial t} - \varepsilon \frac{\partial^2 u(x,t)}{\partial x^2} + a(x,t)u(x,t) = -b(x,t)u(x,t-\tau) + f(x,t),$$

with initial condition and Robin boundary conditions

$$\begin{aligned}
u(x,t) &= \phi_B(x,t), && (x,t) \in [0,1] \times [-\tau, 0],\\
B_{L,\varepsilon}u(0,t) \equiv u(0,t) - \sqrt{\varepsilon}\frac{\partial u(0,t)}{\partial x} &= \phi_L(t), && 0 < t \leq T,\\
B_{R,\varepsilon}u(1,t) \equiv u(1,t) + \sqrt{\varepsilon}\frac{\partial u(1,t)}{\partial x} &= \phi_R(t), && 0 < t \leq T,
\end{aligned}$$

where $0 < \varepsilon \ll 1$ is perturbation parameter, $\tau > 0$ is a delay parameter and $a(x,t) \geq \alpha > 0,\ b(x,t) \geq \beta > 0,\ (x,t) \in \bar{\Omega}$.

Governing Equation-IV: The following singularly perturbed parabolic reaction-diffusion equation without delay is considered [68] on the domain $(x,t) \in \Omega = (0,1) \times (0,T]$

$$\mathcal{L}_\varepsilon u(x,t) \equiv \frac{\partial u(x,t)}{\partial t} - \varepsilon \frac{\partial^2 u(x,t)}{\partial x^2} + a(x,t)u(x,t) = f(x,t),$$

with initial condition and Robin boundary conditions

$$\begin{aligned} u(x,0) &= \phi_B(x), && 0 \le x \le 1, \\ B_{L,\varepsilon} u(0,t) \equiv u(0,t) - \sqrt{\varepsilon}\frac{\partial u(0,t)}{\partial x} &= \phi_L(t), && 0 < t \le T, \\ B_{R,\varepsilon} u(1,t) \equiv u(1,t) + \sqrt{\varepsilon}\frac{\partial u(1,t)}{\partial x} &= \phi_R(t), && 0 < t \le T, \end{aligned}$$

where $0 < \varepsilon \ll 1$ is perturbation parameter and $a(x,t) \ge \alpha > 0,\ (x,t) \in \bar{\Omega}$.

1.6 Organization of the Dissertation

This dissertation consists of seven chapters as outlined in the following manner. It is divided into three main parts.

Firstly, the historical background of the study, objectives of the study, significance of the study, theoretical framework, research design and general mathematical procedures are presented in **Chapter 1**.

Secondly, the main works of this dissertation are outlined from **Chapter 2** up to **Chapter 6**. In the main works, we derived fitted mesh parameter-uniform numerical methods using Shishkin mesh, Bakhvalov-Shishkin and Vulanović-Shishkin meshes.

Finally, a brief summary of the findings, conclusions and recommendations and the scope for further investigations are presented in **Chapter 7**.

Chapter 2

Layer-adapted Upwind Finite Difference Method for Singularly Perturbed Parabolic Convection-diffusion Problems

This chapter deals with an upwind finite difference method on layer-adapted meshes to solve singularly perturbed parabolic convection-diffusion problems with Robin boundary conditions. To discretize the problem, an upwind method in the space direction on layer-adapted Shishkin and Bakhvalov-Shishkin meshes and a backward Euler method in the time direction on uniform meshes are used. The parameter-uniform convergence analysis is well established. To show how the present method can be applied, two examples are taken into account for numerical experimentation. In terms of accuracy, the numerical findings show that the Bakhvalov-Shishkin mesh outperforms the Shishkin mesh. The use of Bakhvalov-Shishkin has an advantage over the Shishkin mesh at the same computational cost because the Bakhvalov-Shishkin mesh is not affected by the logarithmic factor.

2.1 Introduction

Singularly perturbed parabolic convection-diffusion problem with Dirichlet boundary condition which are under consideration are studied by authors in [14], [21], [52], [54], [95] and [117]. A few scholars, for instance, [53] and [80] studied singularly perturbed parabolic problems with Robin boundary conditions. The area of singularly perturbed problems with Robin boundary conditions has received little attention due to difficulties in discretization and analysis of the Robin boundary conditions. This indicates that the area has not been thoroughly researched. Hence, the main aim of this chapter is to develop a parameter-uniformly convergent numerical method for singularly perturbed parabolic convection-diffusion problem with Robin boundary conditions. The present method is simple to apply and provides improved solutions using the Bakhvalov-Shishkin mesh, whereas previous researchers used Shishkin mesh [53] and uniform mesh [80].

2.2 Definition of the Problem

On the domain $\Omega = \Omega_x \times \Omega_t$, where $\Omega_x = (0,1)$, $\Omega_t = (0,T]$, the following singularly perturbed parabolic convection-diffusion problem with non-turning point is considered

$$\mathcal{L}_\varepsilon u(x,t) \equiv \varepsilon \frac{\partial^2 u(x,t)}{\partial x^2} + a(x)\frac{\partial u(x,t)}{\partial x} - b(x)u(x,t) - \frac{\partial u(x,t)}{\partial t} = f(x,t), \quad (x,t) \in \Omega, \quad (2.1)$$

subject to the initial and boundary conditions

$$\begin{cases} u(x,0) = s(x), & 0 \le x \le 1, \\ B_{L,\varepsilon} u(0,t) \equiv u(0,t) - \varepsilon \frac{\partial u(0,t)}{\partial x} = q_0(t), & 0 < t \le T, \\ B_{R,\varepsilon} u(1,t) \equiv u(1,t) + \varepsilon \frac{\partial u(1,t)}{\partial x} = q_1(t), & 0 < t \le T, \end{cases} \quad (2.2)$$

where $0 < \varepsilon \ll 1$ is perturbation parameter. The functions $a(x)$, $b(x)$ and $f(x,t), \forall (x,t) \in \Omega$ in Eq. (2.1); and the initial-boundary functions $s(x)$, $x \in [0,1]$, $q_0(t)$, $q_1(t)$, $t \in (0,T]$

in Eq. (2.2) are sufficiently smooth and bounded functions satisfying the conditions $a(x) \geq \alpha > 0,\ b(x) \geq 0,\ x \in \bar{\Omega}_x$. Under these conditions, the problem in Eqs. (2.1) and (2.2) has a unique solution. Further, assume that the initial function $s^{(k)}(x) = 0,\ \forall k \geq 1$. As the perturbation parameter ε tends to zero, the solution of the problem in Eqs. (2.1) and (2.2) exhibits a boundary layer in the neighbourhood of the left side of the lateral boundary. The presence of ε multiplying the derivative terms in the Robin boundary conditions amplifies the significance of the boundary layer. In the absence of ε, the layer is sufficiently weak for Robin type problems [2]. We assume the data of Eq. (2.1) satisfies an appropriate compatibility conditions of order k, where $k = 0,\ 1,\ 2$ at the points $(0,0)$ and $(1,0)$, see [72]. The k^{th} order compatibility condition for the initial function are given by

$$\begin{aligned}
\frac{\partial^k}{\partial t^k}\left(s - \varepsilon\frac{\partial s}{\partial x}\right)(0) &= \frac{d^k q_0(0)}{\partial t^k},\\
\frac{\partial^k}{\partial t^k}\left(s + \varepsilon\frac{\partial s}{\partial x}\right)(1) &= \frac{d^k q_0(0)}{\partial t^k},\\
-\frac{\partial q_0(0)}{\partial t} + \varepsilon\frac{\partial^2 s(0)}{\partial x^2} + a(0)\frac{\partial s(0)}{\partial x} - b(0)s(0) &= f(0,0),\\
-\frac{\partial q_1(0)}{\partial t} + \varepsilon\frac{\partial^2 s(1)}{\partial x^2} + a(1)\frac{\partial s(1)}{\partial x} - b(1)s(1) &= f(1,0).
\end{aligned}$$

2.3 Properties of the Continuous Solution

The analytical aspects of singularly perturbed problems play an important role in the study of numerical analysis. Setting the value $\varepsilon = 0$, the reduced problem is

$$\begin{cases}
a(x)\frac{\partial u_0(x,t)}{\partial x} - b(x)u_0(x,t) - \frac{\partial u_0(x,t)}{\partial t} = f(x,t), & (x,t) \in \Omega,\\
u_0(x,0) = s(x), & 0 \leq x \leq 1,\\
u_0(1,t) = q_1(t), & 0 < t \leq T.
\end{cases} \tag{2.3}$$

The reduced problem in Eq. (2.3) do not make use of the left boundary condition. As a result, the solution of this problem exhibits the boundary layer in a neighborhood of the boundary $x = 0$ with the width of $O(\varepsilon)$ when $\varepsilon \to 0$. The basic ideas presented in [32] and [100] together with the assumptions given in Eq. (2.1)-(2.2) leads to the following continuous minimum principle.

Lemma 2.3.1. *Assume that $\Upsilon(x,t)$ be a sufficiently smooth function such that $\Upsilon(x,t) \geq 0$ for $(x,t) \in \partial B^0$, where $\{(x,t) : 0 \leq x \leq 1, t = 0\}$, $B_{L,\varepsilon}\Upsilon(0,t) \geq 0$, $B_{R,\varepsilon}\Upsilon(1,t) \geq 0$ for $t \in [0,T]$, and $\mathcal{L}_\varepsilon\Upsilon(x,t) < 0$, $\forall(x,t) \in \Omega$. Then, $\Upsilon(x,t) > 0$, $\forall(x,t) \in \bar{\Omega}$.*

Proof. Suppose that the arbitrary function Υ takes its minimum value at the point $(x^*,t^*) \in \bar{\Omega}$ such that $\Upsilon(x^*,t^*) = \min_{(x,t)\in\bar{\Omega}} \Upsilon(x,t)$ and assume that $\Upsilon(x^*,t^*) < 0$. Clearly, $(x^*,t^*) \notin \partial B^0$.
For $(x^*,t^*) \in \Omega$, we have $\frac{\partial \Upsilon}{\partial t}(x^*,t^*) = 0$, $\frac{\partial \Upsilon}{\partial x}(x^*,t^*) = 0$ and $\frac{\partial^2 \Upsilon}{\partial x^2}(x^*,t^*) \geq 0$.
Consider $(x^*,t^*) \in \{0\}\times[0,T]$. In this case, we have $x^* = 0$ and $\frac{\partial \Upsilon}{\partial x}(x^*,t^*) = \frac{\partial \Upsilon}{\partial x}(0,t^*) \geq 0$. Hence, $\Upsilon(x^*,t^*) - \varepsilon\dfrac{\partial \Upsilon}{\partial x}(x^*,t^*) < 0$, which is a contradiction.
Consider $(x^*,t^*) \in \{1\}\times[0,T]$. In this case, we have $x^* = 1$ and $\frac{\partial \Upsilon}{\partial x}(x^*,t^*) = \frac{\partial \Upsilon}{\partial x}(1,t^*) \leq 0$. Hence, $\Upsilon(x^*,t^*) + \varepsilon\dfrac{\partial \Upsilon}{\partial x}(x^*,t^*) < 0$, which is a contradiction. Now,

$$\mathcal{L}_\varepsilon\Upsilon(x^*,t^*) = \varepsilon\frac{\partial^2 \Upsilon}{\partial x^2}(x^*,t^*) + a(x^*)\frac{\partial \Upsilon}{\partial x}(x^*,t^*) - b(x^*)\Upsilon(x^*,t^*) - \frac{\partial \Upsilon}{\partial t}(x^*,t^*) > 0,$$

which is a contradiction. It follows that $\Upsilon(x,t) > 0$, $\forall(x,t) \in \bar{\Omega}$. □

To show the bounds for the solution $u(x,t)$, we assume, without loss of generality $s(x) = 0$. The next lemma proves the stability estimate to obtain unique solution for Eq. (2.1)-(2.2).

Lemma 2.3.2. *The solution $u(x,t)$ of Eq. (2.1)-(2.2) satisfies the bound*

$$|u(x,t)| \leq \max\left\{|s(x)|, |q_0(t)|, |q_1(t)|\right\} + \frac{\|f\|}{\alpha}, \quad \textit{where } \|f\| = \max_{(x,t)\in\bar{\Omega}} |f(x,t)|.$$

Proof. To prove this lemma, we define two smooth barrier functions as

$$\Theta^{\pm}(x,t) = \max\left\{|s(x)|, |q_0(t)|, |q_1(t)|\right\} + \frac{\|f\|}{\alpha} \pm u(x,t).$$

Now, we evaluate the barrier functions at the initial and boundary conditions.

At $t = 0$, we have

$$\Theta^{\pm}(x,0) = \max\left\{|s(x)|, |q_0(0)|, |q_1(0)|\right\} + \frac{\|f\|}{\alpha} \pm u(x,0) \geq 0.$$

At $x = 0$, we have

$$\Theta^{\pm}(0,t) = \max\left\{|s(0)|, |q_0(t)|, |q_1(t)|\right\} + \frac{\|f\|}{\alpha} \pm u(0,t). \tag{2.4}$$

From Eq. (2.4), we deduce the following

$$\begin{aligned} u(0,t) &= \pm\Theta^{\pm}(0,t) \mp \left[\max\left\{|s(0)|, |q_0(t)|, |q_1(t)|\right\} + \frac{\|f\|}{\alpha}\right], \\ \frac{\partial u(0,t)}{\partial x} &= \pm\frac{\partial \Theta^{\pm}(0,t)}{\partial x} \mp |s'(0)|. \end{aligned} \tag{2.5}$$

Using Eq. (2.5) in the left boundary condition and rearranging gives

$$\Theta^{\pm}(0,t) - \varepsilon\frac{\partial \Theta^{\pm}(0,t)}{\partial x} = \pm q_0(t) + \max\left\{|s(0)|, |q_0(t)|, |q_1(t)|\right\} + \frac{\|f\|}{\alpha} - \varepsilon|s'(0)| \geq 0,$$

since $s'(0) \geq 0$ and $\max\left\{|s(0)|, |q_0(t)|, |q_1(t)|\right\} + \frac{\|f\|}{\alpha} \pm q_0(t) \geq 0$.

At $x = 1$, we have

$$\Theta^{\pm}(1,t) = \max\left\{|s(1)|, |q_0(t)|, |q_1(t)|\right\} + \frac{\|f\|}{\alpha} \pm u(1,t). \tag{2.6}$$

From Eq. (2.6), we deduce the following

$$\begin{cases} u(1,t) = \pm\Theta^{\pm}(1,t) \mp \max\left\{|s(1)|, |q_0(t)|, |q_1(t)|\right\} + \frac{\|f\|}{\alpha}, \\ \frac{\partial u(1,t)}{\partial x} = \pm\frac{\partial \Theta^{\pm}(1,t)}{\partial x} \mp |s'(1)|. \end{cases} \tag{2.7}$$

Using Eq. (2.7) in the right boundary condition and rearranging gives

$$\Theta^{\pm}(1,t) + \varepsilon \frac{\partial \Theta^{\pm}(1,t)}{\partial x} = \pm q_1(t) + \max\big\{|s(1)|, |q_0(t)|, |q_1(t)|\big\} + \frac{\|f\|}{\alpha} + \varepsilon|s'(1)| \geq 0,$$

since $s'(1) \geq 0$ and $\max\big\{|s(1)|, |q_0(t)|, |q_1(t)|\big\} + \frac{\|f\|}{\alpha} \pm q_1(t) \geq 0$.

Now, on the domain Ω, we have

$$\begin{aligned}
\mathcal{L}_\varepsilon \Theta^{\pm}(x,t) &= \varepsilon \frac{\partial^2 \Theta^{\pm}(x,t)}{\partial x^2} + a(x)\frac{\partial \Theta^{\pm}(x,t)}{\partial x} - b(x)\Theta^{\pm}(x,t) - \frac{\partial \Theta^{\pm}(x,t)}{\partial t}, \\
&= \pm f(x,t) + \varepsilon|s''(x)| + a(x)|s'(x)| - \max\{q_0'(t),\ q_1'(t)\} \\
&- b(x) \times \Big(\max\big\{|s(x)|, |q_0(t)|, |q_1(t)|\big\} + \frac{\|f\|}{\alpha}\Big), \\
&= \pm f(x,t) - b(x)\frac{\|f\|}{\alpha} - b(x) \times \max\big\{|s(x)|, |q_0(t)|, |q_1(t)|\big\} \\
&+ \varepsilon|s''(x)| + a(x)|s'(x)| - \max\{q_0'(t),\ q_1'(t)\} \leq 0.
\end{aligned}$$

Using Lemma (2.3.1), it follows that $\Theta^{\pm}(x,t) \leq 0,\ \forall (x,t) \in \bar{\Omega}$. This implies that $|u(x,t)| \leq \max\big\{|s(x)|, |q_0(t)|, |q_1(t)|\big\} + \frac{\|f\|}{\alpha}$. □

The compatibility conditions imposed for the initial condition at the two corners $(0,0)$ and $(0,1)$ guarantee that there exist a constant C such that $\forall (x,t) \in \bar{\Omega}$

$$|u(x,t) - s(x)| \leq Ct, \tag{2.8a}$$

$$|u(x,t) - q_1(t)| \leq C(1-x). \tag{2.8b}$$

The following theorem establishes the bound on the solution and its derivatives.

Lemma 2.3.3. *Let $u(x,t)$ be the solution of Eq.* (2.1)-(2.2)*, then* $|u(x,t)| \leq C,\ (x,t) \in \bar{\Omega}$.

Proof. Without loss of generality, assume initial condition is zero. Equation (2.8a) yields

$$|u(x,t)| \leq Ct, \quad (x,t) \in \bar{\Omega}.$$

Since $t \in (0, T]$, we obtain

$$|u(x,t)| \leq C, \quad (x,t) \in \bar{\Omega},$$

as required. □

Remark 2.1. *To prove the following lemmas, we used* $\frac{\partial^2 u(x,t)}{\partial x^2} = u_{xx}$, $\frac{\partial^2 u(x,t)}{\partial t^2} = u_{tt}$, $\frac{\partial u(x,t)}{\partial x} = u_x$, $\frac{\partial u(x,t)}{\partial t} = u_t$, $\frac{\partial f(x,t)}{\partial x} = f_t$ *etc.*

We make the assertion that both the initial and the boundary conditions are zero.

Lemma 2.3.4. $|u_t(x,t)| \leq C, \quad (x,t) \in \Omega.$

Proof. At $x = 0$ and $x = 1$ of $\bar{\Omega}$, we have $u = 0$ and therefore $u_t = 0$. At $t = 0$, we have $u = 0,\ u_x = 0,\ u_{xx} = 0$, which from Eq. (2.1) yields

$$u_t(x,0) = -f(x,0), \quad 0 \leq x \leq 1.$$

On these three sides of $\bar{\Omega}$ and for C_1 sufficiently large, the following estimate holds

$$|u_t(x,t)| \leq C_1.$$

Differentiating Eq. (2.1) with respect to t and applying the differential operator on the resulting expression yields

$$\begin{aligned}
\mathcal{L}_\varepsilon u_t(x,t) &= \varepsilon u_{txx} + a(x)u_{tx} - b(x)u_t - u_{tt}, \\
&= \Big(\varepsilon u_{xx} + a(x)u_x - b(x)u - u_t\Big)_t, \\
&= f_t.
\end{aligned}$$

Using the fact that f is sufficiently smooth, we have

$$|\mathcal{L}_\varepsilon u_t(x,t)| \leq C_2,$$

for C_2 chosen to be sufficiently large. Since $\mathcal{L}_\varepsilon$ satisfies the minimum principle on $\bar{\Omega}$, we obtain the desired estimate

$$|u_t(x,t)| \le C, \quad \text{on } \bar{\Omega},$$

for $C_2 = C$. □

To prove the subsequent lemmas, we use the concepts established in Kellogg and Tsan [58].

Lemma 2.3.5. $|u_x(x,t)| \le C(1 + \varepsilon^{-1} e^{-\alpha x/\varepsilon}), \;\; (x,t) \in \bar{\Omega}.$

Proof. Eq. (2.1) can be written as

$$h_1(x,t) = \varepsilon u_{xx} + a(x) u_x,$$

where $h_1(x,t) = f(x,t) + u_t + b(x)u(x,t)$. Fixing $t \in (0,T]$ and multiplying both sides of the above equation by the integrating factor $e^{\varepsilon^{-1}A(x)}$, $A(x) = \int_0^x a(s)ds$ results in

$$\begin{aligned}
\varepsilon^{-1} e^{\varepsilon^{-1}A(x)} h_1(x,t) &= e^{\varepsilon^{-1}A(x)} u_{xx} + \varepsilon^{-1} a(x) e^{\varepsilon^{-1}A(x)} u_x, \\
\frac{d}{dx}\left(e^{\varepsilon^{-1}A(x)} \frac{du}{dx} \right) &= \varepsilon^{-1} e^{\varepsilon^{-1}A(x)} h_1(x,t).
\end{aligned}$$

Integrating the above expression from 0 to x gives

$$e^{\varepsilon^{-1}A(0)} u_x(0,t) - e^{\varepsilon^{-1}A(x)} u_x(x,t) = \varepsilon^{-1} \int_0^x h_1(s,t) e^{\varepsilon^{-1}A(s)} ds.$$

This is further simplified to

$$u_x(x,t) = u_x(0,t) e^{\varepsilon^{-1}(A(0)-A(x))} + k_1(x,t),$$

where $k_1(x,t)$ is given by

$$k_1(x,t) = \varepsilon^{-1} \int_0^x h_1(s,t) e^{\varepsilon^{-1}(A(s)-A(x))} ds.$$

Integrating the above equation from x to 1 to derive the bound of $u_x(0,t)$ results in

$$u(x,t) = u(1,t) + u_x(0,t)\int_x^1 e^{\varepsilon^{-1}(A(0)-A(s))}ds + \int_x^1 k_1(s,t)ds.$$

At $x = 0$, it becomes

$$u_x(0,t) = -\frac{\int_0^1 k_1(s,t)ds}{\int_0^1 e^{\varepsilon^{-1}(A(0)-A(s))}ds},$$

since by assumptions $u(0,t) = u(1,t) = 0$. Substitution gives

$$u_x(x,t) = -\frac{e^{\varepsilon^{-1}(A(0)-A(x))}}{\int_0^1 e^{\varepsilon^{-1}(A(0)-A(s))}ds}\int_0^1 k_1(s,t)ds + k_1(x,t),$$

Now taking the norm on both sides yields

$$\begin{aligned}
|u_x(x,t)| &\leq \frac{|e^{\varepsilon^{-1}(A(0)-A(x))}|}{|\int_0^1 e^{\varepsilon^{-1}(A(0)-A(s))}ds|}\left|\int_0^1 k_1(s,t)ds\right| + |k_1(x,t)|,\\
&\leq \frac{|e^{\varepsilon^{-1}A(0)}||e^{-\varepsilon^{-1}A(x)}|}{|e^{\varepsilon^{-1}A(0)}||\int_0^1 e^{-\varepsilon^{-1}A(s)}ds|}\left|\int_0^1 k_1(s,t)ds\right| + |k_1(x,t)|\\
&= \frac{|e^{-\varepsilon^{-1}A(x)}|}{|\int_0^1 e^{-\varepsilon^{-1}A(s)}ds|}\left|\int_0^1 k_1(s,t)ds\right| + |k_1(x,t)|\\
&\leq \tilde{C}\left(1 + \frac{e^{-\varepsilon^{-1}\alpha x}}{\int_0^1 e^{-\varepsilon^{-1}\tilde{\alpha}}ds}\right), \quad \text{since } a(x) \geq \alpha, A(x) = \int_0^x \alpha ds = \alpha x,
\end{aligned}$$

where $\tilde{\alpha}$ is an upper bound of $A(x)$ over $[0,1]$ and $\tilde{C}$ is also an upper bound of $k_1(x,t)$ over $\bar{\Omega}$. Simplifying $\int_0^1 e^{-\varepsilon^{-1}\tilde{\alpha}}ds$ gives $\frac{\varepsilon^{-1}\tilde{\alpha}e^{-\alpha x\varepsilon^{-1}}}{1-e^{-\tilde{\alpha}\varepsilon^{-1}}}$. Using this results in

$$|u_x(x,t)| \leq \tilde{C}\left(1 + \frac{\varepsilon^{-1}\tilde{\alpha}e^{-\alpha x\varepsilon^{-1}}}{(1-e^{-\tilde{\alpha}\varepsilon^{-1}})}\right).$$

Now, from Maclaurin series we have $\tilde{\alpha} \leq (1-e^{-\tilde{\alpha}\varepsilon^{-1}})$, so that the above estimate reduces to

$$|u_x(x,t)| \leq C\big(1 + \varepsilon^{-1}e^{-\alpha x/\varepsilon}\big).$$

which is the desired result. □

Lemma 2.3.6. $|u_{tt}(x,t)| \le C, \quad (x,t) \in \Omega.$

Proof. On the sides $x = 0$ and $x = 1$ of $\bar{\Omega}$, we have $u = 0$ and therefore $u_{tt} = 0$. On the side $t = 0$, we have $u = 0,\ u_x = 0,\ u_{xx} = 0$, which from Eq. (2.1) yields

$$u_t(x,0) = -f(x,0),\ u_{tx}(x,0) = -f_x(x,0),\ u_{txx}(x,0) = -f_{xx}(x,0),\ 0 \le x \le 1.$$

This implies

$$|u_{tx}(x,t)| \le C \ \text{ and } \ |u_{txx}(x,t)| \le C_1 \tag{2.9}$$

on the side $t = 0$. Differentiating Eq. (2.1) with respect to t yields

$$u_{tt} = \varepsilon u_{txx} + a(x)u_{tx} - b(x)u_t - f_t$$

Using the estimates given by Eq. (2.9) and Lemma (2.3.4), we have

$$|u_{tt}(x,t)| \le C_2 \quad \text{on boundary sides} \quad x = 1 \text{and} \ \ t = 0.$$

Twice differentiating Eq. (2.1) with respect to t and applying the differential operator on the resulting expression yields

$$\begin{aligned} \mathcal{L}_\varepsilon u_{tt} &= \varepsilon u_{ttxx} + a u_{ttx} - b(x)u_{tt} - u_{ttt}, \\ &= \big(\varepsilon u_{xx} + a u_x - b(x)u - u_t\big)_{tt}, \\ &= f_{tt}. \end{aligned}$$

Since f_{tt} is bounded function, we have

$$|\mathcal{L}_\varepsilon u_{tt}| \le C.$$

Since the operator $\mathcal{L}_\varepsilon$ satisfies the minimum principle, we obtain the desired estimate

$$|u_{tt}(x,t)| \le C, \quad \text{on } \bar{\Omega},$$

as required. □

Lemma 2.3.7. $|u_{xt}(x,t)| \le C(1+\varepsilon^{-1}e^{-\alpha x/\varepsilon}), \ \ (x,t) \in \bar{\Omega}.$

Proof. Differentiating Eq. (2.1) with respect to t, we get

$$\varepsilon(u_{xt})_x + a(x)u_{xt} - b(x)u_t - u_{tt} = f_t. \tag{2.10}$$

Rewriting the above equation in the form

$$\varepsilon(u_{xt})_x + a(x)u_{xt} = h_2(x,t),$$

where $h_2(x,t) = f_t + u_{tt} + b(x)u_t$. Fixing $t \in (0,T]$ and multiplying both sides of the above equation by the integrating factor $e^{\varepsilon^{-1}A(x)}$, $A(x) = \int_0^x a(\eta)d\eta$ results in

$$\begin{aligned}
&\varepsilon^{-1}e^{-\varepsilon^{-1}A(x)}h_2(x,t) = e^{\varepsilon^{-1}A(x)}u_{xx} + \varepsilon^{-1}a(x)e^{-\varepsilon^{-1}A(x)}u_x,\\
&\frac{d}{dx}\left(e^{\varepsilon^{-1}A(x)}\frac{du_t}{dx}\right) = \varepsilon^{-1}e^{\varepsilon^{-1}A(x)}h_2(x,t).
\end{aligned}$$

Integrating the above expression from 0 to x gives

$$e^{\varepsilon^{-1}A(0)}u_{tx}(0,t) - e^{\varepsilon^{-1}A(x)}u_{xt}(x,t) = \varepsilon^{-1}\int_0^x h_2(\eta,t)e^{\varepsilon^{-1}A(s)}d\eta,$$

which can further be simplified to

$$u_{tx}(x,t) = u_{xt}(0,t)e^{\varepsilon^{-1}(A(0)-A(x))} + k_2(x,t),$$

where $k_2(x,t)$ is given by

$$k_2(x,t) = \varepsilon^{-1} \int_0^x h_2(\eta,t) e^{\varepsilon^{-1}(A(\eta)-A(x))} d\eta.$$

Integrating the above equation from x to 1 to derive the bound of $u_{tx}(0,t)$ gives

$$u_t(x,t) = u_t(1,t) + u_{tx}(0,t) \int_x^1 e^{\varepsilon^{-1}(A(0)-A(s))} ds + \int_x^1 k_2(s,t) ds.$$

Evaluating this equation at $x = 0$ gives

$$u_{xt}(0,t) = -\frac{\int_0^1 k_2(\eta,t) d\eta}{\int_0^1 e^{\varepsilon^{-1}(A(0)-A(\eta))} d\eta},$$

using assumptions $u_t(0,t) = u_t(1,t) = 0$. Substitution yields

$$u_{xt}(x,t) = -\frac{e^{\varepsilon^{-1}(A(0)-A(x))}}{\int_0^1 e^{\varepsilon^{-1}(A(0)-A(\eta))} d\eta} \int_0^1 k_2(\eta,t) d\eta + k_2(x,t),$$

Taking the norm on both sides yields

$$\begin{aligned}
|u_{xt}(x,t)| &\leq \frac{|e^{\varepsilon^{-1}(A(0)-A(x))}|}{|\int_0^1 e^{\varepsilon^{-1}(A(0)-A(\eta))} d\eta|} \left| \int_0^1 k_2(\eta,t) d\eta \right| + |k_2(x,t)|, \\
&\leq \frac{|e^{\varepsilon^{-1}A(0)}||e^{-\varepsilon^{-1}A(x)}|}{|e^{\varepsilon^{-1}A(0)}|| \int_0^1 e^{-\varepsilon^{-1}A(\eta)} d\eta|} \left| \int_0^1 k_2(\eta,t) d\eta \right| + |k_2(x,t)| \\
&= \frac{|e^{-\varepsilon^{-1}A(x)}|}{| \int_0^1 e^{-\varepsilon^{-1}A(\eta)} d\eta|} \left| \int_0^1 k_2(\eta,t) d\eta \right| + |k_2(x,t)| \\
&\leq \tilde{C}\left(1 + \frac{e^{-\varepsilon^{-1}\alpha x}}{\int_0^1 e^{-\varepsilon^{-1}\tilde{\alpha}} d\eta}\right), \quad \text{since } a(x) \geq \alpha, A(x) = \int_0^x \alpha d\eta = \alpha x,
\end{aligned}$$

where $\tilde{\alpha}$ is an upper bound of $A(x)$ over $[0,1]$ and $\tilde{C}$ is also an upper bound of $k_2(x,t)$ over $\bar{\Omega}$. Simplifying $\int_0^1 e^{-\varepsilon^{-1}\tilde{\alpha}} d\eta$ gives $\frac{\varepsilon^{-1}\tilde{\alpha} e^{-\alpha x \varepsilon^{-1}}}{1-e^{-\tilde{\alpha}\varepsilon^{-1}}}$. Using this results in

$$|u_{xt}(x,t)| \leq \tilde{C}\left(1 + \frac{\varepsilon^{-1}\tilde{\alpha} e^{-\alpha x \varepsilon^{-1}}}{(1 - e^{-\tilde{\alpha}\varepsilon^{-1}})}\right).$$

Applying the argument used in the proof of Lemma (2.3.7) yields the estimate

$$|u_{xt}(x,t)| \leq C\big(1 + \varepsilon^{-1} e^{-\alpha x/\varepsilon}\big),$$

which is the desired result. □

Lemma 2.3.8. $|u_{xx}(x,t)| \leq C(1 + \varepsilon^{-2} e^{-\alpha x/\varepsilon}), \;\; (x,t) \in \bar{\Omega}.$

Proof. Differentiating Eq. (2.1) with respect to x, we get

$$\varepsilon(u_{xx})_x + a'(x)u_x + a(x)u_{xx} - b'(x)u - b(x)u_x - u_{tx} = f_x \;\text{ on }\; \bar{\Omega}. \tag{2.11}$$

Equation (2.11) can be rewritten as

$$\varepsilon(u_{xx})_x + a(x)u_{xx} = h_3(x,t) \;\text{ on }\; \bar{\Omega},$$

where

$$h_3(x,t) = f_x - a'(x)u_x + b'(x)u + b(x)u_x + u_{tx}.$$

Using Lemmas (2.3.3), (2.3.5) and (2.3.7), we have

$$|h_3(x,t)| \leq C_4 \varepsilon^{-1}.$$

Fixing $t \in (0,T]$ and multiplying both sides of the above equation by the integrating factor gives

$$u_{xx}(x,t) = u_{xx}(0,t) e^{\varepsilon^{-1}(A(0)-A(x))} + k_3(x,t), \tag{2.12}$$

where $k_3(x,t)$ is given by

$$k_3(x,t) = \varepsilon^{-1} \int_0^x h_3(\gamma,t) e^{\varepsilon^{-1}(A(\gamma)-A(x))} d\gamma.$$

Integrating the Eq. (2.12) from x to 1 gives

$$u_x(1,t) - u_x(1,t) = u_{xx}(0,t)\int_x^1 e^{\varepsilon^{-1}(A(0)-A(\gamma))}d\gamma + \int_x^1 k_3(\gamma,t)d\gamma.$$

Evaluating this equation at $x = 0$ gives

$$u_{xx}(0,t) = \frac{-\int_0^1 k_3(\gamma,t)d\gamma}{\int_0^1 e^{\varepsilon^{-1}(A(0)-A(\gamma))}d\gamma},$$

using assumptions $u_x(0,t) = u_x(1,t) = 0$. Substituting the above results in Eq. (2.12) yield

$$u_{xx}(x,t) = -\frac{e^{\varepsilon^{-1}(A(0)-A(x))}}{\int_0^1 e^{\varepsilon^{-1}(A(0)-A(\gamma))}d\gamma}\int_0^1 k_3(\gamma,t)d\gamma + k_3(x,t),$$

Applying the norm on both sides yields

$$|u_{xx}(x,t)| \leq \varepsilon^{-1}e^{-\alpha x/\varepsilon}\int_0^1 k_3(\gamma,t)d\gamma + k_3(x,t),$$

by similar argument used in the proof of Lemma (2.3.5). Moreover, notice that $z_3(x,t)$ depends on $|h_3(x,t)| \leq C_4\varepsilon^{-1}$, thus we have that

$$|u_{xx}(x,t)| \leq C_4\varepsilon^{-2}e^{-\alpha x/\varepsilon} + C_4\varepsilon^{-1},$$

which reduces to

$$|u_{xx}(x,t)| \leq C_4\big(1 + \varepsilon^{-2}e^{-\alpha x/\varepsilon}\big),$$

since $0 < \varepsilon \ll 1$ and this completes the proof. □

The following theorem summarizes the higher bound on the solution and its derivatives.

Theorem 2.1. *The solution $u(x,t)$ and its partial derivatives satisfy the bound*

$$\left\|\frac{\partial^{l+m}u}{\partial x^l \partial t^m}\right\| \leq C(1 + \varepsilon^{-l}e^{-\alpha x/\varepsilon}), \quad (x,t) \in \bar{\Omega},$$

where l and m are non-negative integers such that $0 \leq l \leq 1,\ 0 \leq l+m \leq 4$.

Proof. The proof follows from Lemmas (2.3.3)-(2.3.8) for the integers $0 \leq l+m \leq 2$ and analogously the higher order derivatives up to the fourth order can be obtained. □

The above classical bounds on the derivatives of the solution are not adequate for the proof of parameter-uniform error estimate. To obtain the stronger bounds on the derivatives of the solution $u(x,t)$ of Eq. (2.1)-(2.2), we seek to express the solution $u(x,t)$ as the sum $v(x,t)+w(x,t)$, where $v(x,t)$ is the regular component and $w(x,t)$ is the singular component. The regular component $v(x,t)$ is further be decomposed into

$$v(x,t) = v_0(x,t) + \varepsilon v_1(x,t) + \varepsilon^2 v_2(x,t), \tag{2.13}$$

where $v_0(x,t)$ satisfies the solution of reduced first-order problem

$$\begin{cases} a(x)\frac{\partial v_0(x,t)}{\partial x} - b(x)v_0(x,t) - \frac{\partial v_0(x,t)}{\partial t} = f(x,t), & (x,t) \in \Omega, \\ B_{R,\varepsilon} v_0(1,t) = q_1(t), & 0 < t \leq T, \\ v_0(x,0) = s(x), & 0 \leq x \leq 1, \end{cases} \tag{2.14}$$

and $v_1(x,t)$ is solution of the following first-order problem

$$\begin{cases} a(x)\frac{\partial v_1(x,t)}{\partial x} - b(x)v_1(x,t) - \frac{\partial v_1}{\partial t} = -\frac{\partial^2 v_0(x,t)}{\partial x^2}, & (x,t) \in \Omega, \\ B_{L,\varepsilon} v_1(0,t) = 0, & 0 < t \leq T, \\ B_{R,\varepsilon} v_1(1,t) = 0, & 0 < t \leq T, \\ v_1(x,0) = 0, & 0 \leq x \leq 1, \end{cases} \tag{2.15}$$

and $v_2(x,t)$ satisfies the following second-order problem

$$\begin{cases} \mathcal{L}_\varepsilon v_2(x,t) = -\frac{\partial^2 v_1(x,t)}{\partial x^2}, & (x,t)\in\Omega, \\ B_{L,\varepsilon} v_2(0,t) = 0, & 0<t\le T, \\ B_{R,\varepsilon} v_2(1,t) = 0, & 0<t\le T, \\ v_2(x,0) = 0, & 0\le x\le 1. \end{cases} \tag{2.16}$$

The regular component $v(x,t)$ is the solution to the following non-homogeneous problem

$$\begin{cases} \mathcal{L}_\varepsilon v(x,t) = f(x,t), & (x,t)\in\Omega, \\ B_{L,\varepsilon} v(0,t) = B_{L,\varepsilon} v_0(0,t), & 0<t\le T, \\ B_{R,\varepsilon} v(1,t) = B_{R,\varepsilon} v_0(1,t), & 0<t\le T, \\ v(x,0) = s(x), & 0\le x\le 1. \end{cases} \tag{2.17}$$

With $v(x,t)$ defined, $w(x,t)$ is the solution of the homogeneous problem

$$\begin{cases} \mathcal{L}_\varepsilon w(x,t) = 0, & (x,t)\in\Omega, \\ B_{L,\varepsilon} w(0,t) = q_0(t) - B_{L,\varepsilon} v_0(0,t), & 0<t\le T, \\ B_{R,\varepsilon} w(1,t) = 0, & 0<t\le T, \\ w(x,0) = 0, & 0\le x\le 1. \end{cases} \tag{2.18}$$

Lemma 2.3.9. *Assume the smoothness assumptions on the data $a,\ b,\ f \in C^2(\bar{\Omega})$, $s \in C^4([0,1]); q_0, q_1 \in C^3([0,1])$ [14] and compatibility conditions on these functions are satisfied, the regular component $v(x,t)$ and its derivatives have the following bounds*

$$\left\| \frac{\partial^{l+m} v}{\partial x^l \partial t^m} \right\|_\Omega \le C(1+\varepsilon^{2-l}), \qquad 0\le l+2m\le 4.$$

where C is a constant independent of ε.

Proof. Since $v_0(x,t)$ and $v_1(x,t)$ are solutions of Eqs. (2.14) and (2.15) respectively, which are independent of ε, therefore we have, for all non-negative integers l, m such that $0 \le l + 2m \le 4$

$$\left\| \frac{\partial^{l+m} v_i}{\partial x^l \partial t^m} \right\|_{\Omega} \le C, \quad i = 0, 1.$$

Since $v_2(x,t)$ is the solution of Eq. (2.16), using Theorem (2.1) for all non-negative integers l, m such that $0 \le l \le 1$ and $0 \le l + 2m \le 4$ we have

$$\left\| \frac{\partial^{l+m} v_2}{\partial x^l \partial t^m} \right\| \le C\big(1 + \varepsilon^{-l} e^{-\alpha x/\varepsilon}\big), \qquad (x,t) \in \bar{\Omega}.$$

From Eq. (2.13), we get

$$\begin{aligned}
\left\| \frac{\partial^{l+m} v}{\partial x^l \partial t^m} \right\| &\le \left\| \frac{\partial^{l+m} v_0}{\partial x^l \partial t^m} \right\| + \varepsilon \left| \frac{\partial^{l+m} v_1}{\partial x^l \partial t^m} \right\| + \varepsilon^2 \left| \frac{\partial^{l+m} v_2}{\partial x^l \partial t^m} \right\| \\
&\le C + C\varepsilon + \varepsilon^2 C\big(1 + \varepsilon^{-l} e^{-\alpha x/\varepsilon}\big), \\
&\le C + C\varepsilon + \varepsilon^2 C + C\varepsilon^{2-l} e^{-\alpha x/\varepsilon}, \\
&\le C + C\varepsilon^{2-l} e^{-\alpha x/\varepsilon}, \ \text{ since } \varepsilon \ll 1 \ \text{ and } e^{-\alpha x/\varepsilon} \le 1, \\
&\le C(1 + \varepsilon^{2-l}),
\end{aligned}$$

as required. □

A sharper bounds and its derivatives on $w(x,t)$ are established as follows.

Lemma 2.3.10. *Assume the smoothness assumptions on the data a, b, $f \in C^2(\bar{\Omega})$, $s \in C^4([0,1]); q_0, q_1 \in C^3([0,1])$ [14] and compatibility conditions on these functions are satisfied and compatibility conditions on these functions, the singular component $w(x,t)$ satisfies the bounds*

$$|w(x,t)| \le Ce^{-\alpha x/\varepsilon}, \qquad \forall (x,t) \in \bar{\Omega}.$$

Proof. Consider the barrier functions

$$\Psi^{\pm}(x,t) = Ce^{-\alpha x/\varepsilon} e^t \pm w(x,t).$$

At the boundaries, the values of $\Psi^{\pm}(x,t)$ are

$$\begin{aligned}\Psi^{\pm}(x,0) &= Ce^{-\alpha x/\varepsilon}e^{0} \pm w(x,0), \quad 0 \le x \le 1,\\ &= Ce^{-\alpha x/\varepsilon}, \quad \text{since } w(x,0)=0,\\ &\ge 0,\end{aligned}$$

$$\begin{aligned}\Psi^{\pm}(0,t) - \varepsilon(\Psi^{\pm}_x)(0,t) &= Ce^{-\alpha(0)/\varepsilon}e^{t} \pm w(0,t) - \varepsilon\left[C(\frac{-\alpha}{\varepsilon})e^{-\alpha(0)/\varepsilon}e^{t} \pm w_x(0,t)\right], \quad 0 < t \le T,\\ &= Ce^{0}e^{t} \pm w(0,t) + Ce^{0}e^{t} \mp \varepsilon w_x(0,t)],\\ &= Ce^{t} \mp (\varepsilon w_x(0,t) - w(0,t)),\\ &\ge 0, \quad \text{by choosing } C \text{ sufficiently large.}\\ \Psi^{\pm}(1,t) + \varepsilon(\Psi^{\pm}_x)(1,t) &= Ce^{-\alpha(1)/\varepsilon}e^{t} \pm w(1,t) + \varepsilon\left[C(\frac{-\alpha}{\varepsilon})e^{-\alpha(1)/\varepsilon}e^{t} \pm w_x(1,t)\right], \quad 0 < t \le T,\\ &= Ce^{-\alpha/\varepsilon}e^{t} \pm w(1,t) - Ce^{-\alpha/\varepsilon}e^{t} \pm \varepsilon w_x(1,t)],\\ &= \pm(w(1,t) + \varepsilon w_x(1,t)), \quad \text{since } \ w(1,t) + \varepsilon w_x(1,t) = 0,\\ &= 0.\end{aligned}$$

Now, on the domain $(x,t) \in \Omega$,

$$\begin{aligned}\mathcal{L}_{\varepsilon}\Psi^{\pm}(x,t) = {} & \varepsilon\left[\left(\frac{C\alpha^2}{\varepsilon^2}\right)e^{-\alpha x/\varepsilon}e^{t} \pm w_{xx}(x,t)\right] + a(x)\left[\left(\frac{-C\alpha}{\varepsilon}\right)e^{-\alpha x/\varepsilon}e^{t} \pm w_x(x,t)\right]\\ & - b(x)\left[Ce^{-\alpha x/\varepsilon}e^{t} \pm w(x,t)\right] - (Ce^{-\alpha x/\varepsilon}e^{t} \pm w_t(x,t)),\\ & = Ce^{-\alpha x/\varepsilon}e^{t}\left(\frac{\alpha^2}{\varepsilon} - \frac{a(x)\alpha}{\varepsilon} - b(x) - 1\right) \pm f(x,t),\\ & \le Ce^{-\alpha x/\varepsilon}e^{t}\left(\frac{\alpha^2}{\varepsilon} - \frac{a(x)\alpha}{\varepsilon} - b(x) - 1\right), \ \text{since } a(x) \ge \alpha > 0, \ b(x) \ge 0,\\ & \le Ce^{-\alpha x/\varepsilon}e^{t},\\ & \le 0.\end{aligned}$$

Using minimum principle on the operator $\mathcal{L}_\varepsilon\Psi^{\pm}(x,t) \leq 0,\ \ \forall(x,t) \in \bar{\Omega}$. This implies

$$
\begin{aligned}
|w(x,t)| &\leq Ce^{-\alpha x/\varepsilon}e^{t},\ \ \forall(x,t)\in\bar{\Omega},\\
&\leq Ce^{-\alpha x/\varepsilon}e^{T},\ \ \text{since } 0<t\leq T \text{ and } e^{t}\leq e^{T},\\
&\leq Ce^{-\alpha x/\varepsilon},\ \ \forall(x,t)\in\bar{\Omega},
\end{aligned}
$$

as required. □

Now, the bound of the derivatives of w is established on the following lemma.

Lemma 2.3.11. *The derivatives of the singular component $w(x,t)$ satisfies the bound*

$$
\left|\frac{\partial^{l+m}w}{\partial x^l\partial t^m}\right| \leq C\varepsilon^{-l}e^{-\alpha x/\varepsilon}, \qquad 0\leq l+2m\leq 4.
$$

where C is a constant independent of ε.

Proof. Letting $\eta = x/\varepsilon$, we set $\tilde{\Omega} = (0,1/\varepsilon)\times(0,T]$ and $\tilde{w}(\eta,t) = w(x,t)$ with similar definitions for $\tilde{a}$ and $\tilde{b}$. Equation (2.18) becomes

$$
\tilde{w}_{\eta\eta} + \tilde{a}\tilde{w}_\eta - \varepsilon\tilde{b}\tilde{w} - \varepsilon\tilde{w}_t = 0, \quad \text{on } \tilde{\Omega}. \tag{2.19}
$$

For each $\zeta \in (0,1/\varepsilon)$ and $\delta > 0$, $R_{\zeta,\delta}$ will denote the rectangle

$$
((\zeta-\delta,\zeta+\delta)\times(0,T])\cap\tilde{\Omega},
$$

and $\bar{R}_{\zeta,\delta}$ is the closure of $R_{\zeta,\delta}$ in the (η,t)-plane. By fixing $(\eta,t)\in\tilde{\Omega}$, we have two cases.

Case (i): For $2 < \eta < 1/\varepsilon$. Since $\tilde{w}$ satisfies Eqs. (2.18) and (2.19) and by using [72], we have

$$
\max_{\bar{R}_{\eta,1}}\left|\frac{\partial^{l+m}\tilde{w}}{\partial x^\eta\partial t^m}\right| \leq C\max_{\bar{R}_{\eta,2}}|\tilde{w}|, \qquad 0\leq l+2m\leq 4. \tag{2.20}
$$

Using Lemma (2.3.10), we in particular have

$$\left|\frac{\partial^{l+m}\tilde{w}(\eta,t)}{\partial x^{\eta}\partial t^{m}}\right| \leq Ce^{-\alpha(\eta-2)} \leq Ce^{-\alpha\eta}.$$

Changing variables, we obtain

$$\left|\frac{\partial^{l+m}w}{\partial x^{l}\partial t^{m}}\right| \leq C\varepsilon^{-l}e^{-\alpha x/\varepsilon}. \tag{2.21}$$

Case (ii): For $0 < \eta \leq 2$. For this case, we apply the results of [72] together with the result from the boundary of $\bar{\Omega}$. As a result, Eq. (2.20) is replaced by

$$\max_{\bar{R}_{\eta,1}}\left|\frac{\partial^{l+m}\tilde{w}}{\partial x^{\eta}\partial t^{m}}\right| \leq C(1+\max_{\bar{R}_{\eta,2}}|\tilde{w}|).$$

Using Lemma (2.3.10), this implies that

$$\left|\frac{\partial^{l+m}\tilde{w}(\eta,t)}{\partial x^{\eta}\partial t^{m}}\right| \leq C.$$

Changing variables, we obtain

$$\left|\frac{\partial^{l+m}w}{\partial x^{l}\partial t^{m}}\right| \leq C\varepsilon^{-l}. \tag{2.22}$$

Combining Eqs. (2.21) and (2.22), we obtain the desired result. □

2.4 Formulation of the Numerical Method

This section utilizes an upwind method to space discretization on Shishkin and Bakhvalov-Shishkin meshes and a backward Euler method for time discretization on a uniform mesh. The first derivatives of the left and right boundary conditions are then discretized using forward and backward difference approximations, respectively.

2.4.1 Shishkin Mesh (S-mesh)

Shishkin mesh is a piecewise uniform mesh which is finer inside of the layer region and coarser outside of the layer region [112]. To construct the Shishkin mesh, let $\bar{\Omega}_x^N = [0, 1]$ and $N \geq 4$ be an even positive integer in the space domain. The space domain is divided into two sub-intervals $[0, \sigma]$ and $[\sigma, 1]$ by placing a uniform mesh with $N/2$ mesh intervals in each of the subintervals. Here the transition point σ is defined as $\sigma = \min\{\frac{1}{2}, \frac{2\varepsilon}{\alpha} \ln N\}$ and $\varepsilon \leq N^{-1}$ is generally in practice. The piecewise equidistant mesh points condensing at the boundary point $x = 0$ is defined as

$$\bar{\Omega}_x^N := x_i = \begin{cases} i\frac{2\sigma}{N}, & \text{for } 0 \leq i \leq \frac{N}{2}, \\ \sigma + (i - \frac{N}{2})\frac{2(1-\sigma)}{N}, & \text{for } \frac{N}{2} < i \leq N, \end{cases}$$

The space mesh widths for $i = 1, 2, \cdots, N$ is defined as

$$h_i = x_i - x_{i-1} = \begin{cases} h = \frac{2\sigma}{N}, & \text{for } 1 \leq i \leq \frac{N}{2}, \\ H = \frac{2(1-\sigma)}{N}, & \text{for } \frac{N}{2} < i \leq N, \end{cases}$$

where h is the space step size in $[0, \sigma]$ and H is the space step size in $[\sigma, 1]$. Throughout the error analysis, we assume that $\sigma = \frac{2\varepsilon}{\alpha} \ln N$, otherwise the mesh is uniform and the analysis is done in a classical way.

2.4.2 Bakhvalov-Shishkin Mesh (BS-mesh)

The BS-mesh is a modification of the S-mesh described above using the Bakhvalov technique [5]. The BS-mesh was first developed and used in [75]. The original Bakhvalov mesh, on the other hand, necessitates the solution of a nonlinear equation to determine the transition point where the mesh transitions from coarse to fine. BS-mesh can be used whenever Shishkin mesh is appropriate, but BS-mesh is easier to handle than Bakhvalov mesh. The interval $[\sigma, 1]$ is uniformly divided into $N/2$ subintervals in BS-mesh, whereas the interval $[0, \sigma]$ is divided into the same number of mesh intervals by effectively inverting the boundary layer function $e^{-\alpha x/2\varepsilon}$. Specifying the $x_i,\ i = 0, 1, \cdots, N/2$ so that $\{e^{\frac{-\alpha x_i}{2\varepsilon}}\}_i$ is a linear function in i, i.e., we set

$$e^{\frac{-\alpha x_i}{2\varepsilon}} = Ai + B$$

and determine the unknowns A and B such that $x_0 = 0$ and $x_{N/2} = \sigma$. From this, for the same transition point as S-mesh, the mesh generating function for a piecewise BS-mesh condensing at the boundary point $x = 0$ is given by [38], [127] and [128]

$$\bar{\Omega}_x^N := x_i = \begin{cases} -\frac{2\varepsilon}{\alpha} \ln\left(1 - 2\left(1 - \frac{1}{N}\right)\frac{i}{N}\right), & \text{for } 0 \le i \le \frac{N}{2}, \\ \sigma + (i - \frac{N}{2})\frac{2(1-\sigma)}{N}, & \text{for } \frac{N}{2} < i \le N. \end{cases}$$

For the above defined meshes on space domain, the time domain $(0, T]$ is divided into the equidistant mesh such that $\Omega_t^M = \{t_j = j\Delta t, \quad j = 0, \cdots, M, \quad \Delta t = \frac{T}{M}\}$ where M is the number of mesh intervals. We fully discretize Eq. (2.1)-(2.2) by replacing the time derivative with a backward Euler method and the space derivatives with an upwind method, yielding the following discrete problem.

$$\mathcal{L}_\varepsilon^{N,\Delta t} U_i^j = \varepsilon \delta_x^2 U_i^j + a_i D_x^+ U_i^j - b_i U_i^j - D_t^- U_i^j = f_i^j, \ \ (x_i, t_j) \in \Omega^{N,\Delta t}, \tag{2.23}$$

with the following discrete initial-boundary conditions

$$\begin{cases} U_i^0 = s_i, & 0 \le i \le 1, \ \ j = 0, \\ B_{L,\varepsilon}^N U_0^j \equiv U_0^j - \varepsilon D_x^+ U_0^j = q_0^j, & 0 < j \le T, \\ B_{R,\varepsilon}^N U_N^j \equiv U_N^j + \varepsilon D_x^- U_N^j = q_1^j, & 0 < j \le T. \end{cases} \tag{2.24}$$

Equations (2.23) and (2.24) gives the following tridiagonal system of linear equations

$$\begin{cases} U_i^0 = s_i, & 0 \le i \le 1, \;\; j = 0, \\ B_{L,\varepsilon}^N U_0^j \equiv r_0^c U_0^j + r_0^+ U_1^j = q_0^j, & \text{for} \;\; i = 0, \;\; 1 \le j < M, \\ \mathcal{L}_\varepsilon^{N,\Delta t} U_i^j \equiv r_i^- U_{i-1}^j + r_i^c U_i^j + r_i^+ U_{i+1}^j = g_i^j, & \text{for} \;\; 1 \le i \le N-1, \;\; 1 \le j < M, \\ B_{R,\varepsilon}^N U_N^j \equiv r_N^- U_{N-1}^j + r_N^c U_N^j = q_N^j, & \text{for} \;\; i = N, \;\; 1 \le j < M, \end{cases} \tag{2.25}$$

where $h_0 := h_1$ and the ghost value $h_{N+1} := h_N$ and the coefficients are

$$\begin{aligned} r_i^- &= \frac{2\varepsilon}{h_i(h_i + h_{i+1})}, \quad r_i^+ = \frac{2\varepsilon}{h_{i+1}(h_i + h_{i+1})} + \frac{a_i}{h_{i+1}}, \\ r_i^c &= -\frac{2\varepsilon}{h_i h_{i+1}} - \frac{a_i}{h_{i+1}} - b_i - \frac{1}{\Delta t}, \quad g_i^j = f_i^j - \frac{U_i^{j-1}}{\Delta t}, \\ r_0^c &= 1 + \frac{\varepsilon}{h_0}, \;\; r_0^+ = -\frac{\varepsilon}{h_0}, \;\; r_N^- = -\frac{\varepsilon}{h_N}, \;\; r_N^c = 1 + \frac{\varepsilon}{h_N}. \end{aligned} \tag{2.26}$$

The coefficient matrix in Eq. (2.26) gives an $(N+1) \times (N+1)$ system of linear equations which can be solved uniquely for the unknowns $U_0, U_1, \cdots, U_{N-1}, U_N$ at j time level. The off-diagonal elements are negative, whereas the main diagonal elements are positive and diagonally dominant. The coefficient matrix is thus an invertible M-matrix. Further, the inverse matrix exists and it is nonnegative. As a result, we solved the linear system of equations in Eq. (2.26) using the matrix inversion method.

2.5 Analysis of the Method

For the present method to be stable if

$$\begin{aligned} &|r_i^c| \ge |r_i^-| + |r_i^+|, \;\; |r_i^-| > 0, \;\; |r_i^+| > 0, \\ &|r_0^c| - |r_0^+| > 0, \qquad |r_N^c| - |r_N^-| > 0. \end{aligned}$$

The coefficient matrix in Eq. (2.26) implies that the coefficient matrix is an M-matrix. The tridiagonal matrix obtained from the system Eq. (2.25) is an M-matrix. This demonstrates that the discrete scheme is stable and free of oscillations. Analogous to the minimum principle stated in Lemma (2.3.1) for the continuous problem, the discrete operator in Eqs. (2.23) and (2.24) satisfies the following discrete minimum principle. This provides the $\varepsilon-$uniform stability for the discrete operator $\mathcal{L}_\varepsilon^{N,\Delta t}$.

Lemma 2.5.1. *Assume $Z(x_i, t_j)$ be sufficiently smooth mesh function defined on $\bar{\Omega}^{N,\Delta t}$ satisfying $B_{L,\varepsilon}^N Z(x_0, t) \geq 0$, $B_{R,\varepsilon}^N Z(x_N, t) \geq 0$ for $t_j \in [0, T]$, $Z(x_i, t_0) \geq 0$ for $x_i \in [0, 1]$ and $\mathcal{L}_\varepsilon^{N,\Delta t} Z(x_i, t_j) \leq 0$, $\forall (x_i, t_j) \in \Omega$, then $Z(x_i, t_j) \geq 0$, $(x_i, t_j) \in \bar{\Omega}$.*

Proof. Assume $(x_i^*, t_j^*) \in \bar{\Omega}$ such that $Z(x_i^*, t_j^*) = \min\limits_{(x_i,t_j)\in\bar{\Omega}} Z(x_i^*, t_j^*)$ and that $Z(x_i^*, t_j^*) < 0$.
For $(x_i^*, t_j^*) \in \Omega$, we have $\frac{\partial Z}{\partial t}(x_i^*, t_j^*) = 0$, $\frac{\partial Z}{\partial x}(x_i^*, t_j^*) = 0$ and $\frac{\partial^2 Z}{\partial x^2}(x_i^*, t_j^*) \geq 0$.
For $(x_i^*, t_j^*) \in S_0$, we have $x_i^* = 0$ and $\frac{\partial Z}{\partial x}(x_i^*, t_j^*) = \frac{\partial Z}{\partial x}(0, t_j^*) = 0$. Hence, $Z(x_i^*, t_j^*) - \varepsilon \dfrac{\partial Z}{\partial x}(x_i^*, t_j^*) < 0$, which is a contradiction.
For $(x_i^*, t_j^*) \in S_1$, we have $x_i^* = 1$ and $\frac{\partial Z}{\partial x}(x_i^*, t_j^*) = \frac{\partial Z}{\partial x}(1, t_j^*) = 0$. Hence, $Z(x_i^*, t_j^*) + \varepsilon \dfrac{\partial Z}{\partial x}(x_i^*, t_j^*) < 0$, which is a contradiction. Also, for $t^* = 0, Z(x^*, 0) < 0$, which is a contradiction. Clearly, $(x_i^*, t_j^*) \notin \partial\Omega$. Now,

$$\mathcal{L}_\varepsilon^{N,\Delta t} Z(x_i^*, t_j^*) = \varepsilon \frac{\partial^2 Z}{\partial x^2}(x_i^*, t_j^*) + a(x^*) \frac{\partial Z}{\partial x}(x_i^*, t_j^*) - b(x^*) Z(x_i^*, t_j^*) - \frac{\partial Z}{\partial t}(x_i^*, t_j^*) > 0,$$

which is a contradiction. It follows that $Z(x_i, t_j) \geq 0$, $\forall (x_i, t_j) \in \bar{\Omega}$. □

Lemma 2.5.2. *The solution U_i^j satisfies the following bound*

$$|U_i^j| \leq \max\left\{|B_{L,\varepsilon}^N U_0^j|, |B_{R,\varepsilon}^N U_N^j|, |U_i^0|\right\} + \frac{\|\mathcal{L}_\varepsilon^{N,\Delta t} U\|}{\alpha}.$$

Proof. Analogues to the continuous case, this lemma can be proved using Lemma (2.5.1) and the barrier functions $\phi^{\pm}(x_i, t_j) = CM \pm U_i^j$, $\forall (x_i, t_j) \in \bar{\Omega}^{N,\Delta t}$, where

$$M = \left\{|B_{L,\varepsilon}^N U_0^j|, |B_{R,\varepsilon}^N U_N^j|, |U_i^0|\right\} + \frac{\|\mathcal{L}_\varepsilon^{N,\Delta t} U\|}{\alpha}.$$

Hence, the proof. □

Next, a parameter-uniform convergence analysis for the discrete scheme in Eq. (2.25) is established. The following truncation error is used in the proof of parameter-uniform convergence.

Lemma 2.5.3. *[128] Let ψ be a smooth function defined on $[0,1]$. Then the following estimates for the truncation error hold true*

$$|\mathcal{L}_\varepsilon^{N,\Delta t}\psi_i^j - \mathcal{L}_\varepsilon \psi(x_i,t_j)| \leq C\left[\varepsilon\int_{x_{i-1}}^{x_{i+1}}|\psi'''(x)|dx + \int_{x_{i-1}}^{x_i}|\psi''(x)|dx + \int_{t_j}^{t_{j+1}}|\psi''(t)|dt\right].$$

Lemma 2.5.4. *[86]. Let $(x_i,t_j)\in\Omega$, then for any mesh function $\varrho(x,t)\in C^2(\bar{\Omega})$*

$$\begin{aligned}
&(a)\ \left|\left(\frac{\partial}{\partial x} - D_x^+\right)\varrho(x_i,t_j)\right| \leq \frac{1}{2}(x_{i+1}-x_i)\left\|\frac{\partial^2\varrho(x_i,t_j)}{\partial x^2}\right\|.\\
&(b)\ \left|\left(\frac{\partial^2}{\partial x^2} - \delta_x^2\right)\varrho(x_i,t_j)\right| \leq \frac{1}{3}(x_{i+1}-x_{i-1})\left\|\frac{\partial^3\varrho(x_i,t_j)}{\partial x^3}\right\|.\\
&(c)\ \left|\left(\frac{\partial}{\partial t} - D_t^-\right)\varrho(x_i,t_j)\right| \leq \frac{\Delta t}{2}\left\|\frac{\partial^2\varrho(x_i,t_j)}{\partial t^2}\right\|.
\end{aligned}$$

The parameter-uniform error bound for the present method is calculated by combining the error estimates in the regular and singular components. To obtain parameter-uniform error estimate, we divide the numerical solution $U_i^j = U(x_i,t_j)$ into discrete regular component V_i^j and discrete singular component W_i^j, which are given by

$$U(x_i,t_j) = V(x_i,t_j) + W(x_i,t_j), \quad \forall (x_i,t_j)\in\Omega,$$

where V_i^j is the solution of the non-homogeneous problem given by

$$\begin{cases}
\mathcal{L}_\varepsilon^{N,\Delta t}V(x_i,t_j) = g(x_i,t_j), & \forall (x_i,t_j)\in\Omega,\\
B_{L,\varepsilon}^N V(0,t_j) = B_{L,\varepsilon}v(0,t_j), & t_j\in\Omega_t^{\Delta t},\\
B_{R,\varepsilon}^N V(1,t_j) = B_{R,\varepsilon}v(1,t_j), & t_j\in\Omega_t^{\Delta t},\\
V(x_i,0) = s_i, & x_i\in\bar{\Omega}_x^N,
\end{cases} \tag{2.27}$$

and W_i^j is the solution of the following homogeneous problem

$$\begin{cases} \mathcal{L}_\varepsilon^{N,\Delta t} W(x_i,t_j) = 0, & \forall (x_i,t_j) \in \Omega, \\ B_{L,\varepsilon}^N W(0,t_j) = q_0^j - B_{L,\varepsilon} v_0(0,t_j), & t_j \in \Omega_t^{\Delta t}, \\ B_{R,\varepsilon}^N W(1,t_j) = 0, & t_j \in \Omega_t^{\Delta t}, \\ W(x_i,0) = 0, & x_i \in \bar{\Omega}_x^N. \end{cases} \tag{2.28}$$

From the above, we can estimate the error at the node (x_i,t_j) by

$$|U_i^j - u(x_i,t_j)| \leq |V_i^j - v(x_i,t_j)| + |W_i^j - w(x_i,t_j)|, \tag{2.29}$$

The error $(U-u)(x_i,t_j)$ can now be obtained from the error estimates for the regular and singular components of the solution as follows.

Theorem 2.2. *Let $V(x_i,t_j)$ be the numerical solution of problem defined by Eq.* (2.27) *and $v(x,t)$ be the solution of Eq.* (2.17) *and assume the bound in Lemma* (2.3.9). *Then, the parameter-uniform error bound satisfied by the regular component on S-mesh is given by*

$$|(V-v)(x_i,t_j)| \leq C(N^{-1} + \Delta t), \quad (x_i,t_j) \in \Omega,$$

and the parameter-uniform error bound on BS-mesh is given by

$$|(V-v)(x_i,t_j)| \leq C(N^{-1} + \Delta t), \quad (x_i,t_j) \in \Omega,$$

where C is a constant independent of ε and mesh points.

Proof. First, the bound of the left boundary is given as follows

$$\begin{aligned} B_{L,\varepsilon}^N (V-v)(x_0,t_j) &= B_{L,\varepsilon}^N V(x_0,t_j) - B_{L,\varepsilon}^N v(x_0,t_j), \\ &= v(x_0,t_j) - \varepsilon v_x(x_0,t_j) - (v(x_0,t_j) - \varepsilon D^+ v(x_0,t_j)), \\ &= -\varepsilon(\frac{\partial}{\partial x} - D^+) v(x_0,t_j). \end{aligned}$$

From this and using Lemma (2.5.4), we obtain

$$|B^N_{L,\varepsilon}(V-v)(x_0,t_j)| \leq C\varepsilon(x_1-x_0)v_{xx}(x_0,t_j).$$

Since $h_1 = x_1 - x_0 = N^{-1}$, we obtain

$$|B^N_{L,\varepsilon}(V-v)(x_0,t_j)| \leq C\varepsilon N^{-1}v_{xx}(x_0,t_j).$$

Using the bound on the derivatives of v in Lemma (2.3.9) and using the fact that $\varepsilon \leq CN^{-1}$, we obtain the error bound at the left boundary point as

$$|B^N_{L,\varepsilon}(V-v)(x_0,t_j)| \leq CN^{-1}, \;\; \forall t_j \in \Omega^{\Delta t}_t.$$

Similarly, we obtain the following at the right boundary

$$|B^N_{R,\varepsilon}(V-v)(x_N,t_j)| \leq C\varepsilon(x_N-x_{N-1})v_{xx}(x_N,t_j).$$

Since $h_N = x_N - x_{N-1} = N^{-1}$, we obtain

$$|B^N_{R,\varepsilon}(V-v)(x_N,t_j)| \leq C\varepsilon N^{-1}v_{xx}(x_N,t_j).$$

Using the bound on the derivatives of v in Lemma (2.3.9) and using the fact that $\varepsilon \leq CN^{-1}$, we obtain the error bound at the right boundary point as

$$|B^N_{R,\varepsilon}(V-v)(x_N,t_j)| \leq CN^{-1}, \;\; \forall t_j \in \Omega^{\Delta t}_t.$$

The estimate of local truncation error at the interior points can be obtained by the classical argument. Thus, the differential and difference equations gives

$$\begin{aligned}
\mathcal{L}_\varepsilon^{N,\Delta t}(V-v)(x_i,t_j) &= f-\mathcal{L}_\varepsilon^{N,\Delta t},\\
&= (\mathcal{L}_\varepsilon-\mathcal{L}_\varepsilon^{N,\Delta t})v(x_i,t_j),\\
&= \varepsilon\left(\frac{\partial^2}{\partial x^2}-\delta_x^2\right)v(x_i,t_j)+a(x_i)\left(\frac{\partial}{\partial x}-D_x^+\right)v(x_i,t_j)\\
&-\left(\frac{\partial}{\partial t}-D_t^-\right)v(x_i,t_j).
\end{aligned}$$

It follows from Lemma (2.5.4) and the truncation error associated with the regular component V of the solution U satisfies the following estimate

$$|\mathcal{L}_\varepsilon^{N,\Delta t}(V-v)(x_i,t_j)|\le\frac{\varepsilon}{3}(x_{i+1}-x_{i-1})\left\|\frac{\partial^3 v}{\partial x^3}\right\|_{\bar\Omega}+\frac{\alpha(x_{i+1}-x_i)}{2}\left\|\frac{\partial^2 v}{\partial x^2}\right\|_{\bar\Omega}+\frac{\Delta t}{2}\left\|\frac{\partial^2 v}{\partial t^2}\right\|_{\bar\Omega}.$$

Since $x_{i+1}-x_{i-1}=2N^{-1}$ and $x_{i+1}-x_i=N^{-1}$ for any piecewise uniform mesh and using the bounds on the derivatives of v given in Lemma (2.3.9), we get

$$\begin{aligned}
|\mathcal{L}_\varepsilon^{N,\Delta t}(V-v)(x_i,t_j)| &\le \frac{\varepsilon}{3}(2N^{-1})(C+C\varepsilon^{-1})+CN^{-1}(C+C)+\frac{\Delta t}{2}(C),\\
&\le CN^{-2}+CN^{-1}+C\Delta t,\quad \text{since } \varepsilon\le CN^{-1},\\
&\le C(N^{-1}+\Delta t).
\end{aligned}$$

Now, introduce the discrete barrier functions

$$\varphi^{\pm}(x_i,t_j)=C[N^{-1}(1-x_i)+t_j\Delta t]\pm(V-v)(x_i,t_j).$$

Using Lemma (2.5.1) to the mesh function $(V-v)(x_i,t_j)$ yields

$$|(V-v)(x_i,t_j)|\le C(N^{-1}+\Delta t),\quad (x_i,t_j)\in\Omega,$$

and a very similar techniques give same error bound on BS-mesh. □

Lemma 2.5.5. *[118] For each $i = 0, \cdots, N$, define the mesh function*

$$Z_i = \prod_{k=1}^{i} \left(1 + \frac{\alpha h_k}{\varepsilon}\right)^{-1}, \qquad i = 1, 2, \cdots, N,$$

with the usual convention that $Z_0 = 1$ for $i = 0$. Then, the following estimate hold

$$\mathcal{L}_\varepsilon^{N,\Delta t} S_i \geq \frac{C Z_i}{\max\{\varepsilon, h_{i+1}\}}, \quad \text{for } 1 \leq i \leq N-1.$$

Lemma 2.5.6. *For each $i = 0, \cdots, N$, we have*

$$e^{-\alpha x_i/\varepsilon} \leq \prod_{k=1}^{i} \left(1 + \frac{\alpha h_k}{\varepsilon}\right)^{-1}.$$

Proof. Using the fact that $e^t \geq 1 + t$, $\forall t \geq 0$, we have

$$e^{-\alpha x_i/\varepsilon} = \left(e^{\alpha h_k/\varepsilon}\right)^{-1} \leq \left(1 + \frac{\alpha h_k}{\varepsilon}\right)^{-1}.$$

Multiplying these inequalities for $k = 1, \cdots, i$, we get the desired result. □

Theorem 2.3. *Let W be the numerical solution defined by Eq.* (2.28) *and w be the continuous solution in Eq.* (2.18) *and assume the bound in Lemma* (2.3.11)*. Then, the parameter-uniform error bound satisfied by the singular component on S-mesh is given by*

$$|(W - w)(x_i, t_j)| \leq C(N^{-1} \ln N + \Delta t), \quad (x_i, t_j) \in \Omega,$$

and the parameter-uniform error bound on BS-mesh is given by

$$|(W - w)(x_i, t_j)| \leq C(N^{-1} + \Delta t), \quad (x_i, t_j) \in \Omega,$$

where C is a constant independent of ε and mesh points.

Proof. Since the error bound on the singular component depends upon mesh parameter

σ, we prove this theorem by considering two cases.

Case (i): For $\sigma = \frac{1}{2}$, the mesh is uniform and then the convergence analysis is made in a classical way by using that $\varepsilon^{-1} \leq C \ln N$. From left boundary condition, we have

$$\begin{aligned}
B^N_{L,\varepsilon}(W - w)(x_0, t_j) &= B^N_{L,\varepsilon} W(x_0, t_j) - B^N_{L,\varepsilon} w(x_0, t_j), \\
&= w(x_0, t_j) - \varepsilon w_x(x_0, t_j) - \big(w(x_0, t_j) - \varepsilon D^+ w(x_0, t_j)\big), \\
&= -\varepsilon(\frac{\partial}{\partial x} - D^+) w(x_0, t_j), \\
|B^N_{L,\varepsilon}(W - w)(x_0, t_j)| &\leq C\varepsilon(x_1 - x_0) w_{xx}(x_0, t_j).
\end{aligned}$$

Using the bound on the derivatives of w in Theorem (2.1) and using the fact that $h_1 = x_1 - x_0$ and $h_1 = 2\sigma/N$, we obtain the error bound at the left boundary point as

$$\begin{aligned}
|B^N_{L,\varepsilon}(W - w)(x_0, t_j)| &\leq C\varepsilon \frac{2\sigma}{N} C\varepsilon^{-2} e^{-\alpha(0)/\varepsilon}, \\
&\leq C\varepsilon^{-1} N^{-1}(2\varepsilon\alpha^{-1} \ln N), \ \text{ since } \sigma = 2\varepsilon\alpha^{-1} \ln N, \\
&\leq C N^{-1} \ln N, \ \ \forall t_j \in \Omega^{\Delta t}_t.
\end{aligned}$$

Similarly, we have at the right boundary point

$$|B^N_{R,\varepsilon}(W - w)(x_N, t_j)| \leq C\varepsilon(x_N - x_{N-1}) w_{xx}(x_N, t_j).$$

From the bound on the derivatives of w in Theorem (2.1) and using the fact that $h_N = x_N - x_{N-1} = \frac{2(1-\sigma)}{N}$, we obtain the error bound at the right boundary point as

$$|B^N_{R,\varepsilon}(W - w)(x_N, t_j)| \leq C N^{-1} \ln N, \ \ \forall t_j \in \Omega^{\Delta t}_t.$$

Now, using the truncation error estimate in Lemma (2.5.3) and Lemma (2.3.10) together with the fact that $x_i - x_{i-1} = N^{-1}$, $x_{i+1} - x_{i-1} = 2N^{-1}$ and $t_{j+1} - t_j = \Delta t$, we get

$$|\mathcal{L}^{N,\Delta t}_\varepsilon (W - w)(x_i, t_j)| \leq C(N^{-1} \ln N + \Delta t), \quad (x_i, t_j) \in \Omega.$$

Applying discrete minimum principle, we have

$$|(W-w)(x_i,t_j)| \leq C(N^{-1}\ln N + \Delta t), \quad (x_i,t_j) \in \Omega.$$

Case (ii): $\sigma = \frac{2\varepsilon}{\alpha}\ln N$. In this case the mesh is piecewise uniform. Now, we give separate proofs in the coarse and fine mesh subintervals. From two boundaries, we have

$$|B^N_{L,\varepsilon}(W-w)(x_0,t_j)| \leq CN^{-1}\ln N, \;\; \forall t_j \in \Omega^{\Delta t}_t,$$
$$|B^N_{R,\varepsilon}(W-w)(x_N,t_j)| \leq CN^{-1}\ln N, \;\; \forall t_j \in \Omega^{\Delta t}_t.$$

Firstly, consider $(x_i,t_j) \in (\sigma,1)\times(0,T]$. Using triangle inequality, we have

$$|(W-w)(x_i,t_j)| \leq |W(x_i,t_j)| + |w(x_i,t_j)|.$$

From the bound on w in Lemma (2.3.10), we have

$$\begin{aligned} |w(x_i,t_j)| &\leq Ce^{-\alpha x_i/\varepsilon} \\ &\leq Ce^{-\alpha\sigma/\varepsilon} \\ &\leq CN^{-1}, \;\; i = N/2,\cdots,N. \end{aligned}$$

In a similar fashion, it is easy to establish the bound

$$|W(x_i,t_j)| \leq CN^{-1}, \;\; i = N/2,\cdots,N.$$

Therefore, for all $(x_i,t_j) \in (\sigma,1)\times(0,T]$, we have

$$|(W-w)(x_i,t_j)| \leq CN^{-1}, \;\; i = N/2,\cdots,N.$$

Secondly, consider $(x_i,t_j)\in(0,\sigma)\times(0,T]$. Then, the truncation error becomes

$$\begin{aligned}|\mathcal{L}_\varepsilon^{N,\Delta t}(W-w)(x_i,t_j)| &\le C\Big[\Delta t+\varepsilon\int_{x_{i-1}}^{x_{i+1}}|w'''(x)|dx+\int_{x_{i-1}}^{x_i}|w''(x)|dx\Big],\\ &\le C\big[\Delta t+\varepsilon^{-2}\int_{x_{i-1}}^{x_{i+1}}e^{-\frac{\alpha x}{\varepsilon}}dx\big],\\ &\le C\big[\Delta t+\varepsilon^{-1}e^{-\alpha x_i/\varepsilon}\big\{e^{\alpha h/\varepsilon}-e^{-\alpha h/\varepsilon}\big\}\big],\\ &\le C\big[\Delta t+\varepsilon^{-1}e^{-\alpha x_i/\varepsilon}\sinh\big(\frac{\alpha h}{\varepsilon}\big)\big].\end{aligned}$$

Since $\sinh(\xi)\le C\xi$, for $0\le\xi\le 2$, we have

$$\begin{aligned}\sinh\big(\frac{\alpha h_i}{\varepsilon}\big) &= \sinh\big(\frac{\alpha h}{\varepsilon}\big),\ \text{ since } i=1,\cdots,\frac{N}{2},\ h_i=h=\frac{2\sigma}{N}=\frac{2}{N}\Big(\frac{2\varepsilon}{\alpha}\ln N\Big),\\ &= \sinh\big(4N^{-1}\ln N\big),\\ &\le CN^{-1}\ln N,\ \ i=1,\cdots,\frac{N}{2}.\end{aligned}$$

Thus, truncation error estimate reduces to

$$\begin{aligned}|\mathcal{L}_\varepsilon^{N,\Delta t}(W-w)(x_i,t_j)| &\le C\big[\Delta t+\varepsilon^{-1}e^{-\alpha x_i/\varepsilon}N^{-1}\ln N\big],\\ &\le C\big[\Delta t+\varepsilon^{-1}N^{-1}\ln N\prod_{k=1}^{i}e^{-\alpha h_k/\varepsilon}\big],\\ &\le C\Bigg[\Delta t+\varepsilon^{-1}N^{-1}\ln N\prod_{k=1}^{i}\Big(1+\frac{-\alpha h_k}{\varepsilon}\Big)^{-1}\Bigg].\end{aligned}\tag{2.30}$$

Using the estimate in Eq. (2.30), we construct the discrete barrier functions

$$\Psi^{\pm}(x_i,t_j)=C\big(N^{-1}+\varepsilon^{-1}(1-x_i)N^{-1}\ln N+t_j\Delta t\big)\pm(W-w)(x_i,t_j).$$

We can easily observe that the barrier functions $\Psi^{\pm}(x_i,t_j)\ge 0$ at all points in the boundaries of the form $(x_N,t_j),(x_0,t_j)$ and (x_i,t_0). Also, we have

$$\begin{aligned}\mathcal{L}_\varepsilon^{N,\Delta t}\Psi^{\pm}(x_i,t_j) &= C\big(N^{-1}+\varepsilon^{-1}\mathcal{L}_\varepsilon^{N,\Delta t}(1-x_i)N^{-1}\ln N+t_j\Delta t\big)\pm\mathcal{L}_\varepsilon^{N,\Delta t}(W-w)(x_i,t_j)\\ &\le 0.\end{aligned}$$

Now, applying discrete minimum principle and combining two cases, we obtain the error estimate at the layer component

$$|(W-w)(x_i,t_j)| \leq C\big(N^{-1}\ln N + \Delta t\big), \;\; \forall (x_i,t_j) \in \bar{\Omega}.$$

and a very similar techniques give the following error bound

$$|(W-w)(x_i,t_j)| \leq C\big(N^{-1} + \Delta t\big), \;\; \forall (x_i,t_j) \in \bar{\Omega},$$

on BS-mesh. □

Combination of the error bound at the boundaries and interior mesh points leads us to the following main convergence theorem.

Theorem 2.4. *Let u be the solution of continuous problem and U be the solution of the discrete problem. Then, the parameter-uniform error bound satisfied by the S-mesh is*

$$\sup_{0<\varepsilon\leq 1} \max_{0\leq i\leq N; 0\leq j\leq M} |U_i^j - u(x_i,t_j)| \leq \begin{cases} C(N^{-1}\ln N + \Delta t), & 0 \leq i \leq \frac{N}{2}, \\ C(N^{-1} + \Delta t), & \frac{N}{2} < i \leq N, \end{cases}$$

and the corresponding parameter-uniform error bound on BS-mesh is given by

$$\sup_{0<\varepsilon\leq 1} \max_{0\leq i\leq N; 0\leq j\leq M} |U_i^j - u(x_i,t_j)| \leq C(N^{-1} + \Delta t), \quad 0 \leq i \leq N.$$

where C is a constant independent of ε and the mesh parameters.

Proof. The proof follows from Eq. (2.29), Theorems (2.2) and (2.3). □

2.6 Numerical Results

This section provides demonstrations of the numerical experiments for the theoretical findings provided in the previous sections.

Example 2.6.1. *From [53], the following test example is considered*

$$\varepsilon\frac{\partial^2 u(x,t)}{\partial x^2}+\frac{\partial u(x,t)}{\partial x}-\frac{\partial u(x,t)}{\partial t}=-4t^3,\qquad (x,t)\in(0,1)\times(0,1],$$

with the initial condition and boundary conditions

$$\begin{cases} u(x,0)=0, & 0\le x\le 1,\\ -\varepsilon\frac{\partial u}{\partial x}(0,t)=t^2, & 0\le t\le 1,\\ u(1,t)=0, & 0\le t\le 1.\end{cases}$$

Example 2.6.2. *Consider the singularly perturbed parabolic problem [53]*

$$\varepsilon\frac{\partial^2 u(x,t)}{\partial x^2}+\frac{\partial u(x,t)}{\partial x}-\frac{\partial u(x,t)}{\partial t}=-20t^3(x+\varepsilon)e^{-\frac{x}{\varepsilon}},\qquad (x,t)\in(0,1)\times(0,1],$$

with the initial condition and boundary conditions

$$\begin{cases} u(x,0)=0, & 0\le x\le 1,\\ -\varepsilon\frac{\partial u(0,t)}{\partial x}=t^5, & 0\le t\le 1,\\ u(1,t)=-t^4(t-5-5\varepsilon)e^{-\frac{1}{\varepsilon}}, & 0\le t\le 1.\end{cases}$$

Since the exact solution for Examples (2.6.1) and (2.6.2) are not available, the maximum absolute error is calculated using the double mesh principle [31]

$$E_\varepsilon^{N,\Delta t}=\max_{(x_i,t_j)\in\bar{\Omega}^{N,M}}\left|U^{N,\Delta t}(x_i,t_j)-U^{2N,\Delta t/2}(x_i,t_j)\right|,\tag{2.31}$$

where $U^{N,\Delta t}(x_i,t_j)$ denote the numerical solution obtained at $(N,\Delta t)$ mesh points whereas $U^{2N,\Delta t/2}(x_i,t_j)$ denote the numerical solution obtained by doubling the mesh points by including the midpoints $x_{i+1/2}=(x_i+x_{i+1})/2,\ t_{j+1/2}=(t_j+t_{j+1})/2$ into the mesh points. The parameter-uniform error and parameter-uniform rate of convergence are computed using the following formulas, respectively

$$E^{N,\Delta t} = \max_{\varepsilon} E_{\varepsilon}^{N,\Delta t} \quad \text{and} \quad R^{N,\Delta t} = \log_2\left(\frac{E^{N,\Delta t}}{E^{2N,\Delta t/2}}\right). \tag{2.32}$$

Table 2.1: Comparison of maximum absolute errors for Example (2.6.1).

	Number of mesh intervals $N = M$, where $M = \frac{1}{\Delta t}$						
$\varepsilon \downarrow$	16	32	64	128	256	512	1024
Present Result (BS-mesh)							
2^{-5}	2.0259e-1	1.0474e-1	5.3188e-2	2.6716e-2	1.3299e-2	6.5441e-3	3.1548e-3
2^{-6}	2.1790e-1	1.1260e-1	5.7043e-2	2.8701e-2	1.4384e-2	7.1858e-3	3.5773e-3
2^{-7}	2.2804e-1	1.1802e-1	5.9552e-2	2.9873e-2	1.4962e-2	7.4863e-3	3.7422e-3
2^{-8}	2.3393e-1	1.2142e-1	6.1153e-2	3.0585e-2	1.5289e-2	7.6448e-3	3.8225e-3
2^{-9}	2.3709e-1	1.2335e-1	6.2117e-2	3.1020e-2	1.5480e-2	7.7321e-3	3.8645e-3
2^{-10}	2.3873e-1	1.2438e-1	6.2656e-2	3.1275e-2	1.5594e-2	7.7822e-3	3.8874e-3
$E^{N,\Delta t}$	2.4039e-1	1.2545e-1	6.3240e-2	3.1569e-2	1.5735e-2	7.8475e-3	3.9167e-3
Result in [53]							
2^{-5}	1.409e+0	8.643e-1	4.916e-1	2.419e-1	1.171e-1	5.464e-2	2.342e-2
2^{-6}	1.448e+0	8.821e-1	5.174e-1	2.931e-1	1.598e-1	8.261e-2	3.875e-2
2^{-7}	1.476e+0	8.965e-1	5.248e-1	2.969e-1	1.616e-1	8.326e-2	3.873e-2
2^{-8}	1.493e+0	9.049e-1	5.291e-1	2.993e-1	1.629e-1	8.391e-2	3.904e-2
2^{-9}	1.502e+0	9.095e-1	5.314e-1	3.005e-1	1.636e-1	8.426e-2	3.920e-2
2^{-10}	1.507e+0	9.119e-1	5.326e-1	3.011e-1	1.639e-1	8.443e-2	3.928e-2
$E^{N,\Delta t}$	1.512e+0	9.143e-1	5.338e-1	3.018e-1	1.642e-1	8.461e-2	3.936e-2

2.7 Discussion and Conclusion

Table (2.1) shows the comparison of maximum absolute errors of the present method using BS-mesh and the method in [53]. Tables (2.2) and (2.3) demonstrate the comparison of maximum absolute errors and the corresponding rate of convergence of the present method on S-mesh and BS-mesh. Figures (2.1)-(2.4) show the physical behavior of the numerical solution U on the S-mesh and BS-mesh for Examples (2.6.1) and (2.6.2), respectively. Based on these sketches, we can see that the BS-mesh condenses more mesh points at the

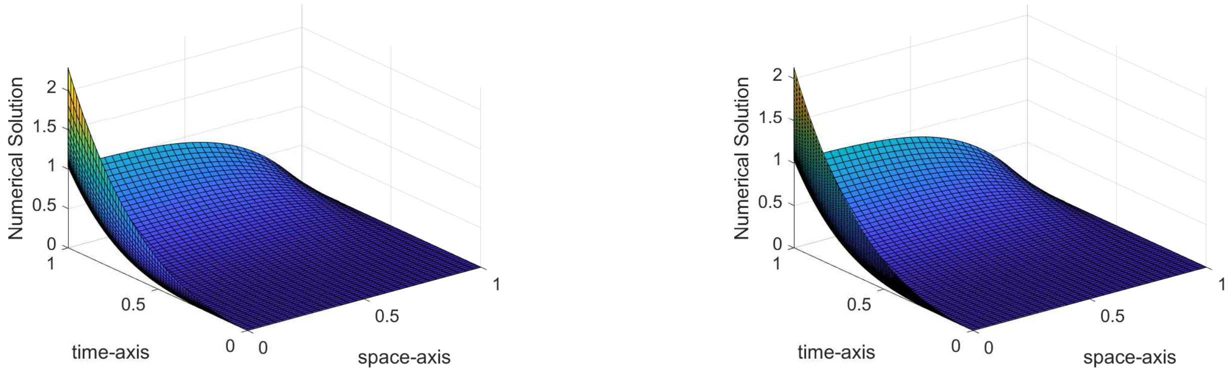

(a) S-mesh. **(b)** BS-mesh.

Figure 2.1: Surface plot of the solution at $N = 64,\ \varepsilon = 10^{-8}$ for Example (2.6.1).

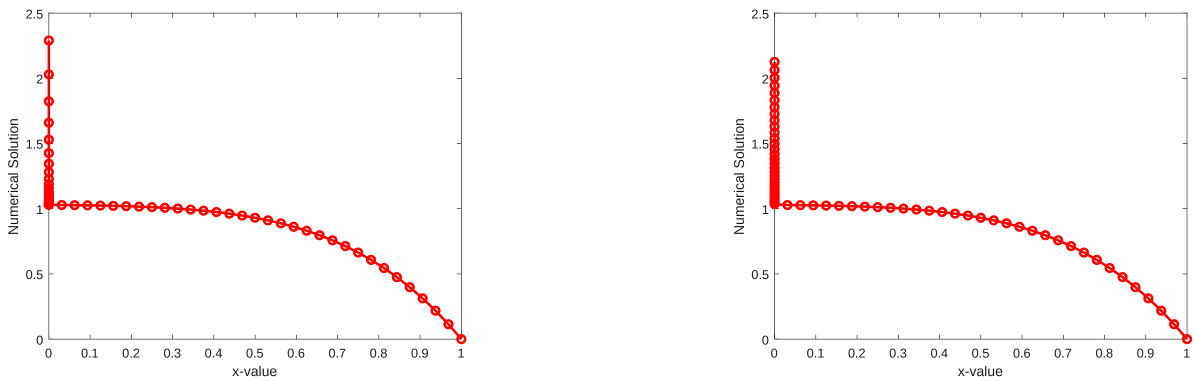

(a) S-mesh. **(b)** BS-mesh.

Figure 2.2: Layer resolving property for $\varepsilon = 10^{-6}, N = M = 64$ for Example (2.6.1).

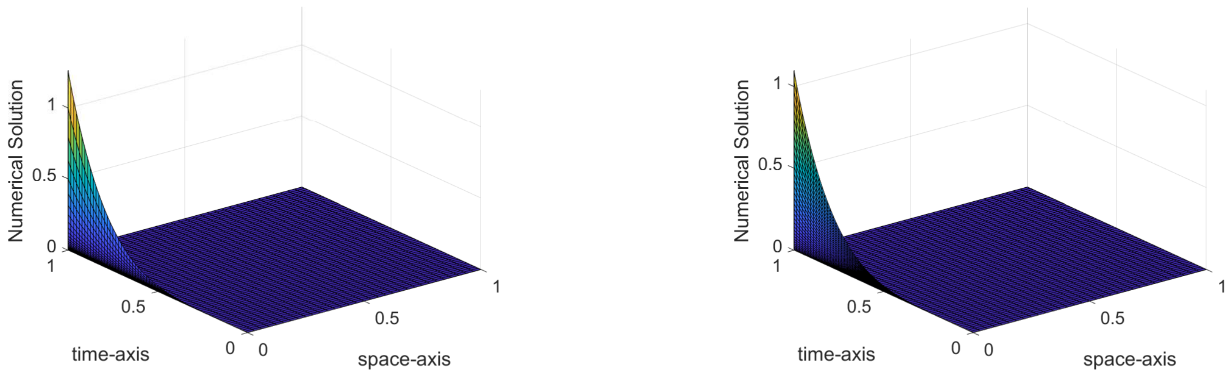

(a) S-mesh. **(b)** BS-mesh.

Figure 2.3: Surface plot of the solution at $N = 64,\ \varepsilon = 10^{-8}$ for Example (2.6.2).

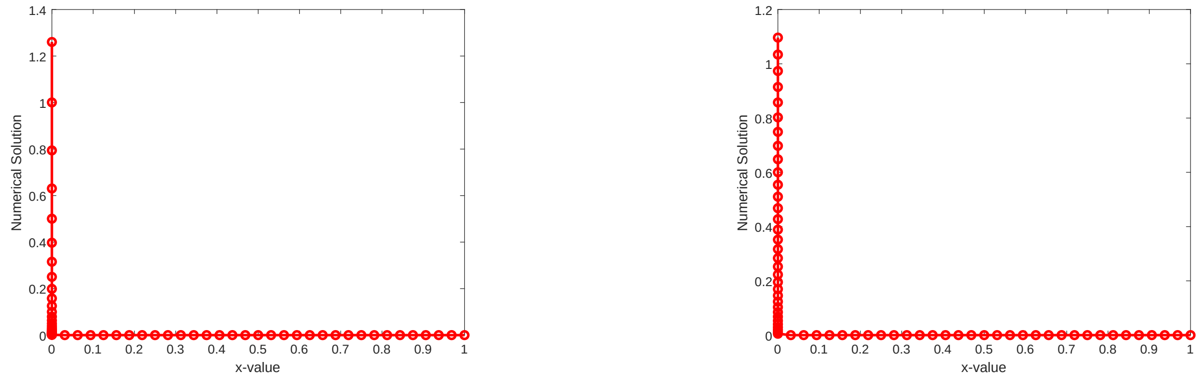

(a) S-mesh. **(b)** BS-mesh.

Figure 2.4: Layer resolving property for $\varepsilon = 10^{-6}, N = M = 64$ for Example (2.6.2).

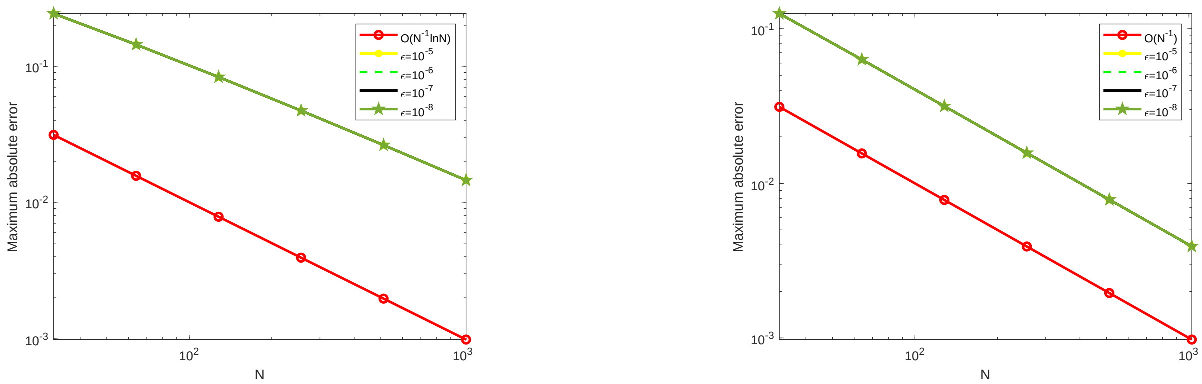

(a) S-mesh. **(b)** BS-mesh.

Figure 2.5: Loglog plot of the maximum absolute errors for Example (2.6.1) using Table (2.2).

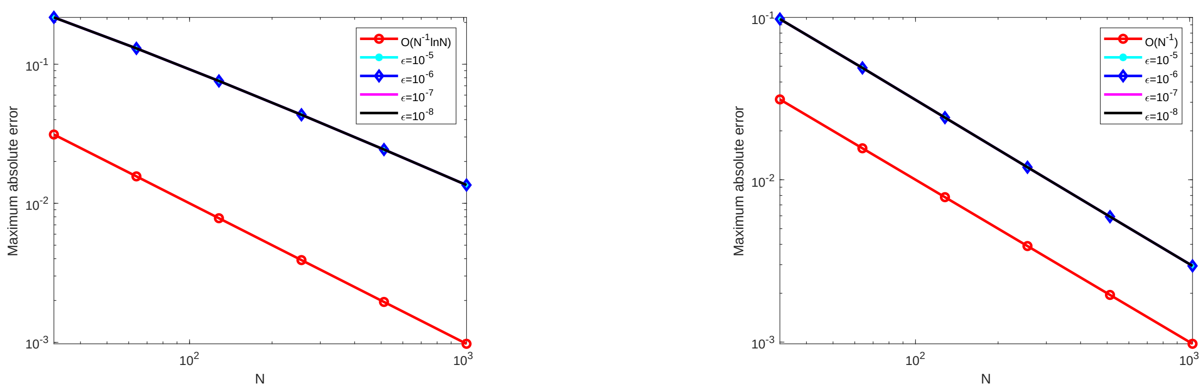

(a) S-mesh. **(b)** BS-mesh.

Figure 2.6: Loglog plot of the maximum absolute errors for Example (2.6.2) using Table (2.3).

Table 2.2: Comparison of $E_{\varepsilon}^{N,\Delta t}, E^{N,\Delta t}$ and $R^{N,\Delta t}$ for Example (2.6.1).

	Number of mesh intervals $N = M$, where $M = \frac{1}{\Delta t}$						
$\varepsilon \downarrow$	16, $\frac{1}{16}$	32, $\frac{1}{32}$	64, $\frac{1}{64}$	128, $\frac{1}{128}$	256, $\frac{1}{256}$	512, $\frac{1}{512}$	1024, $\frac{1}{1024}$
BS-mesh							
10^{-2}	2.2499e-1	1.1635e-1	5.8780e-2	2.9522e-2	1.4794e-2	7.4013e-3	3.6975e-3
10^{-3}	2.3869e-1	1.2435e-1	6.2643e-2	3.1269e-2	1.5591e-2	7.7809e-3	3.8868e-3
10^{-4}	2.4022e-1	1.2534e-1	6.3179e-2	3.1538e-2	1.5719e-2	7.8393e-3	3.9128e-3
10^{-5}	2.4037e-1	1.2544e-1	6.3234e-2	3.1567e-2	1.5734e-2	7.8466e-3	3.9164e-3
10^{-6}	2.4039e-1	1.2545e-1	6.3240e-2	3.1570e-2	1.5735e-2	7.8474e-3	3.9168e-3
10^{-7}	2.4039e-1	1.2545e-1	6.3240e-2	3.1570e-2	1.5736e-2	7.8475e-3	3.9168e-3
10^{-8}	2.4039e-1	1.2545e-1	6.3240e-2	3.1570e-2	1.5736e-2	7.8475e-3	3.9168e-3
$E^{N,\Delta t}$	2.4039e-1	1.2545e-1	6.3240e-2	3.1570e-2	1.5736e-2	7.8475e-3	3.9168e-3
$R^{N,\Delta t}$	0.9383	0.9882	1.0023	1.0045	1.0038	1.0026	
S-mesh							
10^{-2}	3.8932e-1	2.3899e-1	1.4135e-1	8.1504e-2	4.6125e-2	2.5734e-2	1.4199e-2
10^{-3}	3.9636e-1	2.4339e-1	1.4396e-1	8.3045e-2	4.7010e-2	2.6231e-2	1.4473e-2
10^{-4}	3.9706e-1	2.4383e-1	1.4423e-1	8.3205e-2	4.7104e-2	2.6285e-2	1.4503e-2
10^{-5}	3.9713e-1	2.4388e-1	1.4426e-1	8.3221e-2	4.7113e-2	2.6290e-2	1.4506e-2
10^{-6}	3.9714e-1	2.4388e-1	1.4426e-1	8.3222e-2	4.7114e-2	2.6291e-2	1.4506e-2
10^{-7}	3.9714e-1	2.4388e-1	1.4426e-1	8.3222e-2	4.7114e-2	2.6291e-2	1.4506e-2
10^{-8}	3.9714e-1	2.4388e-1	1.4426e-1	8.3222e-2	4.7114e-2	2.6291e-2	1.4506e-2
$E^{N,\Delta t}$	3.9714e-1	2.4388e-1	1.4426e-1	8.3222e-2	4.7114e-2	2.6291e-2	1.4506e-2
$R^{N,\Delta t}$	0.7035	0.7575	0.7936	0.8208	0.8416	0.8579	

boundary layer regions whereas the S-mesh condenses less mesh points. The numerical results show that for a fixed ε, the maximum absolute errors decrease as mesh intervals increase, confirming that the present method provides parameter-uniform convergence for Examples (2.6.1) and (2.6.2). To address this observation, we plotted the maximum absolute errors in log-log scale using the results in the Tables (2.2) and (2.3) on S-mesh and BS-mesh for Examples (2.6.1) and (2.6.2) as depicted in Figures (2.5) and (2.6), respectively. According to all numerical simulations, the problem under consideration has a boundary layer near $x = 0$. On a BS-mesh, the present scheme produces improved numerical results than the S-mesh. Because the BS-mesh is not affected by the logarithmic factor, it has an advantage over the S-mesh at the same computational cost. From the Tables, we see that the maximum absolute errors are getting smaller and the rate of

Table 2.3: Comparison of $E_{\varepsilon}^{N,\Delta t}$, $E^{N,\Delta t}$ and $R^{N,\Delta t}$ for Example (2.6.2).

	Number of mesh intervals $N = M$, where $M = \frac{1}{\Delta t}$						
$\varepsilon \downarrow$	16, $\frac{1}{16}$	32, $\frac{1}{32}$	64, $\frac{1}{64}$	128, $\frac{1}{128}$	256, $\frac{1}{256}$	512, $\frac{1}{512}$	1024, $\frac{1}{1024}$
BS-mesh							
10^{-2}	1.6863e-1	8.5722e-2	4.2787e-2	2.1332e-2	1.0649e-2	5.3199e-3	2.6585e-3
10^{-3}	1.8457e-1	9.6073e-2	4.7981e-2	2.3715e-2	1.1738e-2	5.8319e-3	2.9062e-3
10^{-4}	1.8651e-1	9.7493e-2	4.8769e-2	2.4103e-2	1.1919e-2	5.9139e-3	2.9430e-3
10^{-5}	1.8671e-1	9.7640e-2	4.8851e-2	2.4144e-2	1.1939e-2	5.9238e-3	2.9478e-3
10^{-6}	1.8673e-1	9.7655e-2	4.8860e-2	2.4149e-2	1.1941e-2	5.9248e-3	2.9482e-3
10^{-7}	1.8673e-1	9.7656e-2	4.8860e-2	2.4149e-2	1.1942e-2	5.9249e-3	2.9483e-3
10^{-8}	1.8673e-1	9.7656e-2	4.8860e-2	2.4149e-2	1.1942e-2	5.9249e-3	2.9483e-3
$E^{N,\Delta t}$	1.8673e-1	9.7656e-2	4.8860e-2	2.4149e-2	1.1942e-2	5.9249e-3	2.9483e-3
$R^{N,\Delta t}$	0.9352	0.9990	1.0167	1.0159	1.0112	1.0069	
S-mesh							
10^{-2}	3.3734e-1	2.0950e-1	1.2512e-1	7.2816e-2	4.1554e-2	2.3355e-2	1.2968e-2
10^{-3}	3.4606e-1	2.1648e-1	1.2960e-1	7.5516e-2	4.3135e-2	2.4259e-2	1.3476e-2
10^{-4}	3.4697e-1	2.1725e-1	1.3009e-1	7.5811e-2	4.3307e-2	2.4358e-2	1.3532e-2
10^{-5}	3.4706e-1	2.1733e-1	1.3014e-1	7.5841e-2	4.3325e-2	2.4368e-2	1.3538e-2
10^{-6}	3.4707e-1	2.1734e-1	1.3014e-1	7.5844e-2	4.3326e-2	2.4369e-2	1.3538e-2
10^{-7}	3.4707e-1	2.1734e-1	1.3014e-1	7.5844e-2	4.3326e-2	2.4369e-2	1.3538e-2
10^{-8}	3.4707e-1	2.1734e-1	1.3014e-1	7.5844e-2	4.3326e-2	2.4369e-2	1.3538e-2
$E^{N,\Delta t}$	3.4707e-1	2.1734e-1	1.3014e-1	7.5844e-2	4.3326e-2	2.4369e-2	1.3538e-2
$R^{N,\Delta t}$	0.6753	0.7399	0.7789	0.8078	0.8302	0.8480	

convergence is getting larger for the method using the BS-mesh than the S-mesh. Both theoretical estimates and numerical computations show that the present method is first-order parameter-uniformly convergent using BS-mesh and almost first-order parameter-uniformly convergent using S-mesh. The maximum absolute errors and rate of convergence obtained by the present method on Shishkin and Bakhvalov-Shishkin meshes are compared with the result in [53].

Chapter 3

Hybrid Numerical Method for Singularly Perturbed Parabolic Convection-diffusion Problems on Shishkin Mesh

This chapter presents the numerical solution of singularly perturbed parabolic convection-diffusion problems with Robin boundary conditions. The problem is discretized using an implicit Euler method on uniform mesh for time direction, and a hybrid numerical method that combines the central difference scheme in the boundary layer regions and the mid-point upwind scheme in the outer region on a piecewise uniform Shishkin mesh for space direction. It is demonstrated that the present method is parameter uniformly convergent regardless of the perturbation parameter. The theoretical findings are supported by two computed numerical examples. The present hybrid method is almost second-order convergent and improved the existing methods.

3.1 Introduction

A parameter-uniformly convergent hybrid method for singularly perturbed parabolic convection diffusion problems with Dirichlet boundary conditions have been developed in [29], [38], [46], [90], [119] and [123] for the problem with right boundary layer. In this chapter, a parameter-uniformly convergent hybrid method for the problem under consideration with left boundary layer is developed. The upwind scheme in [53] and the non-standard finite difference method together with the Richardson extrapolation technique in [80] are among the developed numerical scheme for the problem under consideration. Since the upwind method in [53] via Shishkin mesh and Bakhvalov-Shishkin mesh presented in (2) offers low accuracy, this chapter suggested a hybrid method that improved the existing methods and is almost second-order convergent.

3.2 Definition of the Problem

On the domain $\Omega = \Omega_x \times \Omega_t$, where $\Omega_x = (0,1)$, $\Omega_t = (0,T]$, the following singularly perturbed parabolic convection-diffusion non-turning point problem is considered.

$$\mathcal{L}_\varepsilon u(x,t) \equiv \varepsilon\frac{\partial^2 u(x,t)}{\partial x^2} + a(x)\frac{\partial u(x,t)}{\partial x} - b(x)u(x,t) - \frac{\partial u(x,t)}{\partial t} = f(x,t), \quad (x,t) \in \Omega, \quad (3.1)$$

subject to the initial and boundary conditions

$$\begin{cases} u(x,0) = s(x), & 0 \le x \le 1, \\ B_{L,\varepsilon}u(0,t) \equiv u(0,t) - \varepsilon\frac{\partial u(0,t)}{\partial x} = q_0(t), & 0 < t \le T, \\ B_{R,\varepsilon}u(1,t) \equiv u(1,t) + \varepsilon\frac{\partial u(1,t)}{\partial x} = q_1(t), & 0 < t \le T, \end{cases} \quad (3.2)$$

where $0 < \varepsilon \ll 1$ is perturbation parameter and the coefficients $a(x)$, $b(x)$ and $f(x,t)$, $\forall (x,t) \in \Omega$ in Eq. (3.1); and the initial-boundary functions $s(x)$, $\forall x \in [0,1]$, $q_0(t)$, $\forall 0 < t \le T$, $q_1(t)$, $\forall 0 < t \le T$ in Eq. (3.2) are smooth and bounded functions satisfying the conditions $a(x) \geq \alpha > 0,\ b(x) \geq 0,\ (x,t) \in \bar{\Omega}$. Under these conditions, the Eq. (3.1)-(3.2) has a unique solution. Further, the initial function is assumed to satisfy $s^{(k)}(x) = 0,\ \forall k \geq 1$. As the perturbation parameter ε tends to zero, the solution of problem in Eq. (3.1)-(3.2) exhibits the left boundary layer.

3.3 Properties of the Continuous Solution

The assumptions given in Eq. (3.1)-(3.2) admits the following continuous minimum principle.

Lemma 3.3.1. *Assume $\Phi(x,t) \in C^2(\bar{\Omega})$ be a smooth function. If $\Phi(x,0) \geq 0,\ 0 < x < 1$, $B_{L,\varepsilon}\Phi(0,t) \geq 0, 0 \leq t \leq T,\ B_{R,\varepsilon}\Phi(1,t) \geq 0,\ 0 \leq t \leq T$ and $\mathcal{L}_\varepsilon \Phi(x,t) \leq 0$ for all $(x,t) \in \Omega$, then $\Phi(x,t) \geq 0$ for all $(x,t) \in \bar{\Omega}$.*

Proof. For the proof, see Lemma (2.3.1). □

The next lemma proves the stability estimate to obtain unique solution.

Lemma 3.3.2. *The solution $u(x,t)$ of the problem in Eq. (3.1)-(3.2) satisfies the bound*

$$|u(x,t)| \leq \max\left\{|s(x)|, |q_0(t)|, |q_1(t)|\right\} + \frac{\|f\|}{\alpha}, \quad \textit{where } \|f\| = \max_{(x,t)\in\bar{\Omega}} |f(x,t)|.$$

Proof. For the proof, see Lemma (2.3.2). □

The following theorem establishes the bound on the solution and its derivatives.

Theorem 3.1. *The solution $u(x,t)$ and its partial derivatives satisfy the bound*

$$\left|\frac{\partial^{l+m} u}{\partial x^l \partial t^m}\right| \leq C(1 + \varepsilon^{-l} e^{-\alpha x/\varepsilon}), \quad (x,t) \in \bar{\Omega},$$

where l and m are non-negative integers such that $0 \leq l \leq 1,\ 0 \leq l+m \leq 4$.

Proof. For the proof, see Theorem (2.1). □

Lemma 3.3.3. *Assume the smoothness assumptions on the data* $a,\ b,\ f \in C^2(\bar{\Omega})$, $s \in C^4([0,1]); q_0, q_1 \in C^3([0,1])$ *[14] and compatibility conditions on these functions are satisfied, the regular component* $v(x,t)$ *and its derivatives have the following bounds*

$$\left\| \frac{\partial^{l+m} v}{\partial x^l \partial t^m} \right\| \leq C(1 + \varepsilon^{2-l}), \qquad 0 \leq l + 2m \leq 4.$$

where C *is a constant independent of* ε.

Proof. For the proof, see Lemma (2.3.9). □

A sharper bounds and its derivatives on the singular component w are established below.

Lemma 3.3.4. *Assume the smoothness assumptions on the data* $a,\ b,\ f \in C^2(\bar{\Omega})$, $s \in C^4([0,1]); q_0, q_1 \in C^3([0,1])$ *[14] and compatibility conditions on these functions are satisfied, the singular component solution* $w(x,t)$ *satisfies the bounds*

$$|w(x,t)| \leq Ce^{-\alpha x/\varepsilon}, \qquad \forall (x,t) \in \bar{\Omega}.$$

Proof. For the proof, see Lemma (2.3.10). □

Now, we can bound the derivatives of w.

Lemma 3.3.5. *The derivatives of the singular component* $w(x,t)$ *satisfies the bound*

$$\left| \frac{\partial^{l+m} w}{\partial x^l \partial t^m} \right| \leq C\varepsilon^{-l} e^{-\alpha x/\varepsilon}, \qquad 0 \leq l + 2m \leq 4.$$

where C *is a constant independent of* ε.

Proof. For the proof, see Lemma (2.3.11). □

3.4 Formulation of the Numerical Method

In the space domain $\bar{\Omega}_x^N = [0,1]$, let N be an even positive integer that is divisible by 4. The piecewise uniform mesh $S_N = \{x_i\}_0^N$ is constructed by dividing the space domain into two sub-intervals $[0, \sigma]$ and $(\sigma, 1]$ by placing a uniform mesh with $N/2$ mesh intervals in each of the subintervals where the transition point σ is defined as $\sigma = \min\{\frac{1}{2}, \sigma_0 \varepsilon \ln N\}$ where $\sigma_0 \geq 2/\alpha$. The piecewise uniform mesh points condensing at the boundary point $x = 0$ is defined as

$$x_i = \begin{cases} ih, & \text{for } 0 \leq i < \frac{N}{2}, \\ \sigma + (i - \frac{N}{2})H, & \text{for } \frac{N}{2} \leq i \leq N. \end{cases}$$

The space mesh sizes for $i = 0, 1, 2, \cdots, N$ is given by $h_i = x_i - x_{i-1}$ satisfying $h_i = h = \frac{2\sigma}{N} = \frac{4\varepsilon \ln N}{\alpha N}$ for $i = 1, \cdots, \frac{N}{2}$ and $h_i = H = \frac{2(1-\sigma)}{N}$ for $i = \frac{N}{2} + 1, \cdots, N$. Here h and H are the space mesh sizes in $[0, \sigma]$ and $[\sigma, 1]$, respectively. For the error analysis, assume that $\sigma = \sigma_0 \varepsilon \ln N$, otherwise the mesh is uniform and we proceed the analysis in the classical way. The time domain $[0, T]$ is divided into the equidistant mesh such that $\Omega_t^M = \{t_j = j\Delta t, \quad j = 0, \cdots, M, \quad \Delta t = \frac{T}{M}\}$ where M is the number of mesh intervals. Following mesh construction, problem in Eq. (3.1)-(3.2) is discretized using an backward Euler method on a uniform mesh in time direction and a hybrid numerical scheme in space direction on a Shishkin mesh, where we use the central difference scheme in the fine part of the mesh and the mid-point upwind scheme [118] in the coarse part. The first derivatives of the left and right boundary conditions are then approximated using second-order central difference approximation and backward difference approximation, respectively. We define $U^j_{i+\frac{1}{2}}$ as

$$U^j_{i+\frac{1}{2}} = \frac{U^j_i + U^j_{i+1}}{2}.$$

Similarly, we define the following for any given functions

$$a_{i+\frac{1}{2}} = \frac{a_i + a_{i+1}}{2}, \quad b_{i+\frac{1}{2}} = \frac{b_i + b_{i+1}}{2}, \quad f^j_{i+\frac{1}{2}} = \frac{f^j_i + f^j_{i+1}}{2}.$$

The totally discrete numerical scheme now takes the following form

$$\mathcal{L}_{\varepsilon}^{N,M} U_i^j = \begin{cases} \mathcal{L}_{\varepsilon,cen}^{N,M} U_i^j = f_i^j, & \text{for} \quad 0 < i < \frac{N}{2}, \\ \mathcal{L}_{\varepsilon,mup}^{N,M} U_i^j = f_{i+\frac{1}{2}}^j, & \text{for} \quad \frac{N}{2} \leq i < N, \end{cases} \tag{3.3}$$

with the following discrete initial condition

$$U_i^0 = s_i, \qquad\qquad i = 0, \cdots, N, \tag{3.4}$$

and the discrete boundary conditions

$$\begin{cases} B_{L,\varepsilon}^N U_0^j \equiv U_0^j - \varepsilon D_x^0 U_0^j = q_0^j, & j \in (0, T], \\ B_{R,\varepsilon}^N U_N^j \equiv U_N^j + \varepsilon D_x^- U_N^j = q_1^j, & j \in (0, T], \end{cases} \tag{3.5}$$

where

$$\begin{cases} \mathcal{L}_{\varepsilon,cen}^{N,M} U_i^j = \varepsilon \delta_x^2 U_i^j + a_i D_x^0 U_i^j - b_i U_i^j - \delta_t^- U_i^j, \\ \mathcal{L}_{\varepsilon,mup}^{N,M} U_i^j = \varepsilon \delta_x^2 U_i^j + a_{i+\frac{1}{2}} D_x^+ U_i^j - b_{i+\frac{1}{2}} U_{i+\frac{1}{2}}^j - \delta_t^- U_{i+\frac{1}{2}}^j. \end{cases} \tag{3.6}$$

Equation (3.6) yields the following tridiagonal system of equations

$$\begin{cases} r_{cen,i}^- U_{i-1}^j + r_{cen,i}^0 U_i^j + r_{cen,i}^+ U_{i+1}^j = r_i^j & 0 < i < \frac{N}{2}, \\ r_{mup,i}^- U_{i-1}^j + r_{mup,i}^0 U_i^j + r_{mup,i}^+ U_{i+1}^j = r_{i+\frac{1}{2}}^j, & \frac{N}{2} \leq i < N, \end{cases} \tag{3.7}$$

where the coefficients for $0 < i < \frac{N}{2}$ are given by

$$\begin{cases} r_{cen,i}^- = \dfrac{2\varepsilon}{h_i(h_i + h_{i+1})} - \dfrac{a_i}{(h_i + h_{i+1})}, \\ r_{cen,i}^0 = \dfrac{-2\varepsilon}{h_i(h_i + h_{i+1})} - \dfrac{2\varepsilon}{h_{i+1}(h_i + h_{i+1})} - b_i - \dfrac{1}{\Delta t}, \\ r_{cen,i}^+ = \dfrac{2\varepsilon}{h_{i+1}(h_i + h_{i+1})} + \dfrac{a_i}{(h_i + h_{i+1})}, \\ r_i^j = f_i^j - \dfrac{U_i^{j-1}}{\Delta t}, \end{cases}$$

and the coefficients for $\frac{N}{2} \leq i < N$ are given by

$$\begin{cases} r^-_{mup,i} = \dfrac{2\varepsilon}{h_i(h_i + h_{i+1})}, \\ r^0_{mup,i} = -\dfrac{2\varepsilon}{h_i h_{i+1}} - \dfrac{a_{i+\frac{1}{2}}}{h_{i+1}} - \dfrac{b_{i+\frac{1}{2}}}{2} - \dfrac{1}{2\Delta t}, \\ r^+_{mup,i} = \dfrac{2\varepsilon}{h_{i+1}(h_i + h_{i+1})} + \dfrac{a_{i+\frac{1}{2}}}{h_{i+1}} - \dfrac{b_{i+\frac{1}{2}}}{2} - \dfrac{1}{2\Delta t}, \\ r^j_{i+\frac{1}{2}} = f^j_{i+\frac{1}{2}} - \dfrac{U^{j-1}_{i+\frac{1}{2}}}{\Delta t}. \end{cases}$$

From Eq. (3.5), we have

$$\begin{cases} U^j_{-1} = \frac{(h_0+h_1)}{\varepsilon} q^j_0 - \frac{(h_0+h_1)}{\varepsilon} U^j_0 + U^j_1, \\ U^j_N + \varepsilon \frac{U^j_N - U^j_{N-1}}{h_{N+1}} = q^j_1. \end{cases} \tag{3.8}$$

where U^j_{-1} is a value at x_{-1}. Since the node x_{-1} lies outside of the interval $[0,1]$, the value U^j_{-1} is the ghost value. To eliminate the ghost value U^j_{-1}, we define $h_1 := h_0$ and using this by assuming that the difference scheme Eq. (3.7) holds for $i = 0$. By defining $h_{N+1} := h_N$ for the second equation in Eq. (3.8), we obtain the following approximations at the boundary points

$$\begin{cases} \left(\frac{-2\varepsilon}{h_0^2} + \frac{a_0}{\varepsilon} - \frac{2}{h_0} - b_0 - \frac{1}{\Delta t}\right) U^j_0 + \left(\frac{2\varepsilon}{h_0^2}\right) U^j_1 = \varrho, \\ \left(\frac{-\varepsilon}{h_N}\right) U^j_{N-1} + \left(1 + \frac{\varepsilon}{h_N}\right) U^j_N = q^j_1, \end{cases} \tag{3.9}$$

where $\varrho = f^j_0 - \frac{U^{j-1}_0}{\Delta t} + \left(\frac{a_0}{\varepsilon} - \frac{2}{h_0}\right) q^j_0$. The discrete problem in Eq. (3.7) and the discrete boundary conditions in Eq. (3.9) can be written in matrix form as

$$AU^j_i = F, \qquad i = 1, 2, ..., N-1, \quad j = 0, ..., M, \tag{3.10}$$

where U_i^j and F are column vectors of $N+1$ and the matrix A is a tri-diagonal matrix of $(N+1)\times(N+1)$. The entries of coefficient matrix A is given by

$$\begin{cases} A_{0,0} = \frac{-2\varepsilon}{h_0^2} + \frac{a_0}{\varepsilon} - \frac{2}{h_0} - b_0 - \frac{1}{\Delta t}, & i=0,\\ A_{0,1} = \frac{2\varepsilon}{h_0^2}, & i=0,\\ A_{i,i-1} = \frac{2\varepsilon}{h_i(h_i+h_{i+1})} - \frac{a_i}{(h_i+h_{i+1})}, & 1\le i\le \frac{N}{2},\\ A_{i,i} = \frac{-2\varepsilon}{h_i(h_i+h_{i+1})} - \frac{2\varepsilon}{h_{i+1}(h_i+h_{i+1})} - b_i - \frac{1}{\Delta t}, & 1\le i\le \frac{N}{2},\\ A_{i,i+1} = \frac{2\varepsilon}{h_{i+1}(h_i+h_{i+1})} + \frac{a_i}{(h_i+h_{i+1})}, & 1\le i\le \frac{N}{2},\\ A_{i,i-1} = \frac{2\varepsilon}{h_i(h_i+h_{i+1})}, & \frac{N}{2}+1\le i\le N-1,\\ A_{i,i} = -\frac{2\varepsilon}{h_ih_{i+1}} - \frac{a_{i+\frac{1}{2}}}{h_{i+1}} - \frac{b_{i+\frac{1}{2}}}{2} - \frac{1}{2\Delta t}, & \frac{N}{2}+1\le i\le N-1,\\ A_{i,i+1} = \frac{2\varepsilon}{h_{i+1}(h_i+h_{i+1})} + \frac{a_{i+\frac{1}{2}}}{h_{i+1}} - \frac{b_{i+\frac{1}{2}}}{2} - \frac{1}{2\Delta t}, & \frac{N}{2}+1\le i\le N-1,\\ A_{N,N-1} = \frac{-\varepsilon}{h_N}, & i=N,\\ A_{N,N} = 1+\frac{\varepsilon}{h_N}, & i=N. \end{cases}$$

The entries of column vectors F and U are given as follows

$$\begin{cases} F_0^j = f_0^j - \frac{U_0^{j-1}}{\Delta t} + \left(\frac{a_0}{\varepsilon} - \frac{2}{h_0}\right)q_0^j, & i=0,\\ F_i^j = f_i^j - \frac{U_i^{j-1}}{\Delta t}, & 1\le i\le \frac{N}{2},\\ F_i^j = f_{i+\frac{1}{2}}^j - \frac{U_{i+\frac{1}{2}}^{j-1}}{\Delta t}, & \frac{N}{2}+1\le i\le N-1,\\ F_N^j = q_1^j, & i=N,\\ U_i^j = [U_0^j, U_1^j, \cdots, U_N^j]^T. \end{cases}$$

The coefficient matrix of the discrete hybrid numerical scheme in Eq. (3.7) and the discrete boundary conditions in Eq. (3.9) gives an $(N+1)\times(N+1)$ linear systems of equations which can easily be solved using matrix inversion method for the unknowns $U_0^j, \cdots, U_N^j$ at each time level.

3.5 Analysis of the Method

This section establishes the uniform stability results and error analysis for the totally discrete hybrid scheme Eq. (3.3). The next lemma proves the tridiagonal matrix obtained from the system Eq. (3.7) with its corresponding boundary points Eq. (3.9) is an M-matrix. We establish the discrete minimum principle for the operator $\mathcal{L}_{\varepsilon}^{N,M}$.

Lemma 3.5.1. *For all $N \geq N_0$, we have the following mild assumption on the minimum number of mesh points*

$$\frac{N_0}{\ln N_0} \geq \sigma_0 \|a\|_\infty \quad \text{and} \quad (|b|_\infty + 1/\Delta t) \leq \alpha N_0. \tag{3.11}$$

Then, the tridiagonal matrix Eq. (3.7) *with its corresponding boundary points Eq.* (3.9) *is an M-matrix satisfying the following inequalities*

$$\begin{cases} r_{cen,i}^{-} > 0, \;\; r_{cen,i}^{+} > 0, \;\; r_{mup,i}^{-} > 0, \;\; r_{mup,i}^{+} > 0, & 1 \leq i < N, \\ |r_{cen,i}^{-}| + |r_{cen,i}^{+}| < |r_{cen,i}^{0}|, & 1 \leq i < N/2, \\ |r_{mup,i}^{-}| + |r_{mup,i}^{+}| < |r_{mup,i}^{0}|, & N/2 \leq i < N, \\ |r_{cen,1}^{+}| < |r_{cen,1}^{0}|, \qquad |r_{cen,N-1}^{-}| < |r_{cen,N-1}^{0}|, & \\ |r_{mup,1}^{+}| < |r_{mup,1}^{0}|, \qquad |r_{mup,N-1}^{-}| < |r_{mup,N-1}^{0}|. & \end{cases}$$

Lemma (3.5.1) under the hypotheses in Eq. (3.11) shows that the tridiagonal matrix associated with the difference operator $\mathcal{L}_{\varepsilon}^{N,M}$ in Eq. (3.3) at each time level is an M-matrix and, therefore, the operator $\mathcal{L}_{\varepsilon}^{N,M}$ satisfies the discrete minimum principle. Hence, the present method is uniformly stable in the supremum norm.

Lemma 3.5.2. *[46] Let $y(x,t)$ be a smooth function defined on $\bar{\Omega}$ and $y_i^j = y(x_i, t_j)$ be the corresponding discrete function on $\bar{\Omega}^{N,M}$. Then the truncation error at the interior mesh points (x_i, t_j) to the discrete scheme $\mathcal{L}_{\varepsilon}^{N,M}$ is given by*

$$
\begin{aligned}
\tau_i^j &= |\mathcal{L}_\varepsilon^{N,M} y_i^j - \mathcal{L}_\varepsilon y(x_i,t_j)|, \quad 1 \le i < N,\\
&= \begin{cases} |\mathcal{L}_{cen,i}^{N,M} y_i^j - \mathcal{L}_\varepsilon y(x_i,t_j)|, & 1 \le i \le \frac{N}{2},\\ |\mathcal{L}_{mup,i}^{N,M} y_i^j - \mathcal{L}_\varepsilon y(x_{i+\frac{1}{2}},t_j)|, & \frac{N}{2}+1 \le i < N, \end{cases}\\
&\le \begin{cases} C[\Delta t + h\int_{x_{i-1}}^{x_{i+1}} \big(\varepsilon|y_{xxxx}| + |y_{xxx}|\big)dx], & \text{for } 1 \le i \le \frac{N}{2},\\ C[\Delta t + \varepsilon H\int_{x_{i-1}}^{x_{i+1}} |y_{xxxx}| + H\int_{x_{i-1}}^{x_{i+1}}(|y_{xxx}| + |y_{xx}|)], & \text{for } \frac{N}{2}+1 \le i < N. \end{cases}
\end{aligned}
$$

The truncation error at the left boundary point is given by

$$
\begin{aligned}
B_{L,\varepsilon}^N \tau_0^j &= B_{L,\varepsilon}^N y_0^j - B_{L,\varepsilon}^N y(x_0,t_j),\\
&= \left[f_0^j - \frac{y_0^{j-1}}{\Delta t} + \left(\frac{a_0}{\varepsilon} - \frac{2}{h_0}\right) q_0^j \right]\\
&\quad - \left[\left(\frac{-2\varepsilon}{h_0^2} + \frac{a_0}{\varepsilon} - \frac{2}{h_0} - b_0 - \frac{1}{\Delta t}\right) y_0^j + \left(\frac{2\varepsilon}{h_0^2}\right) y_1^j \right].
\end{aligned}
$$

Using $\varepsilon(y_{xx})_0^j + a_0(y_x)_0^j - b_0 y_0^j - \frac{y_0^j - y_0^{j-1}}{\Delta t} = f_0^j$ and Taylor's expansion of y_1^j about h_0 gives

$$
\begin{aligned}
B_{L,\varepsilon}^N \tau_0^j &= \left[\varepsilon(y_{xx})_0^j + a_0(y_x)_0^j - b_0^j y_0^j - \frac{y_0^j - y_0^{j-1}}{\Delta t} - \frac{y_0^{j-1}}{\Delta t} + \left(\frac{a_0}{\varepsilon} - \frac{2}{h_0}\right)\left(y_0^j - \varepsilon (y_x)_0^j \right) \right]\\
&- \left[\left(\frac{-2\varepsilon}{h_0^2} + \frac{a_0}{\varepsilon} - \frac{2}{h_0} - b_0 - \frac{1}{\Delta t}\right) y_0^j + \left(\frac{2\varepsilon}{h_0^2}\right) \left(y_0^j + h_0 (y_x)_0^j + \frac{h_0^2}{2}(y_{xx})_0^j + \frac{h_0^3}{6}(y_{xxx})_0^j \right) \right].
\end{aligned}
$$

Simplifying the above expression results in the error bound at the left boundary point

$$
|B_{L,\varepsilon}^N \tau_0^j| \le C\varepsilon h_0 (y_{xxx})_0^j. \tag{3.12}
$$

Similarly, the truncation error at the right boundary point is given by

$$
\begin{aligned}
B_{R,\varepsilon}^N \tau_N^j &= B_{R,\varepsilon}^N y_N^j - B_{R,\varepsilon}^N y(x_N,t_j),\\
&= y_N^j + \varepsilon(y_x)_N^j - (y_N^j + \varepsilon D_x^- y_N^j),\\
&= \varepsilon\left(\frac{\partial}{\partial x} - D_x^-\right) y(x_N,t_j).
\end{aligned}
$$

The classical estimate gives

$$B^N_{R,\varepsilon}\tau^j_N \leq \frac{\varepsilon}{2}(x_N - x_{N-1})|y_{xx}(x_N, t_j)|.$$

We have the following error bound at the right boundary point

$$|B^N_{R,\varepsilon}\tau^j_N| \leq C\varepsilon h_N|(y_{xx})(x_N, t_j)|. \tag{3.13}$$

To obtain a parameter-uniform error estimate, the numerical solution $U^j_i = U(x_i, t_j)$ of the hybrid scheme Eq. (3.3) is decomposed into discrete regular component V^j_i and discrete singular component W^j_i, which is given by $U(x_i, t_j) = V(x_i, t_j) + W(x_i, t_j)$, $(x_i, t_j) \in \Omega$, where $V(x_i, t_j)$ is the solution of the non-homogeneous problem given by

$$\begin{cases} \mathcal{L}^{N,M}_\varepsilon V(x_i, t_j) = r^j_i, & (x_i, t_j) \in \Omega, \\ B^N_{L,\varepsilon}V(0, t_j) = B_{L,\varepsilon}v(0, t_j), & t_j \in \Omega^M_t, \\ B^N_{R,\varepsilon}V(1, t_j) = B_{R,\varepsilon}v(1, t_j), & t_j \in \Omega^M_t, \\ V(x_i, 0) = s_i, & x_i \in \bar{\Omega}^N_x, \end{cases} \tag{3.14}$$

and $W(x_i, t_j)$ is the solution of the following homogeneous problem

$$\begin{cases} \mathcal{L}^{N,M}_\varepsilon W(x_i, t_j) = 0, & (x_i, t_j) \in \Omega, \\ B^N_{l,\varepsilon}W(0, t_j) = q^j_0 - B_{l,\varepsilon}v(0, t_j), & t_j \in \Omega^M_t, \\ B^N_{r,\varepsilon}W(1, t_j) = 0, & t_j \in \Omega^M_t, \\ W(x_i, 0) = 0, & x_i \in \bar{\Omega}^N_x. \end{cases} \tag{3.15}$$

The error in the numerical solution can be obtained from

$$U^j_i - u(x_i, t_j) = V^j_i - v(x_i, t_j) + W^j_i - w(x_i, t_j), \quad (x_i, t_j) \in \bar{\Omega}.$$

Now, we estimate the error bound in the regular and singular components separately.

Theorem 3.2. *Under the assumption Eq.* (3.11)*, the following error estimate is satisfied by the regular component at each mesh points* $(x_i, t_j) \in \bar{\Omega}$

$$|(V - v)(x_i, t_j)| \le C(N^{-2} + \Delta t).$$

where V is the solution of Eq. (3.14) and v is the solution of the continuous problem in Lemma (3.3.3).

Proof. From Eq. (3.12), the truncation error at the left boundary point is given by

$$|B^N_{L,\varepsilon}(V - v)(x_0, t_j)| \le C\varepsilon h_0 (v_{xxx})(x_0, t_j).$$

Using the bound on the derivatives of v in Lemma (3.3.3), we have

$$\begin{aligned} |B^N_{L,\varepsilon}(V - v)(x_0, t_j)| &\le C\varepsilon h_0(1 + \varepsilon^{-1}) \\ &\le Ch_0(\varepsilon + 1). \end{aligned}$$

Since $\varepsilon \le CN^{-1}$ together with $h_0 = x_1 - x_0 = N^{-1}$, we have the following error estimate at the left boundary point

$$|B^N_{L,\varepsilon}(V - v)(x_0, t_j)| \le CN^{-2}.$$

From Eq. (3.13), the truncation error at the right boundary point is given by

$$|B^N_{R,\varepsilon}(V - v)(x_N, t_j)| \le C\varepsilon h_N (v_{xx})(x_N, t_j).$$

Using the bound on the derivatives of v in Lemma (3.3.3), we have

$$|B^N_{R,\varepsilon}(V - v)(x_N, t_j)| \le C\varepsilon h_N.$$

Since $\varepsilon \leq CN^{-1}$ and noting that $h_N = x_N - x_{N-1} = N^{-1}$, we have the following error estimate at the right boundary point

$$|B^N_{R,\varepsilon}(V-v)(x_N,t_j)| \leq CN^{-2}.$$

From Lemma (3.5.2), we have

$$|\mathcal{L}^{N,M}_{\varepsilon}(V-v)(x_i,t_j)| \leq \begin{cases} C[N^{-2}+\Delta t], & 1 \leq i < \frac{N}{2}, \\ C[N^{-1}(\varepsilon+N^{-1})+\Delta t], & \frac{N}{2} \leq i < N. \end{cases}$$

Since $\varepsilon \leq CN^{-1}$, we get

$$|\mathcal{L}^{N,M}_{\varepsilon}(V-v)(x_i,t_j)| \leq C\big(N^{-2}+\Delta t\big), \;\; 1 \leq i < N.$$

Applying the discrete minimum principle, we obtain the desired result. □

To prove ε-uniform error estimates on the singular component, first we have to state the following two lemmas.

Lemma 3.5.3. *On $\bar{\Omega}^N_x = \{x_i\}^N_0$, define the following mesh functions*

$$S_i = \prod_{k=1}^{i}\left(1+\frac{\alpha h_k}{\varepsilon}\right)^{-1}, \quad 1 \leq i \leq N,$$

with the usual convention that $S_0 = 1$ for $i = 0$. Then, there exists a positive constant C such that for $i = 1, \cdots, N-1$, we have

$$\mathcal{L}^{N,M}_{\varepsilon} S_i \leq \frac{CS_i}{\max\{\varepsilon,\; h_{i+1}\}}.$$

Proof. For the proof, see Lemma (2.5.5). □

Lemma 3.5.4. *[127] The mesh function S_i satisfies the following inequality*

$$e^{-\alpha x_i/\varepsilon} \leq \prod_{k=1}^{i} \left(1 + \frac{\alpha h_k}{\varepsilon}\right)^{-1} = S_i, \quad \textit{for all } 0 \leq i \leq N, \tag{3.16}$$

and on Shishkin mesh, mesh function $S_{\varepsilon,i}$ also satisfies the following inequality

$$\prod_{k=1}^{i} (1 + \frac{\alpha h_k}{\varepsilon})^{-1} \leq \begin{cases} CN^{-4i/N}, & 0 < i < \frac{N}{2}, \\ CN^{-2}, & \frac{N}{2} \leq i < N. \end{cases} \tag{3.17}$$

Lemma 3.5.5. *Let $S_N = \{x_i\}_0^N$ with $h_i = x_i - x_{i-1}$ for all i. Then, the following inequalities hold*

$$N^{-2} \leq \prod_{k=1}^{N/2} \left(1 + \frac{\alpha h_k}{\varepsilon}\right)^{-1} \leq CN^{-2}.$$

Proof. Using inequality $\ln(1 + x) \leq x - x^2/4$ for $0 \leq x \leq 1$, one can express

$$\begin{aligned} \ln \prod_{k=1}^{N/2} \left(1 + \frac{\alpha h_k}{\varepsilon}\right)^{-1} &= -\sum_{k=1}^{N/2} \ln \left(1 + \frac{\alpha h_k}{\varepsilon}\right) \\ &\geq \frac{-\alpha N}{2\varepsilon} h \\ &\geq \frac{-\alpha}{\varepsilon} \lambda = \ln N^{-2}, \end{aligned}$$

from which the left inequality is proved.

For the right inequality, we use $\ln(1 + x) \geq x - x^2/2$ and obtain

$$\begin{aligned} \ln \prod_{k=1}^{N/2} \left(1 + \frac{\alpha h_k}{\varepsilon}\right) &= \sum_{k=1}^{N/2} \ln \left(1 + \frac{\alpha h_k}{\varepsilon}\right) \\ &\geq \sum_{k=1}^{N/2} \left(\frac{\alpha h_k}{\varepsilon} - \frac{\alpha^2 h_k^2}{2\varepsilon^2}\right) \\ &= \frac{\alpha N}{2\varepsilon} h - \frac{\alpha^2}{2\varepsilon^2} \sum_{k=1}^{N/2} h_k^2. \end{aligned}$$

Since $h = \frac{2\sigma}{N}$ and $\sigma = \frac{2\varepsilon \ln N}{\alpha}$, the above expression becomes

$$\ln \prod_{k=1}^{N/2} \left(1 + \frac{\alpha h_k}{\varepsilon}\right)^{-1} \leq \frac{\alpha^2}{2\varepsilon^2} \sum_{k=1}^{N/2} h_k^2 - 2 \ln N,$$

from which the right inequality follows. □

Theorem 3.3. *Under the assumption in Eq.* (3.11)*, the following error estimate is satisfied by the singular component at each mesh points* $(x_i, t_j) \in \bar{\Omega}$*,*

$$|(W - w)(x_i, t_j)| \leq C(N^{-2} \ln^2 N + \Delta t),$$

Proof. Using Eqs. (3.12) and (3.13), we have the following inequalities

$$|B^N_{L,\varepsilon}(W - w)(x_0, t_j)| \leq CN^{-2} \ln^2 N.$$
$$|B^N_{R,\varepsilon}(W - w)(x_N, t_j)| \leq CN^{-2}.$$

When $\sigma = \sigma_0 \varepsilon \ln N$, the mesh is piecewise uniform. There arises two cases.

Case (i): For $(x_i, t_j) \in [\sigma, 1] \times (0, T]$, using triangle inequality and Lemma (3.3.4) gives

$$\begin{aligned}
|(W - w)(x_i, t_j)| &\leq |W(x_i, t_j)| + |w(x_i, t_j)|, \\
&\leq C \prod_{k=i+1}^{N} \left(1 + \frac{\alpha h_k}{\varepsilon}\right)^{-1} + Ce^{-\alpha x_i/\varepsilon}, \\
&\leq C \prod_{k=i+1}^{N} \left(1 + \frac{\alpha h_k}{\varepsilon}\right)^{-1} + C \prod_{k=1}^{i} \left(1 + \frac{\alpha h_k}{\varepsilon}\right)^{-1}, \quad \text{using Eq. (3.16)} \\
&= C \prod_{k=1}^{N} \left(1 + \frac{\alpha h_k}{\varepsilon}\right)^{-1}.
\end{aligned}$$

Using Eq. (3.17) in the above expression, the error bound in the outer layer region is given by:

$$|(W - w)(x_i, t_j)| \leq CN^{-2}, \qquad (x_i, t_j) \in [\sigma, 1] \times (0, T].$$

Case (ii): For $(x_i, t_j) \in [0, \sigma] \times (0, T]$, the truncation error in Lemma (3.5.2) becomes

$$
\begin{aligned}
|\mathcal{L}_{\varepsilon}^{N,M}(W-w)(x_i,t_j)| &\leq C\big[\Delta t + h\int_{x_{i-1}}^{x_{i+1}} \big(\varepsilon|w_{xxxx}| + |w_{xxx}|\big)dx\big],\\
&\leq C\big[\Delta t + h\int_{x_{i-1}}^{x_{i+1}} \Big(\varepsilon\Big(\frac{\alpha^4}{\varepsilon^4}e^{-\alpha x/\varepsilon}\Big) + \Big(\frac{\alpha^3}{\varepsilon^3}e^{-\alpha x/\varepsilon}\Big)\Big)dx\big],\\
&\leq C\left[\Delta t + \frac{h}{\varepsilon^3}\int_{x_{i-1}}^{x_{i+1}} e^{-\alpha x/\varepsilon}dx\right], \quad \text{since } \alpha > 0,\\
&\leq C\left[\Delta t + \frac{h}{\varepsilon^3}(\frac{-\varepsilon}{\alpha})e^{-\alpha x/\varepsilon}|_{x_{i-1}}^{x_{i+1}}\right],\\
&\leq C\big[\Delta t - \frac{h}{\alpha\varepsilon^2}\big(e^{-\alpha x_{i+1}/\varepsilon} - e^{-\alpha x_{i-1}/\varepsilon}\big)\big].
\end{aligned}
$$

Since $h_i = x_i - x_{i-1} \Rightarrow x_{i-1} = x_i - h_i$ and $h_{i+1} = x_{i+1} - x_i \Rightarrow x_{i+1} = x_i + h_{i+1}$, we have

$$
\begin{aligned}
|\mathcal{L}_{\varepsilon}^{N,M}(W-w)(x_i,t_j)| &\leq C\big[\Delta t - \frac{h}{\alpha\varepsilon^2}\big(e^{-\alpha(x_i+h_{i+1})/\varepsilon} - e^{-\alpha(x_i-h_i)/\varepsilon}\big)\big],\\
&\leq C\big[\Delta t - \frac{h}{\alpha\varepsilon^2}\big(e^{-\alpha x_i/\varepsilon}e^{-\alpha h_{i+1}/\varepsilon} - e^{-\alpha x_i/\varepsilon}e^{\alpha h_i/\varepsilon}\big)\big],\\
&\leq C\big[\Delta t + \frac{h}{\alpha\varepsilon^2}e^{-\alpha x_i/\varepsilon}\big(e^{\frac{\alpha h}{\varepsilon}} - e^{\frac{-\alpha h}{\varepsilon}}\big)\big], \quad \text{since } h_i = h_{i+1} = h \text{ on } [0,\sigma],\\
&\leq C\big[\Delta t + \frac{h}{\alpha\varepsilon^2}e^{-\alpha x_i/\varepsilon}\sinh\big(\frac{\alpha h}{\varepsilon}\big)\big], \quad \text{since } \sinh(\frac{\alpha h}{\varepsilon}) = \frac{e^{\frac{\alpha h}{\varepsilon}} - e^{\frac{-\alpha h}{\varepsilon}}}{2}
\end{aligned}
$$

Using the assumption in Eq. (3.11), we get $\frac{\alpha h}{\varepsilon} < 2$ and $\sinh(\xi) \leq C\xi$, for $0 \leq \xi \leq 2$. So, $\sinh\big(\frac{\alpha h}{\varepsilon}\big) \leq \frac{C\alpha h}{\varepsilon}$. Thus, truncation error estimate reduces to

$$
\begin{aligned}
|\mathcal{L}_{\varepsilon}^{N,M}(W-w)(x_i,t_j)| &\leq C\big[\Delta t + \frac{h^2}{\varepsilon^3}e^{-\alpha x_i/\varepsilon}\big],\\
&\leq C\big(\Delta t + \frac{N^{-2}\ln^2 N}{\varepsilon}S_i\big), \quad \text{(by using Eq. (3.16))}.
\end{aligned} \tag{3.18}
$$

Using estimate in Eq. (3.18), we construct the discrete barrier functions

$$
\Psi^{\pm}(x_i,t_j) = C\left(N^{-2} + N^{-2}\ln^2 N e^{-\alpha x_i/\varepsilon}\prod_{k=1}^{i}\big(1 + \frac{\alpha h_k}{\varepsilon}\big) + t_j\Delta t\right) \pm (W-w)(x_i,t_j).
$$

We can easily observe that $\Psi^{\pm}(x_0,t_j) - \varepsilon\Psi_x^{\pm}(x_0,t_j) \geq 0$, $\Psi^{\pm}(x_N,t_j) + \varepsilon\Psi_x^{\pm}(x_N,t_j) \geq 0$ and $\mathcal{L}_{\varepsilon}^{N,M}\Psi^{\pm}(x_i,t_j) \leq 0$. Applying the discrete minimum principle the barrier functions

$\Psi^{\pm}(x_i, t_j) \geq 0$. Using the discrete barrier functions defined above and applying discrete minimum principle, we get

$$|(W - w)(x_i, t_j)| \leq C\big(N^{-2}\ln^2 N + \Delta t\big),$$

on $(x_i, t_j) \in [0, \sigma] \times (0, T]$. $\square$

The above discussions leads us to the following main convergence theorem.

Theorem 3.4. *Let $u(x_i, t_j)$ be the continuous solution and U_i^j be the discrete solution using the hybrid scheme. Then, parameter-uniform error satisfies the following bound*

$$\sup_{0<\varepsilon\leq 1} \max_{0\leq i\leq N; 0\leq j\leq M} |U_i^j - u(x_i, t_j)| \leq \begin{cases} C\big(N^{-2}\ln^2 N + \Delta t\big), & 0 \leq i \leq \frac{N}{2}, \\ C\big(N^{-2} + \Delta t\big), & \frac{N}{2} < i \leq N, \end{cases}$$

where C is a constant independent of ε and the mesh parameters.

Proof. From triangular inequality $|U_i^j - u(x_i, t_j)| \leq |V_i^j - v(x_i, t_j)| + |W_i^j - w(x_i, t_j)|$ and Theorems (3.2) and (3.3), the required result follows. $\square$

3.6 Numerical Results

The numerical experiments that support the theoretical findings presented in the preceding sections are demonstrated in this section.

Example 3.6.1. *From [53], consider the following singularly perturbed parabolic convection-diffusion problem*

$$\varepsilon\frac{\partial^2 u(x,t)}{\partial x^2} + \frac{\partial u(x,t)}{\partial x} - \frac{\partial u(x,t)}{\partial t} = -4t^3, \qquad (x,t) \in (0,1) \times (0,1],$$

with the initial condition and boundary conditions

$$\begin{cases} u(x,0) = 0, & 0 \le x \le 1, \\ -\varepsilon \frac{\partial u(0,t)}{\partial x} = t^2, & 0 \le t \le 1, \\ u(1,t) = 0, & 0 \le t \le 1. \end{cases}$$

Example 3.6.2. *The next example is the following singularly perturbed parabolic convection-diffusion problem [53]*

$$\varepsilon \frac{\partial^2 u(x,t)}{\partial x^2} + \frac{\partial u(x,t)}{\partial x} - \frac{\partial u(x,t)}{\partial t} = -20t^3(x+\varepsilon)e^{-\frac{x}{\varepsilon}}, \quad (x,t) \in (0,1) \times (0,1],$$

with the initial condition and boundary conditions

$$\begin{cases} u(x,0) = 0, & 0 \le x \le 1, \\ -\varepsilon \frac{\partial u(0,t)}{\partial x} = t^5, & 0 \le t \le 1, \\ u(1,t) = -t^4(t-5-5\varepsilon)e^{-\frac{1}{\varepsilon}}, & 0 \le t \le 1. \end{cases}$$

Maximum absolute errors are calculated using the formulas in Eq. (2.31). The parameter-uniform error and rate of convergence are calculated using Eq. (2.32) since the analytical solution for the examples are not available.

Table 3.1: Computation of $E_\varepsilon^{N,\Delta t}$ for Example (3.6.1).

	Number of space mesh interval N = Number of step size in time, $\frac{1}{\Delta t}$						
$\varepsilon \downarrow$	16	32	64	128	256	512	1024
2^{-5}	5.4303e-2	2.7015e-2	1.3561e-2	6.8298e-3	3.4439e-3	1.7377e-3	8.7734e-4
2^{-6}	5.8782e-2	2.9218e-2	1.4595e-2	7.3113e-3	3.6669e-3	1.8398e-3	9.2323e-4
2^{-8}	6.1467e-2	3.0821e-2	1.5388e-2	7.6907e-3	3.8461e-3	1.9239e-3	9.6245e-4
2^{-10}	6.1940e-2	3.1119e-2	1.5561e-2	7.7800e-3	3.8908e-3	1.9458e-3	9.7303e-4
2^{-12}	6.2040e-2	3.1180e-2	1.5595e-2	7.7987e-3	3.9005e-3	1.9508e-3	9.7558e-4
2^{-14}	6.2064e-2	3.1194e-2	1.5603e-2	7.8027e-3	3.9026e-3	1.9519e-3	9.7613e-4
2^{-16}	6.2070e-2	3.1198e-2	1.5605e-2	7.8037e-3	3.9030e-3	1.9521e-3	9.7625e-4
2^{-18}	6.2072e-2	3.1199e-2	1.5605e-2	7.8039e-3	3.9032e-3	1.9522e-3	9.7628e-4
2^{-20}	6.2072e-2	3.1199e-2	1.5605e-2	7.8040e-3	3.9032e-3	1.9522e-3	9.7629e-4

Table 3.2: Comparison of $E^{N,\Delta t}$ and $R^{N,\Delta t}$ for Example (3.6.1).

	Number of space mesh interval N = Number of step size in time, $\frac{1}{\Delta t}$						
	16	32	64	128	256	512	1024
Present Result							
$E^{N,\Delta t}$	6.2072e-2	3.1199e-2	1.5605e-2	7.8040e-3	3.9032e-3	1.9522e-3	9.7629e-4
$R^{N,\Delta t}$	0.9924	0.9995	0.9997	0.9996	0.9996	0.9997	
Result in CH (2) (BS-mesh)							
$E^{N,\Delta t}$	2.4039e-1	1.2545e-1	6.3240e-2	3.1569e-2	1.5735e-2	7.8475e-3	3.9167e-3
$R^{N,\Delta t}$	0.9383	0.9882	1.0023	1.0045	1.0038	1.0026	-
Result in CH-(2) (S-mesh)							
$E^{N,\Delta t}$	3.9714e-1	2.4388e-1	1.4426e-1	8.3222e-2	4.7114e-2	2.6291e-2	1.4506e-2
$R^{N,\Delta t}$	0.7035	0.7575	0.7936	0.8208	0.8416	0.8579	-
Result in [53]							
$E^{N,\Delta t}$	1.512e+0	9.143e-1	5.338e-1	3.018e-1	1.642e-1	8.461e-2	3.936e-2

Table 3.3: Comparison of $E_{\varepsilon}^{N,\Delta t}$ for Example (3.6.2) for $\varepsilon = 2^{-10}$.

	Number of mesh intervals						
$\frac{1}{\Delta t} \downarrow$	$N = 16$	32	64	128	256	512	1024
Present Result							
16	8.9859e-2	3.4862e-2	1.2372e-2	4.0292e-3	1.1310e-3	1.7032e-4	1.5340e-4
32	9.0057e-2	3.5005e-2	1.2505e-2	4.1601e-3	1.2616e-3	3.0087e-4	3.9233e-5
64	9.0163e-2	3.5082e-2	1.2576e-2	4.2305e-3	1.3318e-3	3.7111e-4	6.3656e-5
128	9.0217e-2	3.5121e-2	1.2613e-2	4.2670e-3	1.3682e-3	4.0751e-4	1.0005e-4
256	9.0245e-2	3.5141e-2	1.2632e-2	4.2856e-3	1.3868e-3	4.2603e-4	1.1858e-4
512	9.0259e-2	3.5151e-2	1.2641e-2	4.2949e-3	1.3961e-3	4.3538e-4	1.2792e-4
1024	9.0266e-2	3.5157e-2	1.2646e-2	4.2996e-3	1.4008e-3	4.4007e-4	1.3261e-4
Result in [53]							
	1.40e+0	8.69e-1	5.19e-1	3.02e-1	1.73e-1	9.70e-2	5.39e-2

Table 3.4: Computation of $E_\varepsilon^{N,\Delta t}$ for Example (3.6.2).

	Number of mesh intervals $N = M$						
$\varepsilon \downarrow$	16	32	64	128	256	512	1024
Present Result							
2^{-6}	8.4875e-2	3.2962e-2	1.1623e-2	3.7974e-3	1.1517e-3	3.1738e-4	7.3428e-5
2^{-8}	8.9442e-2	3.4510e-2	1.2349e-2	4.1583e-3	1.3334e-3	4.0873e-4	1.1922e-4
2^{-10}	8.9859e-2	3.5005e-2	1.2576e-2	4.2670e-3	1.3868e-3	4.3538e-4	1.3261e-4
2^{-12}	9.0186e-2	3.5143e-2	1.2640e-2	4.2981e-3	1.4018e-3	4.4262e-4	1.3701e-4
2^{-14}	9.0270e-2	3.5179e-2	1.2657e-2	4.3064e-3	1.4059e-3	4.4462e-4	1.3710e-4
2^{-16}	9.0291e-2	3.5188e-2	1.2661e-2	4.3085e-3	1.4069e-3	4.4514e-4	1.3736e-4
2^{-18}	9.0296e-2	3.5190e-2	1.2663e-2	4.3090e-3	1.4072e-3	4.4527e-4	1.3743e-4
2^{-20}	9.0298e-2	3.5191e-2	1.2663e-2	4.3092e-3	1.4073e-3	4.4531e-4	1.3745e-4

Table 3.5: Comparison of $E^{N,\Delta t}$ and $R^{N,\Delta t}$ for Example (3.6.2).

	Number of mesh intervals $N = M$						
	16	32	64	128	256	512	1024
Present Result							
$E^{N,\Delta t}$	9.0298e-2	3.5191e-2	1.2663e-2	4.3092e-3	1.4073e-3	4.4532e-4	1.3745e-4
$R^{N,\Delta t}$	1.3595	1.4746	1.5551	1.6145	1.6600	1.6959	-
Result in CH (2) (BS-mesh)							
$E^{N,\Delta t}$	1.8673e-1	9.7656e-2	4.8860e-2	2.4149e-2	1.1942e-2	5.9249e-3	2.9483e-3
$R^{N,\Delta t}$	0.9352	0.9990	1.0167	1.0159	1.0112	1.0069	
Result in CH-(2) (S-mesh)							
$E^{N,\Delta t}$	3.4707e-1	2.1734e-1	1.3014e-1	7.5844e-2	4.3326e-2	2.4369e-2	1.3538e-2
$R^{N,\Delta t}$	0.6753	0.7399	0.7789	0.8078	0.8302	0.8480	

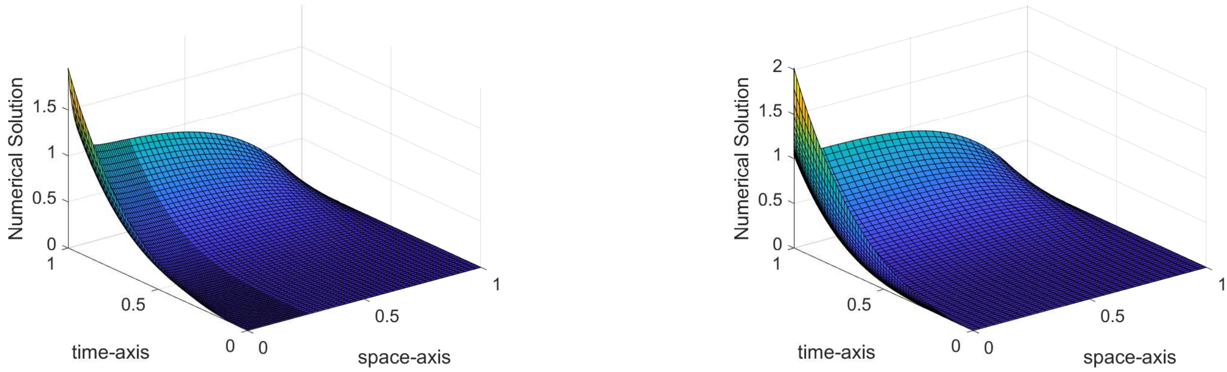

(a) $N = 64 = \frac{1}{\Delta t}$, $\varepsilon = 2^{-5}$ **(b)** $N = 64 = \frac{1}{\Delta t}$, $\varepsilon = 2^{-15}$

Figure 3.1: Surface plot of Example (3.6.1) to show left layer formation as $\varepsilon \to 0$.

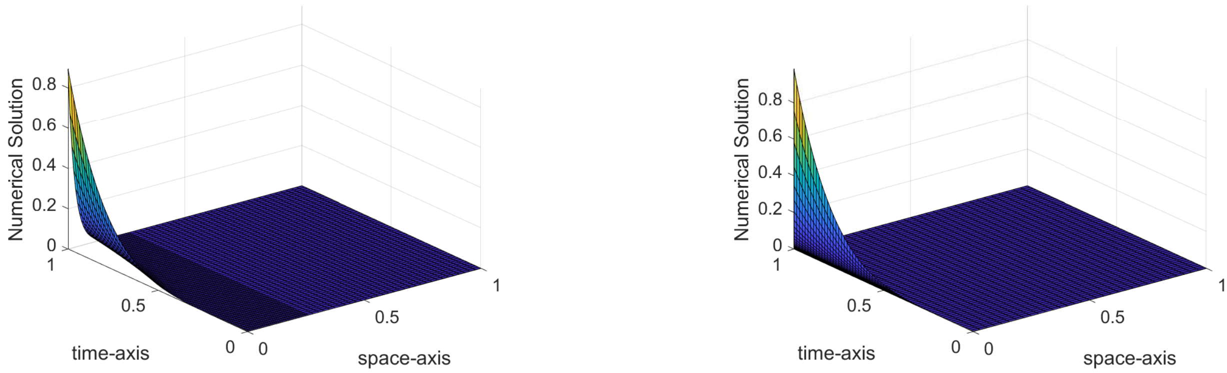

(a) $N = 64 = \frac{1}{\Delta t}$, $\varepsilon = 2^{-5}$ **(b)** $N = 64 = \frac{1}{\Delta t}$, $\varepsilon = 2^{-15}$

Figure 3.2: Surface plot of Example (3.6.2) to show left layer formation as $\varepsilon \to 0$.

3.7 Discussion and Conclusion

Computational results in Table (3.1) show that the current method has improved the upwind method in Chapter (2) for Example (3.6.1). The computed results in Tables (3.1)-(3.3) depict that the present method provides parameter-uniform convergence for Examples (3.6.1) and (3.6.2). The formation of the left boundary layer for different values of ε can be visualized using surface plots, as shown in Figures (3.1)-(3.2) for Examples (3.6.1)-(3.6.2), respectively. All numerical simulations show that the problem under consideration has a boundary layer near $x = 0$. In Figures (3.3), one can observe that a sufficient amount of mesh points and computed solutions are in the boundary layer re-

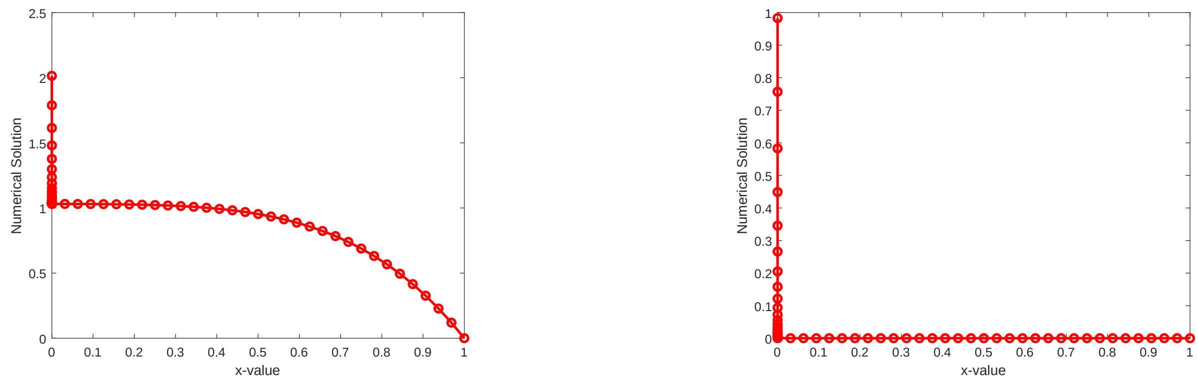

(a) Example (3.6.1). **(b)** Example (3.6.2).

Figure 3.3: Layer resolving property of the method at $\varepsilon = 2^{-15}, N = M = 64$.

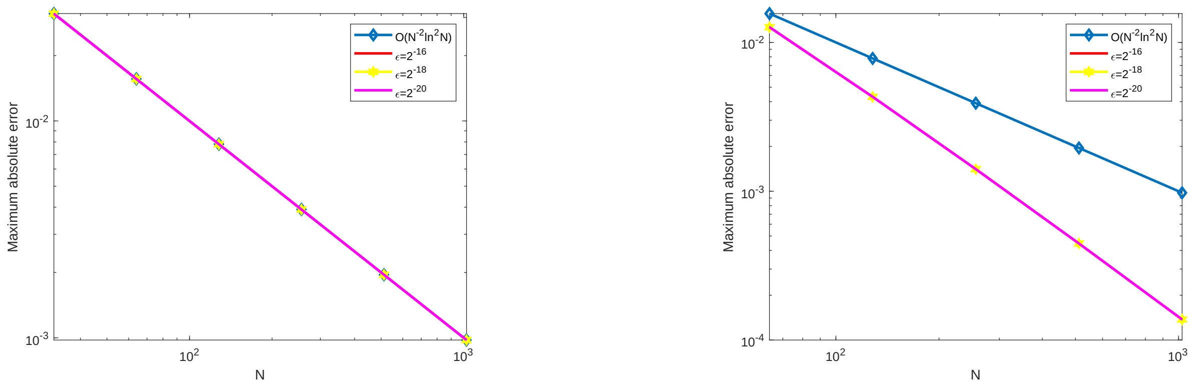

(a) Example (3.6.1) using Table (3.1). **(b)** Example (3.6.2) using Table (3.5).

Figure 3.4: Loglog plot of maximum absolute errors.

gion. Figure (3.4) depicts a plot of the maximum absolute errors in log-log scale using the results in Tables (3.1) and (3.3) for Examples (3.6.1) and (3.6.2), respectively. From the numerical results, we observe that as the number of mesh points rises, the maximum absolute errors decrease and the order of convergence increases. We have shown theoretically that the hybrid finite difference scheme is second-order parameter-uniformly convergent in the space direction with a logarithmic factor and first-order uniformly convergent in the time direction, which is confirmed in Table (3.3) as almost second-order convergent. Our numerical results for Example (3.6.2) in Table (3.3) show that the present method is nearly second-order except for Example (3.6.1) which is first-order convergent. From the loglog plot of Example (3.6.1) in Figure (3.4a), we can observe that the theoretical order of convergence is overlapped with the numerical order of convergence. The theoretical convergence analysis reveals that the present method is second-order in the space direction and first-order in the time direction. From computational result, we found that first-order in time does not reduce the order of convergence of the present method for second example. Even if the accuracy is improved, the rate of convergence of the present method reduces to one for the first example based on the numerical result in Table (3.1). From this table we observe first-order parameter-uniform convergence confirming that the global error is dominated by the time discretization error for this test example and space discretization error cannot be seen. This shows that some of the numerical examples are scheme dependent.

Chapter 4

Fitted Mesh Central Finite Difference Method for Singularly Perturbed Parabolic Convection-diffusion Problem having a Boundary Turning Point

In this chapter, a numerical method for the singularly perturbed parabolic convection-diffusion turning point problem (TPP) with Robin boundary conditions is developed. The solution to the considered problem has a boundary layer on the left side of the domain. The present method comprises an implicit trapezoidal method for time discretization on a uniform mesh and second-order central difference schemes for space discretization on a Shishkin mesh. The stability and convergence analysis of the discrete problem are well established. To validate the present method, some numerical experiments are performed on two examples. It has been demonstrated that the numerical solution generated by the present method converges uniformly to the solution of the continuous solution regardless of the perturbation parameter.

4.1 Introduction

Singularly perturbed parabolic convection-diffusion problems in which the convection coefficient vanishes at some points of the domain of the problem are called singularly perturbed turning point problems and zeros of the convection coefficient are said to be turning points. Zeros that coincide with the boundary are referred as boundary turning points, whereas zeros inside the domain of differential equations are interior turning points.

Different scholars developed various numerical methods for singularly perturbed convection diffusion turning point problems with Dirichlet boundary conditions, see [33], [45], [59], [69], [78], [79], [81], [102], [116], [125] and [126]. However, singularly perturbed convection-diffusion turning point problems with Robin boundary conditions was studied for the first time by Janani Jayalakshmi and Tamilselvan [56]. As far as our knowledge is concerned, no further study has been conducted. Since the previous work is first-order convergent, we developed almost second-order convergent method. In this chapter, the central finite difference methods on Shishkin mesh for space direction and the implicit trapezoidal method on uniform mesh for time direction have been developed for the problem under consideration.

4.2 Definition of the Problem

On the space-time domain $(x,t) \in \Omega = (0,1) \times (0,T]$, where T is some fixed positive value, consider the following singularly perturbed parabolic convection-diffusion-reaction problem having a boundary turning point

$$\mathcal{L}_\varepsilon u(x,t) \equiv \varepsilon \frac{\partial^2 u(x,t)}{\partial x^2} + a(x,t)\frac{\partial u(x,t)}{\partial x} - b(x,t)u(x,t) - \frac{\partial u(x,t)}{\partial t} = f(x,t), \tag{4.1}$$

with the initial condition and the boundary conditions

$$\begin{cases} u(x,0) = \phi_B(x), & 0 \le x \le 1, \\ B_{L,\varepsilon}u(0,t) \equiv u(0,t) - \sqrt{\varepsilon}\frac{\partial u(0,t)}{\partial x} = \phi_L(t), & 0 < t \le T, \\ B_{R,\varepsilon}u(1,t) \equiv u(1,t) + \sqrt{\varepsilon}\frac{\partial u(1,t)}{\partial x} = \phi_R(t), & 0 < t \le T, \end{cases} \tag{4.2}$$

where $0 < \varepsilon \ll 1$ is perturbation parameter. To ensure uniqueness of the solution, we assume the functions involved in Eq. (4.1)-(4.2) are sufficiently smooth and bounded functions such that the convection and reaction coefficients satisfy the conditions $a(x,t) = a_0(x,t)x^p,\ p \ge 1, a_0(x,t) \ge \alpha > 0,\ b(x,t) \ge \beta > 0,\ \forall (x,t) \in \bar{\Omega}$. The problem has left layer of width $O(\sqrt{\varepsilon})$. The convection coefficient $a(x,t)$ in Eq. (4.1) vanishes at $x = 0$, that is, $a(0,t) = 0$, then the turning point coincides with the left boundary. Due to this, the problem in Eq. (4.1) is termed as a boundary turning point problem and the point $x = 0$ is called a turning point. The existence and uniqueness for the solution to Eq. (4.1)-(4.2) can be established under the assumption that the data are Hölder continuous and satisfy an appropriate compatibility conditions at the corner points $(0,0)$ and $(1,0)$. The boundary functions $\phi_L, \phi_R \in C^k([0,T]), \phi_B \in C^{(1,k)}([0,1])$ should satisfy the k^{th} order compatibility condition for the initial function if

$$\frac{\partial^k}{\partial t^k}\left(\phi_B - \sqrt{\varepsilon}\frac{\partial \phi_B}{\partial x}\right)(0,0) = \frac{d^k\phi_L(0)}{\partial t^k},$$
$$\frac{\partial^k}{\partial t^k}\left(\phi_B + \sqrt{\varepsilon}\frac{\partial \phi_B}{\partial x}\right)(1,0) = \frac{d^k\phi_R(0)}{\partial t^k}.$$
$$-\frac{\partial \phi_L(0)}{\partial t} + \varepsilon\frac{\partial^2 \phi_B(0,0)}{\partial x^2} + a(0,0)\frac{\partial \phi_B(0,0)}{\partial x} - b(0,0)\phi_B(0,0) = f(0,0),$$
$$-\frac{\partial \phi_R(1)}{\partial t} + \varepsilon\frac{\partial^2 \phi_B(1,0)}{\partial x^2} + a(1,0)\frac{\partial \phi_B(1,0)}{\partial x} - b(1,0)\phi_B(1,0) = f(1,0).$$

4.3 Properties of the Continuous Solution

When studying the numerical solutions of singularly perturbed problems, the analytical solution plays a vital role. Here, we present the bound for the analytical solution of the continuous problem in Eq. (4.1)-(4.2), which can be used for finding the bounds of the discrete solution and its derivatives. Setting the parameter value $\varepsilon = 0$, the reduced problem corresponding to Eq. (4.1)-(4.2) is

$$\begin{cases} a(x,t)\frac{\partial u_0(x,t)}{\partial x} - b(x,t)u_0(x,t) - \frac{\partial u_0(x,t)}{\partial t} = f(x,t), & (x,t) \in \Omega, \\ u_0(x,0) = \phi_B(x), & 0 \le x \le 1, \\ u_0(1,t) = \phi_R(t), & 0 < t \le T, \end{cases} \tag{4.3}$$

which is a first-order hyperbolic partial differential equation. The boundary $x = 0$ is a characteristic curve of the reduced problem when $a(0,t) = 0$ and $b(0,t) > 0$, and the solution of Eq. (4.1)-(4.2) has a parabolic boundary layer of width $O(\sqrt{\varepsilon})$ in the neighborhood of the left boundary as all the characteristic curves of the reduced problem in Eq. (4.3) is parallel to the left boundary. The assumption for Eq. (4.1)-(4.2) satisfies the continuous minimum principle.

Theorem 4.1. *Let $Z(x,t) \in C^{(2,1)}(\bar{\Omega})$ be smooth function such that $\mathcal{L}_\varepsilon Z(x,t) \le 0, (x,t) \in \Omega,\ B_{L,\varepsilon}Z(0,t) \ge 0,\ t \in [0,T],\ B_{R,\varepsilon}Z(1,t) \ge 0,\ t \in [0,T];\ Z(x,0) \ge 0,\ x \in [0,1]$. Then, $Z(x,t) \ge 0$, for all $(x,t) \in \bar{\Omega}$.*

Proof. Suppose that the arbitrary function Z takes its minimum value at the point $(x^*,t^*) \in \bar{\Omega}$ such that $Z(x^*,t^*) = \min_{(x,t)\in\bar{\Omega}} Z(x,t)$ and assume that $Z(x^*,t^*) < 0$. Clearly, (x^*,t^*) is not in the boundary.

Case (i). For $(0,t^*)$, we have $\frac{\partial Z}{\partial x}(0,t^*) = 0$. Hence, $B_{L,\varepsilon}Z(0,t^*) = Z(0,t^*) - \sqrt{\varepsilon}\dfrac{\partial Z}{\partial x}(0,t^*) < 0$, which is a contradiction.

Case (ii). For $(1,t^*)$, we have $\frac{\partial Z}{\partial x}(1,t^*) = 0$. Hence, $B_{R,\varepsilon}Z(1,t^*) = Z(1,t^*) + \sqrt{\varepsilon}\dfrac{\partial Z}{\partial x}(1,t^*) < 0$, which is a contradiction.

Case (iii). For $(x^*,t^*) \in \Omega$, then $\frac{\partial Z}{\partial t}(x^*,t^*) = 0$ and $\frac{\partial^2 Z}{\partial x^2}(x^*,t^*) \ge 0$. Hence,

$$\mathcal{L}_\varepsilon Z(x^*,t^*) = \varepsilon\frac{\partial^2 Z}{\partial x^2}(x^*,t^*) + a(x^*,t^*)\frac{\partial Z}{\partial x}(x^*,t^*) - \frac{\partial Z}{\partial t}(x^*,t^*) - b(x^*,t^*)Z(x^*,t^*) > 0,$$

which is a contradiction to the assumption that $\mathcal{L}_\varepsilon Z(x,t) \geq 0,\ \forall (x,t) \in \Omega$. It follows that $Z(x^*, t^*) \geq 0$ and thus $Z(x,t) \geq 0,\ \forall (x,t) \in \bar{\Omega}$. □

To show on the bounds of the solution $u(x,t)$, we assume, without loss of generality $\phi_B(x) = 0$. The next lemma proves the stability estimate to obtain unique solution.

Lemma 4.3.1. *The solution $u(x,t) \in C^{(2,1)}(\bar{\Omega})$ of the continuous problem satisfies*

$$|u(x,t)| \leq \max\left\{|\phi_B(x)|,\ |\phi_L(t)|,\ |\phi_R(t)|\right\} + \frac{\|f\|}{\alpha}.$$

Proof. To prove this lemma, we define two smooth barrier functions $\Theta^{\pm}$ as

$$\Theta^{\pm}(x,t) = \max\left\{|\phi_B(x)|, |\phi_L(t)|, |\phi_R(t)|\right\} + \frac{\|f\|}{\alpha} \pm u(x,t).$$

Now, we evaluate the barrier functions at the initial and boundary conditions.
At $t = 0$, we have

$$\Theta^{\pm}(x,0) = \max\left\{|\phi_B(x)|, |\phi_L(0)|, |\phi_R(0)|\right\} + \frac{\|f\|}{\alpha} \pm \phi_B(x) \geq 0.$$

At $x = 0$, we have

$$\Theta^{\pm}(0,t) = \max\left\{|\phi_B(0)|, |\phi_L(t)|, |\phi_R(t)|\right\} + \frac{\|f\|}{\alpha} \pm u(0,t). \tag{4.4}$$

From Eq. (4.4), we deduce the following

$$\begin{aligned} u(0,t) &= \pm\Theta^{\pm}(0,t) \mp \max\left\{|\phi_B(0)|, |\phi_L(t)|, |\phi_R(t)|\right\} + \frac{\|f\|}{\alpha}, \\ \frac{\partial u(0,t)}{\partial x} &= \pm\frac{\partial \Theta^{\pm}(0,t)}{\partial x} \mp |\phi_B'(0)|. \end{aligned} \tag{4.5}$$

Using Eq. (4.5) in the left boundary condition and rearranging gives

$$\Theta^{\pm}(0,t) - \sqrt{\varepsilon}\frac{\partial \Theta^{\pm}(0,t)}{\partial x} = \max\left\{|\phi_B(0)|, |\phi_L(t)|, |\phi_R(t)|\right\} + \frac{\|f\|}{\alpha} \pm \phi_L(t) - \sqrt{\varepsilon}|\phi_B'(0)| \geq 0,$$

for $\phi_B'(0) \leq 0$ and $\max\left\{|\phi_B(0)|, |\phi_L(t)|, |\phi_R(t)|\right\} + \frac{\|f\|}{\alpha} \pm \phi_L(t) \geq 0$. A very similar procedures establish the stability proof for the right boundary condition. On Ω, we have

$$\begin{aligned}\mathcal{L}_\varepsilon\Theta^\pm(x,t) &= \varepsilon\frac{\partial^2\Theta^\pm(x,t)}{\partial x^2} + a(x,t)\frac{\partial\Theta^\pm(x,t)}{\partial x} - b(x,t)\Theta^\pm(x,t) - \frac{\partial\Theta^\pm(x,t)}{\partial t},\\ &= \varepsilon|\phi_B''(x)| + a(x,t)|\phi_B'(t)| - \max\{\phi_L'(t), \phi_R'(t)\}\\ &- b(x,t)\times\left(\max\left\{|\phi_B(x)|, |\phi_L(t)|, |\phi_R(t)|\right\} + \frac{\|f\|}{\alpha}\right) \pm f(x,t) \leq 0.\end{aligned}$$

From the minimum principle, it follows that $\Theta^\pm(x,t) \leq 0, \ \forall (x,t) \in \bar{\Omega}$. □

The next theorem provides the bounds for the solution and its derivatives.

Theorem 4.2. *Let* $a, b, f \in C^{(2+\gamma, 1+\gamma/2)}(\bar{\Omega}), \phi_L, \phi_R \in C^{(\frac{3+\gamma}{2})}([0,T]), \phi_B \in C^{(4+\gamma, 2+\gamma/2)}([0,1])$ $\gamma \in (0,1)$. *Under the smooth conditions, the derivatives of the solution* u *satisfy the bound for all nonnegative integers* l, m *such that* $0 \leq l + 2m \leq 4$

$$\left\|\frac{\partial^{l+m}u}{\partial x^l \partial t^m}\right\|_{\bar{\Omega}} \leq C\varepsilon^{-l/2},$$

where the constant C *is independent of* ε.

Proof. The bounds on the solution and derivatives are obtained by transforming independent variable x to the stretched variable $\hat{x} = x/\sqrt{\varepsilon}$. Under this transformation, Eq. (4.1) is transformed as

$$\frac{\partial^2\hat{u}(\hat{x},t)}{\partial\hat{x}^2} + \hat{a}(\hat{x},t)\varepsilon^{\frac{p-1}{2}}\frac{\partial\hat{u}(\hat{x},t)}{\partial\hat{x}} - \hat{b}(\hat{x},t)\hat{u}(\hat{x},t) - \frac{\partial\hat{u}(\hat{x},t)}{\partial t} = \hat{f}(\hat{x},t), \quad (\hat{x},t) \in \hat{\Omega},$$

with the initial condition and the boundary condition of Robin type

$$\begin{cases}\hat{u}(\hat{x},0) = \phi_B(\hat{x}), & \hat{x} \in (0, \frac{1}{\sqrt{\varepsilon}}),\\ \hat{u}(0,t) - \frac{\partial\hat{u}(0,t)}{\partial\hat{x}} = \phi_L(t), & 0 < t \leq T,\\ \hat{u}(1,t) + \frac{\partial\hat{u}(1,t)}{\partial\hat{x}} = \phi_R(t), & 0 < t \leq T,\end{cases}$$

where $\hat{\Omega} = (0, \frac{1}{\sqrt{\varepsilon}}) \times (0, T]$. For $p = 1$, the transformed differential equation is independent of ε, we use the estimate in [72] to get

$$\left\| \frac{\partial^{l+m} \hat{u}}{\partial \hat{x}^l \partial t^m} \right\|_{\hat{N}_\delta} \leq C(1 + \|\hat{u}\|_{N_{2\delta}}), \qquad l, m \geq 0, \;\; 0 \leq l + 2m \leq 4,$$

for all $\hat{N}_\delta$ in $\hat{\Omega}$. Here, $\hat{N}_\delta$, $\delta > 0$, is a neighborhood with diameter δ in $\hat{\Omega}$ and C is independent of $\hat{N}_\delta$. Similar argument follows for $p > 1$ as we neglect the term involving $\varepsilon^{\frac{p-1}{2}}$ which is very small. Returning back to the original variable x, we get

$$\left\| \frac{\partial^{l+m} u}{\partial x^l \partial t^m} \right\|_{\bar{\Omega}} \leq C\varepsilon^{-l/2}(1 + \|u\|_{\bar{\Omega}}), \qquad l, m \geq 0, \;\; 0 \leq l + 2m \leq 4.$$

for all $\hat{N}_\delta$ in $\hat{\Omega}$. Here, $\hat{N}_\delta$, $\delta > 0$, is a neighborhood with diameter δ in $\hat{\Omega}$ and C is independent of $\hat{N}_\delta$. Similar argument follows for $p > 1$ as we neglect the term involving $\varepsilon^{\frac{p-1}{2}}$ which is very small. Returning back to the original variable x, we get

$$\left\| \frac{\partial^{l+m} u}{\partial x^l \partial t^m} \right\|_{\bar{\Omega}} \leq C\varepsilon^{-l/2}(1 + \|u\|_{\bar{\Omega}}), \qquad l, m \geq 0, \;\; 0 \leq l + 2m \leq 4.$$

The proof is completed by using the bound on u given in Lemma (4.3.1). □

The next theorem provides the bounds for the solution and its derivatives. The above classical bounds on the derivatives of the solution are not adequate for the proof of $\varepsilon-$uniform error estimate. To obtain the stronger bounds on the derivatives of the solution u of Eq. (4.1)-(4.2), we decompose the solution u as the sum $u = v + w$, where v is the solution of the regular and w is the singular components. The regular component v is further be decomposed into

$$v = v_0 + \varepsilon v_1 + \varepsilon^2 v_2,$$

where v_0 satisfies the following solution of reduced first-order problem

$$\begin{cases} a\frac{\partial v_0}{\partial x}(x,t) - bv_0(x,t) - \frac{\partial v_0}{\partial t}(x,t) = f(x,t), & (x,t) \in \Omega, \\ B_{R,\varepsilon}v_0(1,t) = \phi_R(t), & 0 < t \leq T, \\ v_0(x,0) = \phi_B(x), & 0 \leq x \leq 1, \end{cases} \tag{4.6}$$

and v_1 is solution of the following first-order problem

$$\begin{cases} a\frac{\partial v_1}{\partial x}(x,t) - bv_1(x,t) - \frac{\partial v_1}{\partial t}(x,t) = -\frac{\partial^2 v_0}{\partial x^2}(x,t), & (x,t) \in \Omega, \\ B_{L,\varepsilon}v_1(0,t) = 0, & 0 < t \leq T, \\ B_{R,\varepsilon}v_1(1,t) = 0, & 0 < t \leq T, \\ v_1(x,0) = 0, & 0 \leq x \leq 1, \end{cases} \tag{4.7}$$

and v_2 satisfies the following second-order

$$\begin{cases} \mathcal{L}_\varepsilon v_2(x,t) = -\frac{\partial^2 v_1}{\partial x^2}(x,t), & (x,t) \in \Omega, \\ B_{L,\varepsilon}v_2(0,t) = 0, & 0 < t \leq T, \\ B_{R,\varepsilon}v_2(1,t) = 0, & 0 < t \leq T, \\ v_2(x,0) = 0, & 0 \leq x \leq 1. \end{cases} \tag{4.8}$$

The regular component v is the solution to the non-homogeneous problem

$$\begin{cases} \mathcal{L}_\varepsilon v(x,t) = f(x,t), & (x,t) \in \Omega, \\ B_{L,\varepsilon}v(0,t) = B_{L,\varepsilon}v_0(0,t), & 0 < t \leq T, \\ B_{R,\varepsilon}v(1,t) = B_{R,\varepsilon}v_0(1,t), & 0 < t \leq T, \\ v(x,0) = \phi_B(x), & 0 \leq x \leq 1. \end{cases}$$

With v defined, w is the solution of the following homogeneous problem

$$\begin{cases} \mathcal{L}_\varepsilon w(x,t) = 0, & (x,t) \in \Omega, \\ B_{L,\varepsilon} w(0,t) = \phi_L(t) - B_{L,\varepsilon} v_0(0,t), & 0 < t \le T, \\ B_{R,\varepsilon} w(1,t) = 0, & 0 < t \le T, \\ w(x,0) = 0, & 0 \le x \le 1. \end{cases}$$

Therefore, the non-classical bounds in regular and singular components and its derivatives are established in the following theorem.

Theorem 4.3. *Let* $a, b, f \in C^{(4+\gamma, 2+\gamma/2)}(\bar{\Omega})$, $\phi_L, \phi_R \in C^{(\frac{5+\gamma}{2})}([0,T])$, $\phi_B \in C^{(6+\gamma, 3+\gamma/2)}([0,1])$, $\gamma \in (0,1)$. *Assume that the compatibility conditions for* $k = 0,1,2,3$ *are satisfied. Then, for all nonnegative integers* l, m *such that* $0 \le l + 2m \le 4$*, the regular component* v *satisfies the bound*

$$\left\| \frac{\partial^{l+m} v}{\partial x^l \partial t^m} \right\| \le C\big(1 + \varepsilon^{2-l/2}\big),$$

and the singular component w *satisfies the bound*

$$\left| \frac{\partial^{l+m} w}{\partial x^l \partial t^m} \right| \le C\varepsilon^{-l/2} e^{-x\sqrt{\frac{\beta}{\varepsilon}}},$$

where C *is a constant independent of* ε.

Proof. Since the first-order partial differential equations in Eqs. (4.6) and (4.7) do not contain the perturbation parameter ε, we can have the following bound

$$\left\| \frac{\partial^{l+m} v_k}{\partial x^l \partial t^m} \right\|_{\bar{\Omega}} \le C, \quad \text{for } \; k = 0, 1, \tag{4.9}$$

whereas v_2 in Eq. (4.8) is the solution for the second-order homogeneous initial-boundary value problem which is a singular perturbation problem of the form Eq. (4.1). Hence, from Theorem (4.2), we can obtain

$$\left\|\frac{\partial^{l+m}v_2}{\partial x^l\partial t^m}\right\|_{\bar{\Omega}} \leq C\varepsilon^{-l/2}. \tag{4.10}$$

Consider the following inequality to proof the bound in regular component v

$$\left\|\frac{\partial^{l+m}v}{\partial x^l\partial t^m}\right\|_{\bar{\Omega}} \leq \sum_{k=0}^{2}\varepsilon^k\left\|\frac{\partial^{l+m}v_k}{\partial x^l\partial t^m}\right\|_{\bar{\Omega}}. \tag{4.11}$$

Combining the bounds in Eqs. (4.9) and (4.10) into Eq. (4.11), we obtain the required bound for the regular component v as

$$\left\|\frac{\partial^{l+m}v}{\partial x^l\partial t^m}\right\|_{\bar{\Omega}} \leq C(1+\varepsilon^{2-l/2}).$$

The bound for singular component w is obtained by using the barrier functions

$$\Phi^{\pm}(x,t) = Ce^{-x\sqrt{\frac{\beta}{\varepsilon}}}e^t \pm w(x,t), \quad \forall (x,t)\in\bar{\Omega},$$

for sufficiently large C such that $\Phi^{\pm}(x,t)\geq 0$ at all the boundaries. Now, on $(x,t)\in\Omega$,

$$\begin{aligned}\mathcal{L}_\varepsilon\Phi^{\pm}(x,t) &= \varepsilon\left[\frac{\beta}{\varepsilon}Ce^{-x\sqrt{\frac{\beta}{\varepsilon}}}e^t \pm w_{xx}\right] + a(x,t)\left[-\sqrt{\frac{\beta}{\varepsilon}}Ce^{-x\sqrt{\frac{\beta}{\varepsilon}}}e^t \pm w_x\right]\\ &\quad - b(x,t)\left[Ce^{-x\sqrt{\frac{\beta}{\varepsilon}}}e^t \pm w\right] - \left(Ce^{-x\sqrt{\frac{\beta}{\varepsilon}}}e^t \pm w_t\right),\\ &= Ce^{-x\sqrt{\frac{\beta}{\varepsilon}}}e^t\left(\beta - a(x,t)\sqrt{\frac{\beta}{\varepsilon}} - b(x,t) - 1\right) \pm f(x,t), \quad \text{since } b(x,t)\geq\beta>0,\\ &\leq 0, \quad \forall (x,t)\in\Omega.\end{aligned}$$

Using the minimum principle, we have

$$|w| \leq Ce^{-x\sqrt{\frac{\beta}{\varepsilon}}}e^t \leq Ce^{-x\sqrt{\frac{\beta}{\varepsilon}}}, \quad \text{since } 0\leq t\leq T,\ e^t\leq e^T\leq C \ \ \forall (x,t)\in\bar{\Omega}.$$

The bound on the derivatives of w can be obtained based on [72] and [79]. □

4.4 Formulation of the Numerical Method

In this section, the space derivative is discretized using central finite difference methods based on a piecewise-uniform Shishkin mesh and the time derivative is discretized using an implicit trapezoidal method on a uniform mesh.

4.4.1 Time Discretization

To discretize in the time direction, we use an implicit trapezoidal method on a uniform mesh. Let M be a positive integer different from one, we divide the time interval $[0, T]$ with uniform step length Δt. Hence, the interval $[0, T]$ is partitioned into M equal sub-intervals with each nodal points satisfying $0 = t_0 < t_1 < \cdots < t_{M-1} < t_M = T$. Thus, the time nodal points are generated by $t_j = j\Delta t,\ \Delta t = \frac{T}{M},\ j = 0, \cdots, M$, where M denotes the mesh intervals in the time direction. The semi-discretized problem becomes

$$\begin{aligned}\mathcal{L}_\varepsilon^M U^{j+\frac{1}{2}}(x) &\equiv \varepsilon(U_{xx})^{j+\frac{1}{2}}(x) + (aU_x)^{j+\frac{1}{2}}(x) - (bU)^{j+\frac{1}{2}}(x) - \frac{U^{j+1}(x) - U^j(x)}{\Delta t} \\ &= f^{j+\frac{1}{2}}(x),\end{aligned} \tag{4.12}$$

where $U^{j+\frac{1}{2}}(x) = (U^{j+1}(x) + U^j(x))/2$ and $U^{j+1}(x)$ is the numerical solution of $u(x, t_{j+1})$ at $(j+1)^{th}$ time level. The truncated Taylor series expansion gives

$$\begin{aligned}U^{j+1}(x) &= U^{j+\frac{1}{2}}(x) + \frac{\Delta t}{2}\frac{\partial U^{j+\frac{1}{2}}(x)}{\partial t} + \frac{(\Delta t)^2}{8}\frac{\partial^2 U^{j+\frac{1}{2}}(x)}{\partial t^2} + \frac{(\Delta t)^3}{48}\frac{\partial^3 U^{j+\frac{1}{2}}(x)}{\partial t^3}, \\ U^{j}(x) &= U^{j+\frac{1}{2}}(x) - \frac{\Delta t}{2}\frac{\partial U^{j+\frac{1}{2}}(x)}{\partial t} + \frac{(\Delta t)^2}{8}\frac{\partial^2 U^{j+\frac{1}{2}}(x)}{\partial t^2} - \frac{(\Delta t)^3}{48}\frac{\partial^3 U^{j+\frac{1}{2}}(x)}{\partial t^3}.\end{aligned} \tag{4.13}$$

From Eq. (4.13), we obtain

$$\frac{\partial U^{j+\frac{1}{2}}(x)}{\partial t} = \frac{U^{j+1}(x) - U^j(x)}{\Delta t} + \zeta, \tag{4.14}$$

where $\zeta = -\frac{(\Delta t)^2}{24}\frac{\partial^3 U^{j+\frac{1}{2}}(x)}{\partial t^3}$.

Equation (4.14) gives the following global error bound in time semi-discretization

$$\|E_j\|_\infty \leq C(\Delta t)^2, \tag{4.15}$$

where C is an arbitrary constant given by $C = \frac{1}{24}\|\frac{\partial^3 U^{j+\frac{1}{2}}(x)}{\partial t^3}\|$ which is independent of the parameters ε and Δt. From the semi-discrete problem in Eq. (4.12), we have

$$\varepsilon(U_{xx})^{j+1}(x) + a^{j+1}(x)(U_x)^{j+1}(x) - \left(b^{j+1}(x) + \frac{2}{\Delta t}\right) U^{j+1}(x) = Z^j(x), \tag{4.16}$$

with the semi-discrete initial condition and boundary conditions

$$\begin{cases} U^0(x) = \phi_B(x), & 0 \leq x \leq 1, \\ U^{j+1}(0) - \sqrt{\varepsilon}(U_x)^{j+1}(0) = \phi_L^{j+1}, & 0 \leq j \leq M, \\ U^{j+1}(1) + \sqrt{\varepsilon}(U_x)^{j+1}(1) = \phi_R^{j+1}, & 0 \leq j \leq M, \end{cases} \tag{4.17}$$

where $Z^j(x) = -\varepsilon(U_{xx})^j(x) - a^j(x)(U_x)^j(x) + \left(b^j(x) - \frac{2}{\Delta t}\right) U^j(x) + f^{j+1}(x) + f^j(x)$.

4.4.2 Space Discretization

The space domain $\bar{\Omega}_x^N = [0, 1]$ is divided into two sub-domains $[0, \sigma]$ and $[\sigma, 1]$ by placing a uniform mesh with $N/2$ mesh intervals in each of the sub-domains where σ is the transition point defined as $\sigma = \min\{\frac{1}{2}, \frac{2\sqrt{\varepsilon}}{\sqrt{\beta}} \ln N\}$. For $\sigma = 1/2$, the mesh is uniform and for $\sigma = \frac{2\sqrt{\varepsilon}}{\sqrt{\beta}} \ln N$, the mesh points get condensed at the left side of the domain. The space mesh points condensing at the boundary point $x_0 = 0$ is given by

$$x_i = \begin{cases} ih, & \text{for } 0 \leq i \leq \frac{N}{2}, \\ \sigma + \left(i - \frac{N}{2}\right)H, & \text{for } \frac{N}{2} < i \leq N, \end{cases}$$

The space mesh widths for $i = 0, 1, 2, \cdots, N$ can be given as

$$h_i = x_{i+1} - x_i = \begin{cases} h = \frac{2\sigma}{N}, & \text{for } 1 \le i \le \frac{N}{2}, \\ H = \frac{2(1-\sigma)}{N}, & \text{if } \frac{N}{2} < i \le N, \end{cases}$$

where h and H are the space step size in $[0, \sigma]$ and $[\sigma, 1]$, respectively. For error analysis, assume that $\sigma = \frac{2\sqrt{\varepsilon}}{\sqrt{\beta}} \ln N$. We assume $\sqrt{\varepsilon} \le CN^{-1}$ for the numerical solution of singularly perturbed parabolic convection-diffusion turning point problems [79]. As $\varepsilon \to 0$, it is well known that the use of second-order central difference methods for the second- and first-order derivatives in the differential equation gives unstable numerical solution on a uniform mesh. However, as reported in [50] and [77], the use of Shishkin mesh induces stability. Following [16], [17] and [18], we fully discretize the problem in Eq. (4.16) using second-order central finite difference approximation both for the second- and first derivatives in space direction on a Shishkin mesh. To obtain the overall second-order method in space direction, we use the second-order central difference operator for the first derivatives in the left and right boundary conditions in Eq. (4.17). The numerical scheme takes the following form

$$\mathcal{L}_\varepsilon^{N,M} U_i^{j+1} \equiv \varepsilon \delta^2 U_i^{j+1} + a_i^{j+1} D_x^0 U_i^{j+1} - \left(b_i^{j+1} + \frac{2}{\Delta t} \right) U_i^{j+1} = Z_i^j, \tag{4.18}$$

where $Z_i^j = -\varepsilon \delta^2 U_i^j - a_i^j D_x^0 U_i^j + \left(b_i^j - \frac{2}{\Delta t} \right) U_i^j + f_i^{j+1} + f_i^j$. We have the following fully discrete initial condition and boundary conditions

$$\begin{cases} U_i^0 = \phi_B(x_i), & 0 < i < N, \\ U_0^{j+1} - \sqrt{\varepsilon} D_x^0 U_0^{j+1} = \phi_L^{j+1}, & 0 \le j < M, \\ U_N^{j+1} + \sqrt{\varepsilon} D_x^0 U_N^{j+1} = \phi_R^{j+1}, & 0 \le j < M. \end{cases} \tag{4.19}$$

After rearranging the terms in Eq. (4.18), we arrive at the following recurrence relation of the form

$$\mathcal{L}_{\varepsilon}^{N,M}U_i^{j+1} \equiv r_i^- U_{i-1}^{j+1} + r_i^c U_i^{j+1} + r_i^+ U_{i+1}^{j+1} = s_i^- U_{i-1}^{j} + s_i^c U_i^{j} + s_i^+ U_{i+1}^{j} + H_i^j, \tag{4.20}$$

where coefficients for $1 \le i \le N-1$ and $0 \le j < M$ are given as

$$\begin{cases} r_i^- = \dfrac{2\varepsilon}{h_i(h_i+h_{i+1})} - \dfrac{a_i^{j+1}}{h_{i+1}+h_i}, \\ r_i^c = \dfrac{-2\varepsilon}{h_i h_{i+1}} - b_i^{j+1} - \dfrac{2}{\Delta t}, \\ r_i^+ = \dfrac{2\varepsilon}{h_{i+1}(h_i+h_{i+1})} + \dfrac{a_i^{j+1}}{h_{i+1}+h_i}, \end{cases}$$

$$\begin{cases} s_i^- = \dfrac{-2\varepsilon}{h_i(h_i+h_{i+1})} + \dfrac{a_i^{j}}{h_{i+1}+h_i}, \\ s_i^c = \dfrac{2\varepsilon}{h_i h_{i+1}} + b_i^{j} - \dfrac{2}{\Delta t}, \\ s_i^+ = \dfrac{-2\varepsilon}{h_{i+1}(h_i+h_{i+1})} - \dfrac{a_i^{j}}{h_{i+1}+h_i}, \\ H_i^j = f_i^{j+1} + f_i^j. \end{cases}$$

The left boundary condition in Eq. (4.19) can be written as

$$U_0^{j+1} - \sqrt{\varepsilon}\frac{U_1^{j+1} - U_{-1}^{j+1}}{h_0 + h_1} = \phi_L^{j+1}, \tag{4.21}$$

where U_{-1}^{j+1} is a ghost value at $x_{-1} = -h_1$ with $h_0 := h_1$. Thus, we have

$$U_{-1}^{j+1} = \frac{2h_0}{\sqrt{\varepsilon}}\phi_L^{j+1} - \frac{2h_0}{\sqrt{\varepsilon}}U_0^{j+1} + U_1^{j+1} \tag{4.22}$$

The value U_{-1}^{j+1} must be eliminated from the difference scheme Eq. (4.20) at $i = 0$ obtaining

$$r_0^- U_{-1}^{j+1} + r_0^c U_0^{j+1} + r_0^+ U_1^{j+1} = s_0^- U_{-1}^{j} + s_0^c U_0^{j} + s_0^+ U_1^{j} + H_0^j. \tag{4.23}$$

Substituting the expression in Eqs. (4.22) into (4.23) and rearranging, we obtain the following approximation at the left boundary point

$$\begin{aligned} r_0^c U_0^{j+1} + r_0^+ U_1^{j+1} = s_0^c U_0^j + s_0^+ U_1^j + H_0^j + \left(\frac{2\sqrt{\varepsilon}}{h_0} + \frac{a_0^j}{\sqrt{\varepsilon}}\right)\phi_L^j \\ - \left(\frac{2\sqrt{\varepsilon}}{h_0} - \frac{a_0^{j+1}}{\sqrt{\varepsilon}}\right)\phi_L^{j+1}, \end{aligned} \tag{4.24}$$

where the coefficients for $i = 0,\ 0 \le j < M$ are given by

$$\begin{aligned} r_0^c &= \frac{-2\varepsilon}{h_0^2} - \frac{2\sqrt{\varepsilon}}{h_0} + \frac{a_0^{j+1}}{\sqrt{\varepsilon}} - b_0^{j+1} - \frac{2}{\Delta t}; \qquad r_0^+ = \frac{2\varepsilon}{h_0^2}, \\ s_0^c &= \frac{2\varepsilon}{h_0^2} + \frac{2\sqrt{\varepsilon}}{h_0} - \frac{a_0^j}{\sqrt{\varepsilon}} + b_0^j - \frac{2}{\Delta t}; \qquad s_0^+ = \frac{-2\varepsilon}{h_0^2}. \end{aligned}$$

The right boundary condition in Eq. (4.19) can be written as

$$U_N^{j+1} + \sqrt{\varepsilon}\frac{U_{N+1}^{j+1} - U_{N-1}^{j+1}}{h_N + h_{N+1}} = \phi_R^{j+1}, \tag{4.25}$$

where U_{N+1}^{j+1} is a ghost value at $x_{N+1} = 1 + h_N$ with $h_{N+1} := h_N$. Thus, we have

$$U_{N+1}^{j+1} = \frac{2h_N}{\sqrt{\varepsilon}}\phi_R^{j+1} + U_{N-1}^{j+1} - \frac{2h_N}{\sqrt{\varepsilon}}U_N^{j+1}. \tag{4.26}$$

Similarly, the value U_{N+1}^{j+1} must be eliminated from Eq. (4.20) at $i = N$ giving

$$r_N^- U_{N-1}^{j+1} + r_N^c U_N^{j+1} + r_N^+ U_{N+1}^{j+1} = s_N^- U_{N-1}^j + s_N^c U_N^j + s_N^+ U_{N+1}^j + H_N^j. \tag{4.27}$$

Substituting the expression in Eq. (4.26) into Eq. (4.27) and rearranging, we obtain the following approximation at the right boundary point

$$\begin{aligned} r_N^- U_{N-1}^{j+1} + r_N^c U_N^{j+1} = s_N^- U_N^j + s_N^c U_N^j + H_N^j + \left(\frac{-2\sqrt{\varepsilon}}{h_N} - \frac{a_N^j}{\sqrt{\varepsilon}}\right)\phi_R^j \\ - \left(\frac{2\sqrt{\varepsilon}}{h_N} + \frac{a_N^{j+1}}{\sqrt{\varepsilon}}\right)\phi_R^{j+1}, \end{aligned} \tag{4.28}$$

where the coefficients for $i = N,\ 0 \le j < M$ are given by

$$r_N^- = \frac{2\varepsilon}{h_N^2}; \qquad r_N^c = \frac{-2\varepsilon}{h_N^2} - \frac{2\sqrt{\varepsilon}}{h_N} - \frac{a_N^{j+1}}{\sqrt{\varepsilon}} - b_N^{j+1} - \frac{2}{\Delta t},$$
$$s_N^- = \frac{-2\varepsilon}{h_N^2}; \qquad s_N^c = \frac{2\varepsilon}{h_N^2} + \frac{2\sqrt{\varepsilon}}{h_N} + \frac{a_N^{j}}{\sqrt{\varepsilon}} + b_N^{j} - \frac{2}{\Delta t}.$$

The coefficient matrix of the discrete scheme in Eq. (4.20) together with the discrete boundary conditions in Eqs. (4.24) and (4.28) gives an $(N+1)\times(N+1)$ linear systems of equations which can be solved uniquely using matrix inversion method for the unknowns $U_0, U_1, \cdots, U_{N-1}, U_N$ at each time level.

4.5 Analysis of the Method

Following the techniques in [16], [20] and [22], in this section, we first prove the stability analysis and then the consistency of the present scheme. Finally, the convergence analysis via truncation error is presented. First, the stability analysis for solving the tri-diagonal system of equations in Eqs. (4.20), (4.24) and (4.28) is provided. For the present method to be stable if

$$|r_i^c| \ge |r_i^-| + |r_i^+|, \ \ |r_i^-| > 0, \ \ |r_i^+| > 0. \tag{4.29}$$

The above conditions guarantee that the system of linear equations is diagonally dominant. Now, the stability at the left boundary point is established by considering the source function and boundary function equal zero at $i = 0$. At $i = 0$, $a(0,t) = 0$ and $b(x,t) \ge \beta > 0,\ \forall (x,t) \in \bar{\Omega}$ from the continuous problem hold for the discrete problem. From Eq. (4.24), it is obvious that

$$|r_0^c| - |r_0^+| \ge 0 \Rightarrow \left|\frac{2\varepsilon}{h_0^2} + \frac{2\sqrt{\varepsilon}}{h_0} - \frac{a_0^{j+1}}{\sqrt{\varepsilon}} + b_0^{j+1} + \frac{2}{\Delta t}\right| - \left|\frac{2\varepsilon}{h_0^2}\right| > 0. \tag{4.30}$$

Since the above inequality is always true, the present scheme is unconditionally stable at the left boundary point. Similarly, we establish the stability at the right boundary point at $i = N$. At $i = N$, $a(N,t) \geq \alpha > 0$ and $b(x,t) \geq \beta > 0,\ \forall (x,t) \in \bar{\Omega}$ from the continuous problem hold for the discrete problem. From Eq. (4.28), we have

$$|r_N^c| - |r_N^-| \geq 0 \Rightarrow \left| \frac{2\varepsilon}{h_N^2} + \frac{2\sqrt{\varepsilon}}{h_N} + \frac{a_N^{j+1}}{\sqrt{\varepsilon}} + b_N^{j+1} + \frac{2}{\Delta t} \right| - \left| \frac{2\varepsilon}{h_N^2} \right| > 0. \tag{4.31}$$

Since the the above inequality is always true, the discrete scheme is unconditionally stable at the right boundary point.

To establish stability at the interior points, we use Eq. (4.20)

$$\begin{aligned} |r_i^- + r_i^+| &= \left| \frac{2\varepsilon}{h_i(h_i + h_{i+1})} - \frac{a_i^{j+1}}{h_{i+1} + h_i} + \frac{2\varepsilon}{h_{i+1}(h_i + h_{i+1})} + \frac{a_i^{j+1}}{h_{i+1} + h_i} \right| \\ &= \left| \frac{2\varepsilon}{h_i(h_i + h_{i+1})} + \frac{2\varepsilon}{h_{i+1}(h_i + h_{i+1})} \right| \\ &= \frac{2\varepsilon}{h_i h_{i+1}}, \end{aligned} \tag{4.32}$$

provided that $|a_i^{j+1}| \leq \frac{2\varepsilon}{h_i}$ and $|a_i^{j+1}| \leq \frac{2\varepsilon}{h_{i+1}}$. From stability condition in Eqs. (4.29) and (4.32), we have that

$$\begin{aligned} |r_i^- + r_i^+| < |r_i^c| &\Rightarrow \frac{2\varepsilon}{h_i h_{i+1}} < \left| \frac{-2\varepsilon}{h_i h_{i+1}} - b_i^{j+1} + \frac{2}{\Delta t} \right| \\ &\Rightarrow \frac{2\varepsilon}{h_i h_{i+1}} < \frac{2\varepsilon}{h_i h_{i+1}} + b_i^{j+1} - \frac{2}{\Delta t}. \end{aligned}$$

This is always true since $b(x,t) \geq \beta > 0$ on $[0,1]$ and Δt is step size in time direction. Using triangular inequality, we have

$$|r_i^-| + |r_i^+| \leq |r_i^c|,$$

which shows that the given system is diagonally dominant showing that the discrete scheme is stable at the interior points. Combining the stability results in Eq. (4.30), Eq. (4.31) and Eq. (4.32) gives the stability of the discrete scheme in Ω. Next, we establish convergence analysis via truncation error keeping the time direction constant. Truncation error at the left boundary point $i = 0$ is given as follows

$$T_0 = U_0 - \sqrt{\varepsilon}(U_x)_0 - \left(U_0 - \sqrt{\varepsilon}\frac{U_1 - U_{-1}}{h_0 + h_1}\right). \tag{4.33}$$

From Taylor series expansion of the terms U_{-1} and U_1 in space direction, we get

$$\begin{aligned} U_{-1} &\cong U_0 - h_0(U_x)_0 + \frac{h_0^2}{2!}(U_{xx})_0 - \frac{h_0^3}{3!}(U_{xxx})_0 + \cdots, \\ U_1 &\cong U_0 + h_1(U_x)_0 + \frac{h_1^2}{2!}(U_{xx})_0 + \frac{h_1^3}{3!}(U_{xxx})_0 + \cdots, \end{aligned} \tag{4.34}$$

From Eq. (4.34), we have

$$\frac{U_1 - U_{-1}}{h_0 + h_1} = (U_x)_0 + \frac{h_1 - h_0}{2}(U_{xx})_0 + \frac{h_1^3 + h_0^3}{6(h_0 + h_1)}(U_{xxx})_0. \tag{4.35}$$

Using Eq. (4.35) in Eq. (4.33) and simplifying, we have

$$T_0 = \sqrt{\varepsilon}\left(\frac{h_1 - h_0}{2}\right)(U_{xx})_0 + \sqrt{\varepsilon}\left(\frac{h_1^3 + h_0^3}{6(h_0 + h_1)}\right)(U_{xxx})_0, \tag{4.36}$$

as $h_0, h_1 \to 0$, then $T_0 \to 0$. This shows that the discrete scheme is consistent at the left boundary point. Truncation error at the right boundary point $i = N$ can be given by

$$T_N = U_N + \sqrt{\varepsilon}(U_x)_N - \left(U_N + \sqrt{\varepsilon}\frac{U_{N+1} - U_{N-1}}{h_N + h_{N+1}}\right). \tag{4.37}$$

From Taylor series expansion of the terms U_{N-1} and U_{N+1} in space direction, we get

$$\begin{aligned} U_{N-1} &\cong U_N - h_N(U_x)_N + \frac{h_N^2}{2!}(U_{xx})_N - \frac{h_N^3}{3!}(U_{xxx})_N + \cdots, \\ U_{N+1} &\cong U_N + h_{N+1}(U_x)_N + \frac{h_{N+1}^2}{2!}(U_{xx})_N + \frac{h_{N+1}^3}{3!}(U_{xxx})_N + \cdots, \end{aligned} \tag{4.38}$$

From Eq. (4.38), we have

$$\frac{U_{N+1} - U_{N-1}}{h_N + h_{N+1}} = (U_x)_N + \frac{h_{N+1} - h_N}{2}(U_{xx})_N + \frac{h_{N+1}^3 + h_N^3}{6(h_N + h_{N+1})}(U_{xxx})_N. \tag{4.39}$$

Using Eq. (4.39) in Eq. (4.37) and simplifying, we have

$$T_N = -\sqrt{\varepsilon}\left(\frac{h_{N+1} - h_N}{2}\right)(U_{xx})_N - \sqrt{\varepsilon}\left(\frac{h_{N+1}^3 + h_N^3}{6(h_N + h_{N+1})}\right)(U_{xxx})_N. \tag{4.40}$$

as $h_N, h_{N+1} \to 0$, then $T_N \to 0$. This shows that the discrete scheme is consistent at the right boundary point. The truncation error at the interior points is given by

$$\begin{aligned} T_i &= \mathcal{L}_\varepsilon^N(u_i - U_i), \\ &= \mathcal{L}_\varepsilon u_i - \mathcal{L}_\varepsilon^N U_i, \\ &= \varepsilon(u_{xx})_i + a_i(u_x)_i - b_i u_i - \left(\varepsilon\delta_x^2 U_i + a_i\delta_x^0 U_i - b_i U_i\right). \end{aligned} \tag{4.41}$$

At the nodal points x_i, we can write $u_i \cong U_i$ and Eq. (4.41) becomes

$$T_i = \varepsilon(U_{xx})_i + a_i(U_x)_i - \frac{2\varepsilon}{h_i + h_{i+1}}\left(\frac{U_{i+1} - U_i}{h_{i+1}} - \frac{U_i - U_{i-1}}{h_i}\right) - a_i\left(\frac{U_{i+1} - U_{i-1}}{h_i + h_{i+1}}\right). \tag{4.42}$$

From Taylor series expansion of the terms U_{i-1} and U_{i+1} in space direction, we get

$$\begin{aligned} U_{i-1} &\cong U_i - h_i(U_x)_i + \frac{h_i^2}{2!}(U_{xx})_i - \frac{h_i^3}{3!}(U_{xxx})_i + \cdots, \\ U_{i+1} &\cong U_i + h_{i+1}(U_x)_i + \frac{h_{i+1}^2}{2!}(U_{xx})_i + \frac{h_{i+1}^3}{3!}(U_{xxx})_i + \cdots, \end{aligned} \tag{4.43}$$

From Eq. (4.43), we have the following approximations

$$\begin{aligned} \frac{U_{i+1} - U_{i-1}}{h_i + h_{i+1}} &= (U_x)_i + \frac{h_{i+1} - h_i}{2}(U_{xx})_i + \frac{h_{i+1}^3 + h_i^3}{6(h_i + h_{i+1})}(U_{xxx})_i, \\ \frac{U_i - U_{i-1}}{h_i} &= (U_x)_i - \frac{h_i}{2}(U_{xx})_i + \frac{h_i^2}{6}(U_{xxx})_i, \\ \frac{U_{i+1} - U_i}{h_{i+1}} &= (U_x)_i + \frac{h_{i+1}}{2}(U_{xx})_i + \frac{h_{i+1}^2}{6}(U_{xxx})_i. \end{aligned} \tag{4.44}$$

Substituting Eq. (4.44) into Eq. (4.42), we have

$$\begin{aligned} T_i &= \varepsilon(U_{xx})_i + a_i(U_x)_i \\ &- \frac{2\varepsilon}{h_i + h_{i+1}}\left[(U_x)_i + \frac{h_{i+1}}{2}(U_{xx})_i + \frac{h_{i+1}^2}{6}(U_{xxx})_i - \left((U_x)_i - \frac{h_i}{2}(U_{xx})_i + \frac{h_i^2}{6}(U_{xxx})_i\right)\right] \\ &- a_i\left((U_x)_i + \frac{h_{i+1}-h_i}{2}(U_{xx})_i + \frac{h_{i+1}^3 + h_i^3}{6(h_i + h_{i+1})}(U_{xxx})_i\right). \end{aligned} \tag{4.45}$$

Simplifying the expression in Eq. (4.45), we have

$$\begin{aligned} T_i = \varepsilon(U_{xx})_i &- \frac{2\varepsilon}{h_i + h_{i+1}}\left[\left(\frac{h_{i+1}+h_i}{2}\right)(U_{xx})_i + \left(\frac{h_{i+1}^2 - h_i^2}{6}\right)(U_{xxx})_i\right] \\ &- a_i\left(\frac{h_{i+1}-h_i}{2}\right)(U_{xx})_i - a_i\frac{h_{i+1}^3 + h_i^3}{6(h_i + h_{i+1})}(U_{xxx})_i. \end{aligned} \tag{4.46}$$

Further simplification gives the following truncation error at the interior points

$$T_i = -\left(h_{i+1} - h_i\right)\frac{a_i}{2}(U_{xx})_i - \left(\frac{\varepsilon}{3}\left(h_{i+1} - h_i\right) + a_i\frac{h_{i+1}^3 + h_i^3}{6(h_i + h_{i+1})}\right)(U_{xxx})_i, \tag{4.47}$$

as $h_{i+1}, h_i \to 0$, then $T_i \to 0$. This shows the discrete scheme is consistent at the interior points. From Eqs. (4.36), (4.40) and (4.47), we conclude that the discrete scheme is consistent on the domain Ω. We have the following theorem.

Theorem 4.4. *Let u_i be the solution of the continuous problem and U_i be the solution of the discrete problem. Then, the truncation error satisfies the following bound*

$$\sup_{0<\varepsilon\ll 1}\max_{0\le i\le N}|U_i - u_i| \le CN^{-2}\ln^2 N,$$

where C is a constant independent of ε and the mesh parameter N.

Proof. We prove this theorem by considering two cases.

Case (i): Assume $\sigma = \frac{1}{2}$. In this case, the mesh is uniform and the error analysis is done in classical way. The mesh spacing is given by $h_i = \frac{1}{N}$ and $\frac{2\sqrt{\varepsilon}}{\sqrt{\beta}}\ln N \ge \frac{1}{2}$, this gives

$\varepsilon^{-\frac{1}{2}} \leq C \ln N$. Using the definition $h_1 := h_0$ in Eq. (4.36), the truncation error at the left boundary point is given as

$$T_0 = \sqrt{\varepsilon}\left(\frac{h_0^2}{6}\right)(U_{xxx})_0. \tag{4.48}$$

Using $h_0 = \frac{1}{N}$ and Theorem (4.2), the bound on the left boundary point is

$$\begin{aligned} |T_0| &\leq C\sqrt{\varepsilon}N^{-2}(\varepsilon^{-3/2}), \\ &\leq CN^{-3}(C\ln N)^3, \quad \text{since } \varepsilon^{-\frac{1}{2}} \leq C\ln N, \\ &\leq CN^{-2}\ln^2 N. \end{aligned} \tag{4.49}$$

Using the definition $h_{N+1} := h_N$ in Eq. (4.40), the truncation error at the right boundary point is given by

$$T_N = -\sqrt{\varepsilon}\left(\frac{h_N^2}{6}\right)(U_{xxx})_N. \tag{4.50}$$

Using $h_N = \frac{1}{N}$ and Theorem (4.2), we get bound on the right boundary point

$$\begin{aligned} |T_N| &\leq C\sqrt{\varepsilon}N^{-2}(\varepsilon^{-3/2}), \\ &\leq CN^{-3}(C\ln N)^3, \\ &\leq CN^{-2}\ln^2 N. \end{aligned} \tag{4.51}$$

Using $h_i = h_{i+1} = \frac{1}{N}$ in Eq. (4.47), the truncation error at the interior mesh points becomes

$$T_i = -a_i\frac{h_i^2}{6}(U_{xxx})_i. \tag{4.52}$$

Using Theorem (4.2), we obtain the following bound at the interior points

$$\begin{aligned} |T_i| &\leq CN^{-2}(\varepsilon^{-3/2}), \\ &\leq CN^{-2}(C\ln N)^3, \quad \text{since } \varepsilon^{-\frac{1}{2}} \leq C\ln N, \\ &\leq CN^{-2}\ln^2 N, \quad \text{for } i = 1, 2, \cdots, N-1. \end{aligned} \tag{4.53}$$

Combining Eqs. (4.49), (4.51) and (4.53), we have the bound

$$|T_i| \leq CN^{-2} \ln^2 N, \quad \text{for } i = 0, 1, \cdots, N. \tag{4.54}$$

Case (ii): Assume $\sigma = \frac{2\sqrt{\varepsilon}}{\sqrt{\beta}} \ln N$. In this case, the mesh is piecewise uniform with mesh spacing $h_i = \frac{2\sigma}{N}$ in $[0, \sigma]$ and $h_i = \frac{2(1-\sigma)}{N}$ in $[\sigma, 1]$. For $N/2 < i \leq N$, the region is regular, i.e., the interval is $[\sigma, 1]$. Using $h_{N+1} := h_N$ in Eq. (4.40), we obtain

$$T_N = -\sqrt{\varepsilon}\frac{h_N^2}{6}(U_{xxx})_N. \tag{4.55}$$

Using the fact that $h_N = \frac{2(1-\sigma)}{N} \leq CN^{-1}$ in Eq. (4.55) and the regular component bound in Theorem (4.3), we obtain the bound on the right boundary

$$\begin{aligned} |T_N| &\leq C\sqrt{\varepsilon}(CN^{-1})^2(1+\sqrt{\varepsilon}), \text{ since } \sqrt{\varepsilon} \leq CN^{-1}, \\ &\leq CN^{-1}(CN^{-2})(1+N^{-1}), \\ &\leq CN^{-2}. \end{aligned} \tag{4.56}$$

Using $h_i = h_{i+1} = \frac{2(1-\sigma)}{N}$ in Eq. (4.47), we have

$$T_i = -a_i\frac{h_i^2}{6}(U_{xxx})_N. \tag{4.57}$$

Using the regular component bound in Theorem (4.3), we obtain

$$|T_i| \leq CN^{-2}, \text{ for } i = N/2, \cdots, N-1. \tag{4.58}$$

Combining Eqs. (4.56) and (4.58), we obtain the bound in the regular component as

$$|T_i| \leq CN^{-2}, \text{ for } i = N/2, \cdots, N. \tag{4.59}$$

For $0 \leq i \leq N/2$, the region is singular region, i.e., the interval is $[0, \sigma]$. In this case, we have $h_0 = \frac{2\sigma}{N}$ and using the definition $h_1 := h_0$ in Eq. (4.36), we have

$$T_0 = \sqrt{\varepsilon}\left(\frac{h_0^2}{6}\right)(U_{xxx})_0. \tag{4.60}$$

Using the singular component bound in Theorem (4.3), bound on the left boundary is

$$\begin{aligned}|T_0| &\le C\sqrt{\varepsilon}\big(C\sqrt{\varepsilon}N^{-1}\ln N\big)^2\varepsilon^{-3/2}e^{-x_0\sqrt{\frac{\beta}{\varepsilon}}}\\ &\le CN^{-2}\ln^2 N.\end{aligned} \tag{4.61}$$

Using $h_i = h_{i+1} = \frac{2\sigma}{N}$ in Eq. (4.47), we have

$$T_i = -a_i\frac{h_i^2}{6}(U_{xxx})_i. \tag{4.62}$$

Using the fact that $e^{-x_i\sqrt{\frac{\beta}{\varepsilon}}} \le e^{-\sigma\sqrt{\frac{\beta}{\varepsilon}}} = e^{-2\frac{\sqrt{\varepsilon}}{\sqrt{\beta}}\ln N\sqrt{\frac{\beta}{\varepsilon}}} = e^{-2\ln N} = N^{-2}$ and the singular component bound, we have the bound at the interior mesh points

$$\begin{aligned}|T_i| &\le C\big(C\sqrt{\varepsilon}N^{-1}\ln N\big)^2\varepsilon^{-3/2}e^{-x_i\sqrt{\frac{\beta}{\varepsilon}}},\\ &\le CN^{-2}\ln^2 N.\end{aligned} \tag{4.63}$$

Combining Eqs. (4.61) and (4.63), we obtain

$$|T_i| \le CN^{-2}\ln^2 N, \quad \text{for} \quad 0 \le i \le N/2. \tag{4.64}$$

Again, combining Eqs. (4.59) and (4.64), we get

$$|T_i| \le CN^{-2}\ln^2 N, \quad \text{for } 0 \le i \le N,$$

as the required truncation error. □

Combination of the above error bounds lead us to the following main convergence theorem.

Theorem 4.5. *Let $u(x_i, t_j)$ be the solution of the continuous problem and U_i^j be the* *solution of the discrete problem. Then, the parameter-uniform error estimate is given by*

$$\sup_{0<\varepsilon\ll 1} \max_{0\le i\le N, 0\le j\le M} |U_i^j - u(x_i,t_j)| \le C\big((\Delta t)^2 + N^{-2}\ln^2 N\big),$$

where C is a constant independent of ε and the mesh parameters N and Δt.

Proof. The proof follows from the bound of time in Eq. (4.15) and Theorem (4.4). □

4.6 Numerical Results

This section shows numerical experiments for the theoretical findings.

Example 4.6.1. *Consider the singularly perturbed constant coefficient parabolic TPP [56]*

$$\varepsilon\frac{\partial^2 u(x,t)}{\partial x^2} + x^p\frac{\partial u(x,t)}{\partial x} - u(x,t) - \frac{\partial u(x,t)}{\partial t} = x^2 - 1, \quad (x,t) \in (0,1)\times(0,1],$$

with the initial condition and boundary conditions

$$\begin{cases} u(x,0) = 0, & x\in[0,1], \\ u(0,t) - \sqrt{\varepsilon}\frac{\partial u(0,t)}{\partial x} = 0, & t\in[0,1], \\ u(1,t) + \sqrt{\varepsilon}\frac{\partial u(1,t)}{\partial x}) = 0, & t\in[0,1]. \end{cases}$$

Example 4.6.2. *Consider the singularly perturbed variable coefficient parabolic TPP [56]*

$$\varepsilon\frac{\partial^2 u(x,t)}{\partial x^2} + x^p\frac{\partial u(x,t)}{\partial x} - (1+x)u(x,t) - \frac{\partial u(x,t)}{\partial t} = x^2 - 1, \quad (x,t) \in (0,1)\times(0,1],$$

with the initial condition and boundary conditions

$$\begin{cases} u(x,0) = (1-x)^2, & x\in[0,1], \\ u(0,t) - \sqrt{\varepsilon}\frac{\partial u(0,t)}{\partial x} = 1+t^2, & t\in[0,1], \\ u(1,t) + \sqrt{\varepsilon}\frac{\partial u(1,t)}{\partial x} = 0, & t\in[0,1]. \end{cases}$$

Table 4.1: Computed $E_{\varepsilon}^{N,\Delta t}$, $E^{N,\Delta t}$ and $R^{N,\Delta t}$ for Example (4.6.1) with $p = 2$.

	Number of mesh intervals $N = \frac{1}{\Delta t}$						
$\varepsilon \downarrow$	$N = 16$	32	64	128	256	512	1024
Present Result							
2^{-12}	1.1480e-2	4.7679e-3	1.7168e-3	5.6762e-4	1.8264e-4	5.7805e-5	1.7840e-5
2^{-16}	1.4052e-2	5.3475e-3	2.1953e-3	9.0703e-4	3.4737e-4	1.2879e-4	4.3964e-5
2^{-20}	1.4195e-2	5.6796e-3	2.3677e-3	9.5803e-4	3.8126e-4	1.5045e-4	5.9489e-5
2^{-24}	1.4185e-2	5.7532e-3	2.4068e-3	9.5813e-4	3.8201e-4	1.5358e-4	6.1195e-5
2^{-28}	1.4180e-2	5.7685e-3	2.4119e-3	9.5249e-4	3.8419e-4	1.5465e-4	6.1424e-5
2^{-32}	1.4178e-2	5.7721e-3	2.4128e-3	9.5076e-4	3.8491e-4	1.5481e-4	6.1470e-5
2^{-36}	1.4178e-2	5.7730e-3	2.4131e-3	9.5031e-4	3.8509e-4	1.5492e-4	6.1481e-5
2^{-40}	1.4178e-2	5.7732e-3	2.4131e-3	9.5019e-4	3.8514e-4	1.5494e-4	6.1481e-5
	⋮	⋮	⋮	⋮	⋮	⋮	
$E^{N,\Delta t}$	1.4195e-2	5.7733e-3	2.4131e-3	9.5813e-4	3.8515e-4	1.5495e-4	6.1481e-5
$R^{N,\Delta t}$	1.2979	1.2585	1.3326	1.3148	1.3136	1.3336	-
Result in [56]							
$E^{N,\Delta t}$	2.8520e-2	1.4918e-2	7.6326e-3	3.8608e-3	2.1984e-3	1.1464e-3	-
$R^{N,\Delta t}$	0.9349	0.9668	0.9832	0.8124	0.9394	-	-

The exact solution for the considered examples are not given, maximum absolute errors are calculated using the formulas in Eq. (2.31). The parameter-uniform error and rate of convergence are calculated using the formulas in Eq. (2.32).

4.7 Discussion and Conclusion

Computational results in Tables (4.1) and (4.2) confirm that the present method has improved the upwind scheme [56] in the literature for the Examples (4.6.1) and (4.6.2), respectively. Numerical simulation for Example (4.6.1) is plotted in Figure (4.1) and for Example (4.6.2) is plotted in Figure (4.2). More computed solutions are observed in the boundary layer regions as observed from Figures (4.3). The maximum absolute errors for Examples (4.6.1) and (4.6.2) are plotted using log-log scale as can be seen in Figures (4.4). As observed from Figures (4.5) a strong boundary layer is formed near $x = 0$ and as the size of time level increases the thickness of the layer increases for Examples (4.6.1) and (4.6.2). The effect of the singular perturbation parameter on the boundary

Table 4.2: Computed $E_{\varepsilon}^{N,\Delta t}$, $E^{N,\Delta t}$ and $R^{N,\Delta t}$ for Example (4.6.2) with $p = 5$.

	Number of mesh intervals $N = \frac{1}{\Delta t}$						
$\varepsilon \downarrow$	$N = 16$	32	64	128	256	512	1024
Present Result							
2^{-12}	2.6545e-2	1.1602e-2	4.3822e-3	1.5185e-3	4.9899e-4	1.5822e-4	4.4735e-5
2^{-16}	2.6693e-2	1.1667e-2	4.4070e-3	1.5271e-3	5.0184e-4	1.5912e-4	4.9147e-5
2^{-20}	2.6729e-2	1.1684e-2	4.4132e-3	1.5293e-3	5.0254e-4	1.5935e-4	4.9216e-5
2^{-24}	2.6738e-2	1.1688e-2	4.4147e-3	1.5298e-3	5.0272e-4	1.5940e-4	4.9233e-5
2^{-28}	2.6741e-2	1.1689e-2	4.4151e-3	1.5299e-3	5.0276e-4	1.5942e-4	4.9238e-5
2^{-32}	2.6741e-2	1.1689e-2	4.4152e-3	1.5300e-3	5.0277e-4	1.5942e-4	4.9239e-5
2^{-36}	2.6741e-2	1.1689e-2	4.4152e-3	1.5300e-3	5.0278e-4	1.5942e-4	4.9239e-5
2^{-40}	2.6741e-2	1.1689e-2	4.4152e-3	1.5300e-3	5.0278e-4	1.5942e-4	4.9239e-5
	$\vdots$	$\vdots$	$\vdots$	$\vdots$	$\vdots$	$\vdots$	
$E^{N,\Delta t}$	2.6741e-2	1.1689e-2	4.4152e-3	1.5300e-3	5.0278e-4	1.5942e-4	4.9239e-5
$R^{N,\Delta t}$	1.1939	1.4046	1.5289	1.6055	1.6571	1.6950	-
Result in [56]							
$E^{N,\Delta t}$	5.6060e-2	3.2462e-2	1.8415e-2	1.0298e-2	5.8965e-3	3.1267e-3	-
$R^{N,\Delta t}$	0.7882	0.8179	0.8384	0.8045	0.9152	-	-

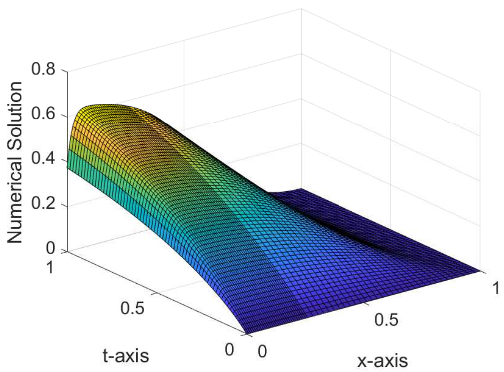

(a) $N = 64 = \frac{1}{\Delta t}$, $\varepsilon = 2^{-10}$.

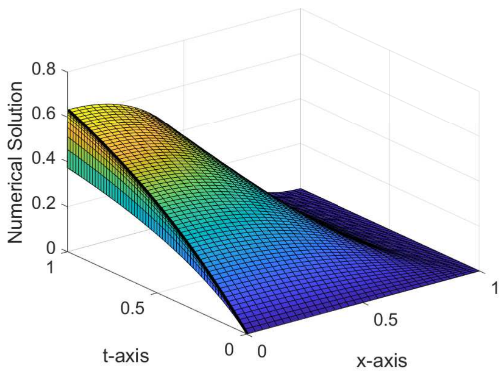

(b) $N = 64 = \frac{1}{\Delta t}$, $\varepsilon = 2^{-20}$.

Figure 4.1: Surface plot of the numerical solution for Example (4.6.1) with $p = 2$.

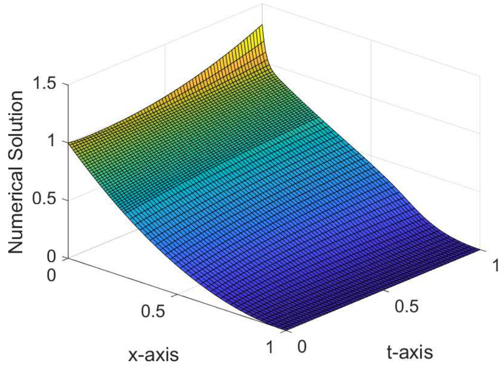

(a) $N = 64 = \frac{1}{\Delta t}$, $\varepsilon = 2^{-10}$.

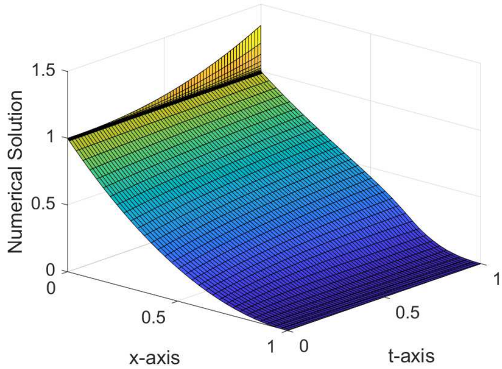

(b) $N = 64 = \frac{1}{\Delta t}$, $\varepsilon = 2^{-20}$.

Figure 4.2: Surface plot of the numerical solution for Example (4.6.2) with $p = 5$.

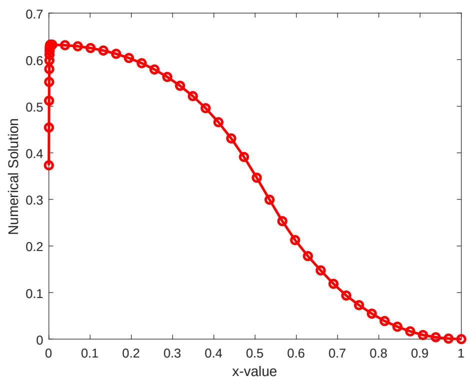

(a) Example (4.6.1).

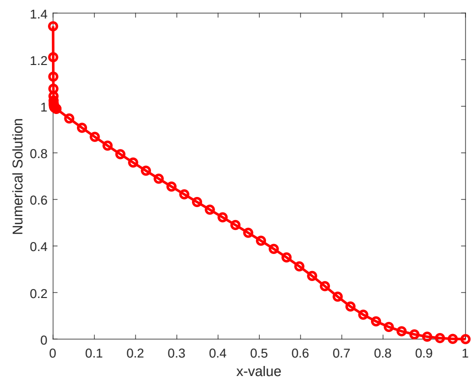

(b) Example (4.6.2).

Figure 4.3: Show boundary layer resolving property for $N = M = 64, \varepsilon = 2^{-20}$.

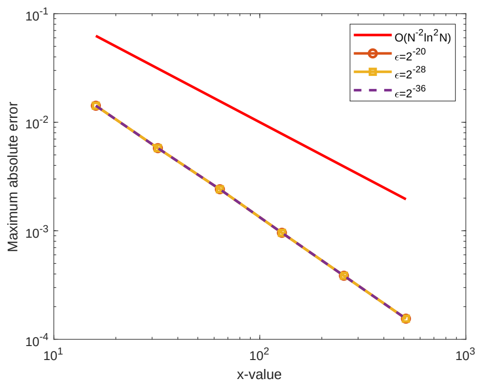

(a) Example (4.6.1) using Table (4.1).

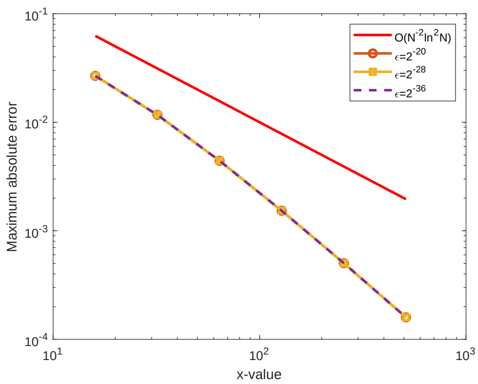

(b) Example (4.6.2) using Table (4.2).

Figure 4.4: Loglog plot of the maximum absolute errors.

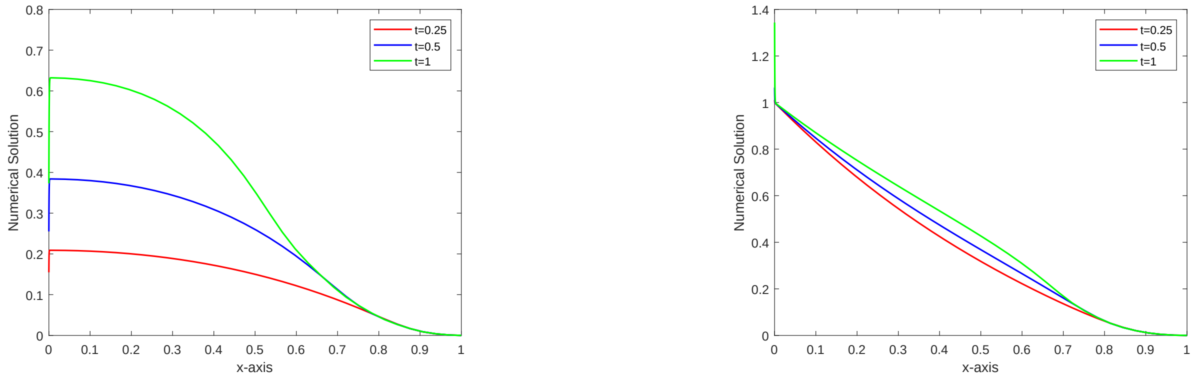

(a) Example (4.6.1). **(b)** Example (4.6.2).

Figure 4.5: Effect of time t level on the solution at $N = 64 = \frac{1}{\Delta t}$, $\varepsilon = 2^{-16}$.

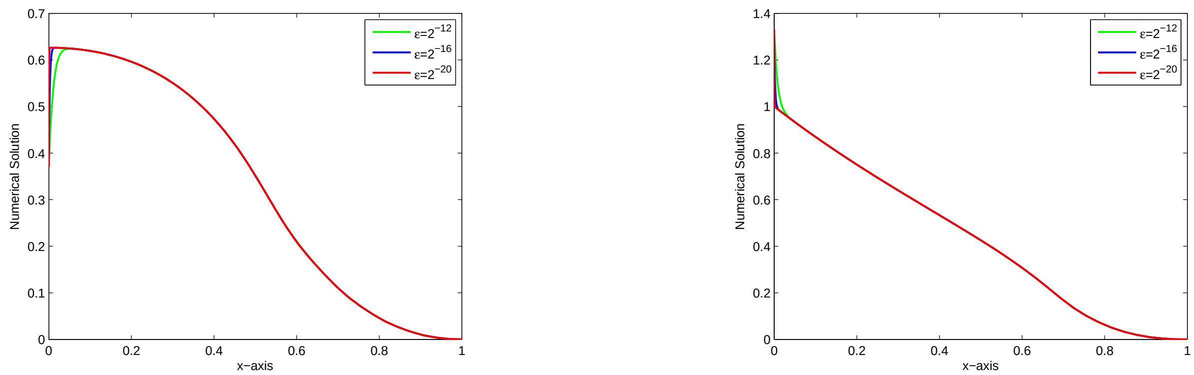

(a) Example (4.6.1). **(b)** Example (4.6.2).

Figure 4.6: Effect of the perturbation parameter ε on the solution at $N = 64 = \frac{1}{\Delta t}$.

layer of the solution for Examples (4.6.1) and (4.6.2) are shown in Figures (4.6). Except in Figures (4.4), when $\varepsilon \to 0$ strong boundary layer is formed near $x = 0$ in all other Figures. A comparison given in Tables clearly indicate that the maximum absolute errors are smaller and rate of convergence is larger in this chapter than those obtained using upwind finite difference method. It verify numerically the theoretical estimates that the present method is almost second order ε-uniformly convergent as opposed to the first-order uniform convergence of upwind finite difference scheme in the literature. Numerical results given in Tables also show that the maximum absolute errors decreases and order of convergence increases as the number of mesh point increases. It can be seen that as ε decreases for a given number of mesh points, both the maximum absolute error and the order of convergence stabilize.

Chapter 5

Fitted Mesh Collocation Method for Singularly Perturbed Parabolic Reaction-diffusion Problem with Time Delay

In this chapter, a numerical solution for singularly perturbed time delay parabolic reaction-diffusion problem with Robin boundary conditions is developed. The problem is discretized by the implicit Euler method on a uniform mesh in time and the extended cubic B-spline collocation method on a Shishkin mesh in space. The convergence analysis of the present method is established, and it is demonstrated to be uniformly convergent of $O(N^{-2}\ln^2 N + \Delta t)$, where Δt and N denote the step size in time and the number of mesh intervals in space, respectively. Numerical experiments are carried out and the obtained results are compared with the method in the literature.

5.1 Introduction

B-spline functions are piecewise polynomial or non-polynomial functions that have been emerged as powerful techniques in the numerical solution of linear and nonlinear partial differential equations. The extended cubic B-spline is the extension of classical cubic B-spline, where its basis is constructed in such a way that one free parameter, λ, is included and the degree of the piecewise polynomial is increased but the continuity of the extended cubic B-splines remains in order three. The extended cubic B-spline has an advantage over the classical cubic B-spline in that the solution obtained by the extended cubic B-spline is better than the solution obtained by the classical cubic B-spline for some optimized value of a free parameter, λ.

Various researchers used the extended cubic B-spline basis function to solve linear and nonlinear ordinary and partial differential equations; see, for example, [88], [109] and [110]. Singularly perturbed semilinear ordinary differential problems of reaction-diffusion and convection-diffusion types, respectively, using the cubic B-spline collocation method on a Shishkin mesh is employed in [103] and [105]. Cubic B-spline collocation method has been developed for time-dependent singularly perturbed differential-difference problems; see [62]. An extended cubic B-spline collocation method has been developed for time-dependent singularly perturbed partial differential problems in [28] and [63]. B-spline methods are better than finite difference method since the former ensures that the solution is continuous in the domain whereas the later gives the solution only at the chosen mesh points, according to [103] and [105].

As far as our knowledge is concerned, no paper deals with the extended cubic B-spline method for singularly perturbed time delay parabolic reaction-diffusion problem with Robin boundary conditions. Thus, we develop such a method for the problem under consideration.

5.2 Definition of the Problem

Let $\Omega = (0,1) \times (0,T]$ be the space-time domain $x-t$. In this chapter, the following singularly perturbed time-delayed parabolic reaction-diffusion problem is considered

$$\mathcal{L}_\varepsilon u(x,t) \equiv \frac{\partial u(x,t)}{\partial t} - \varepsilon \frac{\partial^2 u(x,t)}{\partial x^2} + a(x,t)u(x,t) = -b(x,t)u(x,t-\tau) + f(x,t), \quad (5.1)$$

with the following initial condition and boundary conditions

$$\begin{cases} u(x,t) = \phi_B(x,t), & (x,t) \in [0,1] \times [-\tau, 0], \\ B_{L,\varepsilon}u(0,t) \equiv u(0,t) - \sqrt{\varepsilon}\frac{\partial u(0,t)}{\partial x} = \phi_L(t), & 0 < t \leq T, \\ B_{R,\varepsilon}u(1,t) \equiv u(1,t) + \sqrt{\varepsilon}\frac{\partial u(1,t)}{\partial x} = \phi_R(t), & 0 < t \leq T, \end{cases} \quad (5.2)$$

where $\varepsilon (0 < \varepsilon \ll 1)$ is a diffusion coefficient, $\tau > 0$ is time delay ($\tau = T/k$ for some integer $k > 1$) and $(x,t) \in \Omega$. For the uniqueness of the solution, assume $a(x,t), b(x,t), f(x,t)$, $\phi_B(x,t), \phi_L(t)$ and $\phi_R(t)$ are sufficiently smooth and bounded functions satisfying the conditions $a(x,t) \geq \alpha > 0, b(x,t) \geq \beta > 0,\ \forall (x,t) \in \bar{\Omega}$.

5.3 Properties of the Continuous Solution

Setting $\varepsilon = 0$, the reduced problem corresponding to Eq. (5.1)-(5.2) is

$$\begin{cases} \frac{\partial u_0(x,t)}{\partial t} + a(x,t)u_0(x,t) = -b(x,t)u_0(x,t-\tau) + f(x,t), & (x,t) \in \Omega, \\ u(x,t) = \phi_B(x,t), \quad (x,t) \in [0,1] \times [-\tau, 0]. \end{cases} \quad (5.3)$$

The reduced problem in Eq. (5.3) is an initial value problem which does not make use of the two boundary conditions. Thus, the problem in Eq. (5.1)-(5.2) have boundary layers near $x = 0$ and $x = 1$. For problem of type in Eq. (5.1), where the delay $t - \tau$ are bounded away from t by a positive constant, the existence of the solution can be verified by methods of steps. Assume the solution is known, say

$$u(x,t) = \phi_B(x,t), \quad (x,t) \in [0,1] \times [-\tau, 0].$$

Then $u(x, t-\tau)$ is a known function on $(x,t) \in [0,1] \times [0,\tau]$ and Eq. (5.1) becomes a classical partial differential equation, which can be treated by known existence theories [72]. The methods of steps allows one to represent a delay differential equation equivalently on successive intervals $[0,\tau], [\tau, 2\tau], \cdots, [(n-1)\tau, n\tau]$ as successive systems of ordinary differential equations. Since we know the solution $u(x,t)$ for $(x,t) \in [0,1] \times [0,\tau]$, we can compute the solution for $(x,t) \in [0,1] \times [\tau, 2\tau]$ and so on. Therefore, this method of steps yields the existence and uniqueness results for all $(x,t) \in \bar{\Omega}$ .The existence and uniqueness for a solution of Eq. (5.1)–(5.2) can be established under the assumption that the data are Hölder continuous and also satisfy an appropriate compatibility conditions at the corner points $(0,0)$, $(1,0)$, $(0,-\tau)$ and $(1,-\tau)$. The boundary functions $\phi_L, \phi_R \in C^k([0,T]), \phi_B \in C^{(1,k)}([0,1] \times [-\tau, 0])$ are said to satisfy the k^{th} order compatibility condition at the initial function if

$$\begin{aligned}
\frac{\partial^k}{\partial t^k}\left(\phi_B - \sqrt{\varepsilon}\frac{\partial \phi_B}{\partial x}\right)(0,0) &= \frac{d^k \phi_L(0)}{\partial t^k}, \\
\frac{\partial^k}{\partial t^k}\left(\phi_B + \sqrt{\varepsilon}\frac{\partial \phi_B}{\partial x}\right)(1,0) &= \frac{d^k \phi_R(0)}{\partial t^k}, \\
\frac{\partial \phi_L(0)}{\partial t} - \varepsilon \frac{\partial^2 \phi_B(0,0)}{\partial x^2} + a(0,0)\frac{\partial \phi_B(0,0)}{\partial x} &= -b(0,0)\phi_B(0,0) + f(0,0), \\
\frac{\partial \phi_R(1)}{\partial t} - \varepsilon \frac{\partial^2 \phi_B(1,0)}{\partial x^2} + a(1,0)\frac{\partial \phi_B(1,0)}{\partial x} &= -b(1,0)\phi_B(1,0) + f(1,0).
\end{aligned}$$

Therefore, the problem in Eq. (5.1)–(5.2) have a unique solution, see [1] and [108]. The assumption in Eq. (5.1)-(5.2) admits the following continuous maximum principle.

Lemma 5.3.1. *Assume that φ be a sufficiently smooth function defined on Ω such that $\mathcal{L}_\varepsilon \varphi(x,t) \geq 0, (x,t) \in \Omega$, $B_{L,\varepsilon}\varphi(0,t) \geq 0, t \in (0,T]$, $B_{R,\varepsilon}\varphi(1,t) \geq 0, t \in (0,T]$ and $\varphi(x,t) \geq 0, (x,t) \in [0,1] \times [-\tau, 0]$. Then, $\varphi(x,t) \geq 0$, $\forall (x,t) \in \bar{\Omega}$.*

Proof. Suppose the arbitrary function φ takes its minimum value at the point $(x^*, t^*) \in \bar{\Omega}$

such that $\varphi(x^*,t^*) = \min_{(x,t)\in\bar{\Omega}} \varphi(x,t)$ and assume that $\varphi(x^*,t^*) < 0$. Then, (x^*,t^*) is the interior points.

Case (i): For $(x^*,t^*) \in \{0\} \times (0,T]$, we have $\frac{\partial \varphi}{\partial x}(x^*,t^*) \geq 0$. Hence, $B_{L,\varepsilon}\varphi(x^*,t^*) = \varphi(x^*,t^*) - \sqrt{\varepsilon}\dfrac{\partial \varphi}{\partial x}(x^*,t^*) < 0$, which is a contradiction.

Case (ii): For $(x^*,t^*) \in \{1\} \times (0,T]$, we have $\frac{\partial \varphi}{\partial x}(x^*,t^*) \leq 0$. Hence, $B_{R,\varepsilon}\varphi(x^*,t^*) = \varphi(x^*,t^*) + \sqrt{\varepsilon}\dfrac{\partial \varphi}{\partial x}(x^*,t^*) < 0$, which is a contradiction.

Case (iii): For $(x^*,t^*) \in \Omega$, as it attains minimum at (x^*,t^*), we have $\frac{\partial \varphi}{\partial t}(x^*,t^*) = 0$ and $\frac{\partial^2 \psi}{\partial x^2}(x^*,t^*) \geq 0$. Hence,

$$\mathcal{L}_\varepsilon \varphi(x^*,t^*) = \frac{\partial \varphi}{\partial t}(x^*,t^*) - \varepsilon\frac{\partial^2 \varphi}{\partial x^2}(x^*,t^*) + a(x^*,t^*)\varphi(x^*,t^*) < 0,$$

which is a contradiction to the assumption that $\mathcal{L}_\varepsilon\varphi(x,t) \geq 0$, $\forall (x,t) \in \Omega$. It follows that $\varphi(x^*,t^*) \geq$ and thus $\varphi(x,t) \geq 0$, $\forall (x,t) \in \bar{\Omega}$. □

Stability and $\varepsilon-$uniform bound for Eq. (5.1) is established in the following lemma in the sense of the maximum norm which follows from lemma (5.3.1).

Lemma 5.3.2. *Let $u(x,t)$ be the solution, we have the bound*

$$|u| \leq \max\{|B_{L,\varepsilon}u(x,t)|, |B_{R,\varepsilon}u(x,t)|, |\phi_B(x,t)|\} + \frac{\|f\|}{\alpha}.$$

Proof. This lemma can be proved by using lemma (5.3.1) and the barrier functions

$$\Psi^{\pm}(x,t) = M \pm u(x,t), \quad (x,t) \in \bar{\Omega},$$

where $M = \max\{|B_{L,\varepsilon}u(x,t)|, |B_{R,\varepsilon}u(x,t)|, |\phi_B(x,t)|\} + \frac{\|f\|}{\alpha}$. □

Theorem 5.1. *Let* $a, b, f \in C^{(2+\gamma,1+\gamma/2)}(\bar{\Omega}), \phi_L, \phi_R \in C^{\frac{3+\gamma}{2}}([0,T]), \phi_B \in C^{(4+\gamma,2+\gamma/2)}([0,1]\times[-\tau,0]), \gamma \in (0,1)$. *Assume that the compatibility conditions for $k = 0,1,2$ are fulfilled. Then, the problem has a unique solution and the derivatives of the solution u satisfy the* *bound*

$$\left\| \frac{\partial^{l+m} u}{\partial x^l \partial t^m} \right\|_{\bar{\Omega}} \leq C\varepsilon^{-l/2}, \qquad l, m \geq 0, \quad 0 \leq l + 2m \leq 4,$$

where the constant C is independent of ε.

Proof. The bounds on the solution and derivatives are obtained by transforming independent variable x to the stretched variable $\hat{x} = x/\sqrt{\varepsilon}$. Under the stretched transformation, Eq. (5.1) is transformed as

$$\frac{\partial \hat{u}(\hat{x}, t)}{\partial t} - \frac{\partial^2 \hat{u}(\hat{x}, t)}{\partial \hat{x}^2} + \hat{a}(\hat{x}, t)\hat{u}(\hat{x}, t) = -\hat{b}(\hat{x}, t)\hat{u}(\hat{x}, t - \tau) + \hat{f}(\hat{x}, t), \quad (\hat{x}, t) \in \hat{\Omega},$$

with the initial condition and boundary conditions

$$\begin{cases} \hat{u}(\hat{x}, t) = \phi_B(\hat{x}, t), & (\hat{x}, t) \in (0, \frac{1}{\sqrt{\varepsilon}}) \times [-\tau, 0], \\ \hat{u}(\hat{x}, t) - \frac{\partial \hat{u}(\hat{x}, t)}{\partial \hat{x}} = \phi_{L,\varepsilon}(t), & (\hat{x}, t) \in \{0\} \times (0, T], \\ \hat{u}(\hat{x}, t) + \frac{\partial \hat{u}(\hat{x}, t)}{\partial \hat{x}} = \phi_{R,\varepsilon}(t), & (\hat{x}, t) \in \{(\frac{1}{\sqrt{\varepsilon}}, t) : t \in (0, T]\}, \end{cases}$$

where $\hat{\Omega}_\varepsilon = (0, \frac{1}{\sqrt{\varepsilon}}) \times (0, T]$. Since the transformed differential equation is independent of ε, we use the estimate in [72] to get

$$\left\| \frac{\partial^{l+m} \hat{u}}{\partial \hat{x}^l \partial t^m} \right\|_{\hat{N}_\delta} \leq C(1 + \|\hat{u}\|_{N_{2\delta}}), \qquad l, m \geq 0, \ \ 0 \leq l + 2m \leq 4,$$

for all $\hat{N}_\delta$ in $\hat{\Omega}$. Here, $\hat{N}_\delta$, $\delta > 0$, is a neighborhood with diameter δ in $\hat{\Omega}$ and C is independent of $\hat{N}_\delta$. Returning back to the original variable x, we get

$$\left\| \frac{\partial^{l+m} u}{\partial x^l \partial t^m} \right\|_{\bar{\Omega}} \leq C\varepsilon^{-l/2}(1 + \|u\|_{\bar{\Omega}}), \qquad l, m \geq 0, \ \ 0 \leq l + 2m \leq 4.$$

for all $\hat{N}_\delta$ in $\hat{\Omega}$. Here, $\hat{N}_\delta$, $\delta > 0$, is a neighborhood with diameter δ in $\hat{\Omega}$ and C is independent of $\hat{N}_\delta$. Similar argument follows for $p > 1$ as we neglect the term involving

$\varepsilon^{\frac{p-1}{2}}$ which is very small. Returning back to the original variable x, we get

$$\left\| \frac{\partial^{l+m} u}{\partial x^l \partial t^m} \right\|_{\bar{\Omega}} \leq C\varepsilon^{-l/2}(1 + \|u\|_{\bar{\Omega}}), \qquad l, m \geq 0, \;\; 0 \leq l + 2m \leq 4.$$

The proof is completed by using the bound on u given in Lemma (5.3.2). □

The classical bounds in Theorem (5.1) are not adequate for the proof of ε-uniform error estimate for the numerical method. To get better bounds on the derivatives of the solution, u in Eq. (5.1)-(5.2), we try to express it as $u = v + w$, where v is the regular solution and w is the singular component. The regular component v is further be decomposed into

$$v = v_0 + \varepsilon v_1,$$

where v_0 and v_1 satisfy the following, respectively

$$\begin{cases} \frac{\partial v_0}{\partial t}(x,t) + a(x,t)v_0(x,t) = -b(x,t)v_0(x,t-\tau) + f(x,t), & (x,t) \in \Omega, \\ v_0(x,t) = \phi_B(x,t), & [0,1] \times [-\tau, 0], \end{cases} \tag{5.4}$$

$$\begin{cases} \mathcal{L}_\varepsilon v_1(x,t) = -b(x,t)v_1(x,t-\tau) + \frac{\partial^2 v_0}{\partial x^2}(x,t), & (x,t) \in \Omega, \\ B_{L,\varepsilon} v_1(0,t) = 0, & 0 < t \leq T, \\ B_{R,\varepsilon} v_1(1,t) = 0, & 0 < t \leq T, \\ v_1(x,t) = 0, & [0,1] \times [-\tau, 0]. \end{cases} \tag{5.5}$$

The regular component v is the solution to the non-homogeneous problem

$$\begin{cases} \mathcal{L}_\varepsilon v(x,t) = -b(x,t)v(x,t-\tau) + f(x,t), & (x,t) \in \Omega, \\ B_{L,\varepsilon} v(0,t) = B_{L,\varepsilon} v_0(0,t), & 0 < t \leq T, \\ B_{R,\varepsilon} v(1,t) = B_{R,\varepsilon} v_0(1,t), & 0 < t \leq T, \\ v(x,t) = \phi_B(x,t), & [0,1] \times [-\tau, 0]. \end{cases} \tag{5.6}$$

With $v(x,t)$ defined, $w(x,t)$ is the solution of the homogeneous problem

$$\begin{cases} \mathcal{L}_\varepsilon w(x,t) = -b(x,t)w(x,t-\tau), & (x,t) \in \Omega, \\ B_{L,\varepsilon} w(0,t) = \phi_L(t) - B_{L,\varepsilon} v_0(0,t), & 0 < t \leq T, \\ B_{R,\varepsilon} w(1,t) = \phi_R(t) - B_{R,\varepsilon} v_0(1,t), & 0 < t \leq T, \\ w(x,0) = 0, & [0,1] \times [-\tau, 0]. \end{cases} \tag{5.7}$$

Since Eq. (5.1)-(5.2) have twin boundary layers, we further decompose w as

$$w = w_L + w_R$$

where w_L and w_R are defined respectively by

$$\begin{cases} \mathcal{L}_\varepsilon w_L(x,t) = -b(x,t)w_L(x,t-\tau), & (x,t) \in \Omega, \\ B_{L,\varepsilon} w_L(0,t) = \phi_L(t) - B_{L,\varepsilon} v_0(0,t), & 0 < t \leq T, \\ B_{R,\varepsilon} w_L(1,t) = 0, & 0 < t \leq T, \\ w_L(x,t) = 0, & [0,1] \times [-\tau, 0], \end{cases} \tag{5.8}$$

$$\begin{cases} \mathcal{L}_\varepsilon w_R(x,t) = -b(x,t)w_R(x,t-\tau), & (x,t) \in \Omega, \\ B_{L,\varepsilon} w_R(0,t) = 0, & 0 < t \leq T, \\ B_{R,\varepsilon} w_R(1,t) = \phi_R(t) - B_{R,\varepsilon} v_0(1,t), & 0 < t \leq T, \\ w_R(x,t) = 0, & [0,1] \times [-\tau, 0]. \end{cases} \tag{5.9}$$

Thus, the non-classical bounds of singular and regular components and their derivatives are stated in the following theorem.

Theorem 5.2. *Let* $a, b, f \in C^{(4+\alpha, 2+\alpha/2)}(\bar{\Omega}), \phi_L, \phi_R \in C^{\frac{5+\alpha}{2}}([0,T]), \phi_B \in C^{(6+\alpha, 3+\alpha/2)}([0,1]\times$

$[-\tau,0]),\alpha\in(0,1)$. *Under the compatibility conditions, we have the bounds*

$$\left\|\frac{\partial^{l+m}v}{\partial x^l\partial t^m}\right\|\le C(1+\varepsilon^{1-l/2}),\quad \left|\frac{\partial^{l+m}w_L}{\partial x^l\partial t^m}\right|\le C\varepsilon^{-l/2}e^{-x\sqrt{\frac{\alpha}{\varepsilon}}}$$
$$\left|\frac{\partial^{l+m}w_R}{\partial x^l\partial t^m}\right|\le C\varepsilon^{-l/2}e^{-(1-x)\sqrt{\frac{\alpha}{\varepsilon}}},\quad l,m\ge 0,\quad 0\le l+2m\le 4.$$

Proof. The bounds of regular component and their derivatives are derived as follows. Since v_0 is the solution of a first-order differential equation (reduced problem), a classical argument leads to the estimate

$$\left\|\frac{\partial^{l+m}v_0}{\partial x^l\partial t^m}\right\|_\Omega\le C.$$

Since v_1 is the solution to Eq. (5.1) and using Theorem (5.1), it follows that

$$\left\|\frac{\partial^{l+m}v_1}{\partial x^l\partial t^m}\right\|\le C\varepsilon^{-l/2}.$$

Since

$$\left\|\frac{\partial^{l+m}v}{\partial x^l\partial t^m}\right\|\le\left\|\frac{\partial^{l+m}v_0}{\partial x^l\partial t^m}\right\|+\varepsilon\left\|\frac{\partial^{l+m}v_1}{\partial x^l\partial t^m}\right\|\le C+\varepsilon C\varepsilon^{-l/2}\le C(1+\varepsilon^{1-l/2}),$$

as required. Next, the proof for the bounds on left singular component w_l and its derivatives is given. Define the barrier functions

$$\Psi^{\pm}(x,t)=Ce^{-x\sqrt{\frac{\alpha}{\varepsilon}}}e^t\pm w_L(x,t),$$

Then, the barrier functions are evaluated at the boundaries as follows.

$$\begin{aligned}\Psi^{\pm}(0,t)-\sqrt{\varepsilon}\Psi^{\pm}_x(0,t)&=Ce^t\pm w_L(0,t)-\sqrt{\varepsilon}\left[-C\sqrt{\frac{\alpha}{\varepsilon}}e^t\pm(w_x)_L(0,t)\right],\\&=Ce^t+C\sqrt{\alpha}\pm\left(w_L(0,t)-\sqrt{\varepsilon}(w_x)_L(0,t)\right),\\&=Ce^t+C\sqrt{\alpha}\pm B_{L,\varepsilon}w_L(0,t),\\&\ge 0,\quad \text{choosing C sufficiently large.}\end{aligned}$$

$$\begin{aligned}
\Psi^{\pm}(1,t)+\sqrt{\varepsilon}\Psi_x^{\pm}(1,t) &= Ce^{-\sqrt{\frac{\alpha}{\varepsilon}}}e^{t} \pm w_L(1,t)+\sqrt{\varepsilon}\Big[-C\sqrt{\frac{\alpha}{\varepsilon}}e^{-\sqrt{\frac{\alpha}{\varepsilon}}}e^{t} \pm (w_x)_L(1,t)\Big],\\
&= Ce^{-\sqrt{\frac{\alpha}{\varepsilon}}}e^{t}(1-\sqrt{\alpha}) \pm (w_L(1,t)+\sqrt{\varepsilon}(w_x)_L(1,t)),\\
&= Ce^{-\sqrt{\frac{\alpha}{\varepsilon}}}e^{t}(1-\sqrt{\alpha}) \pm B_{R,\varepsilon}w_L(1,t), \ \text{ since } \ B_{R,\varepsilon}w_L(1,t)=0,\\
&\geq 0.\\
\Psi^{\pm}(x,0) &= Ce^{-x\sqrt{\frac{\alpha}{\varepsilon}}} \pm w_L(x,0) \geq 0, \ \text{ for sufficiently large } \ C.
\end{aligned}$$

We conclude the initial and boundaries that $\Psi^{\pm}(x,t) \geq 0$. Now, on the domain $(x,t) \in \Omega$

$$\begin{aligned}
\mathcal{L}_{\varepsilon}\Psi^{\pm}(x,t) &= Ce^{-x\sqrt{\frac{\alpha}{\varepsilon}}}e^{t} \pm (w_t)_L(x,t) - \varepsilon\left(\frac{C\alpha}{\varepsilon}e^{-x\sqrt{\frac{\alpha}{\varepsilon}}}e^{t} \pm (w_{xx})_L(x,t)\right)\\
&+ a(x,t)\left(Ce^{-x\sqrt{\frac{\alpha}{\varepsilon}}}e^{t} \pm w_L(x,t)\right),\\
&= Ce^{-x\sqrt{\frac{\alpha}{\varepsilon}}}e^{t}(1-\alpha+a(x,t)) \pm f(x,t),\\
&\geq Ce^{-x\sqrt{\frac{\alpha}{\varepsilon}}}e^{t}(1-\alpha+a(x,t)), \ \text{ since f is sufficiently smooth,}\\
&\geq Ce^{-x\sqrt{\frac{\alpha}{\varepsilon}}}e^{t}, \ \text{ since } a(x,t) \geq \alpha > 0,\\
&> 0.
\end{aligned}$$

Applying lemma (5.3.1) on $\mathcal{L}_{\varepsilon}$ yields $\Psi^{\pm}(x,t) \geq 0, \ \forall (x,t) \in \bar{\Omega}$. This implies

$$\begin{aligned}
|w_L(x,t)| &\leq Ce^{-x\sqrt{\frac{\alpha}{\varepsilon}}}e^{t}, \ \forall (x,t) \in \bar{\Omega},\\
&\leq Ce^{-x\sqrt{\frac{\alpha}{\varepsilon}}}, \ \text{ since } 0 \leq t \leq T \text{ and } e^{t} \leq e^{T},
\end{aligned}$$

as required. Let $\tilde{x} = x/\sqrt{\varepsilon}$. Notice the domain of the stretched variable $\tilde{x}$ is clearly $(0, 1/\sqrt{\varepsilon})$. Under the transformation $(x,t) \to (\tilde{x},t)$, the solution of Eq. (5.8) becomes one which is independent of ε. Thus, suitable results in [72] are applied to the solution $\tilde{w}_l$. Two cases rises corresponding to the position $\tilde{x}$. For the neighbourhood $\tilde{N}_{\delta}$ in $(2, 1/\sqrt{\varepsilon}) \times (0,T]$, we have

$$\left|\frac{\partial^{l+m}\tilde{w}_L}{\partial \tilde{x}^l \partial t^m}\right|_{\tilde{N}_{\delta}} \leq C|\tilde{w}_L|_{\tilde{N}_{2\delta}}.$$

Transforming back to the variable x and using the bound on w_l, we obtain

$$\left|\frac{\partial^{l+m} w_L}{\partial x^l \partial t^m}\right| \leq C\varepsilon^{-l/2} e^{-x\sqrt{\frac{\alpha}{\varepsilon}}}.$$

Again, for the neighbourhood $\tilde{N}_\delta$ in $(0, 2] \times (0, T]$, we have

$$\left|\frac{\partial^{l+m} \tilde{w}_L}{\partial \tilde{x}^l \partial t^m}\right|_{\tilde{N}_\delta} \leq C(1 + |\tilde{w}_L|_{\tilde{N}_{2\delta}}).$$

Transforming back to the variable x, using the bound obtained on w_l and noticing that $e^{-\tilde{x}\frac{\alpha}{\sqrt{\varepsilon}}} \geq e^{-2} = C$ for $\tilde{x} \leq 2$, we obtain

$$\left|\frac{\partial^{l+m} w_L}{\partial x^l \partial t^m}\right| \leq C\varepsilon^{-l/2}(1 + e^{-x\sqrt{\frac{\alpha}{\varepsilon}}}).$$

Combining the above two results, we have

$$\left|\frac{\partial^{l+m} w_L}{\partial x^l \partial t^m}\right| \leq C\varepsilon^{-l/2} e^{-x\sqrt{\frac{\alpha}{\varepsilon}}},$$

as required. Similar proof can be given for w_R. This completes the proof. □

5.4 Formulation of the Numerical Method

In this section, the time derivative is discretized using the implicit Euler method, and the space derivative is discretized using the extended cubic B-spline collocation method with the use of a piecewise uniform Shishkin mesh.

5.4.1 Time Discretization

We have two intervals $[-\tau, 0]$ and $[0, T]$ on the time direction. Since $u(x, t - \tau)$ term is there in our problem so in the difference scheme the point $t - \tau$ must coincide with a mesh point. To do this, we first divide the delay interval $[-\tau, 0]$ into s equal parts with spacing $\Delta t = \frac{\tau}{s}$, where τ is the delay parameter and use the same mesh spacing for the non-delay interval $[0, T]$. We divide the non-delay interval $[0, T]$ into M equal parts with spacing $\Delta t = \frac{T}{M}$. Therefore, the time interval $[0, T]$ is divided by the points $0 = t_0 < t_1 < t_2 < \cdots, t_M = T$ with a uniform mesh of step length of Δt defined by $\Omega_t^M = \{t_j : t_j = t_0 + j\Delta t,\ j = 0, \cdots, M\}$, where M denotes the total number of mesh elements in time direction. Thus, uniform meshes Ω_t^M and Ω_t^s with step size Δt, with M and s mesh elements, are used on the interval $[0, T]$ and $[-\tau, 0]$, respectively. The mesh size Δt is chosen in such a way that the delay parameter $\tau = s\Delta t$, where s is a positive integer, $t_j = j\Delta t$, $j \geq -s$. On the same mesh size, we have $T = M\Delta t$, $t_j = j\Delta t$, $0 \leq j \leq M$. We discretize time derivative in Eq. (5.1)-(5.2) by means of the implicit Euler scheme and obtaining the following system of ordinary differential equations

$$\begin{cases} U^{j+1}(x) = \phi_B(x, t_{j+1}), & 0 \leq x \leq 1,\ j \geq -s, \\ (1 + \Delta t \mathcal{L}_\varepsilon^M) U^{j+1}(x) = R^{j+1}(x), & \\ B_{L,\varepsilon} U^{j+1}(0) \equiv U^{j+1}(0) - \sqrt{\varepsilon} U_x^{j+1}(0) = \phi_L^{j+1}, & 0 \leq j \leq M-1, \\ B_{R,\varepsilon} U^{j+1}(1) \equiv U^{j+1}(1) + \sqrt{\varepsilon} U_x^{j+1}(1) = \phi_R^{j+1}, & 0 \leq j \leq M-1, \end{cases} \tag{5.10}$$

where $\mathcal{L}_\varepsilon^M U^{j+1}(x) = -\varepsilon (U_{xx})^{j+1} + a^{j+1}(x) U^{j+1}(x)$ and $R^{j+1}(x) = U^j(x) - \Delta t \big(b^{j+1}(x) U^{j-s+1}(x) - f^{j+1}(x) \big)$. Further, $U^{j+1}(x)$ is the numerical solution at the $(j+1)$th time level. By using the initial condition, we can evaluate the right-hand side as

$$R^{j+1}(x) = \begin{cases} U^j(x) - \Delta t \big(b^{j+1}(x) \phi_B(x, t_{j-s+1})(x) - f^{j+1}(x) \big), & j = 0, 1, ..., s, \\ U^j(x) - \Delta t \big(b^{j+1}(x) U(x, t_{j-s+1})(x) - f^{j+1}(x) \big), & j = s+1, ..., M. \end{cases}$$

For each time step, Eq. (5.10) can be rewritten in the operator form as

$$\begin{cases} U^{j+1}(x) = \phi_B(x, t_{j+1}), & 0 \le x \le 1,\ j \ge -s, \\ \mathcal{L}^M_{\varepsilon,*}U^{j+1}(x) \equiv (1 + \Delta t\mathcal{L}^M_{\varepsilon})U^{j+1}(x) = R^{j+1}(x), & \\ B_{L,\varepsilon}U^{j+1}(0) \equiv U^{j+1}(0) - \sqrt{\varepsilon}U^{j+1}_x(0) = \phi^{j+1}_L, & 0 \le j \le M-1, \\ B_{R,\varepsilon}U^{j+1}(1) \equiv U^{j+1}(1) + \sqrt{\varepsilon}U^{j+1}_x(1) = \phi^{j+1}_R, & 0 \le j \le M-1, \end{cases} \tag{5.11}$$

where the operator $\mathcal{L}^M_{\varepsilon,*}U^{j+1}(x)$ in (5.11) satisfies the semi-discrete maximum principle in the time direction, which ensures the stability of the linear systems of equations in (5.11).

Lemma 5.4.1. *Let the smooth function $Z^{j+1}(x) \in C^2(\Omega)\cup C^0(\bar{\Omega})$ such that $B_{L,\varepsilon}Z^{j+1}(0) \ge 0, B_{R,\varepsilon}Z^{j+1}(1) \ge 0$. Then, $\mathcal{L}^M_{\varepsilon,*}Z^{j+1}(x) \ge 0,\ \forall x \in \Omega$ implies $Z^{j+1}(x) \ge 0,\ \forall x \in \bar{\Omega}$.*

Proof. Let the function $Z^{j+1}(x)$ takes its minimum value at $x^* \in \bar{\Omega}$ such that $Z^{j+1}(x^*) = \min_{x\in\bar{\Omega}} Z^{j+1}(x)$ and assume that $Z^{j+1}(x^*) < 0$. Thus, it is obvious that (x^*, t^{j+1}) does not belong to the boundaries. Also, we have $\frac{\partial Z^{j+1}}{\partial x}(x^*) = 0$ and $\frac{\partial^2 Z^{j+1}}{\partial x^2}(x^*) \ge 0$.

Case (i). We have $B_{L,\varepsilon}Z^{j+1}(x^*) = Z^{j+1}(x^*) - \sqrt{\varepsilon}\dfrac{\partial Z^{j+1}}{\partial x}(x^*) < 0$, which is a contradiction.

Case (ii). We have $B_{R,\varepsilon}Z^{j+1}(x^*) = Z^{j+1}(x^*) + \sqrt{\varepsilon}\frac{\partial Z^{j+1}}{\partial x}(x^*) < 0$, which is a contradiction.

Case (iii). Now,

$$\mathcal{L}^M_{\varepsilon,*}Z^{j+1}(x^*) = -\varepsilon\frac{\partial^2 Z^{j+1}}{\partial x^2}(x^*) + a^{j+1}(x^*)Z^{j+1}(x^*) < 0,$$

which is a contradiction. Thus, it follows that $\mathcal{L}^M_{\varepsilon,*}Z^{j+1}(x^*) \ge 0, \forall x \in \Omega$. □

The local truncation error of for the time semi-discretization is given by $e_{j+1} = u(x, t_{j+1}) - U^{j+1}(x)$, where $U^{j+1}(x)$ is the computed solution for the following boundary value problem

$$\begin{cases} (1 + \Delta t\mathcal{L}^M_{\varepsilon})U^{j+1}(x) = U^j(x) - \Delta t\big(b^{j+1}(x)U^{j-s+1}(x) - f^{j+1}(x)\big), & \\ B_{L,\varepsilon}U^{j+1}(0) \equiv U^{j+1}(0) - \sqrt{\varepsilon}U^{j+1}_x(0) = \phi^{j+1}_L, & 0 \le j \le M-1, \\ B_{R,\varepsilon}U^{j+1}(1) \equiv U^{j+1}(1) + \sqrt{\varepsilon}U^{j+1}_x(1) = \phi^{j+1}_R, & 0 \le j \le M-1. \end{cases}$$

This error measures the contribution of each time step to the global error of the time semi-discretization. We can conclude that the consistency result for the semi-discretized problem is given by the following lemmas.

Lemma 5.4.2. *[27] If*

$$\left|\frac{\partial^k u(x,t)}{\partial t^k}\right| \leq C, \qquad (x,t) \in \bar{\Omega} \times [0,T], \quad 0 \leq k \leq 2,$$

then the local error bound in the time direction is given by

$$\|e_{j+1}\| \leq C(\Delta t)^2.$$

Proof. The computed solution $U^{j+1}(x)$ satisfies

$$(1 + \Delta t \mathcal{L}_\varepsilon^M)U^{j+1}(x) + \Delta t\big(b^{j+1}(x)U^{j-s+1}(x) - f^{j+1}(x)\big) = U^j(x).$$

Since the solution of the continuous problem (5.1) is smooth enough, we have

$$\begin{aligned}
U^j(x) &= U^{j+1}(x) + \Delta t \mathcal{L}_\varepsilon^M U^{j+1}(x) + \Delta t\big(b^{j+1}(x)U^{j-s+1}(x) - f^{j+1}(x)\big) \\
&\quad + \int_{t_j}^{t_{j+1}} (t_j - s)\frac{\partial^2 U}{\partial t^2}(s)ds \\
&= (1 + \Delta t \mathcal{L}_\varepsilon^M)U^{j+1}(x) + \Delta t\big(b^{j+1}(x)U^{j-s+1}(x) - f^{j+1}(x)\big) + O(\Delta t^2).
\end{aligned}$$

Therefore, the local truncation error e_{j+1} satisfies the following boundary value problem

$$\begin{aligned}
(1 + \Delta t \mathcal{L}_\varepsilon^M)e_{j+1}(x) &= O(\Delta t^2), \\
B_{L,\varepsilon}e^{j+1}(0) \equiv e^{j+1}(0) - \sqrt{\varepsilon}e_x^{j+1}(0) &= \phi_L^{j+1}, \\
B_{R,\varepsilon}e^{j+1}(1) \equiv e^{j+1}(1) + \sqrt{\varepsilon}e_x^{j+1}(1) &= \phi_R^{j+1}.
\end{aligned}$$

An application of semi-discrete maximum principle on the operator $(1 + \Delta t \mathcal{L}_\varepsilon^M)$ gives

$$\|e_{j+1}\| \leq C(\Delta t)^2,$$

as required. □

The local truncation error e_{j+1} measures the contribution of each time step to the global error of the time semi-discretization given by $e_j = \sum_{k=1}^{j} e_k$. Then e_j satisfy the following Lemma. The global error is the measure of the contribution of the local error estimate at each time step and is given by $e_j = u(x, t_j) - U^j(x)$.

Lemma 5.4.3. *Under the hypothesis of Lemma* (5.4.2)*, the global error at t_j is given by*

$$\|e_j\| \leq C\Delta t, \quad \forall j \leq T/\Delta t.$$

Proof. The global error estimate is given by

$$\begin{aligned}\|e_j\| = \|\sum_{k=1}^{j} e_k\| &\leq \|e_1\| + \|e_2\| + \cdots + \|e_j\|,\\ &\leq C_1 j(\Delta t)^2, \quad \text{by Lemma 5.4.2},\\ &\leq C_1 T(\Delta t), \quad j\Delta t \leq T,\\ &\leq C\Delta t, \quad C = C_1 T,\end{aligned}$$

where C is a positive constant independent of ε and Δt. □

We conclude that time semi-discretization is first-order uniformly convergent.

5.4.2 Space Discretization

A layer-adapted Shishkin mesh is constructed in such a way that the space domain Ω_x^N is divided into the three non-overlapping intervals $[0, \sigma]$, $(\sigma, 1 - \sigma)$ and $[1 - \sigma, 1]$ with $\frac{N}{4}$, $\frac{N}{2}$ and $\frac{N}{4}$ equidistant subintervals. We define the transition parameter σ as $\sigma =$

$\min\left\{\frac{1}{4}, 2\sqrt{\varepsilon}\ln N\right\}$. Now, we define a piecewise uniform mesh points as

$$x_i = \begin{cases} ih_i, & \text{if } 0 \le i \le \frac{N}{4}, \\ \sigma + \left(i - \frac{N}{4}\right)h_i, & \text{if } \frac{N}{4} \le i \le \frac{3N}{4}, \\ 1 - \sigma + \left(i - \frac{3N}{4}\right)h_i, & \text{if } \frac{3N}{4} \le i \le N, \end{cases}$$

with spacing $h_i = \frac{4\sigma}{N}$, if $1 \le i \le \frac{N}{4}$, $\frac{3N}{4} \le i \le N$ and $h_i = \frac{2(1-2\sigma)}{N}$, if $\frac{N}{4} \le i \le \frac{3N}{4}$. Now, we apply the extended cubic B-spline collocation method to find the approximate solution to Eq. (5.11). Let $\Delta : 0 = x_0 < ... < x_N = 1$ be the space domain $[0, 1]$ with a piecewise uniform mesh spacing $h_i = x_{i+1} - x_i$. The extended cubic B-spline of degree 4, $E_i(x, \lambda), \quad i = -1, 0, \cdots, N, N+1$ is defined by [63] and [113]

$$E_i(x,\lambda) = \frac{1}{24h_i^4} \begin{cases} 4h_i(1-\lambda)(x-x_{i-2})^3 + 3\lambda(x-x_{i-2})^4, & x \in [x_{i-2}, x_{i-1}], \\ (4-\lambda)h_i^4 + 12h_i^3(x-x_{i-1}) + 6h_i^2(2+\lambda)(x-x_{i-1})^2 & \\ -12h_i(x-x_{i-1})^3 - 3\lambda(x-x_{i-1})^4, & x \in [x_{i-1}, x_i], \\ (4-\lambda)h_i^4 + 12h_i^3(x_{i+1}-x) + 6h_i^2(2+\lambda)(x_{i+1}-x)^2 & \\ -12h_i(x_{i+1}-x)^3 - 3\lambda(x_{i+1}-x)^4, & x \in [x_i, x_{i+1}], \\ 4h_i(1-\lambda)(x_{i+2}-x)^3 + 3\lambda(x_{i+2}-x)^4, & x \in [x_{i+1}, x_{i+2}], \\ 0, \quad \text{otherwise}. \end{cases} \tag{5.12}$$

In Eq. (5.12), the free parameter λ is used to change the shape of the B-spline curve and is given by $-m(m-2) \le \lambda \le 1$, where m is the degree of extended cubic B-spline. The variation in m gives different forms of extended cubic B-spline functions [113]. The extended cubic B-spline function has one free parameter, λ. When the free parameter λ tends to zero, the extended cubic B-spline is reduced to convectional cubic B-spline functions. For $\lambda \in [-8, 1]$, cubic B-spline and extended cubic B-spline share the same properties such as local support, non-negativity, partition of unity, and C^2 continuity;

the parameter λ controls the tension of the solution curve. The shape of the extended cubic B-spline functions forces us to add two ghost points, E_{-1} and E_{N+1} to satisfy the boundary conditions. Since B-splines of degree p are $(p-1)$ times continuously differentiable piecewise polynomials that form the basis of the space of splines, let $\varphi_3(\Omega)$ be the space of twice continuously differentiable piecewise extended cubic B-spline on Ω. Since each $E_i(x)$ is also a piecewise cubic with knots at Ω, each $E_i(x) \in \varphi_3(\Omega)$. Suppose that $E_3(\Omega) = \text{span}\,\{E_{-1}, E_0, ..., E_N, E_{N+1}\}$. Since the functions $E_i's$ are linearly independent on $[0,1]$, $E_3(\Omega)$ is an $(N+3)$-dimensional. Let $S(x,\lambda)$ be the B-spline function for $u(x,t_{j+1})$ at the nodal points and $S(x,\lambda) \in E_3(\Omega)$. Therefore, we seek an approximate solution $S(x,\lambda)$ of Eq. (5.11) which is given by

$$S(x,\lambda) = \sum_{i=-1}^{N+1} \gamma_i E_i(x,\lambda), \tag{5.13}$$

where γ_i are unknown real coefficients to be determined by requiring that $S(x,\lambda)$ satisfies Eq. (5.11) at $N+1$ collocation points and imposing the initial and boundary conditions. The values of extended B-splines $E_i(x,\lambda)$ and their derivatives at the nodal points can be calculated from Eq. (5.13) and depicted in Table (5.1). An approximate solution over typical subinterval $[x_i, x_{i+1}]$ can be defined as

$$S(x,\lambda) = \sum_{j=i-1}^{i+2} \gamma_j E_j(x,\lambda). \tag{5.14}$$

Now, substituting the values of E_i for $S_i(\lambda)$ and E_i'' for $S_i''(\lambda)$ as stated in Table (5.1) in

Table 5.1: Values of $E_i(x,\lambda)$ and their derivatives at nodal points.

	x_{i-2}	x_{i-1}	x_i	x_{i+1}	x_{i+2}
$E_i(x,\lambda)$	0	$\frac{4-\lambda}{24}$	$\frac{8+\lambda}{12}$	$\frac{4-\lambda}{24}$	0
$E_i'(x,\lambda)$	0	$\frac{1}{2h_i}$	0	$-\frac{1}{2h_i}$	0
$E_i''(x,\lambda)$	0	$\frac{2+\lambda}{2h_i^2}$	$-\frac{2+\lambda}{h_i^2}$	$\frac{2+\lambda}{2h_i^2}$	0

Eq. (5.11), we get $(N+1)$ linear equations in $(N+3)$ unknowns as

$$\begin{aligned} &-\varepsilon\left(\frac{2+\lambda}{2h_i^2}\gamma_{i-1}-\frac{2+\lambda}{h_i^2}\gamma_i+\frac{2+\lambda}{2h_i^2}\gamma_{i+1}\right)\\ &+p_i^{j+1}\left(\frac{4-\lambda}{24}\gamma_{i-1}+\frac{8+\lambda}{12}\gamma_i+\frac{4-\lambda}{24}\gamma_{i+1}\right)=R_i^{j+1}. \end{aligned} \tag{5.15}$$

After rearranging the terms in Eq. (5.15), we have

$$r_i^-\gamma_{i-1}+r_i^c\gamma_i+r_i^+\gamma_{i+1}=\tilde{R}_i, \quad \text{for } i=0,1,...,N \tag{5.16}$$

where the coefficients are given by

$$\begin{cases} r_i^- = \frac{-\varepsilon(2+\lambda)}{2h_i^2}+\frac{(4-\lambda)}{24}\tilde{p}_i,\\ r_i^c = \frac{\varepsilon(2+\lambda)}{h_i^2}+\frac{(8+\lambda)}{12}\tilde{p}_i,\\ r_i^+ = \frac{-\varepsilon(2+\lambda)}{2h_i^2}+\frac{(4-\lambda)}{24}\tilde{p}_i,\\ \tilde{p}_i=p_i^{j+1}, \quad \tilde{R}_i=R_i^{j+1}. \end{cases}$$

Boundary condition in Eq. (5.11) at x_0 and x_N must be imposed on the system of equations in Eq. (5.16) to obtain the unique solution. At the left boundary, we have

$$\frac{4-\lambda}{24}\gamma_{-1}+\frac{8+\lambda}{12}\gamma_0+\frac{4-\lambda}{24}\gamma_1-\sqrt{\varepsilon}\left(\frac{1}{2h_i}\gamma_{-1}-\frac{1}{2h_i}\gamma_1\right)=\phi_L^{j+1}. \tag{5.17}$$

Rearranging the terms in Eq. (5.17), we have

$$\left(\frac{4-\lambda}{24}-\frac{\sqrt{\varepsilon}}{2h_i}\right)\gamma_{-1}+\frac{8+\lambda}{12}\gamma_0+\left(\frac{4-\lambda}{24}+\frac{\sqrt{\varepsilon}}{2h_i}\right)\gamma_1=\phi_L^{j+1}. \tag{5.18}$$

At the right boundary, we have

$$\frac{4-\lambda}{24}\gamma_{N-1}+\frac{8+\lambda}{12}\gamma_N+\frac{4-\lambda}{24}\gamma_{N+1}+\sqrt{\varepsilon}\left(\frac{1}{2h_i}\gamma_{N-1}-\frac{1}{2h_i}\gamma_{N+1}\right)=\phi_R^{j+1}. \tag{5.19}$$

Rearranging the terms in Eq. (5.19), we have

$$\left(\frac{4-\lambda}{24}+\frac{\sqrt{\varepsilon}}{2h_i}\right)\gamma_{N-1}+\frac{8+\lambda}{12}\gamma_N+\left(\frac{4-\lambda}{24}-\frac{\sqrt{\varepsilon}}{2h_i}\right)\gamma_{N+1}=\phi_R^{j+1}. \tag{5.20}$$

For simplicity, we write Eqs. (5.18) and (5.20) in the following form

$$\begin{aligned} a_1\gamma_{-1}+b_1\gamma_0+c_1\gamma_1&=\phi_L^{j+1},\\ c_1\gamma_{N-1}+b_1\gamma_N+a_1\gamma_{N+1}&=\phi_R^{j+1}, \end{aligned} \tag{5.21}$$

where the coefficients are given by $a_1=\frac{4-\lambda}{24}-\frac{\sqrt{\varepsilon}}{2h_i}, b_1=\frac{8+\lambda}{12}, c_1=\frac{4-\lambda}{24}+\frac{\sqrt{\varepsilon}}{2h_i}$. Equations (5.16) and (5.21) lead to an $(N+3)\times(N+3)$ linear systems with $(N+3)$ unknowns $\gamma_{-1},\gamma_0,...,\gamma_{N+1}$. To be solvable system, we must eliminate the ghost values γ_{-1} and γ_{N+1} from Eq. (5.21). To eliminate γ_{-1}, we set $i=0$ in Eq. (5.16) and obtaining

$$r_0^-\gamma_{-1}+r_0^c\gamma_0+r_0^+\gamma_1=\tilde{R}_0. \tag{5.22}$$

Substituting first equation of Eq. (5.21) into Eq. (5.22), we have

$$r_0^-\left(\frac{\phi_L^{j+1}}{a_1}-\frac{b_1}{a_1}\gamma_0-\frac{c_1}{a_1}\gamma_1\right)+r_0^c\gamma_0+r_0^+\gamma_1=\tilde{R}_0. \tag{5.23}$$

Rearranging Eq. (5.23), we obtain the following equation at the left boundary point

$$\left(r_0^c-\frac{b_1}{a_1}r_0^-\right)\gamma_0+\left(r_0^+-\frac{c_1}{a_1}r_0^-\right)\gamma_1=\tilde{R}_0-\frac{r_0^-}{a_1}\phi_L^{j+1}. \tag{5.24}$$

To eliminate γ_{N+1}, we set $i=N$ in Eq. (5.16) and obtaining

$$r_N^-\gamma_{N-1}+r_N^c\gamma_N+r_N^+\gamma_{N+1}=\tilde{R}_N. \tag{5.25}$$

Substituting the second equation of Eq. (5.21) into Eq. (5.25), we have

$$r_N^- \gamma_{N-1} + r_N^c \gamma_N + r_N^+ \left(\frac{\phi_R^{j+1}}{a_1} - \frac{c_1}{a_1}\gamma_{N-1} - \frac{b_1}{a_1}\gamma_N \right) = \tilde{R}_N. \tag{5.26}$$

Rearranging Eq. (5.26), we obtain the following equation at the right boundary point

$$\left(r_N^- - \frac{c_1}{a_1} r_N^+ \right)\gamma_{N-1} + \left(r_N^c - \frac{b_1}{a_1} r_N^+ \right)\gamma_N = \tilde{R}_N - \frac{r_N^+}{a_1}\phi_R^{j+1}. \tag{5.27}$$

Combining Eq. (5.16) together with Eqs. (5.24) and (5.27) gives solvable system of $(N+1) \times (N+1)$ linear equations in $(N+1)$ unknowns $\gamma_0, ..., \gamma_N$, which can be written in matrix form as

$$M\gamma = G, \qquad i = 1, 2, ..., N-1, \quad j = 0, \cdots, M-1, \tag{5.28}$$

where the entries of the tridiagonal matrix $M = (m_{ij})$ are given by

$$m_{ij} = \begin{cases} r_0^c - \frac{b_1}{a_1} r_0^-, & i = j = 0, \\ r_0^+ - \frac{c_1}{a_1} r_0^-, & i = j = 0, \\ r_i^-, & i = 1, 2, ..., N-1, \ j = 1, \cdots, M-2, \\ r_i^c, & i = 1, 2, ..., N-1, \ j = 1, \cdots, M-2, \\ r_i^+, & i = 1, 2, ..., N-1, \ j = 1, \cdots, M-2, \\ r_N^- - \frac{c_1}{a_1} r_N^+, & i = N, \ j = M-1, \\ r_N^c - \frac{b_1}{a_1} r_N^+, & i = N, \ j = M-1, \\ 0, & \forall |i-j| > 0. \end{cases}$$

The entries of the column vector G is given as

$$G = \begin{cases} \tilde{R}_0^{j+1} - \dfrac{r_0^-}{a_1}\phi_L^{j+1}, & i = 0,\ j = 0, \\ \tilde{R}_i^{j+1}, & i = 1, 2, ..., N-1,\ j = 1, \cdots, M-2, \\ \tilde{R}_N^{j+1} - \dfrac{r_N^+}{a_1}\phi_R^{j+1}, & i = N,\ j = M-1. \end{cases}$$

Since $p_i^{j+1} > 0$, it is easily seen that for $\lambda > -2$ the matrix M is strictly diagonally dominant and hence non-singular. Since M is non-singular, we can solve the system of linear equations in Eq. (5.28) for $\gamma_0, ..., \gamma_N$. Hence, the extended cubic B-spline collocation method applied to Eq. (5.11) has a unique solution $S(x, \lambda)$.

5.5 Analysis of the Method

This section proves the ε-uniform convergence of the present method in the space direction. For this, we use the following lemma.

Lemma 5.5.1. *The extended cubic B-splines* $\{E_{-1}(x,\lambda), E_0(x,\lambda), ..., E_N(x,\lambda), E_{N+1}(x,\lambda)\}$ *defined in Eq.* (5.12) *satisfy the following inequality*

$$\sum_{i=-1}^{N+1} \big|E_i(x,\lambda)\big| \le \frac{7}{4}, \qquad x \in [0,1].$$

Proof. We know that

$$\big|\sum_{i=-1}^{N+1} E_i(x,\lambda)\big| \le \sum_{i=-1}^{N+1} \big|E_i(x,\lambda)\big|.$$

Extended cubic B-splines $E_i(x,\lambda)$ is nonzero at only three nodal points. Thus, at any nodal value x_i, from Table (5.1) we obtain

$$\begin{aligned} \sum_{i=-1}^{N+1} \big|E_i(x,\lambda)\big| &= |E_{i-1}(x_i,\lambda)| + |E_i(x_i,\lambda)| + |E_{i+1}(x_i,\lambda)|, \\ &= \frac{4-\lambda}{24} + \frac{8+\lambda}{12} + \frac{4-\lambda}{24} = 1 < \frac{7}{4}. \end{aligned}$$

From Table (5.1), for $x \in [x_{i-1}, x_i]$, we have

$$|E_i(x, \lambda)| \leq \frac{8+\lambda}{12}, \qquad |E_{i-1}(x, \lambda)| \leq \frac{8+\lambda}{12}.$$

Similarly, for $x \in [x_{i-1}, x_i]$, we have that

$$|E_{i+1}(x, \lambda)| \leq \frac{4-\lambda}{24}, \qquad |E_{i-2}(x, \lambda)| \leq \frac{4-\lambda}{24}.$$

Now, for any point for $x \in [x_{i-1}, x_i]$, we get

$$\sum_{i=-1}^{N+1} \left|E_i(x, \lambda)\right| = |E_{i-1}(x, \lambda)| + |E_i(x, \lambda)| + |E_{i+1}(x, \lambda)| + |E_{i-2}(x, \lambda)| = \frac{20+\lambda}{12}.$$

Since $-8 \leq \lambda \leq 1$, thus $\frac{20+\lambda}{12} \leq \frac{7}{4}$ and this completes the proof. □

Let $Y(x)$ be the unique cubic spline interpolate for an approximate solution $S(x, \lambda)$ of Eq. (5.11) to the solution $U(x_i, t_{j+1})$ which is given by

$$Y(x) = \sum_{i=-1}^{N+1} \bar{\gamma}_i E_i(x, \lambda). \tag{5.29}$$

Lemma 5.5.2. *Let $Y(x)$ be the cubic spline interpolant associated with a solution U_i^{j+1}. If $\tilde{R}_i \in C^2([0,1])$ and $\hat{u}(x_i) = U_i^{j+1} \in C^4([0,1])$, it follows from the estimate of Hall [48] that the standard cubic spline interpolation error estimate holds, for $x \in \Omega_i := [x_i, x_{i+1}] \in \Omega$*

$$\|D^n(\hat{u}(x_i) - Y(x_i))\| \leq \lambda_n h_i^{4-n} \|\hat{u}^{(4)}(x_i)\|, \qquad n = 0, 1, 2, 3$$

where λ_n are constants independent of h_i.

Lemma 5.5.3. *[121] If matrix A is strictly diagonally dominant by rows and the constant $\zeta = \min_i(|a_{i,i}| - \sum_{i\neq j}|a_{i,j}|)$. Then, we have the bound*

$$\|A^{-1}\|_\infty < \frac{1}{\zeta}.$$

Theorem 5.3. *Let $S(x,\lambda)$ be an extended cubic B-spline collocation approximation from the space of extended B-splines $\varphi_3(\Omega)$ to the solution of Eq. (5.11) and $\hat{u}(x_i) = U_i^{j+1}$ is the solution to the problem. If $\tilde{R}(x) \in C^2([0,1])$, then the parameter-uniform error estimate satisfies the bound*

$$\sup_{0<\varepsilon\leq 1} \max_{0\leq i\leq N} |\hat{u}(x_i) - S_i(\lambda)| \leq CN^{-2}(\ln N)^2,$$

where C is a constant independent of ε and N.

Proof. To estimate the error $|\hat{u}(x_i) - S(x_i,\lambda)|$, it follows immediately from the estimates in Lemma (5.5.2) and Eq. (5.29) that

$$\begin{aligned}|\hat{\mathcal{L}}_\varepsilon \hat{u}(x_i) - \hat{\mathcal{L}}_\varepsilon Y(x_i)| &\leq \varepsilon\left(\hat{u}''(x_i) - Y''(x_i)\right) + \tilde{p}(x_i)(\hat{u}(x_i) - Y(x_i)),\\ &\leq \varepsilon(\lambda_2 h_i^2|\hat{u}^{(4)}|) + \|p\|_\infty(\lambda_0 h_i^4|\hat{u}^{(4)}|),\end{aligned}$$

The rearrangement of the above expression gives

$$|\hat{\mathcal{L}}_\varepsilon \hat{u}(x_i) - \hat{\mathcal{L}}_\varepsilon Y(x_i)| \leq \left(\varepsilon\lambda_2 h_i^2 + \|p\|_\infty \lambda_0 h_i^4\right)|\hat{u}^{(4)}|. \tag{5.30}$$

Since the argument depends on whether $\sigma = 1/4$ or $\sigma = 2\sqrt{\varepsilon}\ln N < 1/4$, there arises two cases.

Case (i): When $\sigma = 1/4$, the mesh is uniform with spacing $1/N$, that is, $h_i = 1/N$ and $2\sqrt{\varepsilon}\ln N \geq 1/4$ gives $\varepsilon^{-1/2} \leq C\ln N$. From this, we get $\varepsilon^{-1} \leq (C\ln N)^2$. In this case, we use a classical analysis to prove convergence. Using the classical bound in Theorem (5.1), that is, $|\hat{u}^{(4)}| \leq C\varepsilon^{-2}$ together with Eq. (5.30) yields

$$\begin{aligned}|\hat{\mathcal{L}}_\varepsilon \hat{u}(x_i) - \hat{\mathcal{L}}_\varepsilon Y(x_i)| &\leq C\varepsilon^{-2}\Bigg(\varepsilon\lambda_2 N^{-2} + \|p\|_\infty \lambda_0 N^{-4}\Bigg),\\ &\leq CN^{-2}\Bigg(\varepsilon^{-1} + \varepsilon^{-2}N^{-2}\Bigg),\\ &\leq CN^{-2}\Bigg((C\ln N)^2 + CN^{-2}(\ln N)^4\Bigg).\end{aligned}$$

Since $CN^{-2}(\ln N)^4 \leq C(\ln N)^2$, we obtain the following estimate

$$|\hat{\mathcal{L}}_\varepsilon \hat{u}(x_i) - \hat{\mathcal{L}}_\varepsilon Y(x_i)| \leq CN^{-2}(\ln N)^2.$$

Case (ii): If Ω_i lies in the boundary layer regions, then mesh spacing $h_i = \frac{4\sigma}{N}$ and $\sigma = 2\sqrt{\varepsilon}\ln N$. Then, $h_i \leq C\sqrt{\varepsilon}N^{-1}\ln N$. Using the bounds w_l and w_r in the Theorem (5.2) in the layer regions together with the estimates in Eq. (5.30), we have

$$\begin{aligned}|\hat{\mathcal{L}}_\varepsilon \hat{u}(x_i) - \hat{\mathcal{L}}_\varepsilon Y(x_i)| &\leq C\varepsilon^{-2}\Bigg(\varepsilon\lambda_2 C^2\varepsilon N^{-2}(\ln N)^2 + \|p\|_\infty \lambda_0 C^4\varepsilon^2 N^{-4}(\ln N)^4\Bigg),\\ &\leq CN^{-2}\Bigg((\ln N)^2 + N^{-2}(\ln N)^4\Bigg), \text{ since } e^{-x_0/\sqrt{\varepsilon}} \leq 1 \ \&\ e^{-(1-x_0)/\sqrt{\varepsilon}} \leq 1.\end{aligned}$$

Since $N^{-2}(\ln N)^4 \leq (\ln N)^2$, we obtain the following estimate

$$|\hat{\mathcal{L}}_\varepsilon \hat{u}(x_i) - \hat{\mathcal{L}}_\varepsilon Y(x_i)| \leq CN^{-2}(\ln N)^2.$$

On the other hand, for the subinterval $[\sigma, 1-\sigma]$, that is, for the outer region the mesh spacing is $h_i = 2N^{-1}(1-2\sigma) = 2N^{-1} - C\sqrt{\varepsilon}N^{-1}\ln N \leq C\varepsilon^{1/2}N^{-1}\ln N$. Using this in Eq. (5.30) together with the bound in Theorem (5.2) for v gives us

$$\begin{aligned}|\hat{\mathcal{L}}_\varepsilon \hat{u}(x_i) - \hat{\mathcal{L}}_\varepsilon Y(x_i)| &\leq C\varepsilon^{-2}\Bigg(\varepsilon\lambda_2 C^2\varepsilon N^{-2}\ln^2 N + \|p\|_\infty \lambda_0 C^4\varepsilon^2 N^{-4}\ln^4 N\Bigg)(C(1+\varepsilon^0)),\\ &\leq C\varepsilon^2\Bigg(N^{-2}(\ln N)^2 + N^{-4}(\ln N)^4\Bigg), \text{ since } \sqrt{\varepsilon} \leq CN^{-1},\\ &\leq CN^{-2}\Bigg(N^{-2}(\ln N)^2 + N^{-4}(\ln N)^4\Bigg).\end{aligned}$$

Since $N^{-2}(\ln N)^4$ is very small number, we obtain the following estimate

$$|\hat{\mathcal{L}}_\varepsilon \hat{u}(x_i) - \hat{\mathcal{L}}_\varepsilon Y(x_i)| \leq CN^{-2}(\ln N)^2.$$

Combining the above estimates for both the cases, we have

$$|\hat{\mathcal{L}}_\varepsilon \hat{u}(x_i) - \hat{\mathcal{L}}_\varepsilon Y(x_i)| \leq CN^{-2}(\ln N)^2. \tag{5.31}$$

Therefore, we have

$$\begin{aligned} |\hat{\mathcal{L}}_\varepsilon S(x_i,\lambda) - \hat{\mathcal{L}}_\varepsilon Y(x_i)| = |\hat{R}(x_i) - \hat{\mathcal{L}}_\varepsilon Y(x_i)| &= |\hat{\mathcal{L}}_\varepsilon \hat{u}(x_i) - \hat{\mathcal{L}}_\varepsilon Y(x_i)| \\ &\leq CN^{-2}(\ln N)^2. \end{aligned} \tag{5.32}$$

We know that $\hat{\mathcal{L}}_\varepsilon \tilde{u}(x_i) = \hat{R}(x_i), \quad 0 \leq i \leq N$ with the boundary conditions $\tilde{u}(x_0) - \sqrt{\varepsilon}\tilde{u}'(x_0) = \phi_L^{j+1}$ and $\tilde{u}(x_N) + \sqrt{\varepsilon}\tilde{u}'(x_N) = \phi_R^{j+1}$ leads to the linear system $M\gamma = G$. Assume that $\hat{\mathcal{L}}_\varepsilon Y(x_i) = \bar{R}(x_i), \quad 0 \leq i \leq N$ with the boundary conditions $Y(x_0) - \sqrt{\varepsilon}Y'(x_0) = \bar{\phi_L}^{j+1}$ and $Y(x_N) + \sqrt{\varepsilon}Y'(x_N) = \bar{\phi_R}^{j+1}$ leads to the linear system $M\bar{\gamma} = \bar{G}$. It follows that

$$M(\gamma - \bar{\gamma}) = (G - \bar{G}), \tag{5.33}$$

where $\gamma - \bar{\gamma} = (\gamma_0 - \bar{\gamma}_0, \gamma_1 - \bar{\gamma}_1, ..., \gamma_N - \bar{\gamma}_N)^T$ and

$$G - \bar{G} = \begin{pmatrix} (\tilde{R}_0 - \bar{R}_0) + \frac{r_0^-}{a_1}\left(\bar{\phi_L^{j+1}} - \phi_L^{j+1}\right) \\ (\tilde{R}_1 - \bar{R}_1) \\ \vdots \\ (\tilde{R}_{N-1} - \bar{R}_{N-1}) \\ (\tilde{R}_N - \bar{R}_N) + \frac{r_N^+}{a_1}\left(\bar{\phi_R^{j+1}} - \phi_R^{j+1}\right) \end{pmatrix}$$

Since $M\gamma - M\bar{\gamma} = G - \bar{G}$ from Eq. (5.33) implies that $\hat{\mathcal{L}}_\varepsilon S(x_i) - \hat{\mathcal{L}}_\varepsilon Y(x_i)$, from Eq. (5.31) we have

$$\|G - \bar{G}\| \leq CN^{-2}(\ln N)^2. \tag{5.34}$$

It can be seen that for $\lambda > -2$ and reasonable large N, the matrix M is strictly diagonally dominant and thus non-singular [63]. From the estimate in Lemma (5.5.3), we get

$$\|M^{-1}\| \leq C, \tag{5.35}$$

Combining the bounds in Eqs. (5.33)-(5.35), we obtain

$$\|\gamma - \bar{\gamma}\| \leq CN^{-2}(\ln N)^2. \tag{5.36}$$

Let $e = (e_0, \cdots, e_N)^T$, where $e_i = \gamma_i - \bar{\gamma}_i$. Now, from Eq. (5.27), we have

$$e = M^{-1}(G - \bar{G}). \tag{5.37}$$

Using Eqs. (5.34) and (5.35) in Eq. (5.37), we have the following estimate

$$\|e\| \leq CN^{-2}(\ln N)^2. \tag{5.38}$$

We have the following from the boundaries

$$\begin{aligned} a_1(\gamma_{-1} - \bar{\gamma}_{-1}) + b_1(\gamma_0 - \bar{\gamma}_0) + c_1(\gamma_1 - \bar{\gamma}_1) = \phi_L^{j+1}, \\ c_1(\gamma_{N-1} - \bar{\gamma}_{N-1}) + b_1(\gamma_N - \bar{\gamma}_N) + a_1(\gamma_{N+1} - \bar{\gamma}_{N+1}) = \phi_R^{j+1}, \end{aligned}$$

where a_1, b_1 and c_1 are defined in Eq. (5.21). From this, it is simple task to obtain $|\gamma_{-1} - \bar{\gamma}_{-1}| \leq CN^{-2}(\ln N)^2$ and $|\gamma_{N+1} - \bar{\gamma}_{N+1}| \leq CN^{-2}(\ln N)^2$. Therefore, we have the following estimation from boundary conditions as

$$\max_{-1 \leq i \leq N+1} |\gamma_i - \bar{\gamma}_i| \leq CN^{-2}(\ln N)^2. \tag{5.39}$$

Therefore, the inequality in Eq. (5.39) enables us to estimate $|S_i(\lambda) - Y(x_i)|$ as

$$|S_i(\lambda) - Y(x_i)| = \sum_{i=-1}^{N+1} (\gamma_i - \bar{\gamma}_i)|E_i(x_i, \lambda)|.$$

Using Eq. (5.38) and Lemma (5.5.1), we obtain

$$\max_{0 \le i \le N} |S_i(\lambda) - Y(x_i)| \le CN^{-2}(\ln N)^2. \tag{5.40}$$

From the triangular inequality, we have

$$\begin{aligned} |\hat{u}(x_i) - S_i(\lambda)| &= |\hat{u}(x_i) - Y(x_i)| + |Y(x_i) - S_i(\lambda)|, \\ &\le |\hat{u}(x_i) - Y(x_i)| + |S_i(\lambda) - Y(x_i)|. \end{aligned} \tag{5.41}$$

Using Eq. (5.41) and the results in Eqs. (5.31) and (5.40) gives

$$\sup_{0<\varepsilon\le 1} \max_{0 \le i \le N} |\hat{u}(x_i) - S_i(\lambda)| \le CN^{-2}(\ln N)^2. \tag{5.42}$$

Hence, this completes the proof. □

Theorem 5.4. *Let $S_i^j(\lambda)$ be the extended B-spline collocation approximation to the solution $u(x,t)$ of the problem in Eq. (5.11). Then, the parameter-uniform error estimate of fully discrete scheme is given by*

$$\sup_{0<\varepsilon\le 1} \max_{0\le i\le N, 0\le j\le M} |u(x_i, t_j) - S_i^j(\lambda)| \le C(N^{-2}\ln^2 N + \Delta t).$$

where C is a constant independent of mesh parameters and ε.

Proof. The result of Lemma (5.4.3) and Theorem (5.3) proves this theorem. □

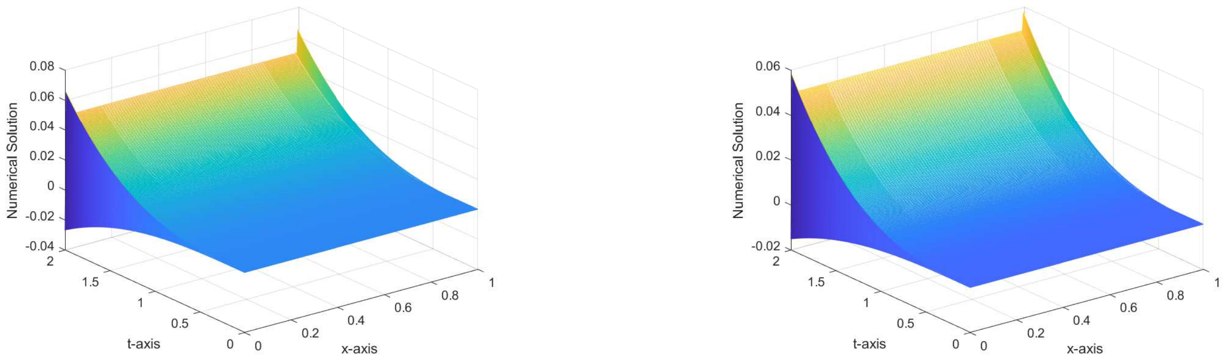

(a) $\lambda = -0.55$. **(b)** $\lambda = 0$.

Figure 5.1: Mesh plot of the numerical solution at $N = 128, \Delta t = \frac{0.1}{2^4}, \varepsilon = 2^{-12}$.

5.6 Numerical Results

To verify the applicability of the present method, an example from the literature is considered. Computations are done for some optimized value as taken in [63] of the free parameter $\lambda = 0.99 \in [-8, 1]$, which gives the minimum error.

Example 5.6.1. *Consider the problem with time delay [108]*

$$\frac{\partial u(x,t)}{\partial t} - \varepsilon \frac{\partial^2 u(x,t)}{\partial x^2} + \frac{1+x^2}{2} u(x,t) = -u(x,t-1) + t^3, \qquad (x,t) \in (0,1) \times (0,2],$$

with the initial condition and boundary conditions

$$\begin{cases} u(x,t) = 0, & (x,t) \in [0,1] \times [-1,0], \\ u(0,t) - \sqrt{\varepsilon}\frac{\partial u(0,t)}{\partial x} = -\frac{128}{35}\pi^{-1/2}t^{7/2}, & t \in [0,2], \\ u(1,t) + \sqrt{\varepsilon}\frac{\partial u(1,t)}{\partial x} = -\frac{128}{35}\pi^{-1/2}t^{7/2}, & t \in [0,2]. \end{cases}$$

The analytical solution for the test example is unknown, we use the double mesh principle to calculate maximum absolute errors using the formula in Eq. (2.31). The uniform error and rate of convergence is calculated by the formula in Eq. (2.32).

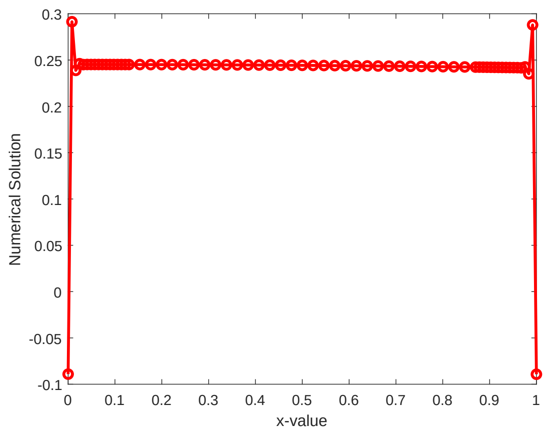

Figure 5.2: Boundary layer property for $N = 64 = M, \varepsilon = 2^{-12}, \lambda = -0.55$.

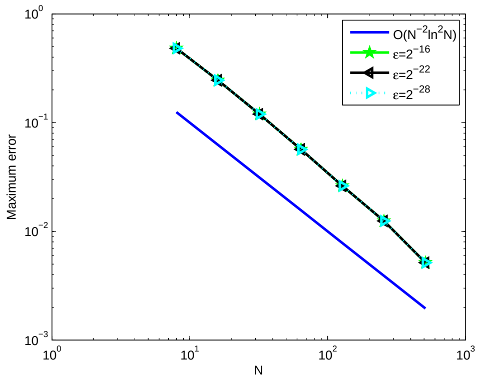

(a) for $\lambda = 0.99$.

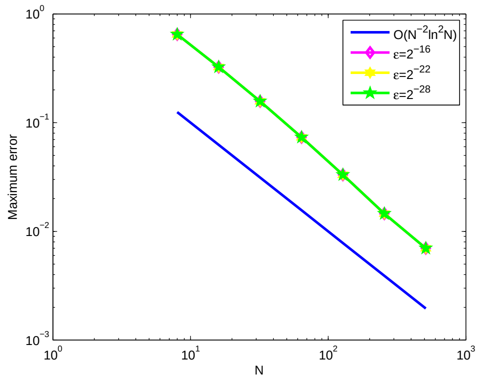

(b) $\lambda = 0$.

Figure 5.3: Loglog plot of the maximum absolute errors using Table (5.4).

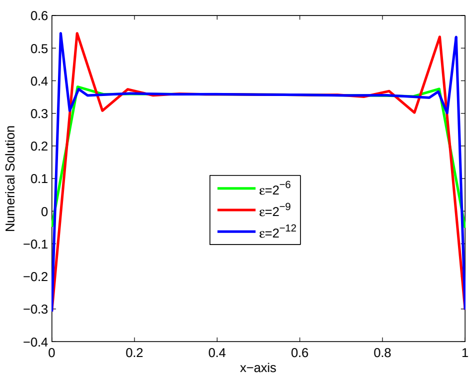

(a) for $\lambda = -0.55$.

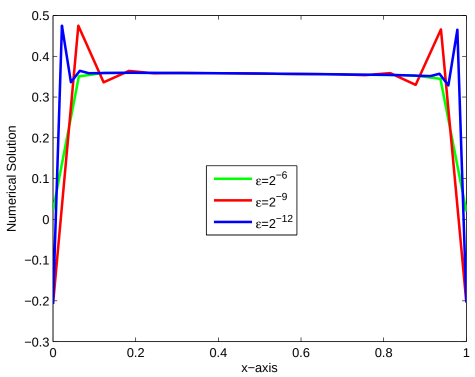

(b) $\lambda = 0$.

Figure 5.4: Effect of perturbation parameter ε on the solution at $N = 16, \Delta t = \frac{0.1}{2}$.

Table 5.2: The values $E_{\varepsilon}^{N,\Delta t}$ for the free parameter $\lambda = 0.99$.

$\varepsilon \downarrow$	$N = 16$, $\Delta t = \frac{0.1}{2}$	32, $\frac{0.1}{2^2}$	64, $\frac{0.1}{2^3}$	128, $\frac{0.1}{2^4}$	256, $\frac{0.1}{2^5}$	512, $\frac{0.1}{2^6}$	1024, $\frac{0.1}{2^7}$
2^{-6}	1.9043e-1	9.7604e-2	4.9405e-2	2.9193e-2	1.7022e-2	4.4560e-3	2.1246e-3
2^{-7}	1.9074e-1	9.7647e-2	4.9411e-2	2.4853e-2	1.4146e-2	4.4571e-3	2.1266e-3
2^{-8}	2.1707e-1	9.7679e-2	4.9415e-2	2.4853e-2	1.2463e-2	5.1580e-3	2.1270e-3
2^{-9}	2.4433e-1	1.1064e-1	4.9417e-2	2.4854e-2	1.2463e-2	5.1580e-3	2.1270e-3
2^{-10}	2.4551e-1	1.1980e-1	5.5853e-2	2.4854e-2	1.2463e-2	5.1580e-3	2.1270e-3
2^{-11}	2.4552e-1	1.1990e-1	5.6763e-2	2.6206e-2	1.2463e-2	5.1580e-3	2.1270e-3
2^{-12}	2.4552e-1	1.1990e-1	5.6763e-2	2.6206e-2	1.2463e-2	5.1580e-3	2.1270e-3
2^{-13}	2.4552e-1	1.1990e-1	5.6763e-2	2.6206e-2	1.2463e-2	5.1580e-3	2.1270e-3
2^{-14}	2.4552e-1	1.1990e-1	5.6763e-2	2.6206e-2	1.2463e-2	5.1580e-3	2.1270e-3
2^{-15}	2.4552e-1	1.1990e-1	5.6763e-2	2.6206e-2	1.2463e-2	5.1580e-3	2.1270e-3
2^{-16}	2.4552e-1	1.1990e-1	5.6763e-2	2.6206e-2	1.2463e-2	5.1580e-3	2.1270e-3
⋮	⋮	⋮	⋮	⋮	⋮	⋮	⋮
2^{-28}	2.4552e-1	1.1990e-1	5.6763e-2	2.6206e-2	1.2463e-2	5.1580e-3	2.1270e-3
2^{-29}	2.4552e-1	1.1990e-1	5.6763e-2	2.6206e-2	1.2463e-2	5.1580e-3	2.1270e-3
2^{-30}	2.4552e-1	1.1990e-1	5.6763e-2	2.6206e-2	1.2463e-2	5.1580e-3	2.1270e-3

5.7 Discussion and Conclusion

The computed maximum absolute errors, $E_{\varepsilon}^{N,\Delta t}$ is given in Table (5.2). From this result, it is clear that the present method gives a parameter-uniform convergence. Computational results in Table (5.3) confirm that the present method has improved the method in the literature [108]. Table (5.4) displays the comparison of computational results using the classical cubic B-spline method for $\lambda = 0$ and extended B-spline method for $\lambda = 0.99$. It is clear from Table (5.4) that extended cubic B-spline collocation method performs better than classical cubic B-spline collocation method. Figure (5.1a) depicts the numerical simulation of the solution profile using the extended cubic B-spline method for $\lambda = -0.55$. To compare the numerical simulation with the extended B-spline method, the solution profile for the classical B-spline method is plotted for $\lambda = 0$ in Figure (5.1b). From Figures (5.1) and (5.2), we see that the problem has parabolic boundary layers near $x = 0$ and $x = 1$ and more computed solutions are observed at the boundary layer regions. The maximum absolute errors are plotted using a log-log scale, as can be seen in Figure (5.3a)

Table 5.3: Comparison of $E^{N,\Delta t}$ using the prsent method and method in [108] for the free parameter $\lambda = 0.99$

Results	$N = 8$ $\Delta t = 0.1$	16 $\frac{0.1}{2}$	32, $\frac{0.1}{2^2}$	64, $\frac{0.1}{2^3}$	128, $\frac{0.1}{2^4}$	256, $\frac{0.1}{2^5}$	512, $\frac{0.1}{2^6}$
Present							
$E^{N,\Delta t}$	4.8306e-1	2.4552e-1	1.1990e-1	5.6763e-2	2.6206e-2	1.2463e-2	5.1580e-3
$R^{N,\Delta t}$	0.9764	1.0340	1.0788	1.1151	1.1722	1.2728	1.2780
In [108]							
$E^{N,\Delta t}$	7.3876e-1	4.2718e-1	2.3070e-1	1.2002e-1	6.1238e-2	3.0931e-2	1.5545e-2
$R^{N,\Delta t}$	0.7903	0.8888	0.9427	0.9709	0.9853	0.9926	0.9963

Table 5.4: Comparison of ε-uniform errors for $\lambda = 0$ and $\lambda = 0.99$.

	$N = 8$ $\Delta t = 0.1$	16 $\frac{0.1}{2}$	32, $\frac{0.1}{2^2}$	64, $\frac{0.1}{2^3}$	128, $\frac{0.1}{2^4}$	256, $\frac{0.1}{2^5}$	512, $\frac{0.1}{2^6}$
$\lambda = 0$							
$E^{N,\Delta t}$	6.4769e-1	3.2519e-1	1.5717e-1	7.3329e-2	3.3118e-2	1.4555e-2	6.9985e-3
$R^{N,\Delta t}$	0.9940	1.0490	1.0999	1.1468	1.1861	1.2232	1.2216
$\lambda = 0.99$							
$E^{N,\Delta t}$	4.8306e-1	2.4552e-1	1.1990e-1	5.6763e-2	2.6206e-2	1.2463e-2	5.1580e-3
$R^{N,\Delta t}$	0.9764	1.0340	1.0788	1.1151	1.1722	1.2728	1.2780

using the extended cubic B-spline method and (5.3b) using classical cubic B-spline. The effect of the singular perturbation parameter on the boundary layers is shown in Figures (5.4a) and (5.4b) for $\lambda = -0.55$ and $\lambda = 0$, respectively. As observed from these Figures, when $\varepsilon \to 0$ strong boundary layers are formed near $x = 0$ and $x = 1$. From the numerical results, we observe that the present method improved the method in the literature. The numerical results show that the extended cubic B-spline collocation approach performs better than the standard cubic B-spline collocation method.

Chapter 6

Hybrid Scheme on Shishkin-type Meshes for Singularly Perturbed Parabolic Reaction-diffusion Problems with Robin Boundary Conditions

In this chapter, a hybrid finite difference method for singularly perturbed parabolic reaction-diffusion problems with Robin boundary conditions is formulated. The problem is discretized in time direction using an implicit Euler method on a uniform mesh and in space direction using a hybrid method that includes a central difference scheme in the outer region and a cubic spline in tension scheme in the boundary layer regions on Shishkin-type meshes. Robin boundary conditions are discretized using second-order finite difference method. The stability and convergence analysis are established. Two numerical examples are computed and the results show that the present method gives almost second-order (up to logarithm factor) parameter-uniformly convergent results using Shishkin mesh, whereas the Bakhvalov-Shishkin and Vulanović-Shishkin meshes yields second-order and improved numerical solutions.

6.1 Introduction

Singularly perturbed parabolic reaction-diffusion problems with Dirichlet boundary conditions have been extensively studied using different numerical methods, for example, see [19], [24], [25], [26], [41], [43], [64], [67], [84], [87], [91], [93], [94] and [104]. Recent literature reported that authors in [68] studied singularly perturbed parabolic reaction-diffusion problems with Robin boundary conditions. No further study has been conducted for singularly perturbed parabolic reaction-diffusion problems with Robin boundary conditions. Inspired by this work and no hybrid method is developed so far for the problem under consideration, in this chapter, a hybrid finite difference scheme for the problem under consideration is developed. The present hybrid finite difference scheme comprises a cubic spline in tension scheme in the boundary layer regions and a classical central finite difference scheme in the outer region on layer-adapted Shishkin-type meshes for space discretization and an implicit Euler method on a uniform mesh for time discretization. The Robin boundary conditions is discretized by the second-order finite difference method.

6.2 Definition of the Problem

Consider the following singularly perturbed parabolic reaction-diffusion problem

$$\mathcal{L}_\varepsilon u(x,t) \equiv \frac{\partial u(x,t)}{\partial t} - \varepsilon \frac{\partial^2 u(x,t)}{\partial x^2} + a(x,t)u(x,t) = f(x,t), \quad (x,t) \in \Omega, \tag{6.1}$$

with the initial condition and boundary conditions

$$\begin{cases} u(x,0) = \phi_B(x), & 0 \le x \le 1, \\ B_{L,\varepsilon} u(0,t) \equiv u(0,t) - \sqrt{\varepsilon}\frac{\partial u(0,t)}{\partial x} = \phi_L(t), & 0 < t \le T, \\ B_{R,\varepsilon} u(1,t) \equiv u(1,t) + \sqrt{\varepsilon}\frac{\partial u(1,t)}{\partial x} = \phi_R(t), & 0 < t \le T, \end{cases} \tag{6.2}$$

where $0 < \varepsilon \ll 1$ is the perturbation parameter. The space-time domain is given by $\Omega = \Omega_x \times \Omega_t = (0,1) \times (0,T]$. The coefficient $a(x,t)$, the source function $f(x,t)$ and the initial-boundary functions $\phi_B(x)$, $\phi_L(t)$ and $\phi_R(t)$ are assumed to be sufficiently smooth and bounded. The reaction term $a(x,t)$ satisfies the condition $a(x,t) \geq \alpha > 0,\ (x,t) \in \bar{\Omega}$. The solution u of Eq. (6.1)–(6.2) is expected to exhibit twin parabolic boundary layers of width $O(\sqrt{\varepsilon})$ near $x = 0$ and $x = 1$.

6.3 Properties of the Continuous Solution

Setting the value $\varepsilon = 0$, the reduced problem corresponding to Eq. (6.1)-(6.2) is

$$\begin{cases} \frac{\partial u_0}{\partial t}(x,t) + a(x,t)u_0(x,t) = f(x,t), & (x,t) \in \Omega, \\ u_0(x,0) = \phi_B(x), & 0 \leq x \leq 1. \end{cases} \tag{6.3}$$

Since the reduced problem in Eq. (6.3) does not make use of the two boundary conditions, the solution to Eq. (6.1)-(6.2) have both left and right boundary layers. The characteristics curve of the reduced problem in Eq. (6.3) is the vertical lines $x=$ constant value, which implies that boundary layers arising in the solution are of parabolic type. The assumptions in problem (6.1) admits the following continuous maximum principle, which ensures the uniform stability of the solution to Eq. (6.1)-(6.2).

Lemma 6.3.1. *Assume that $a \in C^{(0,0)}(\bar{\Omega})$ and let $\varphi \in C^{(2,1)}(\Omega) \cap C^{(0,0)}(\bar{\Omega})$ be a sufficiently smooth function defined on Ω such that $\mathcal{L}_\varepsilon \varphi(x,t) \geq 0, (x,t) \in \Omega$, $B_{L,\varepsilon}\varphi(0,t) \geq 0, t \in (0,T]$, $B_{R,\varepsilon}\varphi(1,t) \geq 0, t \in (0,T]$ and $\varphi(x,0) \geq 0, x \in [0,1]$. Then, $\varphi(x,t) \geq 0$, for all $(x,t) \in \bar{\Omega}$.*

Proof. The proof is given in Theorem (5.3.1). □

The following Lemma proves the stability estimate to obtain unique solution.

Lemma 6.3.2. *Let $u(x,t) \in C^{(2,1)}(\bar{\Omega})$ be the solution to continuous problem in Eq.* (6.1)–(6.2) *satisfying the bound*

$$|u(x,t)| \leq \max\{|\phi_B(x)|, |B_{L,\varepsilon}u(0,t)|, |B_{R,\varepsilon}u(1,t)|\} + \frac{\|f\|}{\alpha}.$$

Proof. To proof this lemma, we define smooth barrier functions $\Theta^{\pm}$ as

$$\Theta^{\pm}(x,t) = \max\{|\phi_B(x)|, |B_{L,\varepsilon}u(0,t)|, |B_{R,\varepsilon}u(1,t)|\} + \frac{\|f\|}{\alpha} \pm u(x,t).$$

Now, evaluating the above-defined barrier functions at the initial and boundary conditions, we obtain the required result. □

The next theorem states the classical bounds on the solution and its derivatives.

Theorem 6.1. *Let $a, f \in C^{(2+\gamma,1+\gamma/2)}(\bar{\Omega}), \phi_L, \phi_R \in C^{\frac{3+\gamma}{2}}([0,T]), \phi_B \in C^{(4+\gamma,2+\gamma/2)}([0,1]), \gamma \in (0,1)$. Under the smooth conditions, the problem has a unique solution $u \in C^{(4+\gamma,2+\gamma/2)}(\bar{\Omega})$. Furthermore, the derivatives of the solution u satisfy the bound*

$$\left\| \frac{\partial^{l+m} u}{\partial x^l \partial t^m} \right\|_{\bar{\Omega}} \leq C\varepsilon^{-l/2}, \qquad l, m \geq 0, \quad 0 \leq l + 2m \leq 4,$$

where C is the constant independent of ε.

Proof. Refer Theorem (5.1) for the proof. □

The classical bounds on the derivatives of the solution given above are insufficient for proving the $\varepsilon-$uniform error estimate. To get better bounds on the derivatives of the problem's solution, u in Eq. (6.1)-(6.2), we try to express it as $u = v + w$, where v is the regular solution and w is the singular component. The regular component v is further be decomposed into

$$v = v_0 + \varepsilon v_1,$$

where v_0 and v_1 satisfy the following

$$\begin{cases} \frac{\partial v_0}{\partial t}(x,t) + av_0(x,t) = f(x,t), & (x,t) \in \Omega, \\ v_0(x,0) = \phi_B(x), & 0 \le x \le 1, \end{cases} \tag{6.4}$$

and

$$\begin{cases} \mathcal{L}_\varepsilon v_1(x,t) = \frac{\partial^2 v_0}{\partial x^2}(x,t), & (x,t) \in \Omega, \\ B_{L,\varepsilon} v_1(0,t) = 0, & 0 < t \le T, \\ B_{R,\varepsilon} v_1(1,t) = 0, & 0 < t \le T, \\ v_1(x,0) = 0, & 0 \le x \le 1, \end{cases} \tag{6.5}$$

The regular component v is the solution to the non-homogeneous problem

$$\begin{cases} \mathcal{L}_\varepsilon v(x,t) = f(x,t), & (x,t) \in \Omega, \\ B_{L,\varepsilon} v(0,t) = B_{L,\varepsilon} v_0(0,t), & 0 < t \le T, \\ B_{R,\varepsilon} v(1,t) = B_{R,\varepsilon} v_0(1,t), & 0 < t \le T, \\ v(x,0) = \phi_B(x), & 0 \le x \le 1. \end{cases} \tag{6.6}$$

With $v(x,t)$ defined, $w(x,t)$ is the solution of the homogeneous problem

$$\begin{cases} \mathcal{L}_\varepsilon w(x,t) = 0, & (x,t) \in \Omega, \\ B_{L,\varepsilon} w(0,t) = \phi_L(t) - B_{L,\varepsilon} v_0(0,t), & 0 < t \le T, \\ B_{R,\varepsilon} w(1,t) = \phi_R(t) - B_{R,\varepsilon} v_0(1,t), & 0 < t \le T, \\ w(x,0) = 0, & 0 \le x \le 1. \end{cases} \tag{6.7}$$

Since the problem in Eq. (6.1)-(6.2) have twin boundary layers, we further decompose w

as $w = w_L + w_R$, where w_L and w_R are defined respectively by

$$\begin{cases} \mathcal{L}_\varepsilon w_L(x,t) = 0, & (x,t) \in \Omega, \\ B_{L,\varepsilon} w_L(0,t) = \phi_L(t) - B_{L,\varepsilon} v_0(0,t), & 0 < t \leq T, \\ B_{R,\varepsilon} w_L(1,t) = 0, & 0 < t \leq T, \\ w_L(x,0) = 0, & 0 \leq x \leq 1, \end{cases} \tag{6.8}$$

and

$$\begin{cases} \mathcal{L}_\varepsilon w_R(x,t) = 0, & (x,t) \in \Omega, \\ B_{L,\varepsilon} w_R(0,t) = 0, & 0 < t \leq T, \\ B_{R,\varepsilon} w_R(1,t) = \phi_R(t) - B_{R,\varepsilon} v_0(1,t), & 0 < t \leq T, \\ w_R(x,0) = 0, & 0 \leq x \leq 1. \end{cases} \tag{6.9}$$

The non-classical bounds of regular and singular components and their derivatives are established in the following theorem.

Theorem 6.2. *Let* $a, f \in C^{(4+\gamma, 2+\gamma/2)}(\bar{\Omega}), \phi_L, \phi_R \in C^{\frac{3+\gamma}{2}}([0,T]), \phi_B \in C^{(6+\gamma, 3+\gamma/2)}([0,1]), \gamma \in (0,1)$. *Under the smoothness conditions, for nonnegative integers* l, m *such that* $0 \leq l + 2m \leq 4$, *we have the bounds*

$$\begin{aligned} \left\| \frac{\partial^{l+m} v}{\partial x^l \partial t^m} \right\| &\leq C(1 + \varepsilon^{1-l/2}), \\ \left| \frac{\partial^{l+m} w_L}{\partial x^l \partial t^m} \right| &\leq C\varepsilon^{-l/2} e^{-x\sqrt{\frac{\alpha}{\varepsilon}}}, \\ \left| \frac{\partial^{l+m} w_R}{\partial x^l \partial t^m} \right| &\leq C\varepsilon^{-l/2} e^{-(1-x)\sqrt{\frac{\alpha}{\varepsilon}}}. \end{aligned}$$

where C *is a constant independent of* ε.

Proof. For the proof, the readers refer Theorem (5.2). □

6.4 Formulation of the Numerical Method

In this section, we discretize the time derivative by means of the implicit Euler method on a uniform mesh. The time domain $[0, T]$ is divided into M equal parts with a uniform time step of Δt so that $\Omega_t^M = \{t_j : t_j = j\Delta t, j = 0, 1, ..., M, \Delta t = T/M\}$, where M denotes the number of mesh elements in the time direction. Then the space derivative is discretized using a hybrid difference method that includes a cubic spline in tension scheme in the boundary layer regions and a central difference scheme in the outer region. In the space direction, a layer-adapted mesh of Shishkin-types are constructed. The space domain Ω_x^N is divided into three subintervals, resulting in $\bar{\Omega} = [0, \sigma) \cup [\sigma, 1-\sigma] \cup (1-\sigma, 1]$. The mesh is equidistant on the subinterval $[\sigma, 1-\sigma]$ with $N/2$ mesh elements and gradually divided into subintervals $[0, \sigma]$ and $[1-\sigma, 1]$ with $N/4$ mesh elements. A mesh transition parameter σ, which depends on the perturbation parameter and the number of mesh intervals, is given as

$$\sigma = \min\left\{\frac{1}{4}, 2\sqrt{\varepsilon}\psi(1/4)\right\}.$$

Let $\bar{\Omega}_x^N = \{x_i\}_{i=0}^N$ be the set of mesh points. Now, the mesh points are defined as

$$x_i = \begin{cases} 2\sqrt{\varepsilon}\psi(t), & \text{for } t_i = \frac{i}{N},\ \ 0 \leq i \leq \frac{N}{4}, \\ \sigma + 2(1-2\sigma)\big(t - 1/4\big), & \text{for } \frac{N}{4} + 1 \leq i \leq \frac{3N}{4}, \\ 1 - 2\sqrt{\varepsilon}\psi(1-t), & \text{for } \frac{3N}{4} + 1 \leq i \leq N. \end{cases}$$

Let the piecewise uniform mesh spacing $h_i = x_i - x_{i-1}$, for $i = 1, \cdots, N$ be the mesh diameter with $\bar{h}_i = (h_{i+1} + h_i)/2$. Under the assumption that $\sqrt{\varepsilon} \leq N^{-1}$, we use $\sigma \geq 2\sqrt{\varepsilon}\ln N$ for the error analysis in all S-type meshes. We considered the layer-adapted meshes in [76] and [82] of S-types, including the Shishkin (S-) mesh, Bakhvalov-Shishkin (BS-) mesh and Vulanović-Shishkin (VS-) mesh with $q = \frac{1}{4} + \frac{1}{4\ln N}$ together with $\varphi = e^{-\psi}$ and the important quantity $\max|\varphi'(t)|$, which arises in error estimates. We discretize the problem in Eq. (6.1) in the outer region $[\sigma, 1-\sigma]$ using central finite difference scheme

Table 6.1: Mesh-generating and mesh-characterising functions of S-type meshes.

	Shishkin mesh	Bakhvalov-Shishkin mesh	Vulanović-Shishkin mesh
$\psi(t)$	$4t\ln N$	$-\ln[1-4(1-N^{-1})t]$	$\frac{t}{q-t}$
$\varphi(t)$	N^{-4t}	$1-4(1-N^{-1})t$	$e^{\frac{-t}{q-t}}$
$\max\lvert\varphi'(t)\rvert$	$C\ln N$	C	C

in space direction and implicit Euler method in time direction as follows.

$$\frac{U_i^{j+1}-U_i^j}{\Delta t}-\frac{\varepsilon}{\bar{h}_i}\left(\frac{U_{i+1}^{j+1}-U_i^{j+1}}{h_{i+1}}-\frac{U_i^{j+1}-U_{i-1}^{j+1}}{h_i}\right)+a_i^{j+1}U_i^{j+1}=f_i^{j+1}. \tag{6.10}$$

After rearranging the terms in Eq. (6.10) for $\frac{N}{4}\leq i\leq\frac{3N}{4}, 0\leq j<M$, we obtain the following scheme in the outer region

$$r_i^-U_{i-1}^{j+1}+r_i^cU_i^{j+1}+r_i^+U_{i+1}^{j+1}=H_i^{j+1}, \tag{6.11}$$

where the coefficients are given as

$$r_i^-=\frac{-2\varepsilon}{h_i(h_i+h_{i+1})},\ r_i^c=\frac{2\varepsilon}{h_ih_{i+1}}+a_i^{j+1}+\frac{1}{\Delta t},\ r_i^+=\frac{-2\varepsilon}{h_{i+1}(h_i+h_{i+1})},\ H_i^{j+1}=\frac{U_i^j}{\Delta t}+f_i^{j+1}.$$

Let $\Omega=[0,1]$ be $x_0=0,\ x_i=\sum_{k=0}^{i-1}h_k,\ h_k=x_{k+1}-x_k,\ x_N=1,\ i=1(1)N-1.$ A function as $S(x,\nu)\in C^2[a,b]$ interpolates $u(x)$ at the mesh points x_i which depends on a parameter ν. When $\nu\to 0$, $S(x,\nu)$ reduces to cubic spline. The spline function $S(x,\nu)=S(x)$ satisfying the differential equation in interval $[x_i,x_{i+1}]$

$$S''(x)+\nu S(x)=[S''(x_i)+\nu S(x_i)]\frac{(x_{i+1}-x)}{h_{i+1}}+[S''(x_{i+1})+\nu S(x_{i+1})]\frac{(x-x_i)}{h_i},$$

where $S(x_i)=U_i$ and $\nu>0$ is termed as tension spline. Following [4], we obtain the following tri-diagonal system

$$\lambda_1h_iM_{i-1}+\lambda_2(h_i+h_{i+1})M_i+\lambda_1h_{i+1}M_{i+1}=\frac{U_{i+1}-U_i}{h_{i+1}}-\frac{U_i-U_{i-1}}{h_i},\ 0<i<N, \tag{6.12}$$

where

$$\lambda_1 = \frac{1}{\lambda^2}(1 - \lambda \csc h\lambda), \lambda_2 = \frac{1}{\lambda^2}(\lambda \coth \lambda - 1),$$

and

$$\lambda = h\nu^1/2,\ M_k = U''(x_k), \quad k = i, i \pm 1.$$

Equating the coefficients of $M_i's$ in Eq. (6.12), we get the following condition

$$\lambda_1 + \lambda_2 = \frac{1}{2}. \tag{6.13}$$

Substituting Eq. (6.13) into Eq. (6.12), we obtain

$$\frac{\lambda}{2} = \tanh\left(\frac{\lambda}{2}\right). \tag{6.14}$$

Solving Eq. (6.14), the smallest positive non-zero root is $\lambda = 0.001$ from infinitely many roots. Discretizing Eq. (6.1) using cubic spline in tension at the boundary layer regions $[0, \sigma)$ and $(1 - \sigma, 1]$ in space and implicit Euler method in time, we obtain

$$\frac{U_k^{j+1} - U_k^j}{\Delta t} - \varepsilon M_k^{j+1} + a_k^{j+1} U_k^{j+1} = f_k^{j+1} \tag{6.15}$$

where $k = i-1, i, i+1$. Equation (6.15) can be written as

$$\begin{cases} -\varepsilon M_{i-1}^{j+1} = \frac{U_{i-1}^j}{\Delta t} + f_{i-1}^{j+1} - \left(a_{i-1}^{j+1} + \frac{1}{\Delta t}\right) U_{i-1}^{j+1}, \\ -\varepsilon M_i^{j+1} = \frac{U_i^j}{\Delta t} + f_i^{j+1} - \left(a_i^{j+1} + \frac{1}{\Delta t}\right) U_i^{j+1}, \\ -\varepsilon M_{i+1}^{j+1} = \frac{U_{i+1}^j}{\Delta t} + f_{i+1}^{j+1} - \left(a_{i+1}^{j+1} + \frac{1}{\Delta t}\right) U_{i+1}^{j+1}. \end{cases} \tag{6.16}$$

Substituting Eq. (6.16) into Eq. (6.12) and rearranging the terms for $1 \le i < \frac{N}{4}$ and $\left(\frac{3N}{4} + 1\right) \le i < N,\ 0 \le j < M$, we obtain the difference scheme in boundary layer regions as

$$r_i^- U_{i-1}^{j+1} + r_i^c U_i^{j+1} + r_i^+ U_{i+1}^{j+1} = H_i^{j+1}, \tag{6.17}$$

where the coefficients are given as

$$\begin{aligned} r_i^- &= \frac{-\varepsilon}{h_i(h_i+h_{i+1})} + \frac{\lambda_1 h_i}{h_{i+1}+h_i}\bigg(a_{i-1}^{j+1} + \frac{1}{\Delta t}\bigg), \quad r_i^c = \frac{\varepsilon}{h_i h_{i+1}} + \lambda_2\bigg(a_i^{j+1} + \frac{1}{\Delta t}\bigg), \\ r_i^+ &= \frac{-\varepsilon}{h_{i+1}(h_i+h_{i+1})} + \frac{\lambda_1 h_{i+1}}{h_{i+1}+h_i}\bigg(a_{i+1}^{j+1} + \frac{1}{\Delta t}\bigg), \\ H_i^{j+1} &= \frac{\lambda_1 h_i}{h_i+h_{i+1}}\bigg(\frac{U_{i-1}^j}{\Delta t} + f_{i-1}^{j+1}\bigg) + \lambda_2\bigg(\frac{U_i^j}{\Delta t} + f_i^{j+1}\bigg) + \frac{\lambda_1 h_{i+1}}{h_i+h_{i+1}}\bigg(\frac{U_{i+1}^j}{\Delta t} + f_{i+1}^{j+1}\bigg). \end{aligned}$$

Therefore, the hybrid method gives second-order accuracy at the interior mesh points in space and the implicit Euler method gives first-order accuracy in time. To obtain the overall second-order accuracy in the space, we use Taylor's expansion and the problem Eq. (6.1)-(6.2) to discretize Robin boundary conditions. To discretize left boundary condition, we use the following Taylor series expansion

$$\frac{U_{i+1}^{j+1} - U_i^{j+1}}{h_{i+1}} = (U_x)_i^{j+1} + \frac{h_{i+1}}{2}(U_{xx})_i^{j+1} + \cdots$$

At $i = 0$, we can write the above equation as

$$D_x^+ U_0^{j+1} = (U_x)_0^{j+1} + \frac{h_1}{2}(U_{xx})_0^{j+1}. \tag{6.18}$$

The discretized left boundary condition in Eq. (6.2) becomes

$$(U_x)_0^{j+1} = \frac{1}{\sqrt{\varepsilon}}[U_0^{j+1} - \phi_L^{j+1}]. \tag{6.19}$$

The discretized form of Eq. (6.1) at $i = 0$ will be

$$(U_{xx})_0^{j+1} = \frac{1}{\varepsilon}[D_t^- U_0^{j+1} + (aU)_0^{j+1} - f_0^{j+1}]. \tag{6.20}$$

Putting Eqs. (6.19) and (6.20) in Eq. (6.18) yields

$$D_x^+ U_0^{j+1} = \frac{1}{\sqrt{\varepsilon}}[U_0^{j+1} - \phi_L^{j+1}] + \frac{h_1}{2\varepsilon}[D_t^- U_0^{j+1} + (aU)_0^{j+1} - f_0^{j+1}].$$

Multiplying both sides of the above equation by $\sqrt{\varepsilon}$, we obtain

$$\sqrt{\varepsilon}D_x^+U_0^{j+1} = U_0^{j+1} - \phi_L^{j+1} + \frac{h_1}{2\sqrt{\varepsilon}}[D_t^-U_0^{j+1} + (aU)_0^{j+1} - f_0^{j+1}].$$

Now, the discrete left boundary condition can be written as

$$U_0^{j+1} - \sqrt{\varepsilon}D_x^+U_0^{j+1} + \frac{h_1}{2\sqrt{\varepsilon}}\left(D_t^-U_0^{j+1} + a_0^{j+1}U_0^{j+1}\right) = \phi_L^{j+1} + \frac{h_1}{2\sqrt{\varepsilon}}f_0^{j+1}. \tag{6.21}$$

Similarly, Taylor series expansion is used to discretize the right boundary condition as

$$\frac{U_i^{j+1} - U_{i-1}^{j+1}}{h_i} = (U_x)_i^{j+1} - \frac{h_i}{2}(U_{xx})_i^{j+1} + \cdots$$

At $i = N$, we can write the above equation as

$$D_x^-U_N^{j+1} = (U_x)_N^{j+1} - \frac{h_N}{2}(U_{xx})_N^{j+1}. \tag{6.22}$$

From the right boundary condition in Eq. (6.2), we have

$$(U_x)_N^{j+1} = \frac{1}{\sqrt{\varepsilon}}[\phi_R^{j+1} - U_N^{j+1}]. \tag{6.23}$$

The discretized form of Eq. (6.1) at $i = N$ will be

$$(U_{xx})_N^{j+1} = \frac{1}{\varepsilon}[D_t^-U_N^{j+1} + (aU)_N^{j+1} - f_N^{j+1}]. \tag{6.24}$$

Inserting Eqs. (6.23) and (6.24) in Eq. (6.22) gives

$$D_x^-U_N^{j+1} = \frac{1}{\sqrt{\varepsilon}}[\phi_R^{j+1} - U_N^{j+1}] - \frac{h_N}{2\varepsilon}[D_t^-U_N^{j+1} + (aU)_N^{j+1} - f_N^{j+1}].$$

Multiplying both sides of the above equation by $\sqrt{\varepsilon}$, we obtain

$$\sqrt{\varepsilon}D_x^- U_N^{j+1} = \phi_R^{j+1} - U_N^{j+1} - \frac{h_N}{2\sqrt{\varepsilon}}[D_t^- U_N^{j+1} + (aU)_N^{j+1} - f_N^{j+1}].$$

Now, the discrete right boundary condition can be written as

$$U_N^{j+1} + \sqrt{\varepsilon}D_x^- U_N^{j+1} + \frac{h_N}{2\sqrt{\varepsilon}}\big(D_t^- U_N^{j+1} + a_N^{j+1}U_N^{j+1}\big) = \phi_R^{j+1} + \frac{h_N}{2\sqrt{\varepsilon}} f_N^{j+1}. \tag{6.25}$$

From Eqs. (6.21) and (6.25), we have the following discrete initial-boundary conditions

$$\begin{cases} U_i^0 = \phi_B(x_i), & 0 < i < N, \\ B_{L,\varepsilon}^N U_0^{j+1} \equiv U_0^{j+1} - \sqrt{\varepsilon}D_x^+ U_0^{j+1} + \frac{h_1}{2\sqrt{\varepsilon}}\big(a_0^{j+1} + D_t^-\big)U_0^{j+1} = A, \ 0 \le j < M, \\ B_{R,\varepsilon}^N U_N^{j+1} \equiv U_N^{j+1} + \sqrt{\varepsilon}D_x^- U_N^{j+1} + \frac{h_N}{2\sqrt{\varepsilon}}\big(a_N^{j+1} + D_t^-\big)U_N^{j+1} = B, \ 0 \le j < M, \end{cases} \tag{6.26}$$

where $A = \phi_L^{j+1} + \frac{h_1}{2\sqrt{\varepsilon}} f_0^{j+1}$ and $B = \phi_R^{j+1} + \frac{h_N}{2\sqrt{\varepsilon}} f_N^{j+1}$. Combining the difference schemes in Eqs. (6.11) and (6.17) together with discrete initial-boundary conditions Eq. (6.26) yields the following hybrid difference scheme

$$\mathcal{L}_\varepsilon^{N,M} U_i^{j+1} \equiv r_i^- U_{i-1}^{j+1} + r_i^c U_i^{j+1} + r_i^+ U_{i+1}^{j+1} = H_i^{j+1}, \quad 0 < i < N, \quad 0 \le j < M, \tag{6.27}$$

where coefficients for $1 \le i < \frac{N}{4}$, $\big(\frac{3N}{4} + 1\big) \le i < N$, $0 \le j < M$ are given as

$$\begin{aligned} r_i^- &= \frac{-\varepsilon}{h_i(h_i + h_{i+1})} + \frac{\lambda_1 h_i}{h_{i+1} + h_i}\left(a_{i-1}^{j+1} + \frac{1}{\Delta t}\right), \quad r_i^c = \frac{\varepsilon}{h_i h_{i+1}} + \lambda_2\left(a_i^{j+1} + \frac{1}{\Delta t}\right), \\ r_i^+ &= \frac{-\varepsilon}{h_{i+1}(h_i + h_{i+1})} + \frac{\lambda_1 h_{i+1}}{h_{i+1} + h_i}\left(a_{i+1}^{j+1} + \frac{1}{\Delta t}\right), \\ H_i^{j+1} &= \frac{\lambda_1 h_i}{h_i + h_{i+1}}\left(\frac{U_{i-1}^j}{\Delta t} + f_{i-1}^{j+1}\right) + \lambda_2\left(\frac{U_i^j}{\Delta t} + f_i^{j+1}\right) + \frac{\lambda_1 h_{i+1}}{h_i + h_{i+1}}\left(\frac{U_{i+1}^j}{\Delta t} + f_{i+1}^{j+1}\right), \end{aligned}$$

and coefficients for $\frac{N}{4} \leq i \leq \frac{3N}{4}, \;\; 0 \leq j < M$ are given as

$$r_i^- = \frac{-2\varepsilon}{h_i(h_i + h_{i+1})}, \;\; r_i^c = \frac{2\varepsilon}{h_i h_{i+1}} + a_i^{j+1} + \frac{1}{\Delta t}, \;\; r_i^+ = \frac{-2\varepsilon}{h_{i+1}(h_i + h_{i+1})}, \;\; H_i^{j+1} = \frac{U_i^j}{\Delta t} + f_i^{j+1},$$

along with the following discrete initial-boundary conditions

$$\begin{cases} U_i^0 = \phi_B(x_i), & 0 < i < N, \\ B_{L,\varepsilon}^N U_0^{j+1} \equiv r_0^c U_0^{j+1} + r_0^+ U_1^{j+1} = \phi_L^{j+1} + \frac{h_1}{2\sqrt{\varepsilon}} f_0^{j+1}, & 0 \leq j < M, \\ B_{R,\varepsilon}^N U_N^{j+1} \equiv r_N^- U_{N-1}^{j+1} + r_N^c U_N^{j+1} = \phi_R^{j+1} + \frac{h_N}{2\sqrt{\varepsilon}} f_N^{j+1}, & 0 \leq j < M, \end{cases} \tag{6.28}$$

where the coefficients for $i = 0$ and $i = N$ at $0 \leq j < M$, respectively are given as

$$r_0^c = 1 + \frac{\sqrt{\varepsilon}}{h_1} + \frac{h_1 a_0^{j+1}}{2\sqrt{\varepsilon}} + \frac{h_1}{2\sqrt{\varepsilon}\Delta t}; \qquad r_0^+ = \frac{-\sqrt{\varepsilon}}{h_1},$$
$$r_N^- = \frac{-\sqrt{\varepsilon}}{h_N}; \qquad r_N^c = 1 + \frac{\sqrt{\varepsilon}}{h_N} + \frac{h_N a_N^{j+1}}{2\sqrt{\varepsilon}} + \frac{h_N}{2\sqrt{\varepsilon}\Delta t}.$$

The coefficient matrix in Eqs. (6.27) and (6.28) gives an $(N+1)\times(N+1)$ system of linear equations which can be solved for $U_0^{j+1}, \cdots, U_N^{j+1}$ at $x_0, \cdots, x_N$. While the main diagonal elements are positive and diagonally dominant, the off-diagonal elements are negative. In this situation, the coefficient matrix is an invertible M-matrix. In addition, the inverse matrix exists and is nonnegative. As a result, we solved the system of linear equations in Eqs. (6.27) and (6.28) via the matrix inversion method.

6.5 Analysis of the Method

In this section, we prove stability analysis as well as an $\varepsilon-$uniform convergence analysis. First, we examine the M-matrix properties at the boundary points $x_0 = 0$ and $x_N = 1$. From Eq. (6.28), it is obvious that $r_0^c > 0, \; r_0^+ < 0$ with

$$|r_0^c| - |r_0^+| = 1 + \frac{h_1 a_0^{j+1}}{2\sqrt{\varepsilon}} + \frac{h_1}{2\sqrt{\varepsilon}\Delta t} > 0.$$

Again, $r_N^c > 0,\ r_N^- < 0$ with

$$|r_N^c| - |r_N^-| = 1 + \frac{h_N a_N^{j+1}}{2\sqrt{\varepsilon}} + \frac{h_N}{2\sqrt{\varepsilon}\Delta t} > 0.$$

Now, from the discretized problem in Eq. (6.27), we clearly see that $r_i^- < 0$ and $r_i^+ < 0$ for $\frac{N}{4} \le i \le \frac{3N}{4}, 0 \le j < M$. For $\frac{N}{4} \le i \le \frac{3N}{4}, 0 \le j < M$, we have

$$\begin{aligned}
|r_i^c| - |r_i^-| - |r_i^+| &= \frac{2\varepsilon}{h_i h_{i+1}} + a_i^{j+1} + \frac{1}{\Delta t} - \frac{2\varepsilon}{h_i(h_i + h_{i+1})} - \frac{2\varepsilon}{h_{i+1}(h_i + h_{i+1})}, \\
&= \frac{2\varepsilon}{h_i h_{i+1}} + a_i^{j+1} + \frac{1}{\Delta t} - \frac{2\varepsilon}{h_i h_{i+1}}, \\
&= a_i^{j+1} + \frac{1}{\Delta t} > 0, \ \text{ since } \ a_i^{j+1} > 0.
\end{aligned}$$

Since the mesh points, the tension parameter λ and the $a(x,t)$ are all positive, it is obvious that $r_i^- < 0$ and $r_i^+ < 0$, for $1 \le i < \frac{N}{4}$ and $\left(\frac{3N}{4} + 1\right) \le i < N, \quad 0 \le j < M$. Again, for $1 \le i < \frac{N}{4}$ and $\left(\frac{3N}{4} + 1\right) \le i < N, \quad 0 \le j < M$, we have

$$\begin{aligned}
|r_i^c| - |r_i^-| - |r_i^+| &= \frac{\varepsilon}{h_i h_{i+1}} + \lambda_2\big(a_i^{j+1} + \frac{1}{\Delta t}\big) - \frac{\varepsilon}{h_i(h_i + h_{i+1})} + \frac{\lambda_1 h_i}{h_{i+1} + h_i}\big(a_{i-1}^{j+1} + \frac{1}{\Delta t}\big), \\
&\quad - \frac{\varepsilon}{h_{i+1}(h_i + h_{i+1})} + \frac{\lambda_1 h_{i+1}}{h_{i+1} + h_i}\big(a_{i+1}^{j+1} + \frac{1}{\Delta t}\big), \\
&= \lambda_2\big(a_i^{j+1} + \frac{1}{\Delta t}\big) - \frac{\lambda_1 h_i}{h_{i+1} + h_i}\big(a_{i-1}^{j+1} + \frac{1}{\Delta t}\big) - \frac{\lambda_1 h_{i+1}}{h_{i+1} + h_i}\big(a_{i+1}^{j+1} + \frac{1}{\Delta t}\big), \\
&= \lambda_2 a_i^{j+1} - \frac{\lambda_1 h_i}{h_{i+1} + h_i} a_{i-1}^{j+1} - \frac{\lambda_1 h_{i+1}}{h_{i+1} + h_i} a_{i+1}^{j+1} + (\lambda_2 - \lambda_1)\frac{1}{\Delta t}, \\
&= (\lambda_2 - \lambda_1) a_i^{j+1} + (\lambda_2 - \lambda_1)\frac{1}{\Delta t},
\end{aligned}$$

using Taylor expansion for the terms a_{i-1}^{j+1} and a_{i+1}^{j+1}. Now, we have

$$|r_i^c| - |r_i^-| - |r_i^+| = (\lambda_2 - \lambda_1)\left(a_i^{j+1} + \frac{1}{\Delta t}\right),$$

Since the tension parameter $\lambda_1 + \lambda_2 = \frac{1}{2}$ that satisfies the inequality $\lambda_2 > \lambda_1$ and the $a(x,t) \ge \alpha > 0$, we have $|r_i^c| - |r_i^-| - |r_i^+| > 0$ implying that the coefficient matrix in Eq. (6.27)-(6.28) leads to an M-matrix. This demonstrates that the discrete scheme satisfies uniform stability. Hence, the discrete operator in Eq. (6.27)-(6.28) satisfies the discrete maximum principle. Next, we prove parameter-uniform convergence analysis for the discrete scheme Eq. (6.27)–(6.28) by dividing the numerical solution U into V as discrete regular and W as discrete singular components given by $U = V + W$. Now, V is the solution of the inhomogeneous problem

$$\begin{cases} \mathcal{L}_{\varepsilon}^{N,M} V(x_i, t_j) = H(x_i, t_j), & \forall (x_i, t_j) \in \Omega, \\ B_{L,\varepsilon}^{N} V(0, t_j) = B_{L,\varepsilon} v(0, t_j) + \frac{h_1}{2\sqrt{\varepsilon}} f(0, t_j), & t_j \in (0, T], \\ B_{R,\varepsilon}^{N} V(1, t_j) = B_{R,\varepsilon} v(1, t_j) + \frac{h_N}{2\sqrt{\varepsilon}} f(1, t_j), & t_j \in (0, T], \\ V(x_i, 0) = \phi_B(x_i, 0), & x_i \in \bar{\Omega}_x^N, \end{cases} \tag{6.29}$$

and W is the solution of the following homogeneous problem

$$\begin{cases} \mathcal{L}_{\varepsilon}^{N,M} W(x_i, t_j) = 0, & \forall (x_i, t_j) \in \Omega, \\ B_{L,\varepsilon}^{N} W(0, t_j) = \phi_L^j - B_{L,\varepsilon} v(0, t_j), & t_j \in (0, T], \\ B_{R,\varepsilon}^{N} W(1, t_j) = \phi_R^j - B_{R,\varepsilon} v(1, t_j), & t_j \in (0, T], \\ W(x_i, 0) = 0, & x_i \in \bar{\Omega}_x^N. \end{cases} \tag{6.30}$$

From the above, we can estimate the error at the node (x_i, t_j) by

$$|U - u| \le |V - v| + |W - w|. \tag{6.31}$$

Theorem 6.3. *Let V be the numerical solution to Eq.* (6.29) *and v be the continuous solution to Eq.* (6.6). *The parameter-uniform error bound for regular component on S-mesh is*

$$|(V - v)(x_i, t_j)| \le \begin{cases} C[N^{-2} + \Delta t], & \textit{if } x_i \ne \sigma, \ x_i \ne 1 - \sigma, \\ C[\sqrt{\varepsilon} N^{-1} + \Delta t], & \textit{if } x_i = \sigma, \ x_i = 1 - \sigma, \end{cases}$$

and parameter-uniform error bound for both BS-mesh and VS-mesh are given as

$$|(V-v)(x_i,t_j)| \le C(N^{-2}+\Delta t),$$

where C is a constant independent of ε and mesh points.

Proof. At the left boundary point, we have

$$\begin{aligned}
B^N_{L,\varepsilon}(V-v)(0,t_j) &= B_{L,\varepsilon}V(0,t_j) - B^N_{L,\varepsilon}v(0,t_j),\\
&= B_{L,\varepsilon}v(0,t_j) + \frac{h_0}{2\sqrt{\varepsilon}}f(0,t_j) - B^N_{L,\varepsilon}v(0,t_j),\\
&= v(0,t_j) - \sqrt{\varepsilon}\frac{\partial v(0,t_j)}{\partial x} + \frac{h_0}{2\sqrt{\varepsilon}}f(0,t_j),\\
&- \big[v(0,t_j) - \sqrt{\varepsilon}D_x^+ v(0,t_j) + \frac{h_0}{2\sqrt{\varepsilon}}\big(a(0,t_j)v(0,t_j) + D_t^- v(0,t_j)\big)\big],\\
&= -\sqrt{\varepsilon}\left[\frac{\partial v(0,t_j)}{\partial x} - D_x^+ v(0,t_j)\right]\\
&+ \frac{h_0}{2\sqrt{\varepsilon}}\left[f(0,t_j) - a(0,t_j)v(0,t_j) - D_t^- v(0,t_j)\right],\\
&= -\sqrt{\varepsilon}\left[\frac{\partial v(0,t_j)}{\partial x} - D_x^+ v(0,t_j)\right]\\
&+ \frac{h_0}{2\sqrt{\varepsilon}}\left[\frac{\partial v(0,t_j)}{\partial t} - \varepsilon\frac{\partial^2 v(0,t_j)}{\partial x^2} - D_t^- v(0,t_j)\right],\\
&\text{since } \frac{\partial^2 v}{\partial x^2}(0,t_{j+1}) = \frac{-1}{\varepsilon}\left(f(0,t_{j+1}) - a(0,t_{j+1})v(0,t_{j+1}) - \frac{\partial v}{\partial t}(0,t_{j+1})\right),\\
&= -\sqrt{\varepsilon}\left[\frac{\partial v(0,t_j)}{\partial x} - \left(D_x^+ v(0,t_j) - \frac{h_0}{2}\frac{\partial^2 v(0,t_j)}{\partial x^2}\right)\right]\\
&+ \frac{h_0}{2\sqrt{\varepsilon}}\left[\frac{\partial v(0,t_j)}{\partial t} - D_t^- v(0,t_j)\right],\\
&= -\sqrt{\varepsilon}\left[-\frac{h_0^2}{6}\frac{\partial^3 v(\eta,t_j)}{\partial x^3}\right] + \frac{h_0}{2\sqrt{\varepsilon}}\left[\frac{\partial v(0,t_j)}{\partial t} - D_t^- v(0,t_j)\right],
\end{aligned}$$

where $0<\eta<h_0$. Using the bound of truncation error, we have

$$|B^N_{L,\varepsilon}(V-v)(0,t_j)| \le \frac{\sqrt{\varepsilon}}{6}h_0^2\left\|\frac{\partial^3 v}{\partial x^3}\right\| + \frac{h_0}{2\sqrt{\varepsilon}}\frac{1}{2}(t_{j+1}-t_j)\left\|\frac{\partial^2 v}{\partial t^2}\right\|.$$

Since $h_0 = x_1 - x_0 = N^{-1}$ and $\frac{h_0}{2\sqrt{\varepsilon}} \le 4$ and using the regular component bound in

Theorem (6.2), we obtain

$$\begin{aligned}|B^N_{L,\varepsilon}(V-v)(0,t_j)| \leq & C\sqrt{\varepsilon}N^{-2}(1+\sqrt{\varepsilon})+C\Delta t,\\ \leq & C(N^{-2}+\Delta t), \ \text{ since } \sqrt{\varepsilon}\leq N^{-1}.\end{aligned}$$

At the right boundary point, we have

$$\begin{aligned}B^N_{R,\varepsilon}(V-v)(1,t_j) &= B_{R,\varepsilon}V(1,t_j) - B^N_{R,\varepsilon}v(1,t_j),\\ &= B_{R,\varepsilon}v(1,t_j) + \frac{h_N}{2\sqrt{\varepsilon}}f(1,t_j) - B^N_{R,\varepsilon}v(1,t_j),\\ &= v(1,t_j) + \sqrt{\varepsilon}\frac{\partial v(1,t_j)}{\partial x} + \frac{h_N}{2\sqrt{\varepsilon}}f(1,t_j),\\ &- \big[v(1,t_j) + \sqrt{\varepsilon}D^-_x v(1,t_j) + \frac{h_N}{2\sqrt{\varepsilon}}\big(a(1,t_j)v(1,t_j) + D^-_t v(1,t_j)\big)\big],\\ &= -\sqrt{\varepsilon}\Bigg[\frac{\partial v(1,t_j)}{\partial x} - D^-_x v(1,t_j)\Bigg]\\ &+ \frac{h_N}{2\sqrt{\varepsilon}}\Bigg[f(1,t_j) - a(1,t_j)v(1,t_j) - D^-_t v(1,t_j)\Bigg],\\ &= -\sqrt{\varepsilon}\Bigg[\frac{\partial v(1,t_j)}{\partial x} - D^-_x v(1,t_j)\Bigg]\\ &+ \frac{h_N}{2\sqrt{\varepsilon}}\Bigg[\frac{\partial v(1,t_j)}{\partial t} - \varepsilon\frac{\partial^2 v(1,t_j)}{\partial x^2} - D^-_t v(0,t_j)\Bigg],\\ &\text{since } f(1,t_j) - a(1,t_j)v(1,t_j) = \frac{\partial v(1,t_j)}{\partial t} - \varepsilon\frac{\partial^2 v(1,t_j)}{\partial x^2},\\ &= -\sqrt{\varepsilon}\Bigg[\frac{\partial v(1,t_j)}{\partial x} - \Bigg(D^-_x v(1,t_j) - \frac{h_N}{2}\frac{\partial^2 v(1,t_j)}{\partial x^2}\Bigg)\Bigg]\\ &+ \frac{h_N}{2\sqrt{\varepsilon}}\Bigg[\frac{\partial v(1,t_j)}{\partial t} - D^-_t v(1,t_j)\Bigg],\\ &= -\sqrt{\varepsilon}\Bigg[-\frac{h_N^2}{6}\frac{\partial^3 v(\eta,t_j)}{\partial x^3}\Bigg] + \frac{h_N}{2\sqrt{\varepsilon}}\Bigg[\frac{\partial v(1,t_j)}{\partial t} - D^-_t v(1,t_j)\Bigg],\end{aligned}$$

where $0<\eta<h_N$. Using the bound of truncation error, we have

$$|B^N_{R,\varepsilon}(V-v)(1,t_j)| \leq \frac{\sqrt{\varepsilon}}{6}h_N^2\left\|\frac{\partial^3 v}{\partial x^3}\right\| + \frac{h_N}{2\sqrt{\varepsilon}}\frac{1}{2}(t_{j+1}-t_j)\left\|\frac{\partial^2 v}{\partial t^2}\right\|.$$

Since $h_N = x_N - x_{N-1} = N^{-1}$ and $\frac{h_N}{2\sqrt{\varepsilon}} \leq 4$ and using the regular component bound in

Theorem (6.2), we obtain the error bound at the right boundary point as

$$|B^N_{R,\varepsilon}(V-v)(1,t_j)| \leq C(N^{-2}+\Delta t).$$

The regular component error $(V-v)$ at the interior points is estimated by the classical argument. Thus, the differential and difference equations give

$$\begin{aligned}\mathcal{L}^{N,M}_{\varepsilon}(V-v) &= f-\mathcal{L}^{N,M}_{\varepsilon}v,\\ &= (\mathcal{L}_{\varepsilon}-\mathcal{L}^{N,M}_{\varepsilon})v,\\ &= -\varepsilon\left(\frac{\partial^2}{\partial x^2}-\delta^2_{\text{hyb}}\right)v+\left(\frac{\partial}{\partial t}-D^-_t\right)v,\end{aligned}$$

where $\delta^2_{\text{hyb}}(.)$ is the hybrid scheme for the second-order space derivative $\partial^2(.)/\partial x^2$ [93]. It follows from classical estimates [86] that at each point (x_i,t_j) in Ω,

$$\begin{aligned}|\mathcal{L}^{N,M}_{\varepsilon}(V-v)(x_i,t_j)| \leq& \left|\varepsilon\left(\frac{\partial^2}{\partial x^2}-\delta^2_{\text{hyb}}\right)v\right|+\left|\left(\frac{\partial}{\partial t}-D^-_t\right)v\right|,\\ \leq& \begin{cases}\frac{\varepsilon}{12}(x_i-x_{i-1})^2\left\|\frac{\partial^4 v}{\partial x^4}\right\|+\frac{1}{2}(t_{j+1}-t_j)\left\|\frac{\partial^2 v}{\partial t^2}\right\|, & \text{if } \ x_i\neq\sigma,\ x_i\neq 1-\sigma,\\ \frac{\varepsilon}{3}(x_{i+1}-x_{i-1})\left\|\frac{\partial^3 v}{\partial x^3}\right\|+\frac{1}{2}(t_{j+1}-t_j)\left\|\frac{\partial^2 v}{\partial t^2}\right\|, & \text{if } \ x_i=\sigma,\ x_i=1-\sigma.\end{cases}\end{aligned}$$

Using the bounds on the solution and its derivatives in Theorem (6.2) for regular component yields the following estimate

$$|\mathcal{L}^{N,M}_{\varepsilon}(V-v)(x_i,t_j)| \leq \begin{cases}C[(x_i-x_{i-1})^2+(t_{j+1}-t_j)], & \text{if } \ x_i\neq\sigma,\ x_i\neq 1-\sigma,\\ C[\sqrt{\varepsilon}(x_{i+1}-x_{i-1})+(t_{j+1}-t_j), & \text{if } \ x_i=\sigma,\ x_i=1-\sigma.\end{cases}$$

Since $x_i-x_{i-1}\leq 2N^{-1}$, $x_{i+1}-x_{i-1}\leq 4N^{-1}$ and $t_{j+1}-t_j\leq\Delta t$, it follows that

$$|\mathcal{L}^{N,M}_{\varepsilon}(V-v)(x_i,t_j)| \leq \begin{cases}C[N^{-2}+\Delta t], & \text{if } \ x_i\neq\sigma,\ x_i\neq 1-\sigma,\\ C[\sqrt{\varepsilon}N^{-1}+\Delta t], & \text{if } \ x_i=\sigma,\ x_i=1-\sigma.\end{cases}$$

Now, introduce the following functions

$$\Phi(x_i,t_j) = C\left[\frac{\sigma}{\sqrt{\varepsilon}}N^{-2}\theta(x_i) + (2+t_j)N^{-2} + (1+t_j)\Delta t\right].$$

where θ is the piecewise linear polynomial given by

$$\theta(x) = \begin{cases} \frac{x}{\sigma}, & \text{for } 0 \le x \le \sigma, \\ 1, & \text{for } \sigma \le x \le 1-\sigma, \\ \frac{1-x}{\sigma}, & \text{for } 1-\sigma \le x \le 1. \end{cases}$$

Since $\frac{\sigma}{\sqrt{\varepsilon}} \ge 2\ln N$, we have

$$0 \le \Phi(x_i,t_j) \le C\big(N^{-2} + \Delta t\big), \quad \text{for all } (x_i,t_j) \in \bar{\Omega},$$

and

$$\mathcal{L}_\varepsilon^{N,M}\Phi(x_i,t_j) \ge \begin{cases} C[N^{-2} + \Delta t], & \forall x_i \ne \sigma,\ x_i \ne 1-\sigma, \\ C[\sqrt{\varepsilon}N^{-1} + N^{-2} + \Delta t], & \forall x_i = \sigma,\ x_i = 1-\sigma. \end{cases} \tag{6.32}$$

Introducing the barrier functions

$$\Psi^{\pm}(x_i,t_j) = \Phi(x_i,t_j) \pm (V-v)(x_i,t_j) \tag{6.33}$$

From Eqs. (6.32) and (6.33), we have

$$\mathcal{L}_\varepsilon^{N,M}\Psi^{\pm}(x_i,t_j) = \mathcal{L}_\varepsilon^{N,M}\Phi(x_i,t_j) \pm \mathcal{L}_\varepsilon^{N,M}(V-v)(x_i,t_j)$$

It follows that

$$\mathcal{L}_\varepsilon^{N,M}\Psi^{\pm}(x_i,t_j) \ge 0, \quad (x_i,t_j) \in \Omega.$$

It is easy to show that

$$B^N_{L,\varepsilon}\Psi^{\pm}(0,t_j) \geq 0, \;\; B^N_{R,\varepsilon}\Psi^{\pm}(1,t_j) \geq 0, \;\; \forall t_j \in \Omega^M_t.$$

Hence, from the discrete maximum principle

$$\Psi^{\pm}(x_i,t_j) \geq 0, \;\; (x_i,t_j) \in \Omega.$$

Applying discrete maximum principle for the mesh function $(V-v)(x_i,t_j)$ yields

$$|(V-v)(x_i,t_j)| \leq C(N^{-2} + \Delta t), \quad (x_i,t_j) \in \Omega.$$

Remark 6.1. *As we know from Table* (6.1) *that*

$$\max_{0\leq i\leq N; 0\leq j<M} |\varphi'| \leq \begin{cases} C \ln N, & \text{(S-mesh)}, \\ C, & \text{(BS-mesh and VS-mesh)}. \end{cases}$$

All same techniques above give the error bound

$$|(V-v)(x_i,t_j)| \leq C(N^{-2} + \Delta t), \quad (x_i,t_j) \in \Omega,$$

on BS-mesh and VS-mesh at regular component. □

Theorem 6.4. *Let W be the numerical solution to Eq.* (6.30) *and w be the continuous solution to Eq.* (6.7). *The parameter-uniform error bound satisfied by the singular component on S-mesh is given by*

$$|(W-w)(x_i,t_j)| \leq C(N^{-2}\ln^2 N + \Delta t), \quad (x_i,t_j) \in \Omega,$$

and parameter-uniform error bound for both BS-mesh and VS-mesh are given by

$$|(W-w)(x_i,t_j)| \le C(N^{-2}+\Delta t), \quad (x_i,t_j)\in\Omega,$$

where C is a constant independent of ε and mesh points.

Proof. Error in the singular component can be estimated by dividing W into the form

$$W = W_L + W_R,$$

where W_L and W_R are defined respectively by

$$\begin{cases} \mathcal{L}_\varepsilon^{N,M} W_L(x_i,t_j) = 0, & (x_i,t_j)\in\Omega, \\ B_{L,\varepsilon}^N W_L(0,t_j) = \phi_L^j - B_{L,\varepsilon} v_0(0,t_j), & 0\le t_j\le T, \\ B_{R,\varepsilon}^N W_L(1,t_j) = 0, & 0\le t_j\le T, \\ W_L(x_i,0) = 0, & 0\le x\le 1, \end{cases} \tag{6.34}$$

and

$$\begin{cases} \mathcal{L}_\varepsilon^{N,M} W_R(x_i,t_j) = 0, & (x_i,t_j)\in\Omega, \\ B_{L,\varepsilon}^N W_R(0,t_j) = 0, & 0\le t_j\le T, \\ B_{R,\varepsilon}^N W_R(1,t_j) = \phi_R^j - B_{R,\varepsilon} v_0(1,t_j), & 0\le t_j\le T, \\ W_R(x_i,0) = 0, & 0\le x\le 1. \end{cases} \tag{6.35}$$

The error in the singular component can then be written in the form

$$W - w = (W_L - w_L) + (W_R - w_R),$$

where the error $W_L - w_L$ is associated with the left boundary layer and $W_R - w_R$ is associated with the right boundary layer. Now, considering the first part $W_L - w_L$. We bound the left boundary as derived above

$$B^N_{L,\varepsilon}(W_L - w_L)(0,t_j) = -\sqrt{\varepsilon}\bigg[-\frac{h_1^2}{6}\frac{\partial^3 w_L}{\partial x^3}(\eta,t_j)\bigg] + \frac{h_1}{2\sqrt{\varepsilon}}\bigg[\frac{\partial w_L}{\partial t}(0,t_j) - D_t^- w_L(0,t_j)\bigg],$$

where $0 < \eta < h_1$. Using the bound of truncation error, we have

$$|B^N_{L,\varepsilon}(W_L - w_L)(0,t_j)| \le \frac{\sqrt{\varepsilon}}{6}h_1^2\bigg\|\frac{\partial^3 w_L}{\partial x^3}\bigg\| + \frac{h_1}{2\sqrt{\varepsilon}}\frac{1}{2}(t_{j+1}-t_j)\bigg\|\frac{\partial^2 w_L}{\partial t^2}\bigg\|.$$

Since $h_1 = \frac{4\sigma}{N} = 8\sqrt{\varepsilon}N^{-1}\ln N,\ \sigma \ge 2\sqrt{\varepsilon}\ln N$ in the case of all S-type meshes together with the bound on the solution and its derivatives in Theorem (6.2) for singular component gives the following estimate

$$\begin{aligned}|B^N_{L,\varepsilon}(W_L - w_L)(0,t_j)| &\le C\sqrt{\varepsilon}(8\sqrt{\varepsilon}N^{-1}\ln N)^2(\varepsilon^{-3/2}e^{-x_0/\sqrt{\varepsilon}}) + C\Delta t,\\ &\le C\sqrt{\varepsilon}\varepsilon N^{-2}\ln^2 N\varepsilon^{-3/2} + C\Delta t,\\ &\le C(N^{-2}\ln^2 N + \Delta t).\end{aligned}$$

The error bound at the right boundary can be obtained similarly as

$$|B^N_{R,\varepsilon}(W_L - w_L)(1,t_j)| \le C(N^{-2}\ln^2 N + \Delta t).$$

To bound the interior points, consider the differential and difference equation

$$\mathcal{L}^{N,M}_\varepsilon(W_L - w_L) = (\mathcal{L}_\varepsilon - \mathcal{L}^{N,M}_\varepsilon)w_L = -\varepsilon\bigg(\frac{\partial^2}{\partial x^2} - \delta^2_{\text{hyb}}\bigg)w_L + \bigg(\frac{\partial}{\partial t} - D_t^-\bigg)w_L.$$

where $\delta^2_{\text{hyb}}(.)$ is the hybrid scheme for the second-order space derivative $\partial^2(.)/\partial x^2$ [93]. It follows that at each point (x_i,t_j) in Ω,

$$|\mathcal{L}^{N,M}_\varepsilon(W_L - w_L)(x_i,t_j)| \le \bigg|\varepsilon\bigg(\frac{\partial^2}{\partial x^2} - \delta^2_{\text{hyb}}\bigg)w_L\bigg| + \bigg|\bigg(\frac{\partial}{\partial t} - D_t^-\bigg)w_L\bigg| \tag{6.36}$$

Using the classical estimate, we obtain

$$\left|\left(\frac{\partial}{\partial t} - D_t^-\right)w_L\right| \leq \frac{1}{2}(t_{j+1} - t_j)\left|\frac{\partial^2 w_L}{\partial t^2}\right|.$$

Since $t-$mesh is uniform with $t_{j+1} - t_j = \Delta t$ and the bounds on the t-derivatives of w_L in Theorem (6.2), it follows that the second term on the right hand side of Eq. (6.36) satisfies

$$\left|\left(\frac{\partial}{\partial t} - D_t^-\right)w_L\right| \leq C\Delta t. \tag{6.37}$$

To bound the first term on the right hand side of Eq. (6.36), there arise two cases. Either $\sigma = \frac{1}{4}$ or $\sigma = 2\sqrt{\varepsilon}\ln N < \frac{1}{4}$ in all S-type meshes.

Case (i): Assume $\sigma = \frac{1}{4}$. In this case, the mesh is uniform and so $h_i = x_i - x_{i-1} = N^{-1}$. With this and a classical argument, leads to

$$\begin{aligned}|\mathcal{L}_\varepsilon^N(W_L - w_L)(x_i)| &\leq \left|\varepsilon\left(\frac{\partial^2}{\partial x^2} - \delta^2_{\text{hyb}}\right)w_L(x_i)\right|,\\ &\leq C\varepsilon(x_i - x_{i-1})^2\left\|\frac{\partial^4 w_L}{\partial x^4}\right\|.\end{aligned}$$

Using bound in Theorem (6.1) yields for all $x_i \in \Omega^N$

$$\begin{aligned}\left|\varepsilon\left(\frac{\partial^2}{\partial x^2} - \delta^2_{\text{hyb}}\right)w_L(x_i)\right| &\leq C\varepsilon(N^{-1})^2\varepsilon^{-2},\\ &\leq C\varepsilon^{-1}N^{-2}.\end{aligned}$$

Since $1/4 \leq 2\sqrt{\varepsilon}\ln N$ and so $\varepsilon^{-1} \leq (8\ln N)^2$, we have the following bound for the case $\sigma = \frac{1}{4}$

$$\left|\varepsilon\left(\frac{\partial^2}{\partial x^2} - \delta^2_{\text{hyb}}\right)w_L(x_i)\right| \leq CN^{-2}\ln^2 N. \tag{6.38}$$

Case (ii): Assume $\sigma = 2\sqrt{\varepsilon}\ln N$. In this case, the mesh is piecewise uniform and $\sigma = 2\sqrt{\varepsilon}\ln N < \frac{1}{4}$, with the mesh spacing $2(1-2\sigma)/N$ in the subinterval $(\sigma, 1-\sigma)$; and $4\sigma/N$ in each of the subintervals $(0,\sigma)$ and $(1-\sigma, 1)$. The argument now depends on the position of the mesh point x_i in Ω_x and there are three distinct possibilities.

At $x_i \in (0, \sigma)$, we have $x_i - x_{i-1} = \frac{4\sigma}{N} = 8\sqrt{\varepsilon}N^{-1}\ln N$. Combining this with a classical estimate and the bound in Theorem (6.2) leads to the bound in Eq. (6.38), we have

$$
\begin{aligned}
\left|\varepsilon\left(\frac{\partial^2}{\partial x^2} - \delta^2_{\text{hyb}}\right)w_L(x_i)\right| &\leq C\varepsilon(x_i - x_{i-1})^2\Big\|\frac{\partial^4 w_L}{\partial x^4}\Big\|, \\
&\leq C\varepsilon(8\sqrt{\varepsilon}N^{-1}\ln N)^2(\varepsilon^{-2}e^{-x_i/\sqrt{\varepsilon}}), \quad \text{since } e^{-x_i/\sqrt{\varepsilon}} \leq e^{-\sigma/\sqrt{\varepsilon}} = N^{-2} \\
&\leq CN^{-2}\ln^2 N, \qquad x_i \in [0, \sigma].
\end{aligned}
$$

At $x_i \in (1-\sigma, 1)$, we have

$$
\begin{aligned}
|\mathcal{L}^{N,M}_{\varepsilon}(W_L - w_L)(x_i)| \leq &\left|\varepsilon\left(\frac{\partial^2}{\partial x^2} - \delta^2_{\text{hyb}}\right)w_L(x_i)\right|, \\
\leq &C\varepsilon(x_i - x_{i-1})^2\Big\|\frac{\partial^4 w_L}{\partial x^4}\Big\|.
\end{aligned}
$$

Since $x_{i-1} > 1-\sigma$ and so $e^{-x_{i-1}/\sqrt{\varepsilon}} \leq e^{-\sigma/\sqrt{\varepsilon}} = e^{-2\ln N} = N^{-2}$ and using bound in Theorem (6.2) yields

$$
\begin{aligned}
\left|\varepsilon\left(\frac{\partial^2}{\partial x^2} - \delta^2_{\text{hyb}}\right)w_L(x_i)\right| &\leq C\varepsilon(8\sqrt{\varepsilon}N^{-1}\ln N)^2(\varepsilon^{-2}e^{-x_{i-1}/\sqrt{\varepsilon}}), \\
&\leq CN^{-2}\ln^2 N e^{-x_{i-1}/\sqrt{\varepsilon}}, \\
&\leq CN^{-2}\ln^2 N.
\end{aligned} \tag{6.39}
$$

At $x_i \in (\sigma, 1-\sigma)$, the local truncation error of the left boundary layer component w_L satisfies

$$
|\mathcal{L}^N_{\varepsilon}(W_L - w_L)(x_i)| = \varepsilon|(\delta^2 w_L - (w_{xx})_L)(x_i)|
$$

But, $|\delta^2 w_L(x_i)| \leq \max_{x_{i-1}\leq x\leq x_{i+1}} |(w_{xx})_L(x_i)|$. Then,

$$
\mathcal{L}^N_{\varepsilon}(W_L - w_L)(x_i)| \leq \left|\varepsilon\left(\frac{\partial^2}{\partial x^2} - \delta^2_{\text{hyb}}\right)w_L(x_i)\right| \leq 2\varepsilon \max_{x_{i-1}\leq x\leq x_{i+1}} \Big\|\frac{\partial^2 w_L}{\partial x^2}\Big\|.
$$

On $x_i \in (\sigma, 1-\sigma)$, consider $x_i = \sigma$. Since $h_i = x_i - x_{i-1}$, we have $x_{i-1} = x_i - h_i = \sigma - \frac{4\sigma}{N}$

and $e^{-x_{i-1}/\sqrt{\varepsilon}} = e^{-\sigma/\sqrt{\varepsilon}}.e^{4\sigma N^{-1}/\sqrt{\varepsilon}}$ together with the bound in Theorem (6.2) yields

$$\begin{aligned}
\mathcal{L}_\varepsilon^N(W_L - w_L)(x_i)| \leq \left|\varepsilon\left(\frac{\partial^2}{\partial x^2} - \delta^2_{\text{hyb}}\right)w_L(x_i)\right| &\leq 2\varepsilon \max_{x_{i-1}\leq x\leq x_{i+1}} \left\|\frac{\partial^2 w_L}{\partial x^2}\right\|,\\
&\leq C\varepsilon\big(\varepsilon^{-1}e^{-x_{i-1}/\sqrt{\varepsilon}}\big),\\
&= Ce^{-\sigma/\sqrt{\varepsilon}}.e^{4\sigma N^{-1}/\sqrt{\varepsilon}},\\
&= Ce^{-2\ln N}.e^{8N^{-1}\ln N},\\
&= C(N^{-2})(N^{1/N})^8,\\
&\leq CN^{-2}, \qquad x_i \in (\sigma, 1-\sigma).
\end{aligned} \tag{6.40}$$

since $N^{1/N} \leq C$, for all $N \geq 1$. Combining this result with a classical estimate and Theorem (6.2) again leads to the bound in Eq. (6.40), which is a slightly stronger result than Eq. (6.38). Adding the results in each domain gives the bound for the first term on the right hand side of Eq. (6.36) satisfying

$$\begin{aligned}
\mathcal{L}_\varepsilon^N(W_L - w_L)(x_i)| &\leq CN^{-2}\ln^2 N + CN^{-2},\\
&\leq CN^{-2}\ln^2 N.
\end{aligned}$$

Combining Eqs. (6.38) and (6.37) with Eq. (6.36) yields the estimate for all $(x_i, t_j) \in \Omega^{N,M}$

$$|\mathcal{L}_\varepsilon^{N,M}(W_L - w_L)(x_i, t_j)| \leq C(N^{-2}\ln^2 N + \Delta t).$$

Applying the discrete maximum principle, we obtain the following bound at the left singular component on S-mesh

$$|(W_L - w_L)(x_i, t_j)| \leq C(N^{-2}\ln^2 N + \Delta t). \tag{6.41}$$

Since $N^{-2} \leq N^{-2}\ln N$ and using Remark (6.1), the above techniques give the error bound

$$|(W_L - w_L)(x_i, t_j)| \leq C(N^{-2} + \Delta t), \quad (x_i, t_j) \in \Omega,$$

on BS-mesh and VS-mesh at left singular component. A completely analogous arguments lead to the error estimate to the right singular component on S-mesh

$$|(W_R - w_R)(x_i, t_j)| \leq C(N^{-2}\ln^2 N + \Delta t).$$

Since $N^{-2} \leq N^{-2}\ln N$, we have the error bound

$$|(W_R - w_R)(x_i, t_j)| \leq C(N^{-2} + \Delta t), \quad (x_i, t_j) \in \Omega,$$

on BS-mesh and VS-mesh at right singular component. □

Combination of the above error bounds lead us to the following main convergence theorem.

Theorem 6.5. *Let u be the continuous solution in Eq.* (6.1)-(6.2) *and U be the discrete solution in Eq.* (6.27)-(6.28)*. The parameter-uniform error bound on S-mesh is given by*

$$\sup_{0<\varepsilon\leq 1} \max_{0\leq i\leq N, 0\leq j\leq M} |U_i^j - u(x_i, t_j)| \leq C(N^{-2}\ln^2 N + \Delta t),$$

and parameter-uniform error bound for both BS-mesh and VS-mesh is given by

$$\sup_{0<\varepsilon\leq 1} \max_{0\leq i\leq N, 0\leq j\leq M} |U_i^j - u(x_i, t_j)| \leq C(N^{-2} + \Delta t).$$

where C is a constant independent of ε and the mesh parameters N and Δt.

Proof. The proof follows from the inequality in Eq. (6.31), Theorems (6.3) and (6.4). □

6.6 Numerical Results

All numerical computations are done for $\lambda_1 = 1/12$ and $\lambda_2 = 5/12$. In the first two tables, we begin with the space mesh size $N = 16$ and the time step $\Delta t = 0.2$ and we multiply N by two and divide Δt by four. The reason of dividing Δt by four is to justify the space direction rate of convergence properly [41] and [42].

Example 6.6.1. *Consider the singularly perturbed parabolic problem [68]*

$$\frac{\partial u(x,t)}{\partial t} - \varepsilon \frac{\partial^2 u(x,t)}{\partial x^2} + \frac{1+x^2}{2} u(x,t) = t^3, \quad (x,t) \in (0,1) \times (0,1],$$

with the initial and boundary conditions

$$\begin{cases} u(x,0) = 0, & x \in [0,1], \\ u(0,t) - \sqrt{\varepsilon}\frac{\partial u(0,t)}{\partial x} = -\frac{128}{35}\pi^{-1/2}t^{7/2}, & t \in [0,1], \\ u(1,t) + \sqrt{\varepsilon}\frac{\partial u(1,t)}{\partial x} = -\frac{128}{35}\pi^{-1/2}t^{7/2}, & t \in [0,1]. \end{cases}$$

The exact solution for the first example is not known, we use the double mesh principle to calculate the maximum absolute errors using the formula

$$E_\varepsilon^{N,\Delta t} = \max_{0 \le i \le N; 0 \le j \le M} \left| U^{N,\Delta t}(x_i, t_j) - U^{2N,\Delta t/4}(x_i, t_j) \right|,$$

where $U^{N,\Delta t}(x_i, t_j)$ denote the numerical solution obtained at $(N, \Delta t)$ mesh points whereas $U^{2N,\Delta t/4}(x_i, t_j)$ denote the numerical solution obtained by doubling the mesh points by including the midpoints $x_{i+1/2} = (x_i + x_{i+1})/2,\ t_{j+1/2} = (t_j + t_{j+1})/2$ into the mesh points.

Example 6.6.2. *Consider the singularly perturbed parabolic reaction-diffusion problem*

$$\frac{\partial u(x,t)}{\partial t} - \varepsilon \frac{\partial^2 u(x,t)}{\partial x^2} + (10 + 0.1\sin(\pi x))u(x,t) = f(x,t), \quad (x,t) \in (0,1) \times (0,1],$$

with the initial and boundary conditions

$$\begin{cases} u(x,0) = 0, & x \in [0,1], \\ u(0,t) - \sqrt{\varepsilon}\frac{\partial u(0,t)}{\partial x} = \phi_l(t), & t \in [0,1], \\ u(1,t) + \sqrt{\varepsilon}\frac{\partial u(1,t)}{\partial x} = \phi_r(t), & t \in [0,1], \end{cases}$$

where the functions $f(x,t), \phi_l(t)$ and $\phi_r(t)$ are chosen from the exact solution

$$u(x,t) = (1 - e^{-t/100})\big(e^{-x\sqrt{10/\varepsilon}} + e^{-(1-x)\sqrt{10/\varepsilon}}\big).$$

Since the exact solution for Example (6.6.2) is known, we calculate the maximum absolute errors using

$$E_{\varepsilon}^{N,\Delta t} = \max_{0\le i\le N; 0\le j\le M} \big|u(x_i,t_j) - U^{N,\Delta t}(x_i,t_j)\big|,$$

where $U^{N,\Delta t}(x_i,t_j)$ denotes the numerical solution and $u(x_i,t_j)$ denotes the exact solution. The parameter-uniform error and parameter-uniform rate of convergence are computed using the following formulas, respectively

$$E^{N,\Delta t} = \max_{0\le i\le N; 0\le j\le M} E_{\varepsilon}^{N,\Delta t} \quad \text{and} \quad R^{N,\Delta t} = \log_2\left(\frac{E^{N,\Delta t}}{E^{2N,\Delta t/4}}\right).$$

6.7 Discussion and Conclusion

Tables (6.2), (6.3), (6.4) and (6.5) depict the comparisons of the maximum absolute errors of the present method using S-mesh, BS-mesh and VS-mesh and the results in [68] and [70] for Example (6.6.1). Table (6.6) show the numerical results using different types of Shishkin-type meshes for Example (6.6.2). The numerical solution for Examples (6.6.1) and (6.6.2) on the S-mesh, BS-mesh and VS-mesh are shown in Figures (6.1) and (6.4), respectively. Based on the sketches in Figures (6.1)-(6.2) for Example (6.6.1) and (6.3)-(6.4) for Example (6.6.2), we can see that the VS-mesh and BS-mesh condense more mesh points and are smoother at the boundary layer regions than the S-mesh. From the numerical results in the Tables for a fixed ε, the maximum absolute errors decrease as mesh intervals increase. To address this observation, we plotted the maximum errors in log-log scale using the results in Table (6.4) on S-mesh, BS-mesh and VS-mesh for Examples

Table 6.2: Comparison of $E_{\varepsilon}^{N,\Delta t}, E^{N,\Delta t}$ and $R^{N,\Delta t}$ for Example (6.6.1).

$\varepsilon \downarrow$	$N=16$ $\Delta t = 0.2$	$N=32$ $\Delta t = \frac{0.2}{4}$	$N=64$ $\Delta t = \frac{0.2}{4^2}$	$N=128$ $\Delta t = \frac{0.2}{4^3}$	$N=256$ $\Delta t = \frac{0.2}{4^4}$	$N=512$ $\Delta t = \frac{0.2}{4^5}$
VS-mesh						
10^{-3}	4.1135e-2	1.0096e-2	2.9334e-3	7.9887e-4	2.1251e-4	5.5563e-5
10^{-4}	4.1548e-2	1.0065e-2	2.9252e-3	7.9847e-4	2.1194e-4	5.5415e-5
10^{-5}	4.1609e-2	1.0056e-2	2.9226e-3	7.9778e-4	2.1176e-4	5.5368e-5
10^{-6}	4.1622e-2	1.0053e-2	2.9218e-3	7.9756e-4	2.1170e-4	5.5353e-5
10^{-7}	4.1625e-2	1.0052e-2	2.9215e-3	7.9749e-4	2.1168e-4	5.5349e-5
10^{-8}	4.1626e-2	1.0051e-2	2.9215e-3	7.9746e-4	2.1168e-4	5.5347e-5
10^{-9}	4.1626e-2	1.0051e-2	2.9214e-3	7.9746e-4	2.1167e-4	5.5346e-5
$E^{N,\Delta t}$	4.1626e-2	1.0096e-2	2.9334e-3	7.9887e-4	2.1251e-4	5.5563e-5
$R^{N,\Delta t}$	2.0437	1.7831	1.8765	1.9104	1.9353	-
BS-mesh						
10^{-3}	4.1124e-2	1.3511e-2	3.8676e-3	1.0218e-3	2.6172e-4	6.6167e-5
10^{-4}	4.1543e-2	1.3476e-2	3.8579e-3	1.0192e-3	2.6105e-4	6.5996e-5
10^{-5}	4.1607e-2	1.3464e-2	3.8548e-3	1.0184e-3	2.6083e-4	6.5942e-5
10^{-6}	4.1621e-2	1.3461e-2	3.8538e-3	1.0182e-3	2.6076e-4	6.5925e-5
10^{-7}	4.1625e-2	1.3460e-2	3.8535e-3	1.0181e-3	2.6074e-4	6.5919e-5
10^{-8}	4.1626e-2	1.3459e-2	3.8534e-3	1.0181e-3	2.6074e-4	6.5917e-5
10^{-9}	4.1626e-2	1.3459e-2	3.8534e-3	1.0180e-3	2.6073e-4	6.5917e-5
$E^{N,\Delta t}$	4.1627e-2	1.3511e-2	3.8676e-3	1.0218e-3	2.6172e-4	6.6167e-5
$R^{N,\Delta t}$	1.6234	1.8046	1.9203	1.9650	1.9838	-
S-mesh						
10^{-3}	1.3320e-1	9.6423e-2	4.6726e-2	1.4534e-2	3.9888e-3	1.0400e-3
10^{-4}	1.3309e-1	9.6359e-2	5.0552e-2	2.1023e-2	7.6183e-3	2.5462e-3
10^{-5}	1.3305e-1	9.6339e-2	5.0537e-2	2.1014e-2	7.6146e-3	2.5449e-3
10^{-6}	1.3304e-1	9.6332e-2	5.0532e-2	2.1011e-2	7.6135e-3	2.5445e-3
10^{-7}	1.3303e-1	9.6330e-2	5.0530e-2	2.1011e-2	7.6131e-3	2.5444e-3
10^{-8}	1.3303e-1	9.6329e-2	5.0530e-2	2.1011e-2	7.6130e-3	2.5443e-3
10^{-9}	1.3303e-1	9.6329e-2	5.0529e-2	2.1010e-2	7.6130e-3	2.5443e-3
$E^{N,\Delta t}$	1.3320e-1	9.6423e-2	5.0552e-2	2.1010e-2	7.6183e-3	2.5462e-3
$R^{N,\Delta t}$	0.4661	0.9316	1.2667	1.4635	1.5811	-

Table 6.3: Comparison of $E^{N,\Delta t}$ and $R^{N,\Delta t}$ for Example (6.6.1).

Results	$N = 32$ $M = 8$	$N = 64$ $M = 32$	$N = 128$ $M = 128$	$N = 256$ $M = 512$	$N = 512$ $M = 2048$
Present results using					
VS-mesh					
$E^{N,\Delta t}$	2.5507e-2	6.1903e-3	1.5349e-3	3.8293e-4	9.5681e-5
$R^{N,\Delta t}$	2.0428	2.0119	2.0030	2.0008	-
BS-mesh					
$E^{N,\Delta t}$	2.5498e-2	6.1903e-3	1.5349e-3	3.8293e-4	9.5683e-5
$R^{N,\Delta t}$	2.0423	2.0119	2.0030	2.0007	-
S-mesh					
$E^{N,\Delta t}$	8.7551e-2	4.8508e-2	2.0595e-2	7.5218e-3	2.5228e-3
$R^{N,\Delta t}$	0.8519	1.2359	1.4531	1.5761	-
Results in [68]					
$E^{N,\Delta t}$	3.2130e-2	8.3210e-3	2.980e-3	5.2559e-4	1.3143e-4
$R^{N,\Delta t}$	1.9490	1.9877	1.9969	1.9995	-

Table 6.4: Values $E^{N,\Delta t}$ and $R^{N,\Delta t}$ for Example (6.6.1).

Results	$N = 32$ $M = 8$	$N = 64$ $M = 16$	$N = 128$ $M = 32$	$N = 256$ $M = 64$	$N = 512$ $M = 128$
Present results using					
VS-mesh					
$E^{N,\Delta t}$	2.5507e-2	1.2509e-2	6.1899e-3	3.0783e-3	1.5349e-3
$R^{N,\Delta t}$	1.0279	1.0150	1.0078	1.0040	-
BS-mesh					
$E^{N,\Delta t}$	2.5498e-2	1.2509e-2	6.1899e-3	3.0783e-3	1.5349e-3
$R^{N,\Delta t}$	1.0274	1.0150	1.0078	1.0040	-
S-mesh					
$E^{N,\Delta t}$	8.7551e-2	4.5279e-2	1.8572e-2	6.4733e-3	1.9890e-3
$R^{N,\Delta t}$	0.9513	1.2857	1.5206	1.7025	-
Results in [68]					
$E^{N,\Delta t}$	3.2130e-2	1.6470e-2	8.3343e-3	4.1915e-3	2.1018e-3
$R^{N,\Delta t}$	0.9641	0.982	0.9916	0.9958	-

Table 6.5: Comparison of $E_\varepsilon^{N,\Delta t}, E^{N,\Delta t}$ and $R^{N,\Delta t}$ using the present method and the method in [70] for Example (6.6.1).

$\varepsilon \downarrow$	$N = 64$ $\Delta t = \frac{1}{16}$	$N = 128$ $\Delta t = \frac{1}{64}$	$N = 256$ $\Delta t = \frac{1}{256}$	$N = 512$ $\Delta t = \frac{1}{1024}$	$N = 1024$ $\Delta t = \frac{1}{4096}$
VS-mesh					
10^{-2}	1.2269e-2	3.0515e-3	7.6714e-4	1.9339e-4	5.3126e-5
10^{-3}	1.2432e-2	3.0762e-3	7.6272e-4	1.9049e-4	4.7611e-5
10^{-4}	1.2500e-2	3.0762e-3	7.6590e-4	1.9127e-4	4.7806e-5
10^{-5}	1.2507e-2	3.0780e-3	7.6632e-4	1.9138e-4	4.7832e-5
10^{-6}	1.2509e-2	3.0783e-3	7.6638e-4	1.9139e-4	4.7836e-5
10^{-7}	1.2509e-2	3.0783e-3	7.6638e-4	1.9139e-4	4.7836e-5
10^{-8}	1.2509e-2	3.0783e-3	7.6638e-4	1.9139e-4	4.7836e-5
$E^{N,\Delta t}$	1.2509e-2	3.0783e-3	7.6714e-4	1.9339e-4	5.3126e-5
$R^{N,\Delta t}$	2.0228	2.0046	1.9880	1.8640	-
BS-mesh					
10^{-2}	1.2269e-2	3.0289e-3	7.5945e-4	1.9339e-4	5.3120e-5
10^{-3}	1.2438e-2	3.0632e-3	7.6274e-4	1.9049e-4	4.7611e-5
10^{-4}	1.2500e-2	3.0763e-3	7.6591e-4	1.9128e-4	4.7807e-5
10^{-5}	1.2508e-2	3.0781e-3	7.6633e-4	1.9138e-4	4.7833e-5
10^{-6}	1.2509e-2	3.0783e-3	7.6638e-4	1.9139e-4	4.7836e-5
10^{-7}	1.2509e-2	3.0783e-3	7.6639e-4	1.9140e-4	4.7836e-5
10^{-8}	1.2509e-2	3.0783e-3	7.6639e-4	1.9140e-4	4.7836e-5
$E^{N,\Delta t}$	1.2509e-2	3.0783e-3	7.6639e-4	1.9339e-4	5.3120e-5
$R^{N,\Delta t}$	2.0228	2.0060	1.9866	1.8642	-
S-mesh					
10^{-2}	1.2008e-2	2.9685e-3	7.3991e-4	1.8484e-4	4.6201e-5
10^{-3}	4.1624e-2	1.3506e-2	3.7571e-3	9.8392e-4	2.5130e-4
10^{-4}	4.5310e-2	1.9925e-2	7.3760e-3	2.4890e-3	7.9527e-4
10^{-5}	4.5288e-2	1.9916e-2	7.3721e-3	2.4876e-3	7.9483e-4
10^{-6}	4.5282e-2	1.9913e-2	7.3709e-3	2.4872e-3	7.9469e-4
10^{-7}	4.5279e-2	1.9912e-2	7.3706e-3	2.4870e-3	7.9464e-4
10^{-8}	4.5279e-2	1.9912e-2	7.3704e-3	2.4870e-3	7.9463e-4
$E^{N,\Delta t}$	4.5310e-2	1.9925e-2	7.3760e-3	2.4890e-3	7.9527e-4
$R^{N,\Delta t}$	1.1852	1.4337	1.5673	1.6460	-
Result in [70]					
$E^{N,\Delta t}$	1.888e-2	7.929e-3	2.821e-3	9.318e-4	2.949e-4
$R^{N,\Delta t}$	1.252	1.490	1.598	1.659	-

Table 6.6: Comparison of $E_\varepsilon^{N,\Delta t}$, $E^{N,\Delta t}$ and $R^{N,\Delta t}$ for Example (6.6.2).

$\varepsilon \downarrow$	$N = 16$ $\Delta t = 0.2$	$N = 32$ $\Delta t = \frac{0.2}{2}$	$N = 64$ $\Delta t = \frac{0.2}{2^2}$	$N = 128$ $\Delta t = \frac{0.2}{2^3}$	$N = 256$ $\Delta t = \frac{0.2}{2^4}$	$N = 512$ $\Delta t = \frac{0.2}{2^5}$
VS-mesh						
10^{-3}	1.5490e-3	4.9785e-4	1.4189e-4	3.8344e-5	1.0107e-5	2.6305e-6
10^{-4}	1.5491e-3	4.9787e-4	1.4190e-4	3.8346e-5	1.0108e-5	2.6306e-6
10^{-5}	1.5491e-3	4.9787e-4	1.4190e-4	3.8347e-5	1.0108e-5	2.6307e-6
10^{-6}	1.5491e-3	4.9787e-4	1.4190e-4	3.8347e-5	1.0108e-5	2.6307e-6
10^{-7}	1.5491e-3	4.9787e-4	1.4190e-4	3.8347e-5	1.0108e-5	2.6307e-6
10^{-8}	1.5491e-3	4.9787e-4	1.4190e-4	3.8347e-5	1.0108e-5	2.6307e-6
10^{-9}	1.5491e-3	4.9787e-4	1.4190e-4	3.8347e-5	1.0108e-5	2.6307e-6
$E^{N,\Delta t}$	1.5491e-3	4.9787e-4	1.4190e-4	3.8347e-5	1.0108e-5	2.6307e-6
$R^{N,\Delta t}$	1.6376	1.8109	1.8877	1.9236	1.9420	-
BS-mesh						
10^{-3}	1.9086e-3	6.4747e-4	1.8527e-4	4.9142e-5	1.2627e-5	3.2023e-6
10^{-4}	1.9086e-3	6.4749e-4	1.8528e-4	4.9144e-5	1.2628e-5	3.2025e-6
10^{-5}	1.9086e-3	6.4749e-4	1.8528e-4	4.9144e-5	1.2628e-5	3.2025e-6
10^{-6}	1.9086e-3	6.4750e-4	1.8528e-4	4.9145e-5	1.2628e-5	3.2025e-6
10^{-7}	1.9086e-3	6.4750e-4	1.8528e-4	4.9145e-5	1.2628e-5	3.2025e-6
10^{-8}	1.9086e-3	6.4750e-4	1.8528e-4	4.9145e-5	1.2628e-5	3.2025e-6
10^{-9}	1.9086e-3	6.4750e-4	1.8528e-4	4.9145e-5	1.2628e-5	3.2025e-6
$E^{N,\Delta t}$	1.9086e-3	6.4750e-4	1.8528e-4	4.9145e-5	1.2628e-5	3.2025e-6
$R^{N,\Delta t}$	1.5596	1.8052	1.9146	1.9604	1.9794	-
S-mesh						
10^{-3}	4.7606e-3	3.2682e-3	1.6943e-3	5.7656e-4	1.6525e-4	4.3875e-5
10^{-4}	4.7607e-3	3.2682e-3	1.8145e-3	8.1208e-4	3.0849e-4	1.0562e-4
10^{-5}	4.7607e-3	3.2682e-3	1.8145e-3	8.1208e-4	3.0849e-4	1.0562e-4
10^{-6}	4.7607e-3	3.2682e-3	1.8145e-3	8.1208e-4	3.0849e-4	1.0562e-4
10^{-7}	4.7607e-3	3.2682e-3	1.8145e-3	8.1208e-4	3.0849e-4	1.0562e-4
10^{-8}	4.7607e-3	3.2682e-3	1.8145e-3	8.1208e-4	3.0849e-4	1.0562e-4
10^{-9}	4.7607e-3	3.2682e-3	1.8145e-3	8.1208e-4	3.0849e-4	1.0562e-4
$E^{N,\Delta t}$	4.7607e-3	3.2682e-3	1.8145e-3	8.1208e-4	3.0849e-4	1.0562e-4
$R^{N,\Delta t}$	0.5427	0.8489	1.1599	1.3964	1.5463	-

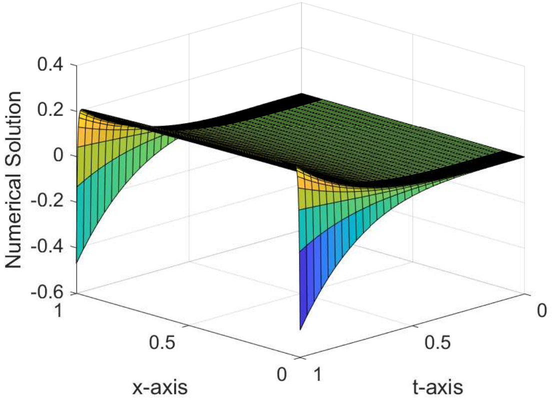

(a) S-mesh

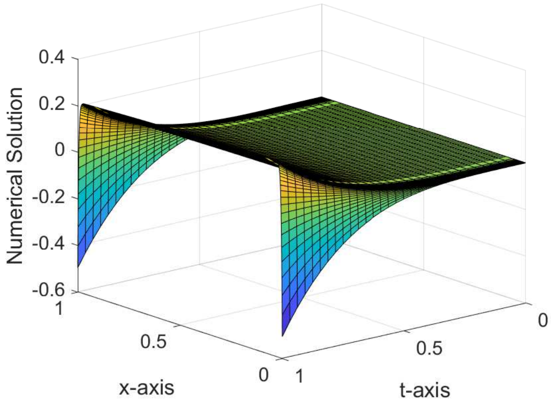

(b) BS-mesh

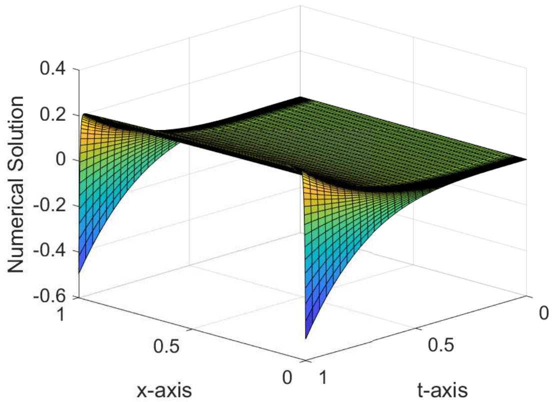

(c) VS-mesh

Figure 6.1: Surface plot at $N = 128, M = 32,\ \varepsilon = 10^{-4}$ for Example (6.6.1).

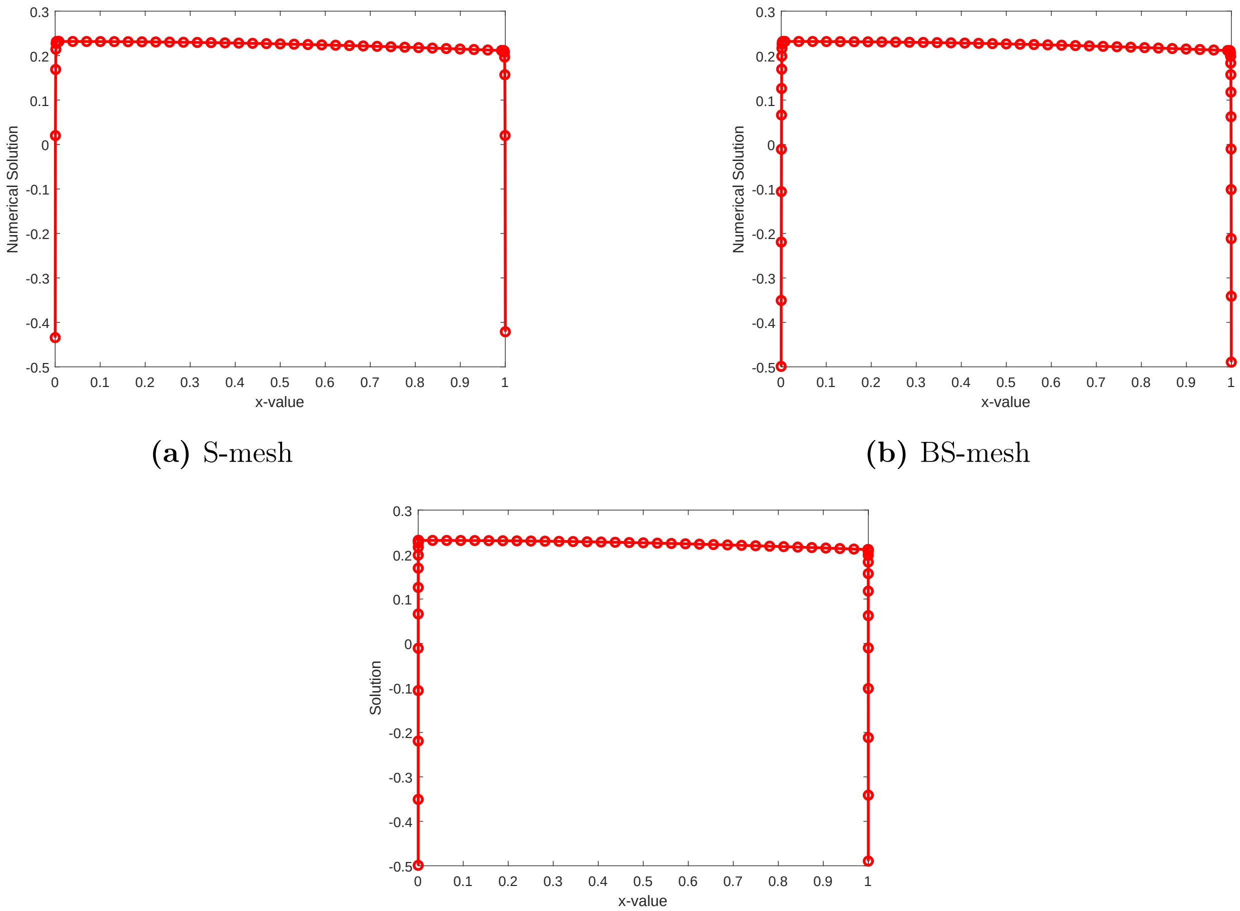

(a) S-mesh **(b)** BS-mesh **(c)** VS-mesh

Figure 6.2: Layer resolving feature for $N = 64, M = 80,\ \varepsilon = 10^{-6}$, Example (6.6.1).

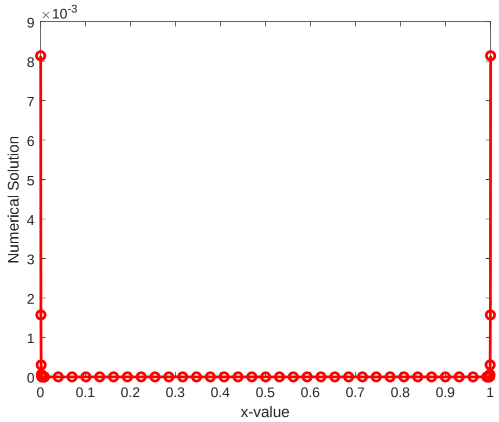

(a) S-mesh

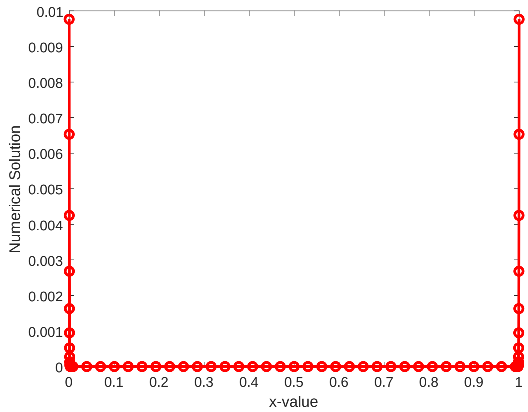

(b) BS-mesh

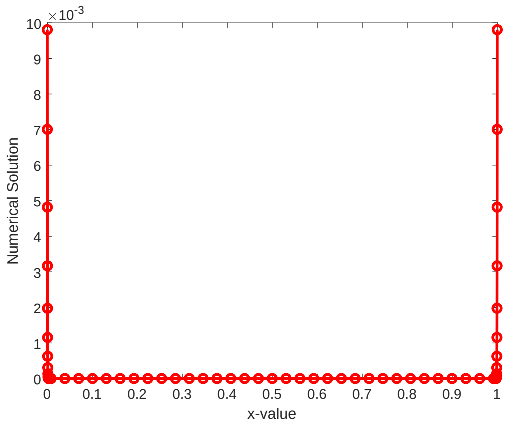

(c) VS-mesh

Figure 6.3: Layer resolving feature for $N = 64, M = 80,\ \varepsilon = 10^{-6}$, Example (6.6.2).

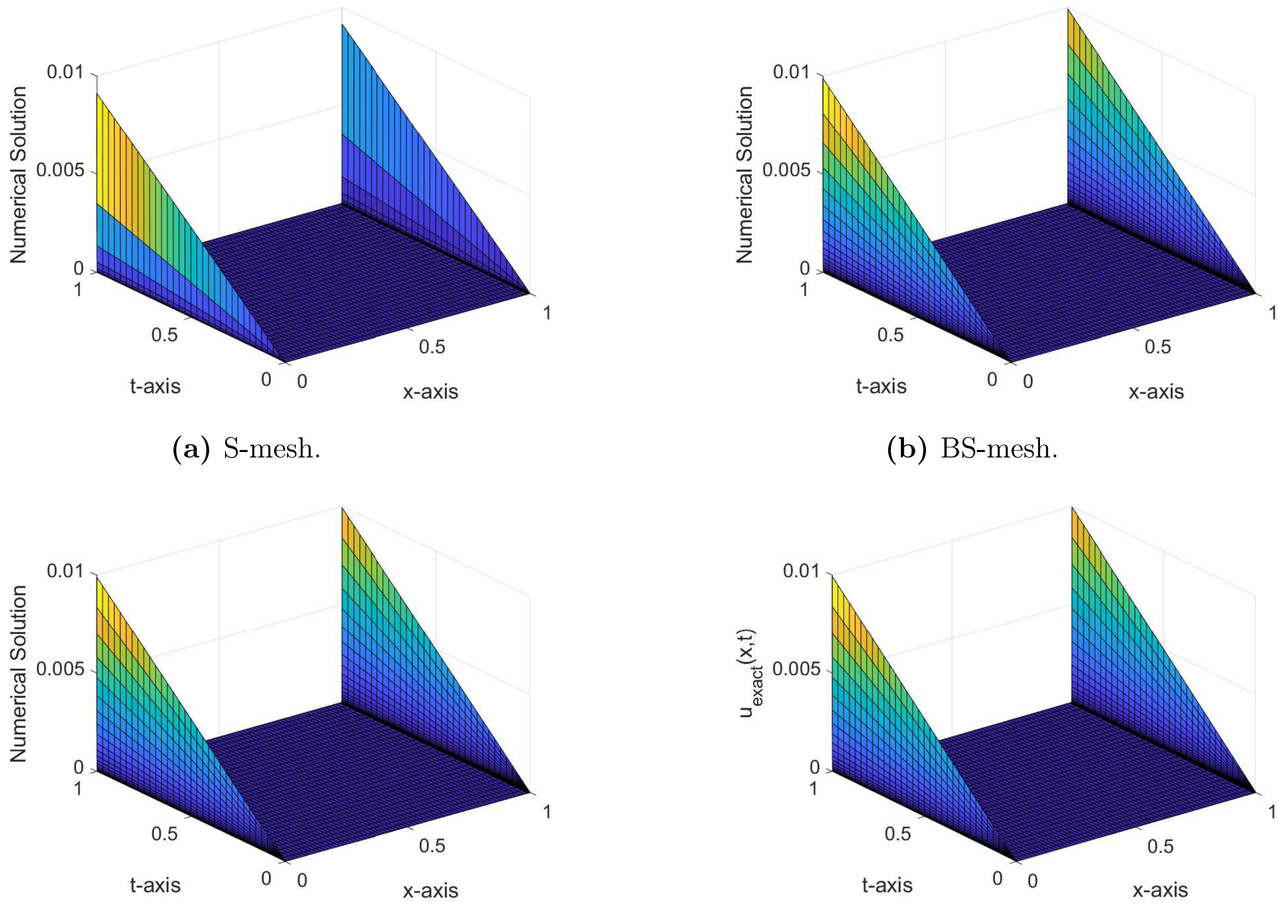

(a) S-mesh.

(b) BS-mesh.

(c) VS-mesh.

(d) Exact solution.

Figure 6.4: Surface plot of the numerical solution U and exact solution for Example (6.6.2) at $N = 128, M = 32,\ \varepsilon = 10^{-6}$.

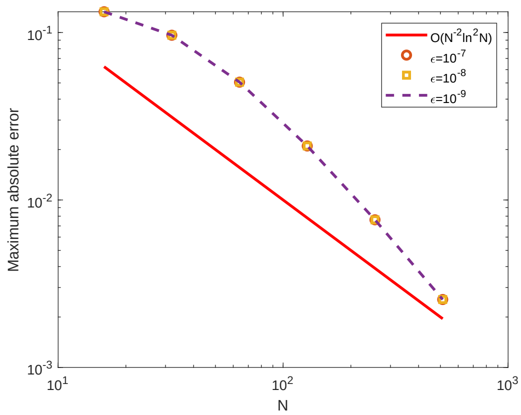

(a) S-mesh.

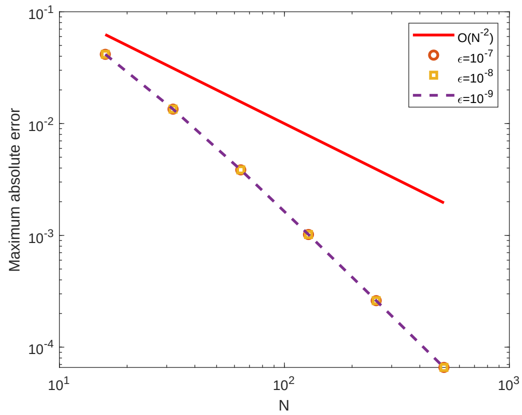

(b) BS-mesh.

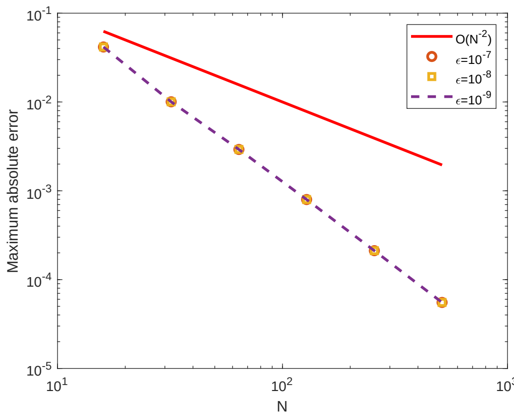

(c) VS-mesh.

Figure 6.5: Log-log plot of the maximum absolute errors in Table (6.4) for Example (6.6.1).

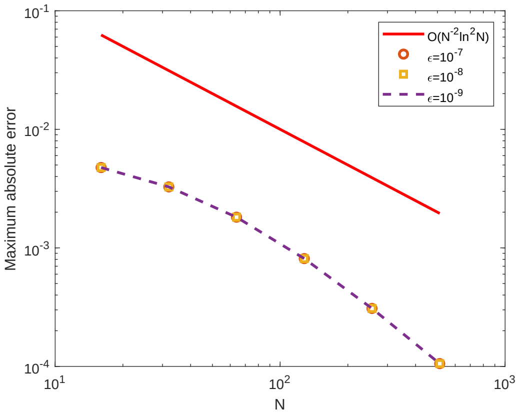

(a) S-mesh.

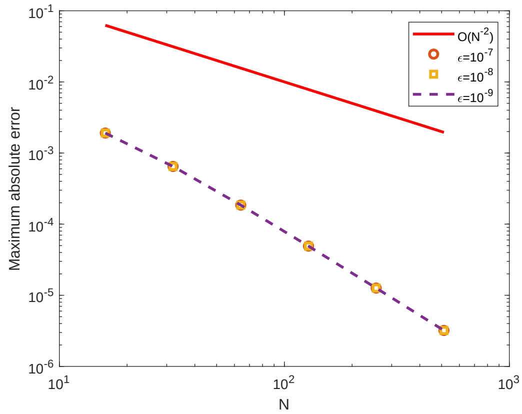

(b) BS-mesh.

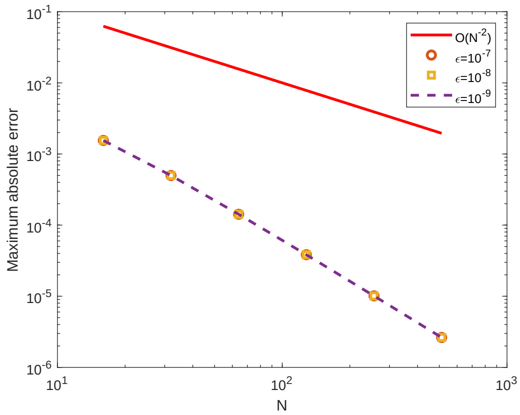

(c) VS-mesh.

Figure 6.6: Log-log plot of the maximum absolute errors in Table (6.4) for Example (6.6.2).

(6.6.1) and (6.6.2) as depicted in Figures (6.5) and (6.6), respectively. The log–log plot shows the slope of maximum point-wise error of the proposed numerical method is of second-order in space direction using BS- and VS meshes. As we observe from Figure (6.4) sub-figures (6.4c) and (6.4d), the numerical solution using the present method on layer-adapted VS-mesh agrees with the exact solution. All the numerical simulations for the examples considered show that the problem (6.1)-(6.2) has a parabolic boundary layer near $x = 0$ and $x = 1$. Both the numerical results in the Tables and the theoretical results confirm that the present method gives an almost second-order (up to logarithmic factor) $\varepsilon-$uniform convergence using S-mesh, whereas using BS-mesh and VS-mesh the numerical results are improved and the rate of convergence is second-order. The present results show betterment than the results in [68] and [70] for Example (6.6.1).

Chapter 7

General Discussions, Conclusions and Recommendations

This chapter provides a brief summary of the key findings of the dissertation. It also provides some recommendations and the scope of future research for the present methods.

7.1 General Discussions

This dissertation developed parameter-uniform numerical methods for singularly perturbed parabolic partial differential equations with Robin boundary conditions.

An upwind finite difference method using S-mesh and BS-mesh in space direction, and implicit Euler method in time direction to solve singularly perturbed parabolic convection-diffusion problems with Robin boundary conditions is discussed in Chapter 2. Forward and backward difference operators are used to discretize Robin boundary conditions. Extensive continuous and discrete analysis are established, which the literature lacks. Theoretical findings and numerical computations using two examples confirm that errors converge at the rate of first order, regardless of the perturbation parameter. It is proved that the optimal error bound, i.e., $O(N^{-1})$ obtained for the present method on the BS-mesh, is in fact more accurate than obtained on the S-mesh.

In Chapter 3, the same governing equation in Chapter 2 is used to develop a hybrid numerical scheme in the space direction on a Shishkin mesh and the implicit Euler method in the time direction on a uniform mesh. The second-order finite difference approximation for the left boundary condition and a backward finite difference approximation for the right boundary condition is constructed. The theoretical convergence analysis reveals that the present method is second-order in the space direction and first-order in the time direction. From computational results, we found that first-order in time does not reduce the proposed hybrid method's order of convergence for second example. However, from the numerical result, the order of the present method reduces to one for first example.

In Chapter 4, a numerical method for solving singularly perturbed parabolic convection-diffusion Robin type problems with a boundary turning point is presented. The implicit trapezoidal method for time discretization on uniform mesh and the second-order central finite difference methods for space discretization on Shishkin mesh is employed. The stability and convergence analysis of the method are established. Two numerical examples are performed to validate the applicability of the present method.

In Chapter 5, both the singularly perturbed time-delayed parabolic reaction-diffusion equation and the Robin boundary conditions are discretized using an extended cubic B-spline collocation method on Shishkin mesh in space direction and an implicit Euler method on uniform mesh in time direction. The convergence analysis of the present method has been proved. Available one example is considered for numerical computations. Comparisons have been made with the method reported in the literature.

Chapter 6 deals with hybrid scheme on S-type meshes for singularly perturbed parabolic reaction-diffusion problems with Robin boundary conditions. Second-order finite difference method is used to handle the Robin boundary conditions. The stability and convergence analysis of the method are proven. The present method converges $\varepsilon-$uniformly with almost second-order accuracy when using S-mesh and second-order accuracy when using BS-mesh and VS-mesh. It is found that using the implicit Euler method for time discretization has no effect on the rate of convergence of the hybrid method.

7.2 Conclusions

This dissertation presented different kinds of parameter-uniform numerical methods for singularly perturbed parabolic partial differential equations of convection-diffusion type and reaction-diffusion type with Robin boundary conditions. All the applied numerical methods such as upwind finite difference method, hybrid method, central finite difference method, and extended cubic B-spline collocation method on layer-adapted meshes of Shishkin, Bakhvalov-Shishkin and Vulanović-Shishkin types are parameter-uniformly convergent. All the methods constructed so far provide improved numerical solutions when compared with the other methods in the literature. The methods applied for solving singularly perturbed parabolic reaction-diffusion and convection-diffusion equations with Robin boundary conditions are conceptually simple, easy to use and readily adaptable for computer implementation. Generally, in all chapters, the stability and convergence analysis of the developed numerical methods are thoroughly established, which most literature lacks. Extensive numerical experiments are carried out to support theoretical findings. In all chapters, we employed matrix inversion method to solve the system of equations. Because of their ease of discretization, the majority of researchers use Dirichlet boundary conditions to solve singularly perturbed problems. The area of singularly perturbed problems with Robin boundary conditions has received little attention due to difficulties in discretization and analysis. Therefore, the main contribution of this dissertation is to apply the layer-adapted mesh methods and to strengthening the discretization and analysis of singularly perturbed parabolic partial differential equations of convection-diffusion and reaction-diffusion types with Robin boundary conditions.

7.3 Recommendations

In the achievement of this dissertation, we faced the some limitations. Even if a second-order accurate numerical method is used at the interior mesh points, using a first-order accurate method for the Neumann boundary conditions affects both the accuracy and rate of convergence of the overall numerical solution. As a result, we recommend the same order of accurate methods to discretize both Robin boundary conditions and the governing differential equation. In general, when the boundary condition contain derivatives of the unknown, it is difficult to obtain higher-order convergence results using direct numerical methods. It is possible to achieve higher-order convergence if acceleration techniques are used. Even though the developed methods are focused mainly on singularly perturbed parabolic partial differential equations with Robin boundary conditions, the following areas still require considerable attention.

- singularly perturbed parabolic semilinear reaction-diffusion problems with Neumann boundary conditions,
- singularly perturbed parabolic problems with integral boundary conditions,
- time fractional singularly perturbed parabolic problems,
- singularly perturbed integro-differential problems with Robin boundary conditions.

As far as the scope for further research is concerned, we intend to

- develop a higher-order parameter-uniform numerical methods,
- apply equidistribution mesh, polynomial-Shishkin mesh, a mesh with a rational function, Vulanović improved Shishkin mesh, harmonic mesh, B-type meshes, Duran mesh, Gartland mesh, and other meshes for the developed methods so far,
- develop spline collocation (quadratic, quartic, quintic) methods to improve the accuracy and rate of convergence for the developed methods so far and the problems under consideration in this dissertation.

Bibliography

[1] A. Ansari, S. Bakr, and G. Shishkin. A parameter-robust finite difference method for singularly perturbed delay parabolic partial differential equations. *Journal of computational and applied mathematics*, 205(1):552–566, 2007.

[2] A. R. Ansari and A. F. Hegarty. Numerical solution of a convection diffusion problem with robin boundary conditions. *Journal of computational and applied mathematics*, 156(1):221–238, 2003.

[3] S. Arora and I. Kaur. Applications of quintic hermite collocation with time discretization to singularly perturbed problems. *Applied Mathematics and Computation*, 316:409–421, 2018.

[4] T. Aziz and A. Khan. A spline method for second-order singularly perturbed boundary-value problems. *Journal of computational and applied mathematics*, 147 (2):445–452, 2002.

[5] N. Bakhvalov. Towards optimization of methods for solving boundary value problems in the presence of boundary layers. zh. vychisl. mat. i mat. fiz., 9: 841–859, 1969.

[6] L. Barbu and G. Morosanu. *Singularly perturbed boundary-value problems*, volume 156. Springer Science & Business Media, 2007.

[7] E. Bashier and K. Patidar. A second-order fitted operator finite difference method

for a singularly perturbed delay parabolic partial differential equation. *Journal of Difference Equations and Applications*, 17(05):779–794, 2011.

[8] E. B. Bashier and K. C. Patidar. An almost second order fitted mesh numerical method for a singularly perturbed delay parabolic partial differential equation. *Neural Parallel Sci. Comput.*, 18(2):137–154, 2010.

[9] E. B. Bashier and K. C. Patidar. A novel fitted operator finite difference method for a singularly perturbed delay parabolic partial differential equation. *Applied mathematics and Computation*, 217(9):4728–4739, 2011.

[10] H. Baumert, P. Braun, E. Glos, W.-D. Müller, and G. Stoyan. Modelling and computation of water quality problems in river networks. In *Optimization Techniques*, pages 482–491. Springer, 1980.

[11] J. Bear and A. Verruijt. Modeling groundwater pollution. In *Modeling Groundwater Flow and Pollution*, pages 153–195. Springer, 1987.

[12] C. M. Bender, S. Orszag, and S. A. Orszag. *Advanced mathematical methods for scientists and engineers I: Asymptotic methods and perturbation theory*, volume 1. Springer Science & Business Media, 1999.

[13] F. Black and M. Scholes. The pricing of options and corporate liabilities. In *World Scientific Reference on Contingent Claims Analysis in Corporate Finance: Volume 1: Foundations of CCA and Equity Valuation*, pages 3–21. World Scientific, 2019.

[14] L. Bobisud. Second-order linear parabolic equations with a small parameter. *Archive for Rational Mechanics and Analysis*, 27(5):385–397, 1968.

[15] J. R. Buchanan and Z. Shao. *A first course in partial differential equations*. World Scientific, 2018.

[16] T. A. Bullo. Accelerated fitted mesh scheme for singularly perturbed turning point boundary value problems. *Journal of Mathematics*, 2022, 2022.

[17] T. A. Bullo, G. A. Degla, and G. F. Duressa. Parameter-uniform finite difference method for singularly perturbed parabolic problem with two small parameters. *International Journal for Computational Methods in Engineering Science and Mechanics*, pages 1–9, 2021.

[18] T. A. Bullo, G. A. Degla, and G. F. Duressa. A parameter-uniform finite difference scheme for singularly perturbed parabolic problem with two small parameters. *European Journal of Computational Mechanics*, pages 197–222, 2021.

[19] T. A. Bullo, G. F. Duressa, and G. Degla. Accelerated fitted operator finite difference method for singularly perturbed parabolic reaction-diffusion problems. *Computational Methods for Differential Equations*, 9(3):886–898, 2021.

[20] T. A. Bullo, G. A. Degla, and G. F. Duressa. Fitted mesh method for singularly perturbed parabolic problems with an interior layer. *Mathematics and Computers in Simulation*, 193:371–384, 2022.

[21] X. Cai and F. Liu. A reynolds uniform scheme for singularly perturbed parabolic differential equation. *ANZIAM Journal*, 47:C633–C648, 2005.

[22] P. P. Chakravarthy and K. Kumar. An adaptive mesh method for time dependent singularly perturbed differential-difference equations. *Nonlinear Engineering*, 8(1): 328–339, 2019.

[23] A. H.-D. Cheng and D. T. Cheng. Heritage and early history of the boundary element method. *Engineering analysis with boundary elements*, 29(3):268–302, 2005.

[24] C. Clavero and J. L. Gracia. On the uniform convergence of a finite difference scheme for time dependent singularly perturbed reaction-diffusion problems. *Applied mathematics and computation*, 216(5):1478–1488, 2010.

[25] C. Clavero and J. L. Gracia. A high order hodie finite difference scheme for 1d

parabolic singularly perturbed reaction–diffusion problems. *Applied Mathematics and Computation*, 218(9):5067–5080, 2012.

[26] C. Clavero and J. L. Gracia. A higher order uniformly convergent method with richardson extrapolation in time for singularly perturbed reaction–diffusion parabolic problems. *Journal of computational and applied mathematics*, 252:75–85, 2013.

[27] C. Clavero, J. Jorge, and F. Lisbona. A uniformly convergent scheme on a nonuniform mesh for convection–diffusion parabolic problems. *Journal of Computational and Applied Mathematics*, 154(2):415–429, 2003.

[28] I. T. Daba and G. F. Duressa. Extended cubic b-spline collocation method for singularly perturbed parabolic differential-difference equation arising in computational neuroscience. *International Journal for Numerical Methods in Biomedical Engineering*, 37(2):e3418, 2021.

[29] I. T. Daba and G. F. Duressa. Hybrid algorithm for singularly perturbed delay parabolic partial differential equations. *Applications and Applied Mathematics: An International Journal (AAM)*, 16(1):21, 2021.

[30] D. de G. Allen and R. Southwell. Relaxation methods applied to determine the motion, in two dimensions, of a viscous fluid past a fixed cylinder. *The Quarterly Journal of Mechanics and Applied Mathematics*, 8(2):129–145, 1955.

[31] E. P. Doolan, J. J. Miller, and W. H. Schilders. *Uniform numerical methods for problems with initial and boundary layers*. Boole Press, 1980.

[32] F. Dorr, S. Parter, and L. F. Shampine. Applications of the maximum principle to singular perturbation problems. *SIAM review*, 15(1):43–88, 1973.

[33] R. K. Dunne, E. O'Riordan, and G. I. Shishkin. A fitted mesh method for a class

of singularly perturbed parabolic problems with a boundary turning point. *Computational Methods in Applied Mathematics*, 3(3):361–372, 2003.

[34] D. Edwards, J. Gier, K. Nelson, and R. Roddick. Spectral and directional thermal radiation characteristics of selective sufaces for solar collectors. *Solar Energy*, 6(1): 1–8, 1962.

[35] R. E. Ewing. *The mathematics of reservoir simulation.* SIAM, 1983.

[36] P. Farrell, A. Hegarty, J. M. Miller, E. O'Riordan, and G. I. Shishkin. *Robust computational techniques for boundary layers.* Chapman and hall/CRC, 2000.

[37] K. O. Friedrichs and W. R. Wasow. Singular perturbations of non-linear oscillations. *Duke Mathematical Journal*, 13(3):367–381, 1946.

[38] L. Govindarao and J. Mohapatra. Numerical analysis and simulation of delay parabolic partial differential equation involving a small parameter. *Engineering Computations*, 2019.

[39] L. Govindarao and J. Mohapatra. Richardson extrapolation technique for singularly perturbed delay parabolic partial differential equation. *International Journal of Advanced Trends in Computer Applications*, (1):44–48, 2019.

[40] L. Govindarao, J. Mohapatra, and A. Das. A fourth-order numerical scheme for singularly perturbed delay parabolic problem arising in population dynamics. *Journal of Applied Mathematics and Computing*, 63(1):171–195, 2020.

[41] S. Gowrisankar and S. Natesan. The parameter uniform numerical method for singularly perturbed parabolic reaction–diffusion problems on equidistributed grids. *Applied Mathematics Letters*, 26(11):1053–1060, 2013.

[42] S. Gowrisankar and S. Natesan. A robust numerical scheme for singularly perturbed delay parabolic initial-boundary-value problems on equidistributed grids. *Electron. Trans. Numer. Anal*, 41:376–395, 2014.

[43] J. L. Gracia and E. O'Riordan. Numerical approximation of solution derivatives in the case of singularly perturbed time dependent reaction–diffusion problems. *Journal of Computational and Applied Mathematics*, 273:13–24, 2015.

[44] A. Gupta, A. Kaushik, and M. Sharma. A higher-order hybrid spline difference method on adaptive mesh for solving singularly perturbed parabolic reaction–diffusion problems with robin-boundary conditions. *Numerical Methods for Partial Differential Equations*, 39(2):1220–1250, 2023.

[45] V. Gupta and M. K. Kadalbajoo. A layer adaptive b-spline collocation method for singularly perturbed one-dimensional parabolic problem with a boundary turning point. *Numerical Methods for Partial Differential Equations*, 27(5):1143–1164, 2011.

[46] V. Gupta, M. Kumar, and S. Kumar. Higher order numerical approximation for time dependent singularly perturbed differential-difference convection-diffusion equations. *Numerical Methods for Partial Differential Equations*, 34(1):357–380, 2018.

[47] S.-Y. Hahn, J. Bigeon, and J.-C. Sabonnadiere. An 'upwind'finite element method for electromagnetic field problems in moving media. *International journal for numerical methods in engineering*, 24(11):2071–2086, 1987.

[48] C. Hall. On error bounds for spline interpolation. *Journal of approximation theory*, 1(2):209–218, 1968.

[49] T. C. Hanks. Model relating heat-flow values near, and vertical velocities of mass transport beneath, oceanic rises. *Journal of Geophysical Research*, 76(2):537–544, 1971.

[50] A. F. Hegarty, J. J. Miller, E. O'Riordan, and G. Shishkin. Use of central-difference operators for solution of singularly perturbed problems. *Communications in numerical methods in engineering*, 10(4):297–302, 1994.

[51] P. Hemker, G. Shishkin, and L. Shishkina. The numerical solution of a neumann problem for parabolic singularly perturbed equations with high-order time accuracy. In *Recent Advances in Numerical Methods and Applications II*, pages 27–39. World Scientific, 1999.

[52] P. Hemker, G. Shishkin, and L. Shishkina. High-order time-accuracy schemes for parabolic singular perturbation problems with convection. *Russian journal of numerical analysis and mathematical modelling*, 17(1):1–24, 2002.

[53] P. W. Hemker, G. I. Shishkin, and L. P. Shishkina. High-order time-accurate schemes for singularly perturbed parabolic convection-diffusion problems with robin boundary conditions. *Computational Methods in Applied Mathematics*, 2(1):3–25, 2002.

[54] P. W. Hemker, G. I. Shishkin, and L. P. Shishkin. Novel defect-correction high-order, in space and time, accurate schemes for parabolic singularly perturbed convection-diffusion problems. *Computational Methods in Applied Mathematics*, 3(3):387–404, 2003.

[55] C. Hirsch. *Numerical computation of internal & external flows: fundamentals of numerical discretization.* John Wiley & Sons, Inc., 1988.

[56] G. Janani Jayalakshmi and A. Tamilselvan. An $\varepsilon-$uniform method for a class of singularly perturbed parabolic problems with robin boundary conditions having boundary turning point. *Asian-European Journal of Mathematics*, 13(01):2050025, 2020.

[57] S. Jiang, M. Sun, and Y. Yang. Reduced multiscale computation on adapted grid for the convection-diffusion robin problem. *J. Appl. Anal. Comput*, 7(4):1488–1502, 2017.

[58] R. B. Kellogg and A. Tsan. Analysis of some difference approximations for a singular

perturbation problem without turning points. *Mathematics of computation*, 32(144): 1025–1039, 1978.

[59] S. Ku Sahoo and V. Gupta. Second-order parameter-uniform finite difference scheme for singularly perturbed parabolic problem with a boundary turning point. *Journal of Difference Equations and Applications*, 27(2):223–240, 2021.

[60] Y. Kuang. *Delay differential equations: with applications in population dynamics*. Academic press, 1993.

[61] D. Kumar and K. Deswal. Wavelet-based approximation for two-parameter singularly perturbed problems with robin boundary conditions. *Journal of Applied Mathematics and Computing*, pages 1–25, 2022.

[62] D. Kumar and P. Kumari. A parameter-uniform collocation scheme for singularly perturbed delay problems with integral boundary condition. *Journal of Applied Mathematics and Computing*, 63(1):813–828, 2020.

[63] D. Kumar and P. Kumari. A parameter-uniform scheme for singularly perturbed partial differential equations with a time lag. *Numerical Methods for Partial Differential Equations*, 36(4):868–886, 2020.

[64] M. Kumar and S. Chandra Sekhara Rao. High order parameter-robust numerical method for time dependent singularly perturbed reaction–diffusion problems. *Computing*, 90(1):15–38, 2010.

[65] P. Kumar and A. Ravi Kanth. Computational study for a class of time-dependent singularly perturbed parabolic partial differential equation through tension spline. *Computational and Applied Mathematics*, 39(3):1–19, 2020.

[66] S. Kumar and M. Kumar. High order parameter-uniform discretization for singularly perturbed parabolic partial differential equations with time delay. *Computers & Mathematics with Applications*, 68(10):1355–1367, 2014.

[67] S. Kumar and S. C. S. Rao. A robust overlapping schwarz domain decomposition algorithm for time-dependent singularly perturbed reaction–diffusion problems. *Journal of computational and applied mathematics*, 261:127–138, 2014.

[68] S. Kumar, H. Ramos, et al. Parameter-uniform approximation on equidistributed meshes for singularly perturbed parabolic reaction-diffusion problems with robin boundary conditions. *Applied Mathematics and Computation*, 392:125677, 2021.

[69] S. Kumar, J. Vigo-Aguiar, et al. A parameter-uniform grid equidistribution method for singularly perturbed degenerate parabolic convection–diffusion problems. *Journal of Computational and Applied Mathematics*, 404:113273, 2022.

[70] S. Kumar, J. Singh, and H. Ramos. Parameter-uniform convergence analysis of a domain decomposition method for singularly perturbed parabolic problems with robin boundary conditions. *Journal of Applied Mathematics and Computing*, 69(2): 2239–2261, 2023.

[71] A. Kumari and V. Kukreja. Shishkin mesh based septic hermite interpolation algorithm for time-dependent singularly perturbed convection–diffusion models. *Journal of Mathematical Chemistry*, 60(10):2029–2053, 2022.

[72] O. A. Ladyzhenskaia, V. A. Solonnikov, and N. N. Ural'tseva. *Linear and quasi-linear equations of parabolic type*, volume 23. American Mathematical Soc., 1988.

[73] B. E. Launder, D. B. Spalding, et al. Lectures in mathematical models of turbulence. 1972.

[74] S. D. Lawley and J. P. Keener. A new derivation of robin boundary conditions through homogenization of a stochastically switching boundary. *SIAM Journal on Applied Dynamical Systems*, 14(4):1845–1867, 2015.

[75] T. Linß. An upwind difference scheme on a novel shishkin-type mesh for a linear

convection–diffusion problem. *Journal of computational and applied mathematics*, 110(1):93–104, 1999.

[76] T. Linß. Layer-adapted meshes for convection–diffusion problems. *Computer Methods in Applied Mechanics and Engineering*, 192(9-10):1061–1105, 2003.

[77] T. Linß and M. Stynes. Numerical methods on shishkin meshes for linear convection–diffusion problems. *Computer methods in applied mechanics and engineering*, 190 (28):3527–3542, 2001.

[78] A. Majumdar and S. Natesan. Second-order uniformly convergent richardson extrapolation method for singularly perturbed degenerate parabolic pdes. *International Journal of Applied and Computational Mathematics*, 3(1):31–53, 2017.

[79] A. Majumdar and S. Natesan. An $\varepsilon-$uniform hybrid numerical scheme for a singularly perturbed degenerate parabolic convection–diffusion problem. *International Journal of Computer Mathematics*, 96(7):1313–1334, 2019.

[80] N. A. Mbroh, S. C. O. Noutchie, and R. Y. M. Massoukou. A uniformly convergent finite difference scheme for robin type singularly perturbed parabolic convection diffusion problem. *Mathematics and Computers in Simulation*, 174:218–232, 2020.

[81] N. A. Mbroh, C. O. Noutchie, and R. Y. Massoukou. A second order fitted operator finite difference scheme for a singularly perturbed degenerate parabolic problem. *International Journal of Nonlinear Analysis and Applications*, 12(Special Issue): 677–687, 2021.

[82] Y. Mei, S. Wang, Z. Xu, C. Song, and Y. Cheng. Convergence analysis of the ldg method for singularly perturbed reaction-diffusion problems. *Symmetry*, 13(12): 2291, 2021.

[83] R. E. Mickens. *Nonstandard finite difference models of differential equations*. world scientific, 1994.

[84] J. Miller, E. O'Riordan, G. Shishkin, and L. Shishkina. Fitted mesh methods for problems with parabolic boundary layers. In *Mathematical Proceedings of the Royal Irish Academy*, pages 173–190. JSTOR, 1998.

[85] J. J. Miller. *Singular perturbation problems in chemical physics: analytic and computational methods*. Wiley Online Library, 1997.

[86] J. J. Miller, E. O'riordan, and G. I. Shishkin. *Fitted numerical methods for singular perturbation problems: error estimates in the maximum norm for linear problems in one and two dimensions*. World scientific, 1996.

[87] P. Mishra, K. K. Sharma, A. K. Pani, and G. Fairweather. High-order discrete-time orthogonal spline collocation methods for singularly perturbed 1d parabolic reaction–diffusion problems. *Numerical Methods for Partial Differential Equations*, 36(3):495–523, 2020.

[88] S. T. Mohyud-Din, T. Akram, M. Abbas, A. I. Ismail, and N. H. Ali. A fully implicit finite difference scheme based on extended cubic b-splines for time fractional advection–diffusion equation. *Advances in Difference Equations*, 2018(1):1–17, 2018.

[89] N. Mphephu. *Numerical solution of 1-D convection-diffusion-reaction equation*. PhD thesis, Master Thesis, University of Pretoria, South Africa, 25 October, 2013.

[90] K. Mukherjee and S. Natesan. Parameter-uniform hybrid numerical scheme for time-dependent convection-dominated initial-boundary-value problems. *Computing*, 84 (3):209–230, 2009.

[91] J. B. Munyakazi and K. C. Patidar. A fitted numerical method for singularly perturbed parabolic reaction-diffusion problems. *Computational and applied mathematics*, 32(3):509–519, 2013.

[92] J. B. Munyakazi, K. C. Patidar, and M. T. Sayi. A fitted numerical method for

parabolic turning point singularly perturbed problems with an interior layer. *Numerical Methods for Partial Differential Equations*, 35(6):2407–2422, 2019.

[93] S. Natesan and R. Deb. A robust numerical scheme for singularly perturbed parabolic raction-diffusion problems. *Neural, Parallel and Scientific Computations*, 16(3):419, 2008.

[94] S. Natesan and S. Gowrisankar. Robust numerical scheme for singularly perturbed parabolic initial-boundary-value problems on equidistributed mesh. *Computer Modeling in Engineering & Sciences(CMES)*, 88(4):245–267, 2012.

[95] M. J. Ng-Stynes, E. O'Riordan, and M. Stynes. Numerical methods for time-dependent convection-diffusion equations. *Journal of Computational and Applied mathematics*, 21(3):289–310, 1988.

[96] R. E. O'Malley. *Singular perturbation methods for ordinary differential equations*, volume 89. Springer, 1991.

[97] A. Peiraviminaei and F. Ghoreishi. Numerical solutions based on chebyshev collocation method for singularly perturbed delay parabolic pdes. *Mathematical Methods in the Applied Sciences*, 37(14):2112–2119, 2014.

[98] S. Polak, C. Den Heijer, W. Schilders, and P. Markowich. Semiconductor device modelling from the numerical point of view. *International Journal for Numerical Methods in Engineering*, 24(4):763–838, 1987.

[99] L. Prandtl. International mathematical congress, heidelberg. *Uber Flussigkeits Bewegung bei sehr kleiner Reibung*, pages 484–491, 1904.

[100] M. H. Protter and H. F. Weinberger. *Maximum principles in differential equations*. Springer Science & Business Media, 2012.

[101] J. Pudykiewicz. Simulation of the chernobyl dispersion with a 3-d hemispheric tracer model. *Tellus B*, 41(4):391–412, 1989.

[102] P. Rai and S. Yadav. Robust numerical schemes for singularly perturbed delay parabolic convection-diffusion problems with degenerate coefficient. *International Journal of Computer Mathematics*, 98(1):195–221, 2021.

[103] S. Rao, S. Kumar, and M. Kumar. A parameter-uniform b-spline collocation method for singularly perturbed semilinear reaction-diffusion problems. *Journal of optimization theory and applications*, 146(3):795–809, 2010.

[104] S. Rao, S. Kumar, and J. Singh. A discrete schwarz waveform relaxation method of higher order for singularly perturbed parabolic reaction–diffusion problems. *Journal of Mathematical Chemistry*, 58(3):574–594, 2020.

[105] S. C. S. Rao and S. Kumar. A robust numerical method for singularly perturbed semilinear convection-diffusion problems. *Neural, Parallel & Scientific Computations*, 18(2):155–166, 2010.

[106] H.-G. Roos, M. Stynes, and L. Tobiska. *Robust numerical methods for singularly perturbed differential equations: convection-diffusion-reaction and flow problems*, volume 24. Springer Science & Business Media, 2008.

[107] H. Schlichting and K. Gersten. *Boundary layer theory.* Springer, 2015.

[108] P. A. Selvi and N. Ramanujam. A parameter uniform difference scheme for singularly perturbed parabolic delay differential equation with robin type boundary condition. *Applied Mathematics and Computation*, 296:101–115, 2017.

[109] S. Sharifi and J. Rashidinia. Numerical solution of hyperbolic telegraph equation by cubic b-spline collocation method. *Applied Mathematics and Computation*, 281: 28–38, 2016.

[110] S. Sharifi and J. Rashidinia. Collocation method for convection-reaction-diffusion equation. *Journal of King Saud University-Science*, 31(4):1115–1121, 2019.

[111] K. K. Sharma, P. Rai, and K. C. Patidar. A review on singularly perturbed differential equations with turning points and interior layers. *Applied Mathematics and computation*, 219(22):10575–10609, 2013.

[112] G. I. Shishkin. Approximation of the solutions of singularly perturbed boundary-value problems with a parabolic boundary layer. *USSR Computational Mathematics and Mathematical Physics*, 29(4):1–10, 1989.

[113] H. Shukla and M. Tamsir. Extended modified cubic b-spline algorithm for nonlinear fisher's reaction-diffusion equation. *Alexandria Engineering Journal*, 55(3):2871–2879, 2016.

[114] J. Singh, S. Kumar, and M. Kumar. A domain decomposition method for solving singularly perturbed parabolic reaction-diffusion problems with time delay. *Numerical Methods for Partial Differential Equations*, 34(5):1849–1866, 2018.

[115] S. Singh, D. Kumar, and K. Deswal. Trigonometric b-spline based ε-uniform scheme for singularly perturbed problems with robin boundary conditions. *Journal of Difference Equations and Applications*, 28(7):924–945, 2022.

[116] S. Singh, D. Kumar, and H. Ramos. A uniformly convergent quadratic b-spline based scheme for singularly perturbed degenerate parabolic problems. *Mathematics and Computers in Simulation*, 2022.

[117] M. Stynes and E. O'Riordan. Uniformly convergent difference schemes for singularly perturbed parabolic diffusion-convection problems without turning points. *Numerische Mathematik*, 55(5):521–544, 1989.

[118] M. Stynes and H.-G. Roos. The midpoint upwind scheme. *Applied Numerical Mathematics*, 23(3):361–374, 1997.

[119] I. Takele Daba and G. File Duressa. A hybrid numerical scheme for singularly per-

turbed parabolic differential-difference equations arising in the modeling of neuronal variability. *Computational and Mathematical Methods*, 3(5):e1178, 2021.

[120] M. Van Dyke. Perturbation methods in fluid mechanics. academic. *New York*, 1964.

[121] J. M. Varah. A lower bound for the smallest singular value of a matrix. *Linear Algebra and its applications*, 11(1):3–5, 1975.

[122] W. R. Wasow. *On boundary layer problems in the theory of ordinary differential equation.* New York University, 1942.

[123] M. M. Woldaregay and G. F. Duressa. Uniformly convergent hybrid numerical method for singularly perturbed delay convection-diffusion problems. *International Journal of Differential Equations*, 2021, 2021.

[124] J. Wu. *Theory and applications of partial functional differential equations*, volume 119. Springer Science & Business Media, 1996.

[125] S. Yadav and P. Rai. A parameter uniform scheme for delay parabolic singularly perturbed turning point problem. *Differential Equations and Dynamical Systems*, pages 1–16, 2021.

[126] S. Yadav, P. Rai, and K. K. Sharma. A higher order uniformly convergent method for singularly perturbed parabolic turning point problems. *Numerical Methods for Partial Differential Equations*, 36(2):342–368, 2020.

[127] Q. Zheng, F. Huang, X. Feng, M. Han, et al. The uniform convergence of upwind schemes on layer-adapted meshes for a singularly perturbed robin bvp. *Open Journal of Applied Sciences*, 2(4):66–69, 2012.

[128] Q. Zheng, J. He, and Y. Liu. Higher-order layer-adapted finite difference schemes for singularly perturbed robin problems. In *Journal of Physics: Conference Series*, volume 1053, page 012007. IOP Publishing, 2018.

Appendix A

CV of the PhD Candidate

Personal Information

- Name: Fasika Wondimu Gelu
- Place and Date of Birth: 27 May 1986, SNNPR State, Ethiopia.
- Academic Qualification: BEd and MSc.
- Academic Rank: Currently lecturer at Dilla University, Ethiopia.

Educational Background

- July 19, 2007: Bachelor of Education from Dilla University, Ethiopia.
- June 25, 2015: Master of Science (Numerical Analysis) from Jimma University, Ethiopia.
- Since October 18, 2019: PhD scholar (Numerical Analysis) at Jimma University, Ethiopia.

Work Experience

- Ph.D. scholar at Jimma University, Ethiopia since October 18, 2019.
- Lecturer at Dilla University since September 2016-to-June 2018.
- Mathematics teacher at Waka preparatory and secondary school, SNNPR state, Dawuro Zone since September 2008-to-August 2015.

Research Interest

His research interest focuses on numerical solution of:

- singularly perturbed ordinary and partial differential equations.
- initial and boundary value problems.

CV of the PhD Candidate

List of Publications

1. A robust higher-order fitted mesh numerical method for solving singularly perturbed parabolic reaction-diffusion problems. *Results in Applied Mathematics.* **20**, 100405, 2023.

2. A parameter-uniform numerical method for singularly perturbed Robin type parabolic convection-diffusion turning point problems. *Applied Numerical Mathematics*, **190**:50-64, 2023.

3. A novel numerical approach for singularly perturbed parabolic convection-diffusion problems on layer-adapted meshes. *Research in Mathematics.* **9**(1), 1-15, 2022.

4. Parameter-uniform numerical scheme for singularly perturbed parabolic convection-diffusion Robin type problems with a boundary turning point. *Results in Applied Mathematics.* **15**(2), 100324, 2022.

5. Computational method for singularly perturbed parabolic reaction-diffusion equations with Robin boundary conditions. *Journal of Applied Mathematics & Informatics.* **40**(1-2), 25-45, 2022.

6. A uniformly convergent collocation method for singularly perturbed delay parabolic reaction-diffusion problems. *Abstract and Applied Analysis.* **2021**, Article ID 8835595, 11 pages, 2021.

7. Hybrid scheme on S-type meshes for singularly perturbed parabolic reaction-diffusion problems with Robin boundary conditions (Under Review).

8. Hybrid numerical method for singularly perturbed parabolic convection-diffusion problems on Shishkin mesh (Under Review).

9. An accelerated numerical scheme for solving singularly perturbed Robin-type parabolic problems with two small parameters (Ready for Submission).

10. Sixth order compact finite difference method for solving singularly perturbed 1D Reaction Diffusion Equations with Dirichlet Boundary conditions, *Journal of Taibah University for Science*, **11**, 302-308, 2017.

11. Fourth order compact finite difference method for solving singularly perturbed 1D Reaction Diffusion Equations with Dirichlet Boundary conditions. *Momona Ethiopian Journal of Science*, **8**(2), 168-181, 2016.

12. Tenth order compact finite difference method for solving singularly perturbed 1D Reaction Diffusion Equations. *International Journal of Engineering and Applied Science (IJEAS)*, **8**(3), 15-24, 2016.

MSc Thesis Supervised:

Since 2016, I have been supervised more than 5 MSc student.

Appendix B

Declaration Form

Letter for Declaration

I, undersigned, declared that this is my bona fide original work has never been presented in this or any other university, and that all resources and materials used for the dissertation, have been fully acknowledged.

Name: ....

Signature:..................................

Date:...

Place:..

Date of Submission:.......................................

This dissertation has been submitted for examination with my approval as

Candidate's Supervisor

Name: ....

Signature:..................................

Date:...